



# **THE MATHEMATICAL MODEL OF OXY-FUEL COMBUSTION OF MUNICIPAL SOLID WASTE ON THE GRATE FURNACE INTEGRATED WITH CO<sub>2</sub> CAPTURE**

by Paulina Copik

Doctoral Thesis in Environmental Engineering, Mining and Energy

Silesian University of Technology Gliwice

Poland, 2024

**Author:**

Paulina Copik, MSc

Joint Doctoral School at Silesian University of Technology

e-mail: [paulina.wienchol@polsl.pl](mailto:paulina.wienchol@polsl.pl)

**Supervisor:**

Andrzej Szlęk, Professor

Department of Thermal Technology

Silesian University of Technology

Konarskiego 22, 44-100 Gliwice, Poland

e-mail: [andrzej.szlek@polsl.pl](mailto:andrzej.szlek@polsl.pl)

**Co-Supervisor:**

Mario Ditaranto, PhD

SINTEF Energy Research

Sem Sælands vei 11, 7034 Trondheim, Norway

e-mail: [marioditaranto@sintef.no](mailto:marioditaranto@sintef.no)

**Polish title:**

Opracowanie modelu matematycznego spalania tlenowego stałych odpadów komunalnych na palenisku rusztowym zintegrowanym z wychwytem dwutlenku węgla

©Copyright 2024 by Paulina Copik

*“An expert is a man  
who has made all the mistakes  
which can be made  
in a very narrow field”*

**Niels Bohr** (1885-1962)

*I dedicate this work to my beloved Husband, Kuba*

# Preface

This thesis is submitted as the fulfilment of the requirements for the degree “Doctor of Philosophy” at the Silesian University of Technology (SUT), Gliwice, Poland.

The work was carried out at the Faculty of Energy and Environmental Engineering at the Department of Thermal Technology, with Professor Andrzej Szlęk and Dr. Mario Ditaranto as supervisors.

This work has been part of the “Experimental investigation and modelling of the oxy-incineration of municipal solid waste process for the development of technology for utilization of waste with negative CO<sub>2</sub> emission” (2021/41/N/ST8/02548) research project funded by the National Science Centre in Poland and carried out in cooperation with SINTEF Energy Research in Norway. The author also expresses his gratitude for providing financial support.

# Acknowledgments

I would like to express my sincere gratitude to my supervisor, Prof. Andrzej Szlęk, for his significant help, knowledge sharing, patience and professional and life guidance. I am deeply grateful for all the time devoted, valuable advice and commitment to my doctoral research.

I gratefully acknowledge the support of my co-supervisor, Dr. Mario Ditaranto, especially for the trust he placed in me and for giving me the opportunity to experience working in an international environment and using the laboratory facility at SINTEF Energy Research.

At this point, I would also like to acknowledge the people I had the opportunity to work with over the years. I am very grateful for the company of Agnieszka Korus, with whom I spent many hours in the laboratory, shared all my worries and celebrated successes. Thank you for your invaluable help, knowledge sharing in connection with experimental research, and support with my research.

Above all, my deepest gratitude goes to my family and friends. I am extremely grateful for the care, the opportunities and the right direction you have shown me, thanks to you I am in this place.

Finally, my deep sincere goes to my husband, Jakub. I am really grateful for his constant support, particularly in difficult times, his encouragement, and his patience, which I truly appreciate.

# Contents

1	Preface.....	IV
2	Acknowledgments.....	V
4	Contents .....	VI
6	Abstract.....	IX
7	Streszczenie.....	X
8	List of publications .....	XI
9	Supplementary activities.....	XIII
10	Other publications not included in the thesis .....	XV
11	Nomenclature .....	XVI
1	Introduction.....	1
1.1	Background.....	1
1.1.1	Waste generation and composition .....	2
1.1.2	Waste management: situation and trends in Europe .....	4
1.1.3	Incineration systems in the past and now .....	6
1.2	BECCS technologies.....	10
1.2.1	Carbon capture techniques.....	11
2	Objectives of this study.....	13
2.1	Scope of the thesis .....	14
3	Waste incineration integrated with carbon capture – paper I .....	16
3.1	Waste-to-energy with CCUS facilities.....	16
3.1.1	Novel concept of oxy-WtE .....	17
3.2	Conclusions for the next steps .....	19

## VII

4	Thermogravimetric and kinetic analysis of the waste material under different atmospheres – II paper .....	20
4.1	Kinetic theory.....	20
4.2	Methodology .....	21
4.2.1	Experimental procedure .....	21
4.2.2	Materials .....	22
4.3	Thermogravimetric analysis results .....	22
4.4	The kinetic data results .....	25
5	Experimental investigation of waste decomposition in various conditions – III paper .....	29
5.1	Experimental rig and the procedure .....	29
5.2	Results and discussion .....	30
5.2.1	Gas evolution .....	30
5.2.2	Kinetic analysis of waste-derived chars.....	32
6	Mathematical modelling of the oxy-waste incineration – IV paper .....	35
6.1	Model development .....	35
6.1.1	Model overview .....	35
6.1.2	Model equations.....	36
6.2	Results.....	38
6.2.1	Air-fired mode .....	38
6.2.2	Oxy-fired mode.....	39
7	Summary and conclusions .....	43
8	Bibliography .....	46
9	List of tables.....	54
10	List of figures .....	55

VIII

11   Appendixes ..... 56



# Abstract

Greenhouse gas (GHG) emissions are a serious environmental issue that humankind must face soon. Bio-energy carbon capture technology (BioCCS or BECCS) that results in negative-CO<sub>2</sub> power generation will be a vital in the transition toward a sustainable economy. Due to the biogenic origin of a considerable part of carbon contained in municipal solid waste (MSW), implementing carbon capture in waste incineration plants can be classified as BioCCS. Nowadays, there are four incinerators, in which CO<sub>2</sub> capture is applied; however, they use the post-combustion technique since it is the most mature method and does not require many changes in the system. Nevertheless, the separation of CO<sub>2</sub> from the flue gas stream, which contains mostly nitrogen, is expensive and causes a large drop in the system's total performance.

A more superior solution is oxy-fuel combustion technology. OFC involves the replacement of air as an oxidizer with oxygen and recirculated exhaust gas. As a result, the produced gas is composed mainly of CO<sub>2</sub> and H<sub>2</sub>O, which makes its sequestration more cost-effective. Nevertheless, changing the atmosphere from N<sub>2</sub> to CO<sub>2</sub> affects combustion behaviour. To study the impact of atmosphere on the thermal degradation process, evaluate the quantitative differences between air and oxy-waste combustion, and to better understand the process principles, the mathematical model of waste combustion under different atmospheres was developed. The model included all important stages of waste decomposition taking place within the chamber, such as moisture evaporation, pyrolysis, char burnout, and gas combustion over the grate. The individual processes were described using chemical data determined based on experimental results obtained through an experimental campaign on a thermogravimetric (TG) instrument and a lab-scale experimental rig. Isoconversional methods were employed to determine kinetic data.

The results of the work will contribute to the development of waste incineration plants integrated with carbon capture, expanding knowledge about the thermal degradation of waste in various conditions and will be useful for the design of oxy-waste combustion chambers.

# Streszczenie

Emisja gazów cieplarnianych (GHG) stanowi poważny środowiskowy problem, który obecnie skupia uwagę wielu naukowców. Technologia wychwytywania dwutlenku węgla z bioenergii (BioCCS lub BECCS), która skutkuje wytwarzaniem energii o ujemnej emisji CO<sub>2</sub> będzie miała kluczowe znaczenie w transformacji energetycznej. Ze względu na biologiczne pochodzenie części węgla zawartego w odpadach komunalnych (MSW), zastosowanie wychwytywania dwutlenku węgla w spalarniach odpadów można zaliczyć jako technologię BioCCS. Obecnie na świecie działają cztery spalarnie, w których CO<sub>2</sub> jest wychwytywane. Jednak następuje to po spalaniu powietrznym (ang. post-combustion) z uwagi na dojrzałość tej techniki i brak konieczności wielu zmian w istniejącym systemie. Niemniej jednak separacja CO<sub>2</sub> ze strumienia gazów spalinowych, który zawiera głównie azot, jest złożone i powoduje duży spadek całkowitej wydajności instalacji. Lepszym rozwiązaniem wychwyty CO<sub>2</sub> jest technologia spalania tlenowego (OFC), które polega na zastąpieniu powietrza jako utleniacza tlenem o wysokiej czystości i recykulowanymi spalinami. Dzięki temu wytwarzany gaz składa się głównie z CO<sub>2</sub> i H<sub>2</sub>O, co sprawia, że jego sekwestracja jest bardziej efektywna i opłacalna. Niemniej jednak zmiana atmosfery z N<sub>2</sub> na CO<sub>2</sub> wpływa znacząco na zachowanie paliwa podczas spalania. Aby lepiej zrozumieć ten proces, zbadano degradację termiczną reprezentatywnych odpadów komunalnych (MSW) w atmosferze N<sub>2</sub>, CO<sub>2</sub> i O<sub>2</sub>/CO<sub>2</sub> za pomocą termograwimetru (TG), a także użyto stanowiska doświadczalnego w skali laboratoryjnej. Eksperymenty przeprowadzono z dynamicznym programem temperaturowym w trzech szybkościach ogrzewania. Do określenia danych kinetycznych zastosowano metody izokonwersji. Przedstawione parametry kinetyczne dostarczyły podstawowych informacji na temat konwersji odpadów stałych i zostały wykorzystane w matematycznym modelowaniu spalania odpadów tlenowych. Opracowany model uwzględnia wszystkie istotne etapy rozkładu odpadów zachodzące w komorze, takie jak odparowanie wilgoci, piroliza, dopalenie karbonizatu i spalanie gazów nad rusztem. Wyniki prac przyczynią się do rozwoju spalarni odpadów zintegrowanych z wychwytem dwutlenku węgla, poszerzenia wiedzy o termicznej degradacji odpadów w różnych warunkach i będą przydatne do celów projektowych komór spalania tlenowego odpadów.

# List of publications

The presented doctoral thesis consists of 4 monothematic papers listed below. The full texts of this publications can be found in the Appendices chapter.

- I. **P. Wienchol\***, A. Szlęk, M. Ditaranto, Waste-to-energy technology integrated with carbon capture – Challenges and opportunities, Energy (IF: 9.000), Volume 198, 2020, 117352, <https://doi.org/10.1016/j.energy.2020.117352>

Number of citations: **120**

- II. **P. Wienchol\***, A. Korus, A. Szlęk, M. Ditaranto, Thermogravimetric and kinetic study of thermal degradation of various types of municipal solid waste (MSW) under N<sub>2</sub>, CO<sub>2</sub> and oxy-fuel conditions, Energy (IF: 9.000), Volume 248, 2022, 123573, <https://doi.org/10.1016/j.energy.2022.123573>

Number of citations: **17**

- III. **P. Copik\***, A. Korus, A. Szlęk, M. Ditaranto, A comparative study on thermochemical decomposition of lignocellulosic materials for energy recovery from waste: Monitoring of evolved gases, thermogravimetric, kinetic and surface analyses of produced chars, Energy (IF: 9.000), Volume 285, 2023, 129328, <https://doi.org/10.1016/j.energy.2023.129328>.

Number of citations: **2**

- IV. **P. Copik\***, A. Szlęk, M. Ditaranto, Simplified mathematical model of oxy-fuel combustion of municipal solid waste on the grate furnace: effect of different flue gas recirculation rates and comparison with conventional mode, Archives of Thermodynamics (IF: 0.800), Volume 4, 2024, doi: 10.24425/ather.2024.151233

Number of citations: **0**

\*corresponding author

The author's contribution for each paper was following:

## XII

I. Paulina Copik's contribution was to collect, review, and analyse the available literature on the waste-to-energy sector coupled with different carbon capture technologies to develop conclusions and formulate hypotheses, which were assessed during the doctoral thesis execution. Preparation, submission and revision of the manuscript. According to the author's statement, Paulina Copik's contribution was equal to 80%.

II. Paulina Copik's contribution was to prepare the scope of the experimental analysis, develop the experimental methodology, acquire waste materials, prepare and analyse the waste samples before the tests, obtain research funding, execute experimental tests and perform thermogravimetric and kinetic analysis, validate the results with literature data, and prepare and submit the manuscript. According to the author's statement, Paulina Copik's contribution was equal to 60%.

III. Paulina Copik's contribution was to formulate the methodology of the tests using a lab-scale reactor, conduct an experimental campaign, prepare waste-derived chars and their thermogravimetric and kinetic analysis, examine the results and draw conclusions, prepare and submit the manuscript, as well as obtain research funding. According to the author's statement, Paulina Copik's contribution was equal to 60%.

IV. Paulina Copik's contribution consisted in developing a mathematical model of waste incineration in the air and  $O_2/CO_2$  atmosphere, conducting simulations and analysing the described system in order to obtain the results and draw conclusions, prepare and submit the manuscript, as well as obtain research funding. According to the author's statement, Paulina Copik's contribution amounted to 80%.

# Supplementary activities

The author of this thesis is the co-author of 6 conference papers and presentations related to oxy-fuel combustion of waste and 3 presentations not related to subject of this thesis. The papers are listed below. The presenter is underlined.

1. **P. Wienchol**, A. Szlęk, M. Ditaranto, *Mathematical modeling of oxy-fuel combustion of municipal solid waste on the grate furnace integrated with CO<sub>2</sub> capture*, Contemporary Problems of Thermal Engineering CPOTE 20, 20-24.09.2020, Kraków, Poland.
2. **P. Wienchol**, A. Szlęk, *A study of a multi-zone combustion of municipal solid waste (MSW) in O<sub>2</sub>/CO<sub>2</sub> atmosphere*, V International Scientific and Technical Conference Modern Power Systems and Units, MPSU 21, 19-21.05.2021, Kraków, Poland.
3. **P. Wienchol**, A. Korus, A. Szlęk, M. Ditaranto, *Thermogravimetric analysis of thermal degradation of municipal solid waste (MSW) in N<sub>2</sub>, CO<sub>2</sub> and O<sub>2</sub>/CO<sub>2</sub> atmospheres*, 34<sup>th</sup> International Conference on Efficiency, Cost, Optimization, Simulation and Environmental Impact of Energy Systems, ECOS 2021, 27.06-02.07.2021, Taormina, Italy.
4. **P. Wienchol**, A. Korus, A. Szlęk, M. Ditaranto, *Experimental investigation on thermal decomposition of waste materials under different conditions for oxy-waste incineration technology development*, 16<sup>th</sup> Conference on Sustainable Development of Energy, Water and Environmental Systems, SDEWES 2021, 10-15.10.2021, Dubrovnik, Croatia.
5. **P. Wienchol**, A. Szlęk, M. Ditaranto, *Optimization of the ratio and feeding of the O<sub>2</sub>/CO<sub>2</sub> mixture to the municipal solid waste incineration process in a moving grate boiler*, 13th European Conference on Industrial Furnaces and Boilers (INFUB-13), 19-22.04.2022, Algarve, Portugal.
6. **P. Copik**, A. Szlęk, M. Ditaranto, *Oxy-incineration of the municipal solid waste in a moving grate boiler*, 11th European Combustion Meeting, 26-28.04.2023, Rouen, France.

7. H. Jaroszek, **P. Copik**, A. Korus, *Flow-electrode capacitive deionization (FCDI) in desalination: the effect of membrane type*, XIV Konferencja Naukowa „Membrany i Procesy Membranowe w Ochronie Środowiska” MEMPEP 2023, 21-24.06.2023, Zakopane, Poland, Politechnika Śląska, 145 s., ISBN 978-83-7880-909-8
8. A. Korus, H. Jaroszek, **P. Copik**, *Dual 2D-NLDFT model of CO<sub>2</sub> & O<sub>2</sub> adsorption for detailed understanding of micropore development in biochar during two-stage gasification*, The World Conference on Carbon, 16-21.07.2023, Cancun, Mexico.
9. A. Korus, H. Jaroszek, **P. Copik**, *The effect of leaching pre-treatment on the electrochemical properties of activated carbon and biochar electrodes for flow capacitive deionisation*, The World Conference on Carbon, 16-21.07.2023, Cancun, Mexico.

# Other publications not included in the thesis

J. Domin, M. Górski, R. Białecki, J. Zając, K. Grzyb, P. Kielan, W. Adamczyk, Z. Ostrowski, P. Wienchol, K. Lamkowski, *Wheeled Robot Dedicated to the Evaluation of the Technical Condition of Large-Dimension Engineering Structures*. *Robotics* 2020, 9, 28. <https://doi.org/10.3390/robotics9020028>

H. Jaroszek, A. Siekierka, P. Copik, A. Korus, *Insight into the impacts of acid and base pre-treatment on activated carbon and biochar electrodes in flow-electrode capacitive deionization*, *Desalination and Water Treatment*, 2023, vol. 314, s.1-15. [DOI:10.5004/dwt.2023.30090](https://doi.org/10.5004/dwt.2023.30090)

A. Korus, J. Jagiello, H. Jaroszek, P. Copik, A. Szlęk, *Variation of Pore Development Scenarios by Changing Gasification Atmosphere and Temperature*, *Energy*, Volume 289, 2024, Elsevier Ltd. doi:10.1016/j.energy.2023.129897.

# Nomenclature

A	pre-exponential factor, 1/s
$c_p$	the specific heat capacity, kJ/kgK
E	Energy activation, J/mol
H	enthalpy, kJ
k	reaction rate, 1/s
m	mass, kg
t	time, s
T	temperature, K
R	the universal gas constant, J(molK) <sup>-1</sup>
v	velocity, m/s

## Abbreviations and Acronyms

BECCS	Bioenergy Carbon Capture and Storage
CCS	Carbon Capture and Storage
CDR	Carbon dioxide removal
GHG	Greenhouse gas
ICM	Industrial carbon management
MSW	Municipal Solid Waste
OFC	Oxy-fuel combustion
RES	Renewable energy sources



**Greek letters**

$\alpha$	conversion rate
$\beta$	heating rate
$\varepsilon$	emissivity
$\sigma$	Stefan–Boltzmann constant

# Chapter 1

## Introduction

### 1.1 Background

The overall recognition is that the climate is changing, as evidenced by observations of rising average sea levels, widespread melting of snow and ice, and increases in average air and ocean temperatures [1]. Figure 1 presents the global and European surface air temperature anomalies between 1979 and 2023, where it can be observed that August 2023 was 0.71°C warmer than the 1991-2020 average temperature for August. The main reason for this phenomenon is a very high concentration of anthropogenic carbon dioxide (CO<sub>2</sub>), i.e., around 400 ppm by volume, which is the most radiative, non-condensing, and longest-lived greenhouse gas (GHG) that can remain in the atmosphere for millennia [2].

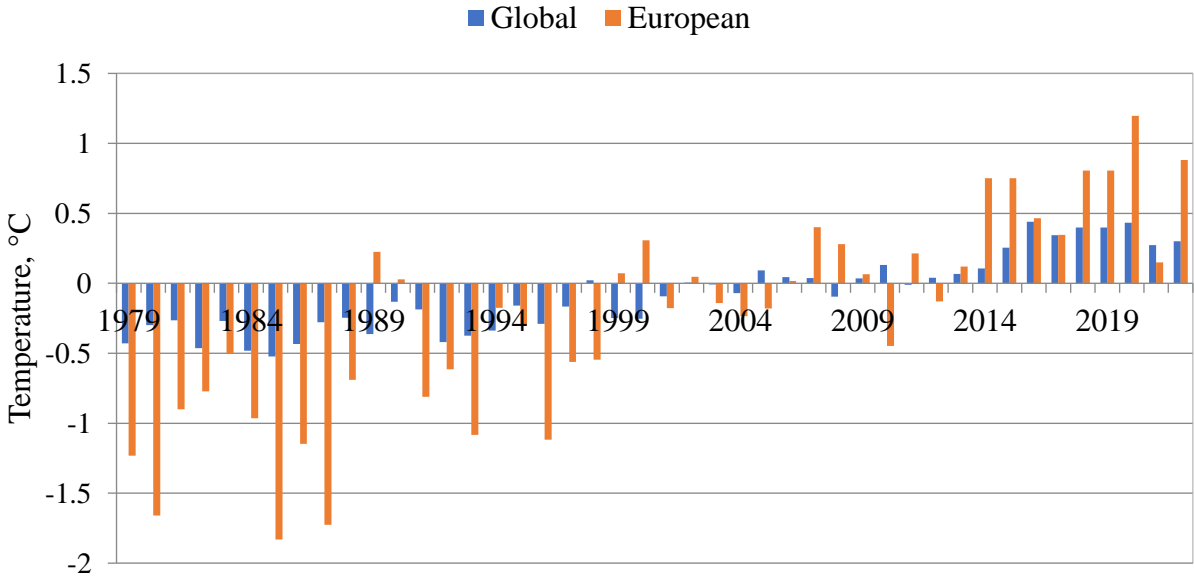


Figure 1 Global-mean and European-mean surface air temperature anomalies relative to 1991-2020 for each August from 1979 to 2023 (adapted from [3])

There are several approaches to facing global warming, such as adaptation, mitigation, and industrial carbon management (ICM). Adaptation involves simply living with and modifying behaviours of society around global warming issues. Mitigation is aimed at limiting the increase in global warming, which is performed by virtue of different acts, such as the Paris Agreement. Representatives of member states established the common goal of decreasing GHGs emissions to keep a global average temperature well below 2°C above pre-industrial levels and to pursue efforts to limit the growth to 1.5°C [4]. Since then, a massive energy transition towards renewable energy sources (RES) has started, resulting in a decrease in the consumption of conventional fuels, switching to other lower-carbon alternatives, e.g., nuclear, gas, or biomass, and an improvement in energy efficiency in industry and the power sector. ICM consists of the development of carbon capture, utilization, and storage techniques with persistent consumption of fossil-based fuels [2], [5].

According to leading climate scientists [6], coming back to the level of atmospheric concentration of CO<sub>2</sub> from the pre-industrial era is very unlikely to be obtained in this century, but keeping global warming at around 1.5°C more than in the pre-industrial era is still feasible but will involve the implementation of carbon dioxide removal (CDR) technologies, which must ensure the removal of between 100 and 1000 GtCO<sub>2</sub> by 2100.

### **1.1.1 Waste generation and composition**

Another serious global issue, municipal solid waste (MSW), is considered an unavoidable by-product of human activities, urbanization, and economic development. The current “take, make, use and dispose” model of economy causes the management of MSW to be a growing challenge worldwide. Nowadays, global waste generation is estimated at level of 2.01 billion tonnes and it is expected to rise to 3.4 billion tonnes by 2050 [7]. Figure 2 presents the composition of the MSW in Poland in 2020. As can be observed, the majority of waste constitutes organics (30.1%) that contains both kitchen and yard waste, plastics (16.1%), and paper with paperboard (12.8%). Waste of unknown origin (other) also constitutes a significant part (11.6%), while inert (1.7%), wood (0.6%) and hazardous waste (0.3%) are the least numerous [8].

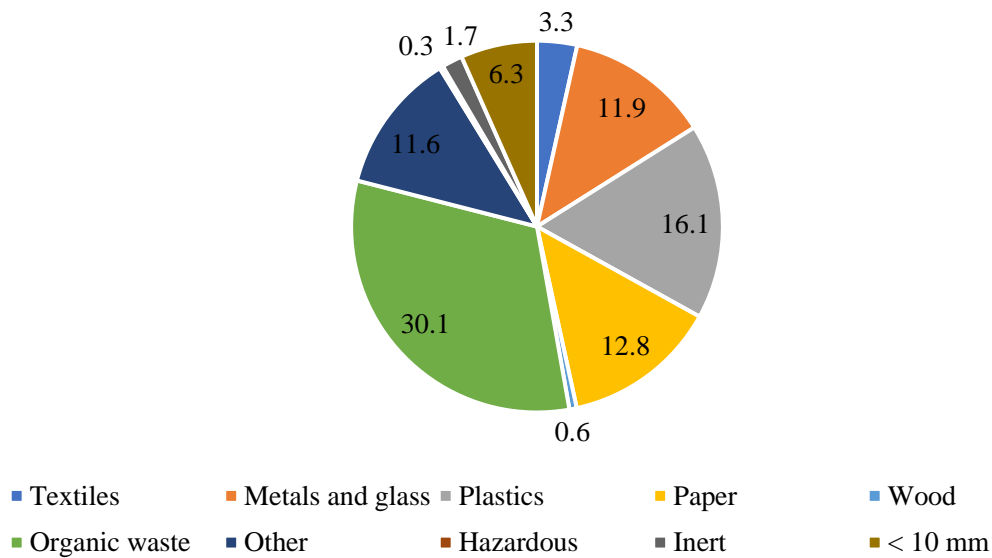


Figure 2 Municipal solid waste composition in Poland (2020). Based on data available [8]

Figure 3 presents the composition of the MSW in the USA in 2018. As can be observed, the majority of waste constitutes organics (31.6%), plastics (18.5%), and metals with glass (14.7%). Inert waste has the smallest share (2.24%). As can be seen, except for a few waste material groups, the morphology of the waste is similar for the USA and Poland, which can be explained by the similar lifestyle patterns and therefore consumption habits in these two industrialized countries. Comparison with developing countries would show major differences since, as explained in [7], waste composition depends on gross domestic product (GDP) value. The “other” fraction represents, in both cases, several percent, a better characterisation of this fraction may result in a more adjusted management [9].

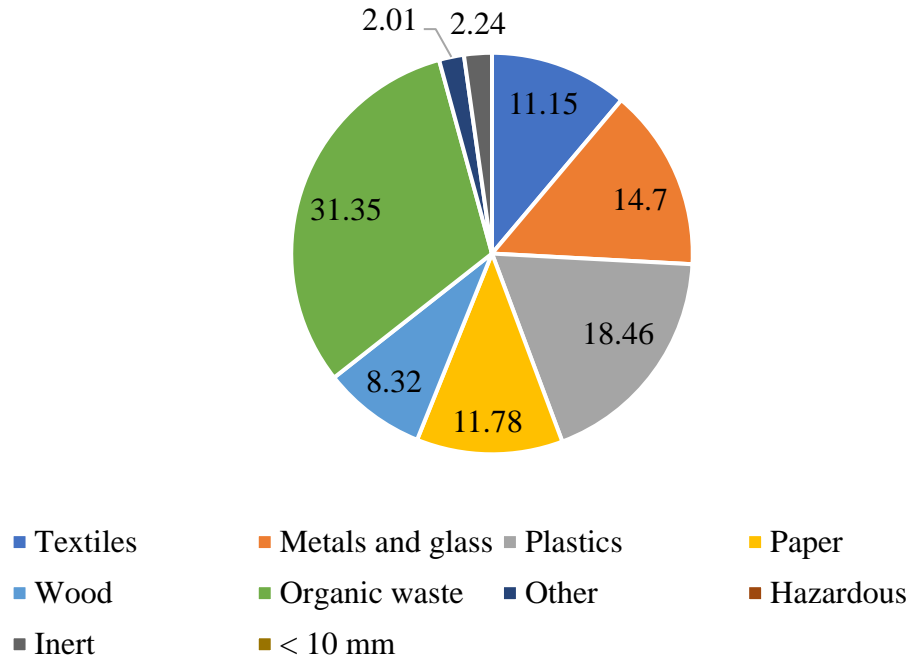


Figure 3 Municipal solid waste composition in USA (2018). Based on data available [10].

### 1.1.2 Waste management: situation and trends in Europe

European waste management from 1995 to 2019 is shown in Figure 4 [11]. As can be observed, at the end of the last century, landfilling was the most common method of waste disposal, while the amount of waste that was treated by other methods of disposal was negligible. As the 21<sup>st</sup> century began, waste management started to be more sustainable, and thus other technologies have gained importance. Recycling and energy recovery were of particular interest and gradually increased their share in waste management until 2014, when, for the first time in Europe, more waste was recycled and thermally processed than landfilled.

In the most recent years, recycling has played a leading role in the waste disposal process as it allows for recovering materials. Considering new regulations adopted by the EU, such as the Green Deal or Circular Economy Package, prevention, reuse, and recycling still will be promoted to achieve the target of reducing overall waste production and halving the amount of remaining (non-recycled) municipal solid waste by 2030 [12].

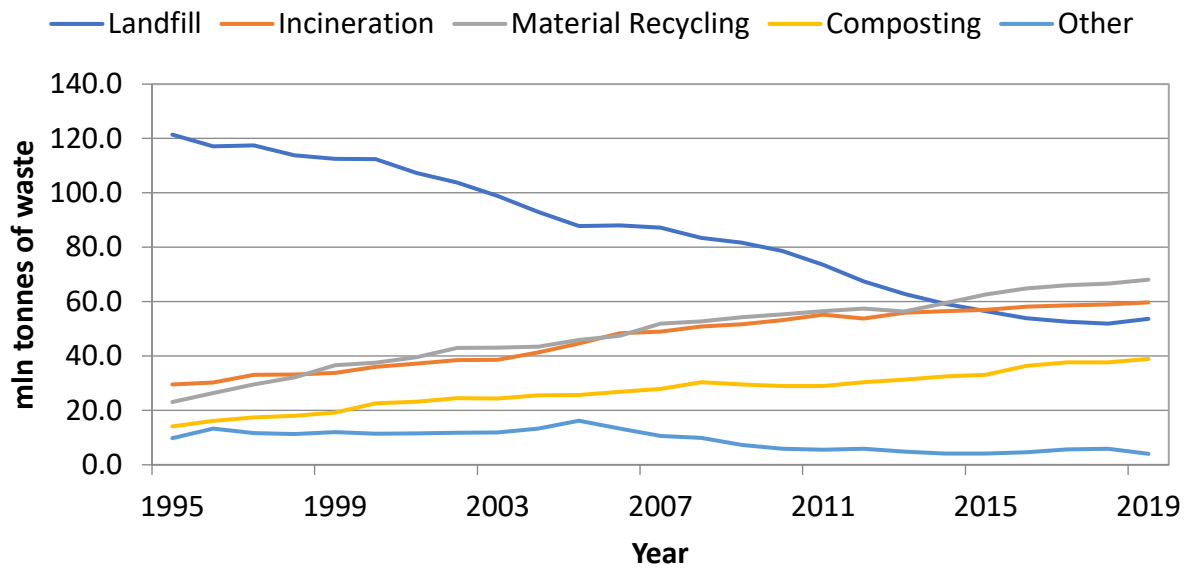


Figure 4 Municipal waste landfilled, incinerated, recycled, and composted, EU-27, 1995-2019 (Eurostat [11])

Regarding the development of waste-to-energy (WtE) technologies, the EU has a skeptical view since the Commission is concerned that, by increasing WtE capacity, waste recycling and reuse will be threatened. Despite the Commission's conclusion that WtE could play a key role in the transition to a circular economy, the waste hierarchy (Fig. 4) must be used as a guiding principle to ensure that prevention, reuse, and recycling are not averted and should be a priority. On the other hand, biomass, which includes a fraction of municipal solid waste with a biological origin, is one of the renewable energy sources defined by the RED [13]. Therefore, waste can cease to be an issue and become a valuable source of energy. The inclusion of the organic part of MSW in the definition of potential sources of RES has enabled the Member States to meet their domestic renewable energy goals through the WtE industry [14].

Despite doubts as to whether thermal treatment methods are necessary, a fundamental question arises how to dispose of waste that cannot be recycled, and significant amounts are currently landfilled in Europe, which is the source for public health issues. This causes methane release with a global warming potential (GWP) 20 times higher than that of carbon dioxide, the penetration of hazardous pollutants into groundwater as well as the emission of toxic fumes and dust from landfill sites into the atmosphere [15].

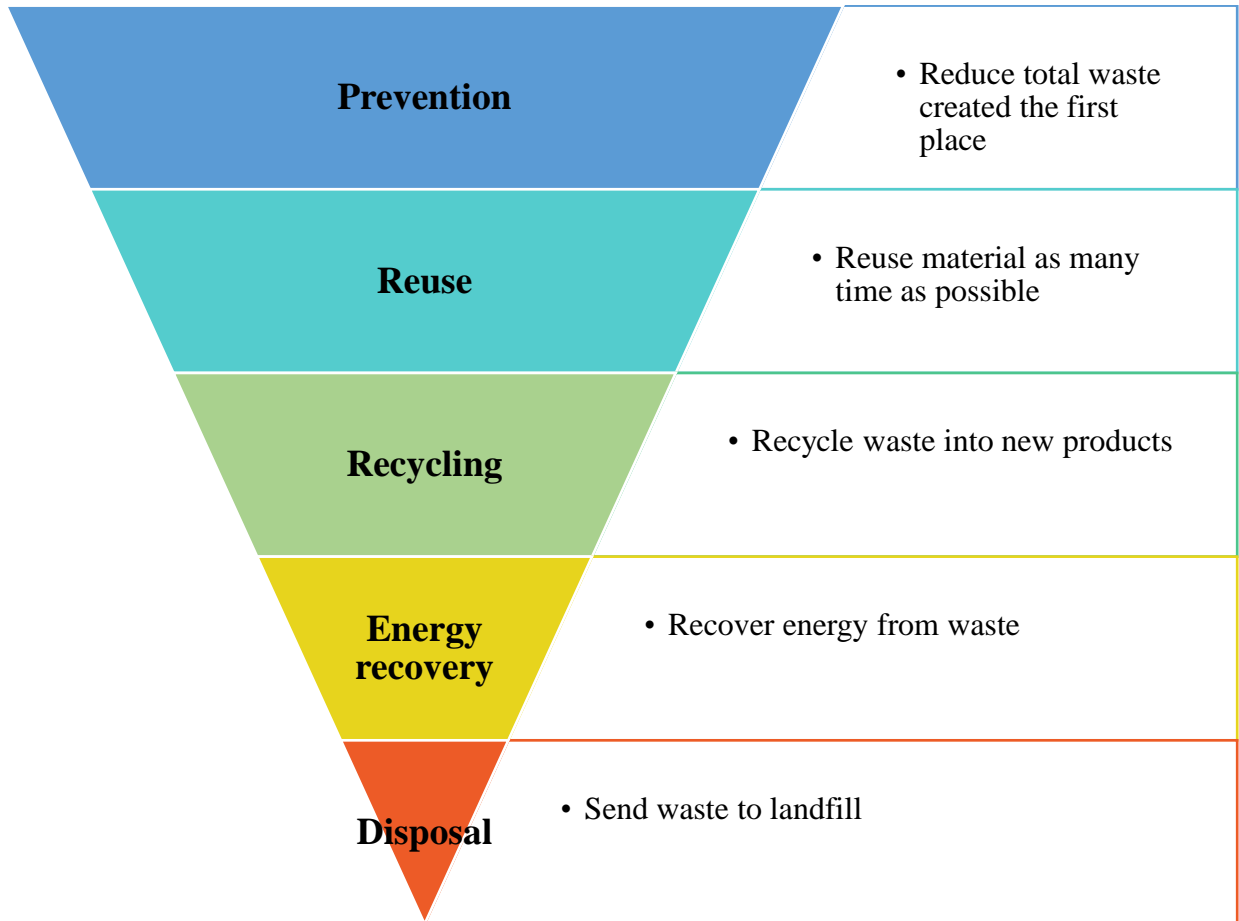


Figure 5 EU waste hierarchy [12]

### 1.1.3 Incineration systems in the past and now

The discussion about incinerators as a way of waste management system began during the Industrial Revolution. At that time, the practice of throwing garbage in the open and on riverbanks was common. Only increased public awareness that an unclean environment creates favourable conditions for the growth of bacteria and other disease-causing agents has led society to demand action from city authorities, which finally yielded to the pressure and in 1929, the first regulations were formulated in the USA. First incineration plants were intended only to reduce the volume of waste, without using the generated heat. Energy recovery from waste combustion began in the late 19<sup>th</sup> century in Europe and in the middle of 20<sup>th</sup> century in the USA (caused by the increased oil prices) [16], [17].

In the case of combustion technology, early incinerators were divided into continuous feed, batch-feed, ram-feed, metal conical and waste heat recovery incinerators. Among the first heat recovery systems were low-pressure and high-pressure boilers, as well as water wall furnaces. Only the continuous feed incinerators survived to these days. Nowadays, the MSWI technologies are categorized into three main groups, namely, moving grate, rotary kiln, and fluidized bed [16], [18].

Over the decades, the greatest progress has been made in the development of air pollution control (APC) systems, driven by public protests and pressure to close waste incinerators. As reported in the literature [16], the first electrostatic precipitators were developed around the 1970s and more advanced APC systems were adopted in the late 1980s. In the late 20th century, when the emission of harmful dioxins from MSWI plants was discovered, APC equipment had to be adjusted to facilitate the destruction of dioxins from the exhaust gas. Now, the emission of all known harmful substances (for example, fly ashes, heavy metals (Hg, Cd, Tl, As, Ni, Pb), carbon compounds (CO, hydrocarbons (VOCs) (PCDD/F, PCB), acid and other gases (HCl, HF, HBr, HI, SO<sub>2</sub>, NO<sub>x</sub>, NH<sub>3</sub>) is strictly limited by legal regulations [19].

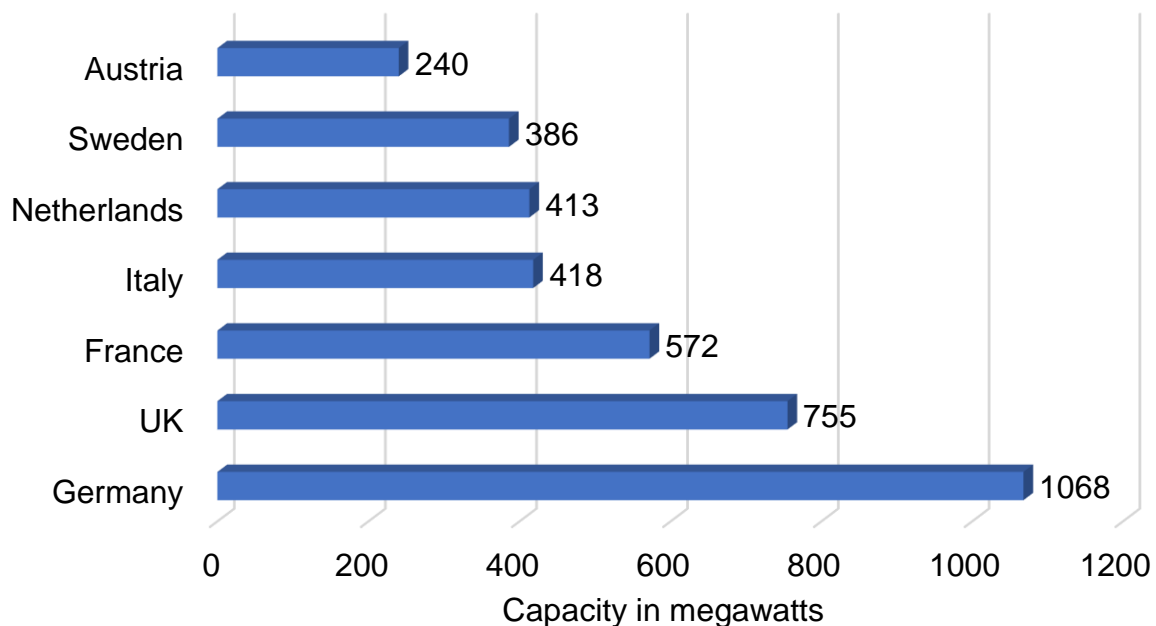


Figure 6 Installed capacity of municipal waste energy in Europe in 2022



Currently, incineration involves controlled combustion of waste in the air atmosphere to produce ash, flue gas, and heat used to generate electricity. The process should be organized so that the flue gas reaches a temperature of at least 850°C for 2 seconds to ensure proper destruction of toxic organic substances, and in the case of hazardous materials a temperature of at least 1150°C must be achieved [20]. Waste is processed in over 1400 incinerators globally with a total capacity exceeding 700 000 MT/d and the most widely used combustion technology is the moving grate system [21].

In Europe, the amount of MSW incinerated has risen from 30 million tonnes in 1995 to 59 million tonnes in 2022, i.e., from 70 to 133 kg per capita [11]. The total capacity of WtE installations in the countries with the largest number of incineration plants is shown in Figure 6. The distribution of waste incineration plants in Europe is shown in Figure 7. As can be observed, most waste incineration plants are located in Western Europe, especially in Germany, France, and Italy. The large number of the WtE plants are also located in Scandinavia and Great Britain.

It should be also noted that between 1995 and 2017 GHG emissions from MSW management (excluding energy recovery) have decreased by 42% and the sector will continue to play an important part in the EU's ambition to achieve net zero by 2050 [14].

The data presented confirms that WtE plants have grown to be a vibrant industry and will continue to develop. Nevertheless, some crucial issues remained unsolved. Firstly, MSW volumes continue to be on the rise which suggests that the linear economy is still predominant worldwide. Secondly, despite major achievements made in the evolution of APC systems, social phobia against pollutants, particularly dioxins has not been diminished [16]. Moreover, the Not In My Back Yard (NIMBY) effect, caused by misinformation, distrust of authority and risk aversion, is prevalent when speaking of MSW incinerators that forces local governments to postpone, relocate, or even cancel new projects [22]. Therefore, there is now a great need for action to dispel negative public perception and make MSW incineration a more acceptable technology.

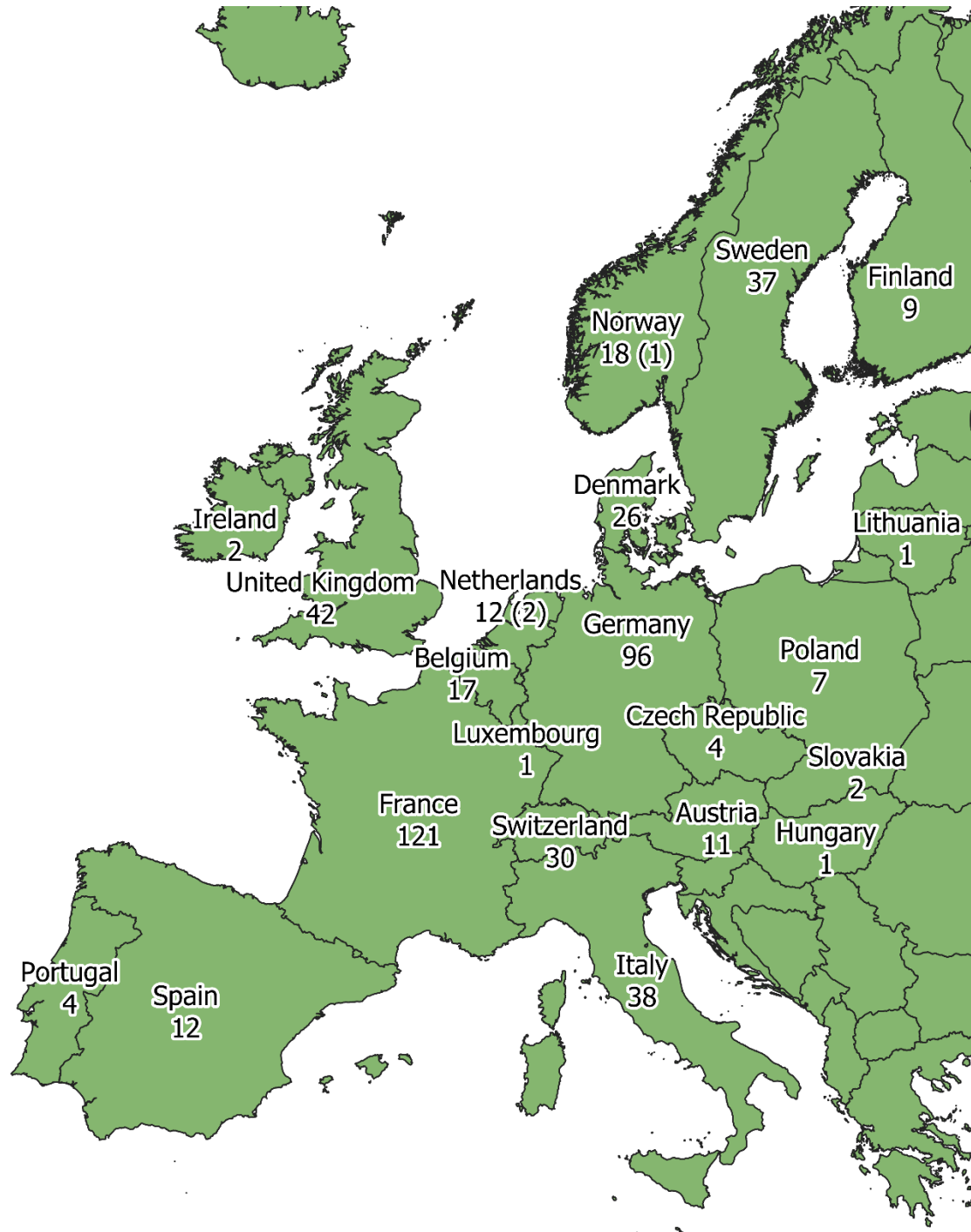


Figure 7 The number and distribution of waste incineration plants in Europe (2020) [23]

## 1.2 BECCS technologies

One of the solutions to the global warming problem mentioned in most climate change mitigation pathways may be one of the CDR technologies, i.e., bioenergy with carbon capture and storage (BECCS) [24]. In the BECCS system (Fig. 8), CO<sub>2</sub> is removed from the atmosphere through the process of photosynthesis, which occurs in plant cells, and then biomass is utilized to produce energy. The obtained biogenic CO<sub>2</sub> is captured and permanently stored, for example, in a geological formation or a sea floor, and the biomass is cultivated again. Therefore, BECCS can result in negative emissions and, thus, a decrease in atmospheric CO<sub>2</sub> [24],[25].

There are at least 20 BECCS projects worldwide, comprising various technologies, for example, ethanol plants in France, Brazil and Sweden, biomass combustion and co-firing in Japan, two pulp and paper plants in Sweden, biomass gasification in the US, biogas plant in Sweden as well as incineration plants in the Netherlands, Norway, and Japan. These BECCS projects together correspond to 2.6 million tonnes (Mt) of CO<sub>2</sub> captured per year, of which 93% is related to ethanol production [26], [27].

### Atmospheric CO<sub>2</sub>

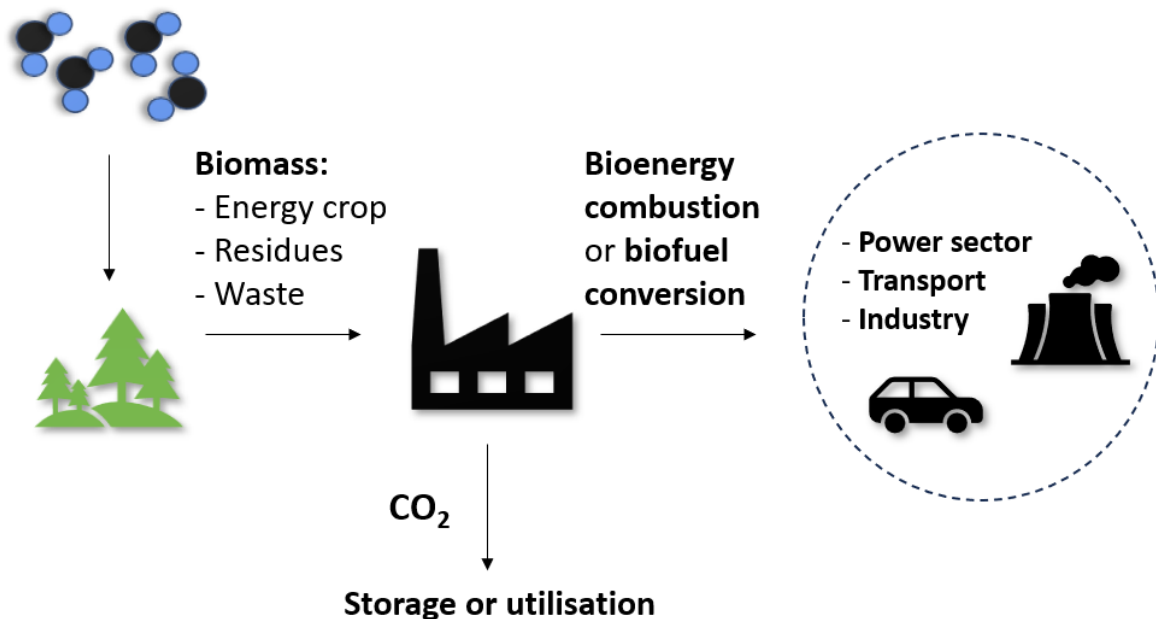


Figure 8 BECCS schematic draw

It should be remembered that typically, within a range from 50% to 70%, the carbon contained in municipal solid waste is of biological origin [28]. The organic part of MSW is a source of bioenergy with carbon capture and storage (BECCS). As shown in [29], for each kg of wet MSW incinerated, around  $-0.7$  kg of  $\text{CO}_{2,\text{eq}}$  was formed, which is very promising from the environmental impact point of view. Despite this, the lack of sufficient economic support programs and policy instruments is a barrier to their large-scale deployment. Therefore, introducing renewable energy certificates or a negative emission refunding system by the EU would significantly influence the economic viability of these technologies.

### 1.2.1 Carbon capture techniques

In  $\text{CO}_2$  capture, three main technologies are used: pre-combustion, post-combustion and oxy-fuel combustion. Pre-combustion includes the gasification of fuel in air or oxygen (and steam) to produce synthesis gas, which is a mixture of carbon monoxide (CO) and hydrogen ( $\text{H}_2$ ), also known as syngas. Then, the produced syngas is cooled down, cleaned up from contamination, and subjected to the water-gas shift reaction (WGSR), according to Eq. (1), to increase the content of  $\text{CO}_2$  along with the production of  $\text{H}_2$  as a carbon-free fuel, which only generates  $\text{H}_2\text{O}$  when combusted. Finally,  $\text{CO}_2$  is separated through various physical and chemical absorption processes for either storage or utilization [30].



The post-combustion technique involves combusting fuel under air conditions and then capturing and separating  $\text{CO}_2$  from the flue gas in an absorber that contains the solvent. Later, the scrubbed gas is washed with water, and the  $\text{CO}_2$  is regenerated. Typically, the captured  $\text{CO}_2$  is compressed into supercritical fluid and transported for storage in geological formations or saline aquifers. Currently, post-combustion technology is the most mature and widely used technique since it does not require many modifications to the combustion system [31]. Post-combustion is cheaper, however less effective compared to pre-combustion technology due to the dilution of  $\text{CO}_2$  in the flue gas by  $\text{N}_2$  from air that reduces the partial pressure of  $\text{CO}_2$  and increases the energy required for the process [32].

Oxy-fuel combustion consists of the replacement of air as an oxidant with high-purity oxygen, usually above 95 vol%, and recirculated flue gas to control the flame temperature to within the allowable limits of the boiler materials. Consequently, the produced flue gas stream mostly contains carbon dioxide and water vapour that can be easily removed by condensation [33]. Switching the atmosphere from diatomic nitrogen to three-atomic gases like CO<sub>2</sub> and water vastly affects the combustion chemistry and radiative heat transfer in the boiler, and thus, oxy-fuel combustion requires a larger change in plant configuration when compared to post-combustion [34]. Many studies indicate that oxy-fuel combustion should be the most energy-efficient, cost-effective as well as ecological of the available carbon capture technologies. This conclusion is based on assumptions of higher boiler efficiency caused by a smaller flue gas volume and the reduced necessity for flue gas cleaning, including the resulting decrease in capital costs (CAPEX) and operational costs (OPEX) [35], [36].

## Chapter 2

# Objectives of this study

As shown in the previous chapter, excessive waste generation and global warming are the key issues that need to be addressed. The answer to these challenges seems to be the development of waste utilization technologies with heat recovery integrated with CO<sub>2</sub> capture. In this thesis, the status of the waste-to-energy industry coupled with carbon capture with the main emphasis on oxy-fuel combustion of waste, which was identified as the least recognized and most promising technology, was first presented. Then, the objectives were formulated, namely development of the oxy-waste combustion model that could be used for real-time optimization.

The work contains both experimental research and mathematical modelling to deepen the fundamental knowledge about the technology, provide a better understanding of the organisation of the process in a real incineration plant to make it feasible and effective and verify the following research hypotheses:

- 1) It is possible to represent the processes occurring in the grate furnace with a simple model that can be used to optimize the operation of the furnace
- 2) The presence of CO<sub>2</sub> can improve the conversion of heavy hydrocarbons by enhanced cracking, and thus promoting CO, H<sub>2</sub> and CO<sub>2</sub> production.
- 3) By using diluted O<sub>2</sub> by the CO<sub>2</sub>, it is possible to decrease the temperature of the char bed (below the ash melting point), while achieving a high temperature above the bed, where less diluted O<sub>2</sub> is introduced.

The following research activities were formulated to reach the objectives of this thesis:

- comprehensive review of the waste-to-energy technologies integrated with carbon capture to establish the status of the knowledge, opportunities, and challenges of this technique in terms of technical, environmental, and socio-political feasibility

- identification of processes occurring during the oxy-fuel combustion of waste, formulation of mathematical model assumptions and equations.
- preparation of experimental procedures on thermogravimetric instrument and conducting a series of experimental analyses to obtain the TG and DTG curves under different conditions
- determination of kinetic parameters of individual steps (pyrolysis, char burnout) of various feedstocks' thermal decomposition in different conditions
- investigation of the impact of the atmosphere on the thermal degradation of waste materials using lab-scale equipment
- development of the mathematical model of combustion of waste under air atmosphere and its validation with full-scale data
- modification of the mathematical model into combustion of waste under oxy-fired conditions and the evaluation of the effect of different oxidant distribution routes

## 2.1 Scope of the thesis

The doctoral thesis consists of 6 following chapters.

**Chapter 1** provides the significance of the research and the general background and motivation of this study.

**Chapter 2** is this chapter.

**Chapter 3** presents an overall concept of waste-to-energy technology integrated with carbon capture. The state-of-the-art of this negative CO<sub>2</sub> emission technology along with the crucial opportunities and challenges of this technique in terms of technical, environmental, and socio-political feasibility.

**Chapter 4** is devoted to the thermogravimetric and kinetic analysis of the thermal degradation of waste materials under various conditions, namely different atmospheres and heating rates are examined to obtain kinetic data of the thermal decomposition of waste materials.

**Chapter 5** shows the experimental campaign using a lab-scale test rig performed to analyse the gas evolution profiles during the thermal degradation under different conditions and prepare waste-derived chars for kinetic analysis.

**Chapter 6** is focused on explaining model development, including model assumptions and equations, and a summary of the most important results of simulations. This chapter verifies the third hypothesis regarding the possibility of lowering the bed temperature using recycled flue gases while achieving a high temperature above the bed.

**Chapter 7** presents a summary and conclusions of this work.

Chapters 3 to 6 highlight the most significant aspects of Articles I to IV, which are included in the appendix section.



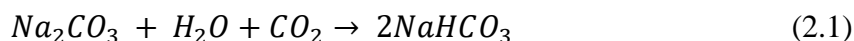
# Chapter 3

## Waste incineration integrated with carbon capture – paper I

Coupling waste-to-energy plants with carbon capture is a novel idea that has sparked great interest among scientists, however, only a few studies have been published to date [37]. In the first paper, the state-of-the-art of this technology was presented, along with the crucial opportunities and challenges of this technique in terms of technical, environmental, and socio-political feasibility.

### 3.1 Waste-to-energy with CCUS facilities

Currently, four MSW incineration plants integrated with CO<sub>2</sub> capture worldwide are planned or in operation; but they employ the post-combustion capture method, which consists of absorption using, for example, sodium bicarbonate solvent according to Eq. (2) [27]. They can be found in Norway (Klemetsrud CHP), Japan (Saga City), and the Netherlands (Twence and AVR plants). AVR Plant, Twence, and Saga City are examples of CCU facilities.



In Japan, an alkaline aqueous amine method of CO<sub>2</sub> capture was introduced and designed by Toshiba, capturing 10 tonnes of carbon dioxide every day. The obtained carbon dioxide is used in the agriculture sector for local crop cultivation and algae culture formation.

The Dutch AVR plant is the first waste-to-energy company with a large-scale CO<sub>2</sub> capture system. As of 2019, 60 000 tons of carbon dioxide per year were captured, liquefied, and transported to end users, which were the greenhouse horticulture industry. [83]. While, at the

Twence waste incineration plant, 830 000 tonnes of waste are processed annually, producing 405 000 MWh of electricity and 1.5 million GJ of thermal energy for district heating.

A waste incineration plant in Oslo (Klemetsrud) processes around 400,000 tonnes of non-recyclable waste. As a result, 55 MW of heat and 10.5 MW of electricity is produced for city residents. The carbon capture method that will be implemented in the plant is based on amine absorption and it will reduce the carbon dioxide emission by 400 000 tonnes every year from 2025. The plant in Klemetsrud will be an example of a CCS facility, therefore it is foreseen that carbon dioxide will be permanently stored in the North Sea.

### **3.1.1 Novel concept of oxy-WtE**

The above examples have shown that carbon capture can be successfully implemented in a MSW incineration plant resulting in zero (or even negative) CO<sub>2</sub> emission power generation. However, the separation of CO<sub>2</sub> after air combustion is problematic and reduces efficiency by 14.7%. Studies showed that oxy-fuel combustion reduces the efficiency of the incineration plant by 12.6% [35]. Moreover, after the oxy-fuel incinerator optimisation, the efficiency drop can reach 9.57% [38]. Key parameters, which could improve the oxy-fuel combustion process are the recirculation of flue gas, which can be used to heat the molecular sieve regeneration gas of ASU and the primary condensate as well as the waste heat generated by ASU compressors, which also can be utilized to heat the primary condensate.

Although oxy-fuel combustion is a known technology, up to now, it has been mostly investigated and employed for fossil fuels [33], [39], [40]. Nevertheless, to the best knowledge of the author, currently, there are no commercial oxy-fuel power plants or other facilities.

Oxy-MSW combustion (Fig. 9) is promising technology since, except carbon capture, it can bring several advantages, such as an increase in process temperature due to higher oxygen concentration and the decrease of the auxiliary fossil fuel consumption that is usually used to keep the required temperature and thus causes inevitable emissions of CO<sub>2</sub>.

Since the atmosphere affects the combustion chemistry, obtaining experimental data on thermal behaviour and retrieving kinetic parameters that can be used during the mathematical modelling of an oxy-fired combustion chamber is important. Therefore, the first step of the development of

such systems should be the analysis of the thermal decomposition of various waste feedstocks, separately and as fuel mixture, under different conditions using thermogravimetric analysis (TGA), which is often coupled with Fourier-transform infrared spectroscopy (FTIR), gas chromatography (GC) or mass spectrometry (MS) to identify gaseous products that are released during the process.

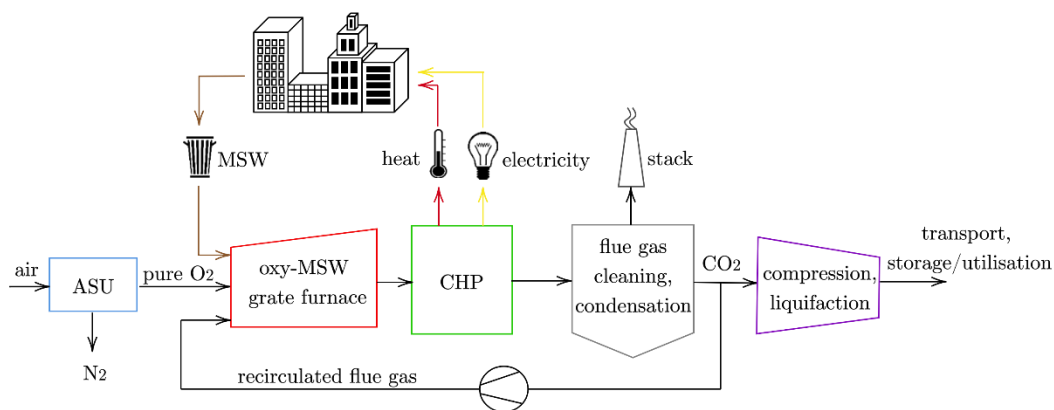


Figure 9 Schematic diagram of the oxy-fuel incineration plant

Most studies on oxy-MSW combustion available in the literature compared the thermal degradation of MSW individual compounds and their blends using thermogravimetric analyses under N<sub>2</sub> and CO<sub>2</sub> atmospheres [41]–[43]. The results indicated that the direct replacement of nitrogen by carbon dioxide affects weight loss rates and the reactions occurring above 600 °C, while at lower temperatures CO<sub>2</sub> acts as an inert atmosphere. Moreover, it was shown that atmosphere affects the composition and amount of the obtained gaseous products. The authors also noticed that blends of materials can hinder the burnout and char-CO<sub>2</sub> reaction.

The combustion behaviour in N<sub>2</sub>/O<sub>2</sub> and CO<sub>2</sub>/O<sub>2</sub> was investigated for the mixed wastes only [44]–[47]. The authors claimed that the 30% oxygen content in the CO<sub>2</sub>/O<sub>2</sub> atmosphere achieved a similar combustion performance as air, and thus oxyfuel combustion technique needs knowledge from oxygen-enriched combustion technology. Besides, some researchers investigated emissions of pollutants [48], [49] and heavy metals migration under N<sub>2</sub>/O<sub>2</sub> and CO<sub>2</sub>/O<sub>2</sub> [50], [51]. Nevertheless, currently, there is a lack of reliable kinetic data of MSW

decomposition under  $\text{CO}_2$  and  $\text{O}_2/\text{CO}_2$ , which would express the quantitative differences between the atmospheres and could be used for oxy-MSW combustion process modelling.

The first tests on a lab-scale reactor dedicated to oxy-MSW combustion were described in Ref. [28]. This study showed that the model MSW can be successfully incinerated under various oxy-fuel conditions, provided that the oxygen concentration in the oxidiser is carefully adjusted.

### **3.2 Conclusions for the next steps**

As can be observed, the research to date has been focused on understanding the thermal behaviour of MSW, while the kinetic analysis has not been carried out exhaustively. Therefore, the next step of the research is to develop a mathematical model of the oxy-MSW combustion as well as determine a reliable set of kinetic parameters of decomposition for typical MSW components under  $\text{CO}_2$  and  $\text{O}_2/\text{CO}_2$  that could be applied in the mathematical model.

# Chapter 4

## Thermogravimetric and kinetic analysis of the waste material under different atmospheres – II paper

The next paper aimed to deepen the fundamental knowledge of the effect of the atmosphere on the selected waste thermal degradation. The thermogravimetric technique was used for analysis and N<sub>2</sub>, CO<sub>2</sub> and O<sub>2</sub>/CO<sub>2</sub> atmospheres were tested. Few types of municipal solid waste (MSW), such as textiles (Tex), spent coffee grounds (SCG), and PVC were examined. The further goal of this research was to determine the global kinetic parameters, such as energy activation (E<sub>a</sub>) and pre-exponential factor (A) of pyrolysis process various atmospheres using different approaches.

### 4.1 Kinetic theory

The rate of the chemical process is generally expressed as follows:

$$\frac{d\alpha}{dt} = k(T)f(\alpha) \quad (3.1)$$

where  $t$  - time, s;  $T$  - temperature, K;  $\alpha$  - conversion rate, dimensionless;  $f(\alpha)$  - reaction model; and  $k(T)$  - rate constant that is represented by the Arrhenius equation:

$$k(T) = A \exp\left(\frac{-E}{RT}\right) \quad (3.2)$$

where  $A$  - the pre-exponential (frequency) factor, s<sup>-1</sup>;  $E$  - the activation energy, J/mol;  $R$  - the gas constant, J(molK)<sup>-1</sup>

$$\alpha(T) = \frac{m_0 - m_{(T)}}{m_0 - m_f} \quad (3.3)$$

where  $m_0$  – initial mass, mg;  $m_{(T)}$  – mass at given temperature, mg;  $m_f$  – final mass, mg.

Thermal degradation of waste is highly complex due to its heterogeneity and high moisture content; thus, fast and accurate kinetic calculations are required. Thanks to recent advancements in the study of kinetics, isoconversional methods have demonstrated its ability to provide precise activation energy values for biomass, including pre-exponential factor and reaction models. With that information, it is plausible to model biofuel decomposition without reaction model pre-assumption, providing physically unbiased calculation results, giving  $n$  sets of isoconversional kinetic triplets for  $n$  conversion discretized points, and forming modelled conversion profiles [52].

In this thesis, different methods: a) differential, i.e., Friedman, and b) integral, like Vyazovkin, Ozawa-Flynn-Wall and Kissinger-Akahira-Sunose. were used and compared. According to the isoconversional principle, the process rate at a constant extent of conversion  $\alpha$  is a function of temperature [53]. For the  $\alpha = const$ , the following assumptions can be derived from Eq. (3.4) taking the first logarithmic derivative:

$$\left[ \frac{\partial \ln (d\alpha/dt)}{\partial T^{-1}} \right]_{\alpha} = \left[ \frac{\partial \ln k (T)}{\partial T^{-1}} \right]_{\alpha} + \left[ \frac{\partial \ln f (\alpha)}{\partial T^{-1}} \right]_{\alpha} \quad (3.4)$$

Because at  $\alpha = const$ ,  $f(\alpha)$  is also constant, and the second term in the right-hand side of Eq. (3.5) is zero, thus:

$$\left[ \frac{\partial \ln (d\alpha/dt)}{\partial T^{-1}} \right]_{\alpha} = \frac{-E_{\alpha}}{R} \quad (3.5)$$

A detailed presentation and explanation of isoconversional methods is provided in the Appendix section.

## 4.2 Methodology

### 4.2.1 Experimental procedure

The experimental procedure was developed on the basis of preliminary research. The tests were carried out at standard atmospheric pressure using a TGA/DSC analyser (Netzsch STA 409 PC Luxx) with a sensitivity of 0.001 mg. The initial weight of the samples was  $5 \pm 0.1$  mg. Sample mass loss profiles were determined based on dynamic heating runs, in the temperature range from 100 to 1000 °C at heating rates ( $\beta$ ) of 5, 10 and 15 K/min.

To evaluate the effect of the atmosphere on the process, three different conditions were employed: (a) inert 100 vol% N<sub>2</sub>, (b) gasifying 70/30 vol% CO<sub>2</sub>/N<sub>2</sub> and (c) oxidising with 63/7/30 vol% CO<sub>2</sub>/O<sub>2</sub>/N<sub>2</sub>.

### **4.2.2 Materials**

Textiles (Tex), used coffee grounds (SCG) and polyvinyl chloride (PVC) were selected for research due to their high prevalence in waste and difficulty in disposal [54], [55].

The proximate, ultimate as well as ash and chemical composition analyses were performed to obtain detailed characterisation of the used materials. The results of the analyses of the feedstock are presented in II and III paper (Appendix section). The analyses were outsourced to an accredited laboratory, where all parameters were determined using accredited methods. The results of proximate analysis for PVC and textiles were similar, since both materials are polymers, even though the textile is a natural polymer and PVC is synthetic [9]. The SCG, being an organic material, is rich in hemicellulose, cellulose, lignin, fat, and protein [56].

## **4.3 Thermogravimetric analysis results**

As the result of the experimental campaign, the mass loss (TGA) and the mass loss rate (DTG) profiles of each studied waste materials, namely for textile, spent coffee grounds and PVC samples, under inert, gasifying, and oxidising atmospheres at studied heating rates were collected and analysed (Figs. 10-12).

The results of TGA curves indicated that Tex sample mostly contains cellulose since the reaction appeared in one step between 230 and 400 °C. SCG sample's thermal degradation started at 190.3 °C and finished at 560.2 °C with a relatively high amount of solid residue, meaning that

cellulose, hemicellulose and lignin occur in the material. Shifting atmosphere from inert to gasifying does not affect the thermal decomposition of samples below 600 °C [43], [57], [58].

Different specific heat capacities and diffusion rates of nitrogen and carbon dioxide reduce the rate of mass loss of peaks corresponding to the release of volatile matters [42]. In the gasifying atmosphere, the second peak appeared above 600 °C during the decomposition of lignocellulosic materials that was attributed to CO<sub>2</sub>-char reactions, for example, the Boudouard reaction [59]. In the O<sub>2</sub>/CO<sub>2</sub> atmosphere, the presence of oxygen accelerated thermal decomposition and, consequently, the pyrolysis and char oxidation processes occurred almost simultaneously.

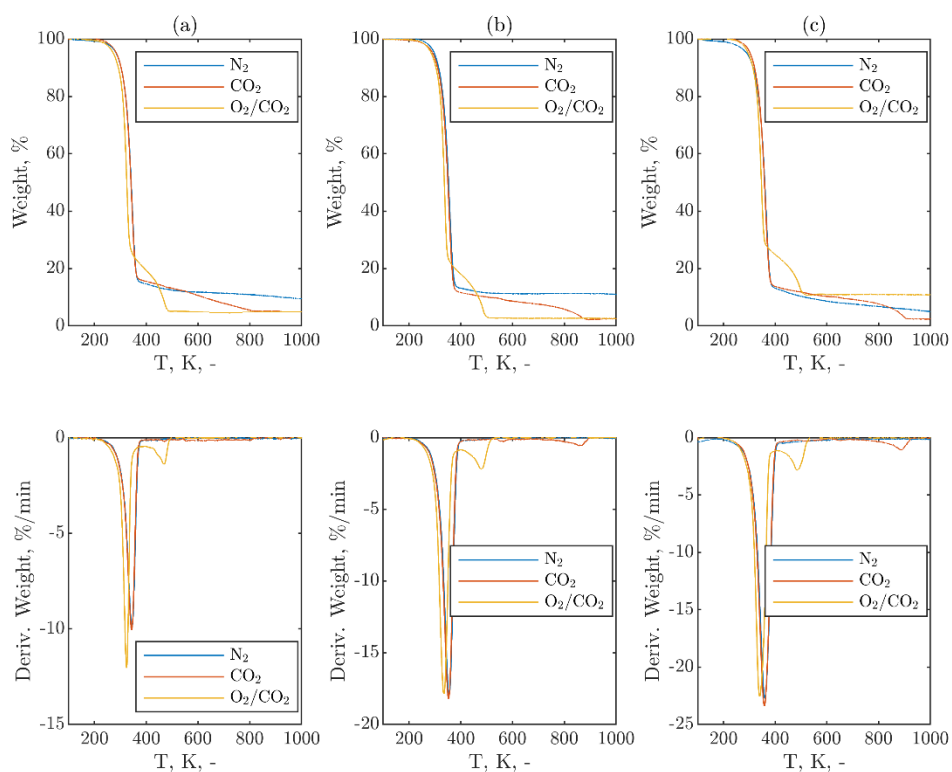


Figure 10 TGA and DTG curves of Tex sample under N<sub>2</sub>, CO<sub>2</sub> and O<sub>2</sub>/CO<sub>2</sub> atmospheres at a) 5, b) 10 and c) 15 Kmin<sup>-1</sup>

In the case of the PVC sample, decomposition involved a two-step reaction when carrier gas was N<sub>2</sub> and CO<sub>2</sub>. In oxidising atmosphere, degradation consists of three-step reaction. The first step is prescribed for dehydrochlorination and polyene chain formation (between 220 and 380 °C). The second step is linked to the degradation of polyene chains between 380 and 530 °C [60], the formation of alkyl aromatics with remaining char, including condensation and dehydrogenation



reactions with deep dealkylation, isomerization, chain scission, crosslinking, and aromatization [61].

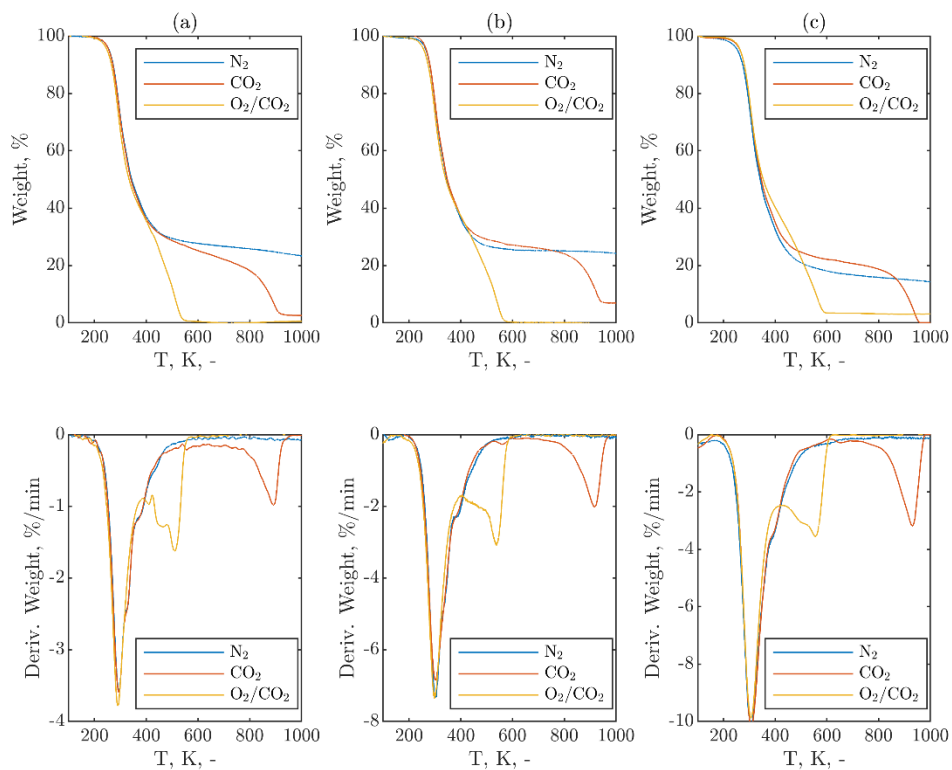


Figure 11 TGA and DTG curves of SCG under  $N_2$ ,  $CO_2$  and  $O_2/CO_2$  atmospheres at a) 5, b) 10 and c) 15  $Kmin^{-1}$

In general, with increasing heating rate, the DTG peaks shifted toward a higher temperature range without a significant change in their shape. The maximum values of DTG peaks were generally greater for higher heating rates, which was also noticed by other researchers. It demonstrated that the process is delayed with the raised heating rate. It can be caused by the fact that the heat transfer of the sample particles is decreased at the high heating rate, which is not favourable to the degradation of the feedstock [62].

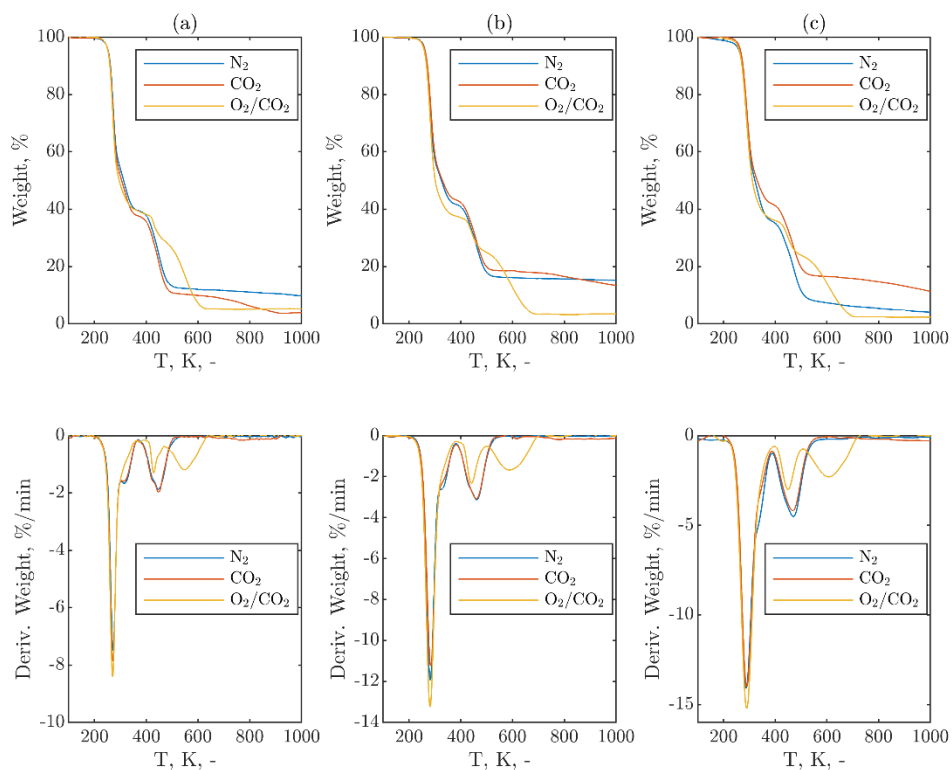


Figure 12 TGA and DTG curves of PVC under  $N_2$ ,  $CO_2$  and  $O_2/CO_2$  atmospheres at a) 5, b) 10 and c) 15  $Kmin^{-1}$

#### 4.4 The kinetic data results

The main results of kinetic analysis are summarised in Table 1. As can be observed, the Friedman differential method and Vyazovkin method yielded almost identical average values of  $E\alpha$ , which were slightly lower than those from the other integral methods. The average  $E\alpha$  values calculated by the KAS method were very similar as those calculated by the OFW method.

In the case of the spent coffee sample, the average value of  $E\alpha$  was generally greater than for textiles, meaning that SCG decomposition was more energy-intensive, most likely due to its more complex composition.

Under oxidising conditions, the average values of  $E\alpha$  is the smallest, which can be ascribed to the presence of highly reactive oxygen which facilitated decomposition.

Table 1 Kinetic data of pyrolysis process under different conditions

Atmosphere	Sample	Parameter	Friedman	OFW	KAS	Vyazovkin
inert	SCG	Ea, kJ/mol	232.1	242.1	241.9	233.4
		A, log(1/s)	17.7	19.1	19.1	17.8
		R <sup>2</sup>	0.99959	0.98783	0.98759	0.99956
	Tex	Ea, kJ/mol	179.4	198.8	198.7	190.5
		A, log(1/s)	12.9	14.6	14.6	13.8
		R <sup>2</sup>	0.99991	1.00000	1.00000	0.99986
	PVC (first peak)	Ea, kJ/mol	153.0	189.8	189.7	166.7
		A, log(1/s)	11.9	15.5	15.6	13.2
		R <sup>2</sup>	0.99974	0.99009	0.98340	0.99932
	PVC (second peak)	Ea, kJ/mol	216.4	248.0	247.9	216.9
		A, log(1/s)	13.2	15.6	15.7	13.3
		R <sup>2</sup>	0.99732	0.99073	0.98827	0.99997
gasifying	SCG	Ea, kJ/mol	274.7	266.7	266.6	274.6
		A, log(1/s)	21.3	21.2	21.2	21.3
		R <sup>2</sup>	0.99991	0.99085	0.98897	0.99984
	Tex	Ea, kJ/mol	188.9	189.0	188.9	188.8

		A, log(1/s)	13.7	13.7	13.8	13.7	
		R <sup>2</sup>	0.99976	0.99917	0.99817	0.99978	
	PVC (first peak)	Ea, kJ/mol	171.9	175.3	175.2	171.0	
		A, log(1/s)	13.6	14.0	14.1	13.5	
		R <sup>2</sup>	0.97352	0.97106	0.99340	0.99951	
	PVC (second peak)	Ea, kJ/mol	216.5	261.1	261.0	217.2	
		A, log(1/s)	13.3	16.7	16.7	13.3	
		R <sup>2</sup>	0.99732	1.00000	1.00000	0.55475	
	oxidising	SCG	Ea, kJ/mol	192.0	190.1	190.0	191.0
			A, log(1/s)	14.8	14.9	15.0	14.7
			R <sup>2</sup>	0.99998	0.98712	0.98708	0.99996
		Tex	Ea, kJ/mol	158.8	152.8	152.6	157.5
A, log(1/s)			11.6	10.9	10.9	11.5	
R <sup>2</sup>			0.99989	0.98847	0.99064	0.99985	
PVC (first peak)		Ea, kJ/mol	131.2	153.1	153.0	130.9	
		A, log(1/s)	10.0	12.1	12.1	9.9	
		R <sup>2</sup>	0.99982	0.99631	0.99753	0.99976	
PVC		Ea, kJ/mol	207.1	253.3	253.1	206.7	

	(second peak)	A, log(1/s)	12.9	16.3	16.3	12.9
		R <sup>2</sup>	0.99823	0.99014	0.99023	0.99809

These sets of kinetic data calculated using different isoconversional methods in the presented investigation will be directly used in the modelling of oxy-MSW incineration systems. This study also confirmed that the model-free methods can be successfully applied to different types of waste materials.

# Chapter 5

## Experimental investigation of waste decomposition in various conditions – III paper

In the next step of the work, a laboratory-scale reactor was used to compare the thermal behaviour of TEX and SCG under different conditions and evaluate if the presence of gasifying agent elevates the conversion of hydrocarbons by enhanced cracking and secondary reactions. Moreover, waste-derived chars were produced and subjected to thermogravimetric analysis to retrieve the kinetic data of char burnout under oxy-fired conditions.

### 5.1 Experimental rig and the procedure

The main part of the test rig is a tubular reactor located inside an electrical furnace (Fig. 13). Gases of defined composition were introduced into the upper part of the quartz tube reactor. Three different atmospheres were used: (a) inert 100 vol.% N<sub>2</sub>, (b) gasifying 100 vol.% CO<sub>2</sub> and (c) oxidising with 90/10 vol.% CO<sub>2</sub>/O<sub>2</sub>, with a total flow of 400 ml/min to assess the gas evolution profiles during different processes, such as pyrolysis, gasification and oxy-combustion.

The temperature of the process varied from ambient temperature to 800 °C, in the case of an inert atmosphere, and to 1100 °C in the gasifying and oxidising atmospheres, with a heating rate of 15 K/min. After the process, samples were kept in the reactor for a 30 min isotherm at the final temperature for the given atmosphere. Gas samples were taken at 90 s intervals and analysed post-run with GC-TCD. Each test was repeated to assess the reproducibility of the experimental results. The temperature of the sample was registered with a thermocouple inserted into the reactor and the mean value was reported for each sampling interval.

The detailed research methodology is presented in the Appendix (Paper III).

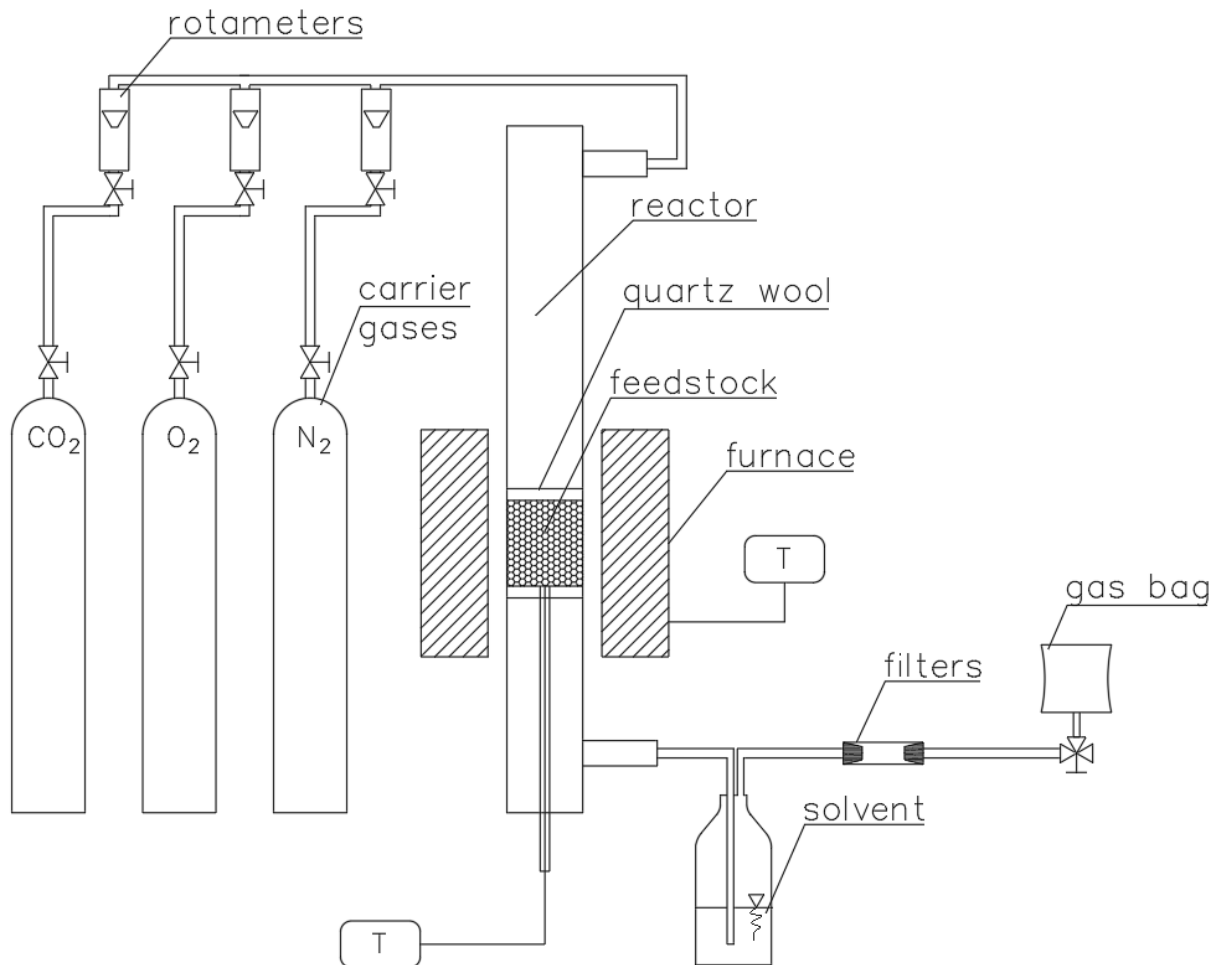


Figure 13 Custom-built test stand for waste thermal degradation

## 5.2 Results and discussion

This part presents and discusses the most important findings published in Paper III, namely gas evolution profiles during the thermal degradation of textiles and ground coffee under inert, gasifying and oxidising atmosphere. In addition, the chemical kinetic constants of char burning in an  $O_2/CO_2$  atmosphere were tabulated since they were used in the oxy-combustion model.

### 5.2.1 Gas evolution

Comparing the inert atmosphere and the gasifying atmosphere, similar findings can be noticed as before, namely below 600 °C there are no significant differences in gaseous products. In both

atmospheres, the maximum peak of CO is around 0.15 mmol/min and appears at 380 °C for Tex and 0.50 mmol/min at 350 °C for SCG, while the CH<sub>4</sub> peak height is of 0.03 mmol/min and occurs at 550 °C for Tex, and 0.19 mmol/min at 560 °C for SCG. However, in the gasifying atmosphere, the second peak of CO can be distinguished above 700 °C with a height of 2.5 mmol/min (Tex) and 5.8 mmol/min (SCG), which results from the secondary reactions, such as Boudouard reaction of char with CO<sub>2</sub>.

In the oxidising atmosphere, most gases are released at the temperature range of 300 to 550 °C, because of the occurrence of reactive oxygen. The peaks of CH<sub>4</sub> and CO correspond with the highest oxygen uptake. In this atmosphere, the formation of CH<sub>4</sub> occurs at the same temperature as the initial CO and CO<sub>2</sub> release. These results suggest the differences in the devolatilization of the samples in the presence of oxygen. In the inert conditions, methane and hydrogen are produced at higher temperature (above 500 °C) due to the secondary reactions of tars adsorbed on the char (demethylation and dehydrogenation), whereas, when oxygen is supplied, tars undergo homogenous reactions with O<sub>2</sub> immediately after their release from the sample, i.e. at the temperatures around 300 °C. Tar decomposition in the gas phase results in the loss of functional groups, releasing CH<sub>4</sub>, and the ring opening reactions, which yields CO and CO<sub>2</sub>, significantly increasing the molar flows of these compounds. Hydrogen was not detected in the oxidation tests of both materials as it was instantaneously combusted to H<sub>2</sub>O.

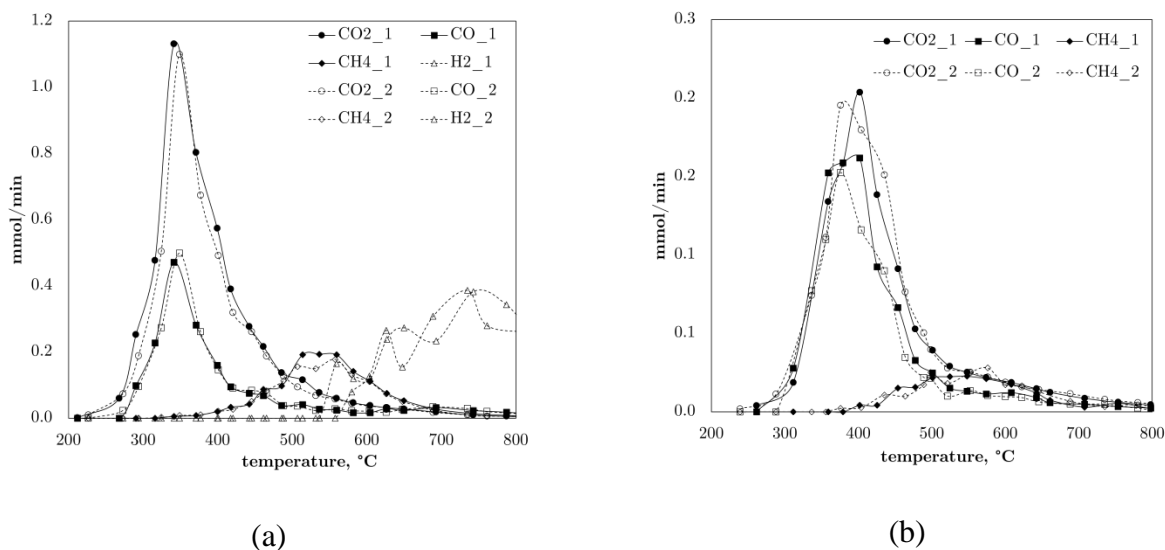


Figure 14 Gas evolution during the thermal degradation of a) SCG and b) textiles under N<sub>2</sub> atmosphere



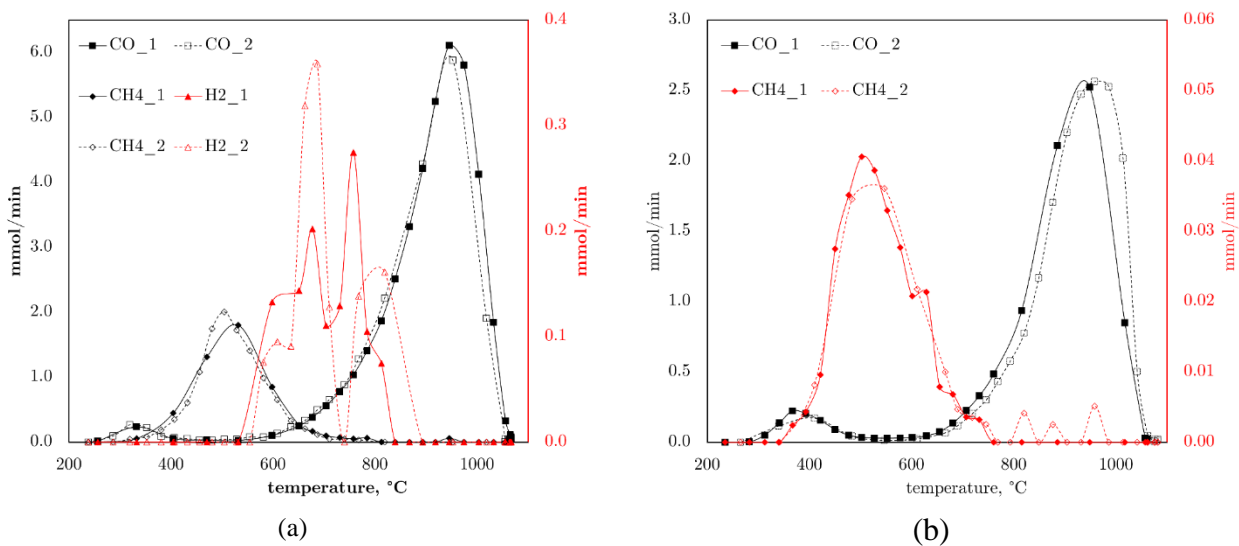


Figure 15 Gas evolution during the thermal degradation of a) SCG and b) textiles under CO<sub>2</sub> atmosphere

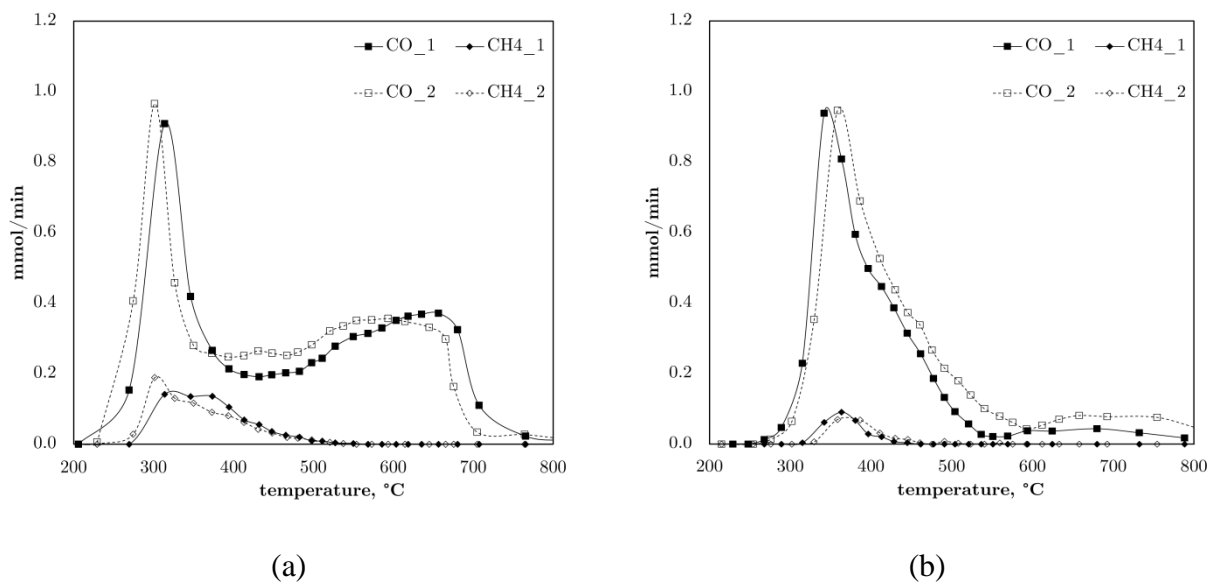


Figure 16 Gas evolution during the thermal degradation of a) SCG and b) textiles under O<sub>2</sub>/CO<sub>2</sub> atmosphere

## 5.2.2 Kinetic analysis of waste-derived chars

Tables 2-3 list the average  $E_a$  and  $\log(A)$  values for the thermal degradation of chars originating from SCG and TEX in an O<sub>2</sub>/CO<sub>2</sub> atmosphere.

The results showed that with the increasing the heating rate, higher  $E_a$  can be observed. It can be explained by the fact that slow pyrolysis developed significantly greater porosity compared to the fast devolatilization process.

Based on kinetic analysis, it was observed that in the case of SCG sample, higher heating itself did not have a strong influence on the activation energy of the char; it was slightly decreased by around 3 kJ/mol. However, char produced by using muffle furnace resulted in more reactive sample. It can be caused by the entry of oxygen into the furnace during the pyrolysis process, and thus more developed porosity and reactivity.

The necessary data were obtained from the conducted experimental campaign to develop a model for oxy-waste combustion. This study also showed that occurrence of  $\text{CO}_2$  promotes secondary pyrolysis reaction, thus verifies the second hypothesis.

Table 2 Kinetic parameters of oxy-combustion of SCG derived chars

Sample	SCG_slow		SCG_fast		SCG_muffle	
	Friedman	Vyazovkin	Friedman	Vyazovkin	Friedman	Vyazovkin
Average value of energy activation, kJ/mol	73.5	72.8	69.5	70.6	51.9	52.0
Average value of pre-exponential factor, Log(1/s)	2.162	2.104	2.057	2.144	1.130	1.173

Table 3 Kinetic parameters of oxy-combustion of Tex derived chars

<b>Sample</b>	<b>TEX_slow</b>		<b>TEX_fast</b>	
<b>Method</b>	<b>Friedman</b>	<b>Vyazovkin</b>	<b>Friedman</b>	<b>Vyazovkin</b>
Average value of energy activation, kJ/mol	80.2	80.1	116.1	116.4
Average value of pre-exponential factor, Log(1/s)	2.905	2.908	5.308	5.333

# Chapter 6

## Mathematical modelling of the oxy-waste incineration – IV paper

In the last of a cycle which PhD thesis is composed of, a mathematical model of waste combustion for a full-scale moving grate MSWI plant under air- and oxy-fired conditions is demonstrated and validated. The model is developed using MATLAB Software. First, the combustion model under air-fired mode is developed and validated by comparison with full-scale plant data. The validated model is then modified for an oxy-fired system and used to study the effects of the atmosphere and oxidant distribution on the process.

### 6.1 Model development

#### 6.1.1 Model overview

The scheme of the considered MSW grate furnace is shown in Figure 17. It is divided into three separate areas: (a) grate, (b) intermediate zone, and (c) freeboard. During the process, fresh MSW is fed into the furnace, where in the first stage is heated by surrounding gases by radiative heat transfer. Then, the waste reacts with oxidiser, which is supplied to the furnace, mainly generating CO and CO<sub>2</sub>.

When furnace is air combustion mode, the primary and secondary air is considered to be humid air. Temperature and relative humidity determine the absolute water content of air. For oxy-combustion mode, the oxidant is oxygen from the ASU and recycled exhaust gases.

The intermediate zone was defined as the immediate area above the grate where the released gases and volatile substances are partially combusted with the remaining oxidant.

In the freeboard, oxidiser is supplied again to ensure the complete combustion of combustible gases. The produced flue gas contains mainly  $\text{CO}_2$ ,  $\text{H}_2\text{O}$ , and excess  $\text{O}_2$ .

It is assumed that the model is steady state. Grate and intermediate zones are treated as one dimensional. The freeboard is modelled as 0-d. Grate and intermediate zones are discretized in the direction of the moving grate as a series of control volumes. State variables within each control volume are homogeneous. Pyrolysis and char burnout zones that take place on the grate are taken into account based on one-step chemical kinetics. Combustion of volatiles and gases produced during char burnout zone that takes place over the grate is complete.

Physical data and process data of the full-scale incineration plant were provided by the Returkraft WtE plant in Kristiansand (Norway). A description of the waste incineration process at the studied plant is available in the article [63] and in Appendix (Paper IV).

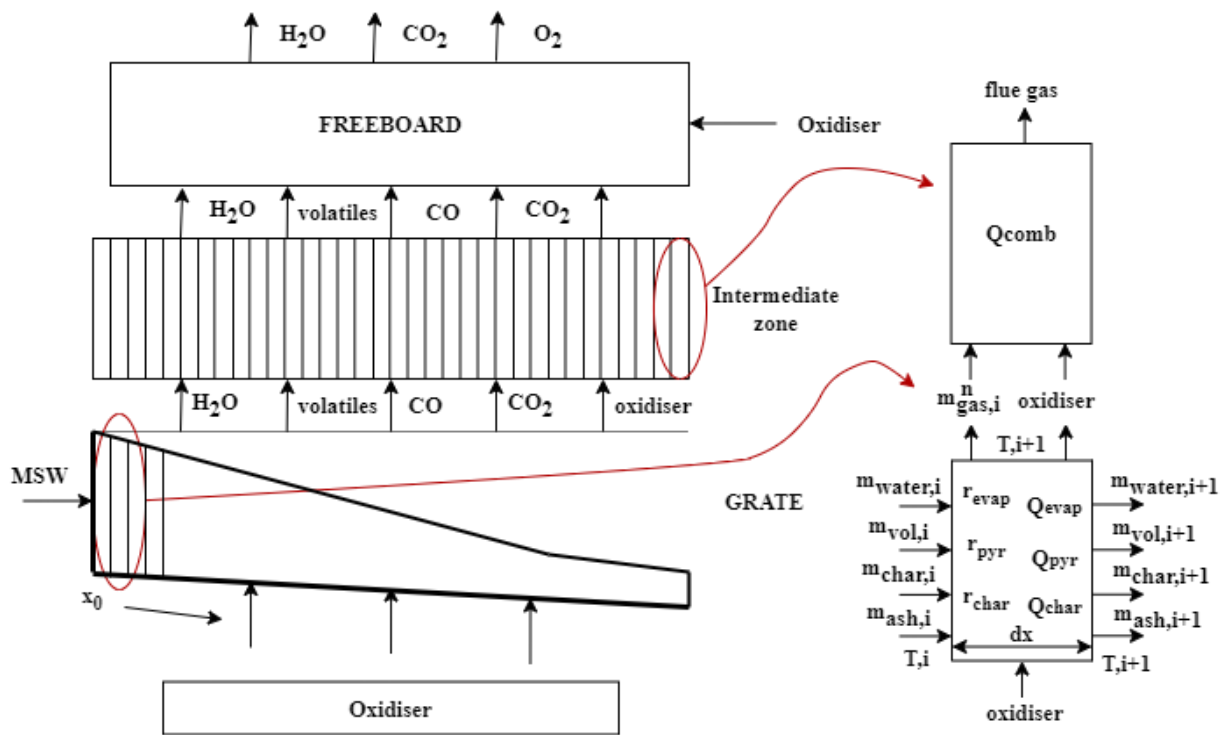


Figure 17 Model of MSW combustion chamber

## 6.1.2 Model equations

The mass balance equation in each control volume is formulated as follows:

$$\frac{d\dot{m}_i}{dx} = -k_i \cdot dt \cdot \dot{m}_i \quad (5.1)$$

where  $k_i$  is the rate of the  $i$ -th process (drying, pyrolysis, char burn-out), 1/s,  $dt$  is fuel residence time, s, described as:

$$dt = \frac{dx}{v} \quad (5.2)$$

where  $dx$  is the length of the control volume, m,  $v$  is grate velocity, m/s.

The energy balance for the municipal solid waste bed is modelled as:

$$\frac{\dot{m}_{tot,i} C_{tot,i} dT_i}{dx} = H_{bed,i} - H_{bed,i+1} + Q_{rad,i} + H_{ox,i}^{in,grate} - H_{ox,i}^{out,grate} + Q_{reac,i} - H_{gas,i}^{out,grate} \quad (5.3)$$

where  $Q_{rad,i}$  is heat of radiation between gases in the furnace and grate surface, kW/m;  $H_{ox,i}^{in,grate}$  and  $H_{ox,i}^{out,grate}$  are the enthalpy of the oxidant at the inlet and outlet of the  $i$ -th control volume, kW/m;  $Q_{reac,i}$  is the heat of the reactions (evaporation, pyrolysis, char oxidation) of the  $i$ -th control volume, kW/m;  $H_{bed,i-1}$  and  $H_{bed,i+1}$  are the physical enthalpy of the solid bed in the adjacent  $i$ -th control volume, kW/m;  $H_{gas,i}^{out}$  is the physical enthalpy of the gaseous phase escaping  $i$ -th control volume, kW/m,  $\dot{m}_{tot,i}$  is defined as:

$$\dot{m}_{tot,i} = \dot{m}_{water,i} + \dot{m}_{waste,i} + \dot{m}_{char,i} + \dot{m}_{ash,i} \quad (5.4)$$

Where  $\dot{m}_{water,i}$ ,  $\dot{m}_{waste,i}$ ,  $\dot{m}_{char,i}$  and  $\dot{m}_{ash,i}$  are the mass flow of the water, dry waste, char and ash in the solid bed, kg/(s·m).

In this work, it was assumed that the temperature at the outlet above the grate is equal to the temperature in the next control volume ( $i+1$ ).

Since high temperature occurs in the combustion chamber, this model assumes that radiation is the dominant heat transfer mechanism (Eq. 5.5).

$$Q_{rad,i} = \frac{\varepsilon_{bed} + 1}{2} A \sigma (\varepsilon_{gas} T_{gas}^4 - \sigma_{gas} T_{bed}^4) \quad (5.5)$$

The emissivity  $\varepsilon_{bed}$  depends on the material, temperature and surface condition. In simulations a constant emissivity of  $\varepsilon_{bed} = 0.8$  for waste bed was used, but various emissivity can be used for different fractions if data are available.  $T_{gas}$  is a temperature of the freeboard, K.  $T_{bed}$  is a temperature of the grate, K.

To calculate the radiative properties of the gases in the furnace ( $\varepsilon_{gas}$  and  $\alpha_{gas}$ ), the weighted sum of the gray gases model (WSGGM) is used, which was introduced by Hottel and Sarofim [64] and due to its simplicity and relatively high accuracy, it was further developed and used by many researchers [63], [65].

The energy balance of intermediate zone is calculated as follow:

$$\frac{\dot{m}_{gas,i} c_{gas,i} dT_i}{dx} = H_{ox,i}^{out,grate} + H_{gas,i}^{out,grate} + Q_{comb,i} - H_{gas,i}^{out,intermediate\ zone} \quad (5.6)$$

where  $Q_{comb,i}$  is heat of partial combustion of volatiles and combustible gases, kW/m;  $H_{gas,i}^{out,intermediate\ zone}$  is the physical enthalpy of the produced gas at the outlet of the i-th control volume, kW/m.

## 6.2 Results

In this section, the most important results of performed simulations are presented.

### 6.2.1 Air-fired mode

Figures 18a presents grate and intermediate zone temperature as well as mass flow of the fuel in the function of the grate length. As shown, firstly, the fuel heats up and dries, then when the grate reaches a temperature of 450 °C, volatile matters are released. Directly above the grate, in

the intermediate zone, the volatiles partially burn, releasing heat and causing the growth of the temperature. After the pyrolysis process, the waste char begins to slowly oxidize, and over a grate length of 8 m the fuel is burned out. In the last zone, the air mass flow is reduced and only ash remains. Similar findings regarding weight loss on the grate, burnout and grate temperatures have been found in the literature [21], [63], [66]–[68]. As can be seen in Fig. 18b, oxygen is consumed during most of the process on the grate, which means that the air is distributed correctly. After the complete combustion of the fuel, the intermediate zone is filled only with air. Results indicate that during the char oxidation  $\text{CO}_2$  generation is more intensive. The produced carbon monoxide will be further combusted in the intermediate zone over the grate generating heat. In the Appendix (Paper IV) model validation is presented in detail.

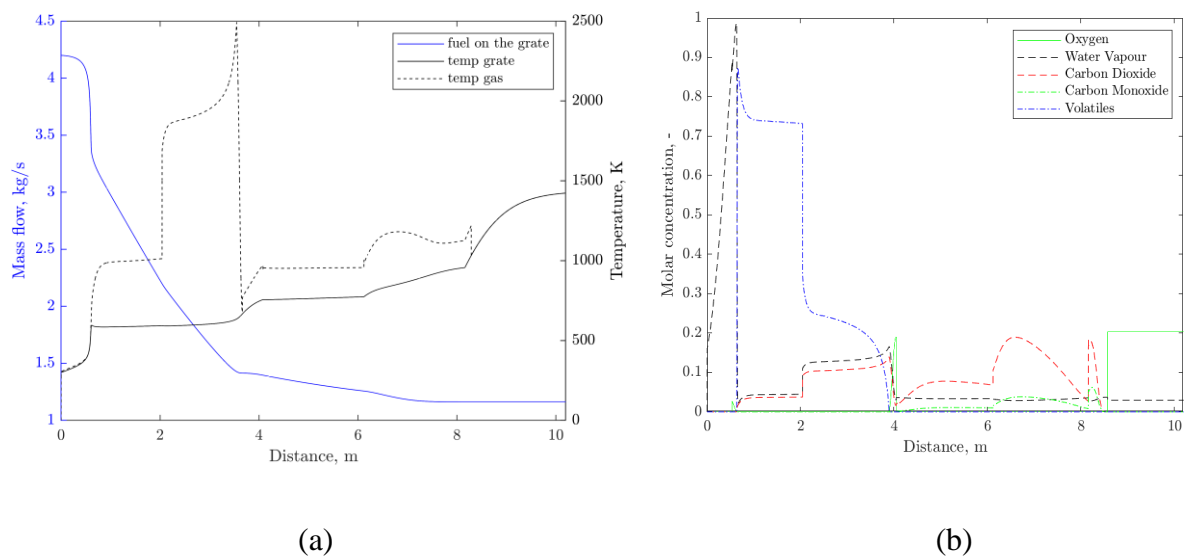


Figure 18 (a) Temperature of the grate and intermediate zone as well as mass flow of the fuel in the function of the grate length; (b) Molar fractions of gas species in the intermediate zone

## 6.2.2 Oxy-fired mode

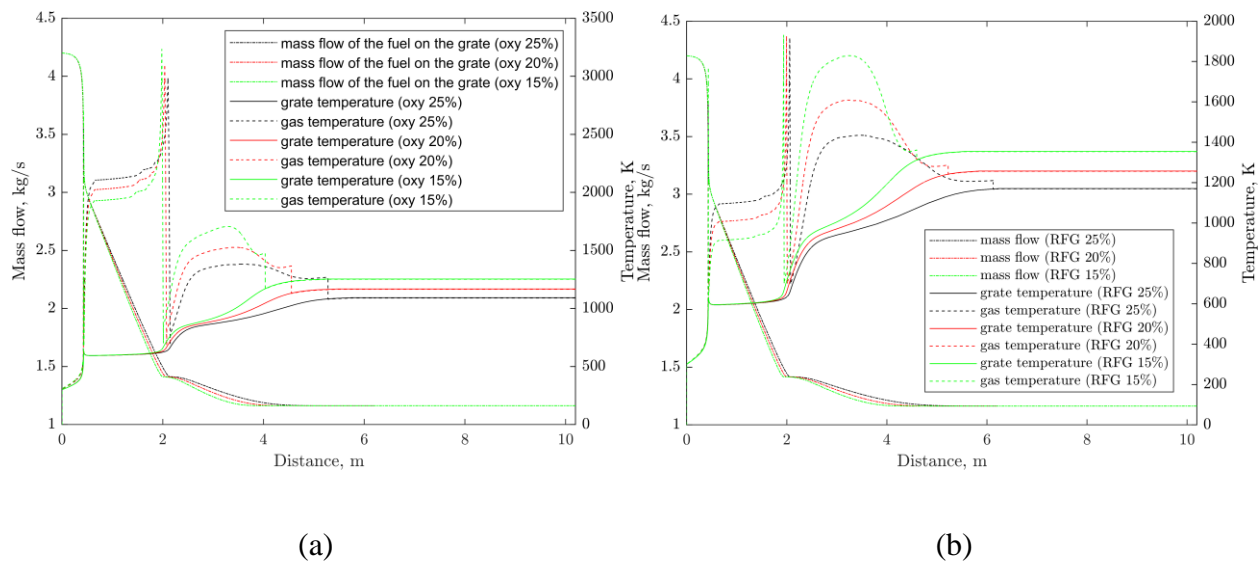
This section presents the results of the simulations of the oxy-waste combustion chamber. To evaluate the effect of different factors, we studied various cases of oxidant distribution. The first analysed case involved introducing oxygen into the combustion chamber, with lambda ( $\lambda$ ) equal to 0.52, along with recirculated flue gas in the ratio of 15, 20, and 25%. The second analysed case comprised checking the influence of oxidant distribution. This was achieved by first

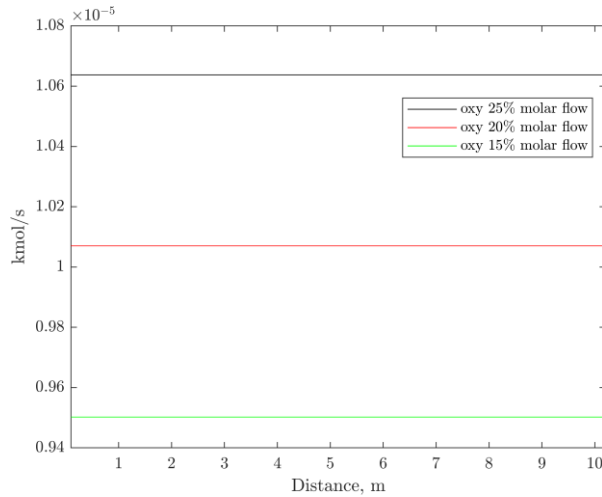


supplying recirculated flue gas to the grate, and after devolatilization process, introducing oxygen (in the amount as in the first case).

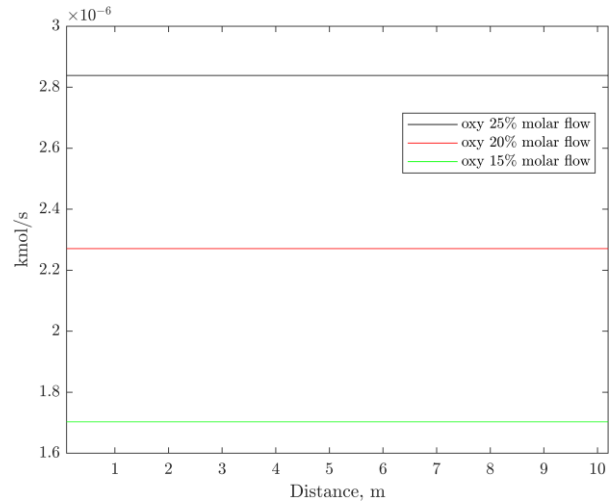
As can be observed, the higher the degree of flue gas recirculation, the lower the temperature of the grate and the intermediate zone, which confirms that recirculation can effectively control the temperature in the combustion chamber. The reason for that is the change in the environment of the furnace, as  $\text{CO}_2$  and  $\text{H}_2\text{O}$  contained in flue gas have a different specific heat capacity than  $\text{N}_2$ . The increased amount of recycled flue gas, and thus the higher amount of heat released by combustion, is absorbed, which decreases the temperature of the process [69], [70].

The next finding obtained in this research is that using oxygen during waste combustion increases the temperature of the process and shortens it. For example, for a recirculation rate of 15%, combustion ends at 4 m, for 20% at 4.5 m, and for 25% at 5.5 m (Fig. 19a). The results imply that the use of recirculated flue gas for evaporation and pyrolysis processes is feasible (Fig. 19b). Limiting oxygen slightly extends the process and significantly decreases the temperature in the combustion chamber. This means that not only the size of the equipment employed for flue gas cleaning can be smaller due to the lower volume of exhaust gas, but also the size of combustion chambers working under oxy-fuel conditions may be reduced by 30-50% compared to the conventional mode of combustion.





(c)



(d)

Figure 19 Temperature of the grate and intermediate zone as well as mass flow of the fuel in the function of the grate length for a) different recirculation of flue gas rates and b) different distribution of oxygen recirculation of flue gas rates together with c) and d) oxidant distribution along the grate

Tables 4 and 5 summarize the required amount of oxygen to carry out the oxy-waste combustion process (total and oxygen produced in ASU). As can be seen, the higher ratio of the flue gas recirculation, the higher the usage of oxygen. This is due to the fact that the recirculated gases contain oxidizing compounds such as oxygen, carbon dioxide and water vapour. Besides, the share of oxygen in the oxidant was calculated for the each case, which varies from 33% up to 34%.

Table 4 Oxygen demand for different oxy-fired conditions from the first examined case (Fig. 19a)

Parameter	Unit	Value		
FGR ratio	%	15	20	25
Total oxygen demand	kmol/s	0.0969	0.1027	0.1085
Oxygen from ASU	kmol/s	0.0795		
The share of oxygen in	%	33	37	43

the oxidant				
-------------	--	--	--	--

Table 5 Oxygen demand for different oxy-fired conditions from the second examined case (Fig. 19b)

Parameter	Unit	Value		
FGR ratio	%	15%	20%	25%
Total oxygen demand	kmol/s	0.0290	0.0232	0.0174
The share of oxygen in the oxidant	%	25		

# Chapter 7

## Summary and conclusions

Global warming and excessive waste generation are major challenges that are currently attracting the attention of many scientists, environmental activists and policymakers. Nowadays, global waste generation is estimated at level of 2.01 billion tonnes and it is expected to rise to 3.4 billion tonnes by 2050. One of the methods to fight climate change with simultaneous waste treatment can be bioenergy carbon capture, utilization, and storage. Currently, four MSW incineration plants integrated with carbon capture are planned or in operation; but they employ the post-combustion method.

In this thesis, carbon capture based on oxy-fuel combustion technology is proposed, since it can bring several advantages to incineration process, such as an increase in temperature due to higher oxygen concentration and a decrease in the auxiliary fossil fuel consumption that is usually used to keep the required by law temperature and thus cause inevitable CO<sub>2</sub> emission. Although oxy-fuel combustion is a known technology, up to now, it has been mostly investigated for fossil fuels and there is a lack of research on such complex fuel as waste combustion under oxy-fired conditions.

Therefore, this study contains both experimental research and mathematical modelling to obtain the new knowledge about the technology, provide a better understanding of the organisation of the process in a real incineration plant to make it feasible and efficient.

In this work, firstly wide literature review is presented to underline the most important challenges and opportunities of the oxy-fuel combustion. Then, thermogravimetric and kinetic analysis is performed to investigate the effect of atmosphere on thermal behaviour of the waste and determine kinetic data of the individual processes during the thermal degradation. Next, an experimental campaign on the thermal degradation of waste using a lab-scale rig is done to study

the effect of the atmosphere on the gas evolution profile. Afterwards, a mathematical model of a real-scale oxy-waste incinerator is developed.

Results showed that shifting atmosphere from inert to gasifying does not influence the thermal decomposition of samples below 600 °C, and the kinetic parameters for pyrolysis are similar in N<sub>2</sub> and CO<sub>2</sub> atmosphere. However, in the gasifying atmosphere, the second peak appears above 600 °C during the decomposition of lignocellulosic materials that is ascribed to CO<sub>2</sub>-char reactions. In the case of lignocellulosic materials, the O<sub>2</sub>/CO<sub>2</sub> atmosphere causes that reactions with char and carrier gas is more rapid and occurs at a lower temperature, thus it partially overlaps the pyrolysis process, which is demonstrated by DTG curves as well as larger fluctuations in the activation energy above a certain value of  $\alpha$ .

It was found that the kinetic parameters calculated by isoconversional methods can be applied to waste materials. Methods of Friedman and Vyazovkin are more efficient than OFW and KAS for studied materials, because the theoretical curves reproduced based on kinetic data obtained using these methods best reflected the measurement results.

The study also shows the importance of the atmosphere during waste devolatilization and solid residue formation. Gasifying and oxidising atmospheres enhanced the secondary reactions. Regarding the properties of chars produced during the slow and fast pyrolysis of investigated waste, it can be concluded that a higher heating rate resulted in chars with lower porosity and thus they were less reactive.

The presented results showed that such combustion parameters as temperature and the length of the process highly depend on oxidant composition. Increased content of oxygen in the supplied gas shortens the combustion process by around 30-50% and elevates the temperature in the gaseous reactions area as well as in the grate. Study also confirmed that flue gas recirculation effectively control the temperature of the process. Moreover, the results indicate that the use of recirculated exhaust gases as an oxidant is sufficient for the drying and pyrolysis process. Thus, oxy-fuel combustion of waste in a grate furnace can provide improved burnout and higher temperature with a sustainable “CO<sub>2</sub>-less” thermal conversion of fuel.

The results of the work will contribute to the development of waste incineration plants integrated with carbon capture, expanding knowledge about the thermal degradation of waste in various conditions and will be useful for the design of oxy-waste combustion chambers.

# Bibliography

- [1] K. Tanaka and B. C. O'Neill, "The Paris Agreement zero-emissions goal is not always consistent with the 1.5 °C and 2 °C temperature targets," *Nat. Clim. Chang.*, vol. 8, no. 4, pp. 319–324, 2018, doi: 10.1038/s41558-018-0097-x.
- [2] A. Sodiq *et al.*, "A review on progress made in direct air capture of CO<sub>2</sub>," *Environ. Technol. Innov.*, vol. 29, p. 102991, 2023, doi: 10.1016/j.eti.2022.102991.
- [3] "Climate Change Service. Surface Air Temperature for September 2023." <https://climate.copernicus.eu/surface-air-temperature-august-2023>.
- [4] United Nations Framework Convention on Climate Change, "Paris Agreement," 2015.
- [5] M. Yusuf and H. Ibrahim, "A comprehensive review on recent trends in carbon capture, utilization, and storage techniques," *J. Environ. Chem. Eng.*, vol. 11, no. 6, p. 111393, 2023, doi: <https://doi.org/10.1016/j.jece.2023.111393>.
- [6] K. J. Joeri Rogelj, Drew Shindell, "Mitigation Pathways Compatible with 1.5°C in the Context of Sustainable Development," *Glob. Warm. 1.5°C. An IPCC Spec. Rep. impacts Glob. Warm. 1.5°C above pre-industrial levels Relat. Glob. Greenh. gas Emiss. pathways, Context Strength. Glob. response to Threat Clim. Chang.*, 2018.
- [7] S. Kaza, L. Yao, P. Bhada-Tata, and F. Van Woerden, *What a Waste 2.0: A Global Snapshot of Solid Waste Management to 2050*. 2018.
- [8] J. Szczepański, K; Waszczyłko-Miłkowska, B; Kamińska-Borak, "Morfologia odpadów komunalnych wytwarzanych w Polsce," 2022. [Online]. Available: <https://ios.edu.pl/wp-content/uploads/2022/08/ios-pib-morfologia-odpadow-komunalnych-wytwarzanych-w-polsce-w-systemie-gminnym.pdf>.
- [9] M. Becidan, "Experimental Studies on Municipal Solid Waste and Biomass Pyrolysis," Norwegian University of Science and Technology, 2007.

- [10] epa, “2022 Household Municipal Waste Characterisation,” no. September, 2023, [Online]. Available: <https://www.epa.ie/publications/monitoring--assessment/waste/national-waste-statistics/2022-household-municipal-waste-characterisation-report.php>.
- [11] Eurostat, “Municipal waste statistics,” 2021. [https://ec.europa.eu/eurostat/statistics-explained/index.php/Municipal\\_waste\\_statistics#Municipal\\_waste\\_generation](https://ec.europa.eu/eurostat/statistics-explained/index.php/Municipal_waste_statistics#Municipal_waste_generation).
- [12] European Commission, “COMMUNICATION FROM THE COMMISSION TO THE EUROPEAN PARLIAMENT, THE COUNCIL, THE EUROPEAN ECONOMIC AND SOCIAL COMMITTEE AND THE COMMITTEE OF THE REGIONS A new Circular Economy Action Plan For a cleaner and more competitive Europe,” 2020. [Online]. Available: <https://eur-lex.europa.eu/legal-content/EN/TXT/?uri=COM%3A2020%3A98%3AFIN>.
- [13] European Commission, “DIRECTIVE (EU) 2023/2413 OF THE EUROPEAN PARLIAMENT AND OF THE COUNCIL of 18 October 2023 amending Directive (EU) 2018/2001, Regulation (EU) 2018/1999 and Directive 98/70/EC as regards the promotion of energy from renewable sources, and repealing Council,” 2023. [Online]. Available: <https://eur-lex.europa.eu/legal-content/EN/TXT/?uri=CELEX%3A32023L2413&qid=1699364355105>.
- [14] J. Malinauskaite *et al.*, “Municipal solid waste management and waste-to-energy in the context of a circular economy and energy recycling in Europe,” *Energy*, vol. 141, pp. 2013–2044, 2017, doi: 10.1016/j.energy.2017.11.128.
- [15] F. Cucchiella, I. D’Adamo, and M. Gastaldi, “Sustainable waste management: Waste to energy plant as an alternative to landfill,” *Energy Convers. Manag.*, vol. 131, pp. 18–31, 2017, doi: 10.1016/j.enconman.2016.11.012.
- [16] L. Makarichi, W. Jutidamrongphan, and K. Techato, “The evolution of waste-to-energy incineration: A review,” *Renew. Sustain. Energy Rev.*, vol. 91, pp. 812–821, Aug. 2018, doi: 10.1016/J.RSER.2018.04.088.
- [17] A. Kumar and S. R. Samadder, “A review on technological options of waste to energy for effective management of municipal solid waste,” *Waste Manag.*, vol. 69, pp. 407–422,



- 2017, doi: 10.1016/j.wasman.2017.08.046.
- [18] L. Lombardi, E. Carnevale, and A. Corti, “A review of technologies and performances of thermal treatment systems for energy recovery from waste,” *Waste Manag.*, vol. 37, pp. 26–44, Mar. 2015, doi: 10.1016/J.WASMAN.2014.11.010.
- [19] M. Jurczyk, M. Mikus, and K. Dziejczak, “FLUE GAS CLEANING IN MUNICIPAL WASTE-TO-ENERGY PLANTS – PART I,” no. Iv, pp. 1179–1193, 2016.
- [20] R. Carrasco-hern, P. E. Escamilla-garcía, R. H. Camarillo-l, J. M. Legal-hern, and E. Fern, “Technical and economic analysis of energy generation from waste incineration in Mexico,” vol. 31, 2020, doi: 10.1016/j.esr.2020.100542.
- [21] T. Gu, C. Yin, W. Ma, and G. Chen, “Municipal solid waste incineration in a packed bed: A comprehensive modeling study with experimental validation,” *Appl. Energy*, vol. 247, pp. 127–139, Aug. 2019, doi: 10.1016/j.apenergy.2019.04.014.
- [22] H. Lu, “Learning from failure: Breaking the waste incineration NIMBY cycle through participatory governance,” *Clean. Waste Syst.*, vol. 5, no. April, p. 100089, 2023, doi: 10.1016/j.clwas.2023.100089.
- [23] Confederation of European Waste-to-Energy Plants, “Waste-to-Energy Plants in Europe in 2020,” 2020. <https://www.cewep.eu/waste-to-energy-plants-in-europe-in-2020/>.
- [24] S. E. T. K. B. A. Ramírez, “Decarbonising Industry via BECCS : Promising Sectors , Challenges , and Techno - economic Limits of Negative Emissions,” *Curr. Sustain. Energy Reports*, pp. 253–262, 2021, doi: 10.1007/s40518-021-00195-3.
- [25] S. V Hanssen, V. Daioglou, Z. J. N. Steinmann, J. C. Doelman, D. P. Van Vuuren, and M. A. J. Huijbregts, “The climate change mitigation potential of bioenergy with carbon capture and storage,” *Nat. Clim. Chang.*, vol. 10, pp. 1023–1029, 2020, doi: 10.1038/s41558-020-0885-y.
- [26] A. Lefvert and S. Gr, “Lost in the scenarios of negative emissions : The role of bioenergy with carbon capture and storage ( BECCS ),” vol. 184, no. November 2023, 2024, doi: 10.1016/j.enpol.2023.113882.

- [27] P. Wienchol, A. Szlęk, and M. Ditaranto, “Waste-to-energy technology integrated with carbon capture – Challenges and opportunities,” *Energy*, vol. 198, p. 117352, May 2020, doi: 10.1016/j.energy.2020.117352.
- [28] M. Becidan, M. Ditaranto, P. Carlsson, J. Bakken, M. N. P. Olsen, and J. Stuen, “Oxyfuel Combustion of a Model MSW—An Experimental Study,” *Energies 2021, Vol. 14, Page 5297*, vol. 14, no. 17, p. 5297, Aug. 2021, doi: 10.3390/EN14175297.
- [29] N. Pour, P. A. Webley, and P. J. Cook, “Potential for using municipal solid waste as a resource for bioenergy with carbon capture and storage (BECCS),” *Int. J. Greenh. Gas Control*, vol. 68, pp. 1–15, 2018.
- [30] A. I. Osman, M. Hefny, M. I. A. Abdel Maksoud, A. M. Elgarahy, and D. W. Rooney, *Recent advances in carbon capture storage and utilisation technologies: a review*, vol. 19, no. 2. Springer International Publishing, 2021.
- [31] T. Wilberforce, A. Baroutaji, B. Soudan, A. H. Al-Alami, and A. G. Olabi, “Outlook of carbon capture technology and challenges,” *Sci. Total Environ.*, vol. 657, 2019, doi: 10.1016/j.scitotenv.2018.11.424.
- [32] R. M. Cuéllar-Franca and A. Azapagic, “Carbon capture, storage and utilisation technologies: A critical analysis and comparison of their life cycle environmental impacts,” *J. CO<sub>2</sub> Util.*, vol. 9, pp. 82–102, Mar. 2015, doi: 10.1016/J.JCOU.2014.12.001.
- [33] M. B. Toftegaard, J. Brix, P. A. Jensen, P. Glarborg, and A. D. Jensen, “Oxy-fuel combustion of solid fuels,” *Prog. Energy Combust. Sci.*, vol. 36, no. 5, pp. 581–625, 2010, doi: 10.1016/j.pecs.2010.02.001.
- [34] C. Huanying *et al.*, “Effects of CO<sub>2</sub> and H<sub>2</sub>O on oxy-fuel combustion characteristics and structural evolutions of Zhundong coal pellet at fast heating rate,” *Fuel*, vol. 294, no. March, p. 120525, 2021, doi: 10.1016/j.fuel.2021.120525.
- [35] Y. T. Tang, X. Q. Ma, Z. Y. Lai, and Y. Chen, “Energy analysis and environmental impacts of a MSW oxy-fuel incineration power plant in China,” *Energy Policy*, vol. 60, pp. 132–141, 2013, doi: 10.1016/j.enpol.2013.04.073.

- [36] A. Pettinau, F. Ferrara, V. Tola, and G. Cau, “Techno-economic comparison between different technologies for CO<sub>2</sub>-free power generation from coal,” *Appl. Energy*, 2017, doi: 10.1016/j.apenergy.2017.02.056.
- [37] D. Su, L. Herraiz, M. Lucquiaud, C. Thomson, and H. Chalmers, “Thermal integration of waste to energy plants with Post-combustion CO<sub>2</sub> capture,” *Fuel*, vol. 332, no. P1, p. 126004, 2023, doi: 10.1016/j.fuel.2022.126004.
- [38] G. Ding *et al.*, “Process simulation and optimization of municipal solid waste fired power plant with oxygen/carbon dioxide combustion for near zero carbon dioxide emission,” *Energy Convers. Manag.*, vol. 157, pp. 157–168, Feb. 2018, doi: 10.1016/j.enconman.2017.11.087.
- [39] B. J. P. Buhre, L. K. Elliott, C. D. Sheng, R. P. Gupta, and T. F. Wall, “Oxy-fuel combustion technology for coal-fired power generation,” *Prog. energy Combust. Sci.*, vol. 31, no. 4, pp. 283–307, 2005.
- [40] L. Chen, S. Z. Yong, and A. F. Ghoniem, “Oxy-fuel combustion of pulverized coal: Characterization, fundamentals, stabilization and CFD modeling,” *Prog. Energy Combust. Sci.*, vol. 38, no. 2, pp. 156–214, Apr. 2012, doi: 10.1016/j.pecs.2011.09.003.
- [41] Z. Lai, X. Ma, Y. Tang, and H. Lin, “Thermogravimetric analysis of the thermal decomposition of MSW in N<sub>2</sub>, CO<sub>2</sub> and CO<sub>2</sub>/N<sub>2</sub> atmospheres,” *Fuel Process. Technol.*, vol. 102, pp. 18–23, 2012, doi: 10.1016/j.fuproc.2012.04.019.
- [42] Y. T. Tang, X. Q. Ma, Z. H. Wang, Z. Wu, and Q. H. Yu, “A study of the thermal degradation of six typical municipal waste components in CO<sub>2</sub> and N<sub>2</sub> atmospheres using TGA-FTIR,” *Thermochim. Acta*, 2017, doi: 10.1016/j.tca.2017.09.009.
- [43] M. Ali, S. Yousef, J. Eimontas, and N. Stri, “Pyrolysis and gasification kinetic behavior of mango seed shells using TG-FTIR-GC-MS system under N<sub>2</sub> and CO<sub>2</sub> atmospheres,” vol. 173, 2021, doi: 10.1016/j.renene.2021.04.034.
- [44] Z. Y. Lai, X. Q. Ma, Y. T. Tang, and H. Lin, “A study on municipal solid waste (MSW) combustion in N<sub>2</sub>/O<sub>2</sub> and CO<sub>2</sub>/O<sub>2</sub> atmosphere from the perspective of TGA,” *Energy*, vol. 36, no. 2, pp. 819–824, 2011, doi: 10.1016/j.energy.2010.12.033.

- [45] Z. Y. Lai, X. Q. Ma, Y. T. Tang, H. Lin, and Y. Chen, "Thermogravimetric analyses of combustion of lignocellulosic materials in N<sub>2</sub>/O<sub>2</sub> and CO<sub>2</sub>/O<sub>2</sub> atmospheres," *Bioresour. Technol.*, vol. 107, pp. 444–450, 2012, doi: 10.1016/j.biortech.2011.12.039.
- [46] Y. Tang, X. Ma, Z. Lai, and Y. Fan, "Thermogravimetric analyses of co-combustion of plastic, rubber, leather in N<sub>2</sub>/O<sub>2</sub> and CO<sub>2</sub>/O<sub>2</sub> atmospheres," *Energy*, vol. 90, pp. 1066–1074, 2015.
- [47] L. Wang, T. Li, G. Várhegyi, Ø. Skreiberg, and T. Løvås, "CO<sub>2</sub> Gasification of Chars Prepared by Fast and Slow Pyrolysis from Wood and Forest Residue: A Kinetic Study," *Energy and Fuels*, vol. 32, no. 1, pp. 588–597, 2018, doi: 10.1021/acs.energyfuels.7b03333.
- [48] Y. Tang, X. Ma, Z. Lai, D. Zhou, and Y. Chen, "Thermogravimetric characteristics and combustion emissions of rubbers and polyvinyl chloride in N<sub>2</sub>/O<sub>2</sub> and CO<sub>2</sub>/O<sub>2</sub> atmospheres," *Fuel*, vol. 104, no. x, pp. 508–514, 2013, doi: 10.1016/j.fuel.2012.06.047.
- [49] Y. Tang, X. Ma, Z. Lai, D. Zhou, H. Lin, and Y. Chen, "NO<sub>x</sub> and SO<sub>2</sub> emissions from municipal solid waste (MSW) combustion in CO<sub>2</sub>/O<sub>2</sub> atmosphere," *Energy*, vol. 40, no. 1, pp. 300–306, 2012, doi: 10.1016/j.energy.2012.01.070.
- [50] C. Ke, X. Ma, Y. Tang, W. Zheng, and Z. Wu, "The volatilization of heavy metals during co-combustion of food waste and polyvinyl chloride in air and carbon dioxide/oxygen atmosphere," *Bioresour. Technol.*, vol. 244, no. August, pp. 1024–1030, 2017, doi: 10.1016/j.biortech.2017.08.075.
- [51] Y. Tang, X. Ma, C. Zhang, Q. Yu, and Y. Fan, "Effects of sorbents on the heavy metals control during tire rubber and polyethylene combustion in CO<sub>2</sub>/O<sub>2</sub> and N<sub>2</sub>/O<sub>2</sub> atmospheres," *Fuel*, vol. 165, pp. 272–278, Feb. 2016, doi: 10.1016/J.FUEL.2015.10.038.
- [52] S. Sobek and S. Werle, "Isoconversional determination of the apparent reaction models governing pyrolysis of wood, straw and sewage sludge, with an approach to rate modelling," *Renew. Energy*, vol. 161, pp. 972–987, 2020, doi: 10.1016/j.renene.2020.07.112.
- [53] S. Vyazovkin, "Isoconversional kinetics of thermally stimulated processes," *Springer*,

2015.

- [54] S. Yousef *et al.*, “A sustainable bioenergy conversion strategy for textile waste with self-catalysts using mini-pyrolysis plant,” vol. 196, no. June, pp. 688–704, 2019, doi: 10.1016/j.enconman.2019.06.050.
- [55] X. Li, V. Strezov, and T. Kan, “Energy recovery potential analysis of spent coffee grounds pyrolysis products,” *J. Anal. Appl. Pyrolysis*, 2014, doi: 10.1016/j.jaap.2014.08.012.
- [56] H. A. Kibret, Y.-L. Kuo, T.-Y. Ke, and Y.-H. Tseng, “Gasification of spent coffee grounds in a semi-fluidized bed reactor using steam and CO<sub>2</sub> gasification medium,” *J. Taiwan Inst. Chem. Eng.*, vol. 119, pp. 115–127, 2021, doi: <https://doi.org/10.1016/j.jtice.2021.01.029>.
- [57] C. Yue, P. Gao, L. Tang, and X. Chen, “Effects of N<sub>2</sub>/CO<sub>2</sub> atmosphere on the pyrolysis characteristics for municipal solid waste pellets,” *Fuel*, vol. 315, no. November 2021, p. 123233, 2022, doi: 10.1016/j.fuel.2022.123233.
- [58] M. Policella, Z. Wang, K. G. Burra, and A. K. Gupta, “Characteristics of syngas from pyrolysis and CO<sub>2</sub>-assisted gasification of waste tires,” *Appl. Energy*, vol. 254, no. April, p. 113678, 2019, doi: 10.1016/j.apenergy.2019.113678.
- [59] Y. Lin *et al.*, “Combustion, pyrolysis and char CO<sub>2</sub>-gasification characteristics of hydrothermal carbonization solid fuel from municipal solid wastes,” *Fuel*, vol. 181, pp. 905–915, 2016, doi: 10.1016/j.fuel.2016.05.031.
- [60] W. Ma, G. Rajput, M. Pan, F. Lin, L. Zhong, and G. Chen, “Pyrolysis of typical MSW components by Py-GC/MS and TG-FTIR,” *Fuel*, vol. 251, no. March, pp. 693–708, 2019, doi: 10.1016/j.fuel.2019.04.069.
- [61] G. Özsın, “TGA / MS / FT-IR study for kinetic evaluation and evolved gas analysis of a biomass / PVC co-pyrolysis process,” vol. 182, no. December 2018, pp. 143–153, 2019, doi: 10.1016/j.enconman.2018.12.060.
- [62] G. Ding, B. He, H. Yao, Y. Cao, L. Su, and Z. Duan, “Co - combustion behaviors of municipal solid waste and low - rank coal semi - coke in air or oxygen / carbon dioxide

- atmospheres,” *J. Therm. Anal. Calorim.*, no. 0123456789, 2019, doi: 10.1007/s10973-019-09170-z.
- [63] E. Magnanelli, O. L. Tranås, P. Carlsson, J. Mosby, and M. Becidan, “Dynamic modeling of municipal solid waste incineration,” *Energy*, vol. 209, p. 118426, Oct. 2020, doi: 10.1016/J.ENERGY.2020.118426.
- [64] A. F. S. C. Hottel, “Radiative Heat Transfer.” McGraw-Hill, New York, 1967.
- [65] H. Sadeghi, S. Hostikka, G. Crivelli, and H. Bordbar, “Weighted-sum-of-gray-gases models for non-gray thermal radiation of hydrocarbon fuel vapors , CH<sub>4</sub> , CO and soot,” *Fire Saf. J.*, vol. 125, no. September 2020, p. 103420, 2021, doi: 10.1016/j.firesaf.2021.103420.
- [66] Z. Yu, X. Ma, and Y. Liao, “Mathematical modeling of combustion in a grate-fired boiler burning straw and effect of operating conditions under air- and oxygen-enriched atmospheres,” *Renew. Energy*, vol. 35, no. 5, pp. 895–903, 2010, doi: 10.1016/j.renene.2009.10.006.
- [67] Q. N. Hoang, J. Van Caneghem, T. Croymans, R. Pittoors, and M. Vanierschot, “A novel comprehensive CFD-based model for municipal solid waste incinerators based on the porous medium approach,” *Fuel*, vol. 326, p. 124963, 2022, doi: <https://doi.org/10.1016/j.fuel.2022.124963>.
- [68] Y. B. Yang, H. Yamauchi, V. Nasserzadeh, and J. Swithenbank, “Effects of fuel devolatilisation on the combustion of wood chips and incineration of simulated municipal solid wastes in a packed bed,” *Fuel*, vol. 82, no. 18, pp. 2205–2221, Dec. 2003, doi: 10.1016/S0016-2361(03)00145-5.
- [69] R. Karim, A. Ahmed, A. Alhamid, R. Sarhan, and J. Naser, “CFD simulation of biomass thermal conversion under air / oxy-fuel conditions in a reciprocating grate boiler,” *Renew. Energy*, vol. 146, pp. 1416–1428, 2020, doi: 10.1016/j.renene.2019.07.068.
- [70] M. Mureddu, F. Dessì, A. Orsini, F. Ferrara, and A. Pettinau, “Air- and oxygen-blown characterization of coal and biomass by thermogravimetric analysis,” *Fuel*, vol. 212, no. April, pp. 626–637, 2018, doi: 10.1016/j.fuel.2017.10.005.

# List of tables

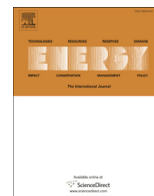
TABLE 1 KINETIC DATA OF PYROLYSIS PROCESS UNDER DIFFERENT CONDITIONS.....	26
TABLE 2 KINETIC PARAMETERS OF OXY-COMBUSTION OF SCG DERIVED CHAR.....	33
TABLE 3 KINETIC PARAMETERS OF OXY-COMBUSTION OF TEX DERIVED CHAR.....	34
TABLE 4 OXYGEN DEMAND FOR DIFFERENT OXY-FIRED CONDITIONS.....	41
TABLE 5 OXYGEN DEMAND FOR DIFFERENT OXY-FIRED CONDITIONS.....	42

# List of figures

FIGURE 1 GLOBAL-MEAN AND EUROPEAN-MEAN SURFACE AIR TEMPERATURE ANOMALIES RELATIVE TO 1991-2020 FOR EACH AUGUST FROM 1979 TO 2023 (ADAPTED FROM [3]) .....	1
FIGURE 2 MUNICIPAL SOLID WASTE COMPOSITION IN POLAND (2020). BASED ON DATA AVAILABLE [8].....	3
FIGURE 3 MUNICIPAL SOLID WASTE COMPOSITION IN USA (2018). BASED ON DATA AVAILABLE [10]. .....	4
FIGURE 4 MUNICIPAL WASTE LANDFILLED, INCINERATED, RECYCLED, AND COMPOSTED, EU-27, 1995-2019 (EUROSTAT [11]).....	5
FIGURE 5 EU WASTE HIERARCHY [12] .....	6
FIGURE 6 INSTALLED CAPACITY OF MUNICIPAL WASTE ENERGY IN EUROPE IN 2022.....	7
FIGURE 7 THE NUMBER AND DISTRIBUTION OF WASTE INCINERATION PLANTS IN EUROPE (2020) [23].....	9
FIGURE 8 BECCS SCHEMATIC DRAW .....	10
FIGURE 9 SCHEMATIC DIAGRAM OF THE OXY-FUEL INCINERATION PLANT .....	18
FIGURE 10 TGA AND DTG CURVES OF TEX SAMPLE UNDER N <sub>2</sub> , CO <sub>2</sub> AND O <sub>2</sub> /CO <sub>2</sub> ATMOSPHERES AT A) 5, B) 10 AND C) 15 KMIN <sup>-1</sup> .....	23
FIGURE 11 TGA AND DTG CURVES OF SCG UNDER N <sub>2</sub> , CO <sub>2</sub> AND O <sub>2</sub> /CO <sub>2</sub> ATMOSPHERES AT A) 5, B) 10 AND C) 15 KMIN <sup>-1</sup> .....	24
FIGURE 12 TGA AND DTG CURVES OF PVC UNDER N <sub>2</sub> , CO <sub>2</sub> AND O <sub>2</sub> /CO <sub>2</sub> ATMOSPHERES AT A) 5, B) 10 AND C) 15 KMIN <sup>-1</sup> .....	25
FIGURE 13 CUSTOM-BUILT TEST STAND FOR WASTE THERMAL DEGRADATION .....	30
FIGURE 14 GAS EVOLUTION DURING THE THERMAL DEGRADATION OF A) SCG AND B) TEXTILES UNDER N <sub>2</sub> ATMOSPHERE .....	31
FIGURE 15 GAS EVOLUTION DURING THE THERMAL DEGRADATION OF A) SCG AND B) TEXTILES UNDER CO <sub>2</sub> ATMOSPHERE.....	32
FIGURE 16 GAS EVOLUTION DURING THE THERMAL DEGRADATION OF A) SCG AND B) TEXTILES UNDER O <sub>2</sub> /CO <sub>2</sub> ATMOSPHERE .....	32
FIGURE 17 MODEL OF MSW COMBUSTION CHAMBER.....	36
FIGURE 18 (A) TEMPERATURE OF THE GRATE AND INTERMEDIATE ZONE AS WELL AS MASS FLOW OF THE FUEL IN THE FUNCTION OF THE GRATE LENGTH; (B) MOLAR FRACTIONS OF GAS SPECIES IN THE INTERMEDIATE ZONE.....	39
FIGURE 19 TEMPERATURE OF THE GRATE AND INTERMEDIATE ZONE AS WELL AS MASS FLOW OF THE FUEL IN THE FUNCTION OF THE GRATE LENGTH FOR A) DIFFERENT RECIRCULATION OF FLUE GAS RATES AND B) DIFFERENT DISTRIBUTION OF OXYGEN RECIRCULATION OF FLUE GAS RATES TOGETHER WITH C) AND D) OXIDANT DISTRIBUTION ALONG THE GRATE.....	41



# Appendixes



# Waste-to-energy technology integrated with carbon capture – Challenges and opportunities

Paulina Wienchol<sup>a, \*</sup>, Andrzej Szłęk<sup>a</sup>, Mario Ditaranto<sup>b</sup>

<sup>a</sup> Department of Thermal Engineering, Silesian University of Technology, Gliwice, Poland

<sup>b</sup> SINTEF Energy Research, Trondheim, Norway

## ARTICLE INFO

### Article history:

Received 17 December 2019

Received in revised form

24 February 2020

Accepted 8 March 2020

Available online 12 March 2020

### Keywords:

Oxy-fuel combustion

MSW

Waste

Incineration

BECCS

## ABSTRACT

Carbon dioxide emission is a serious environmental issue that humankind must face soon. One of the promising technologies for reducing global CO<sub>2</sub> emissions is oxy-fuel combustion (OFC) technology, which belongs to the carbon capture methods. OFC involves the use of oxygen and recirculated flue gas as an oxidizer in the combustion process. Application of oxy-fuel combustion in waste incineration can result in negative CO<sub>2</sub> emission since some part of the carbon in municipal solid waste is biogenic. Such technology is often described as BECCS or Bio-CCS and it has attracted the attention of scientists recently. In addition to easier CO<sub>2</sub> capture, oxy-fuel combustion of municipal solid waste offers other advantages, such as reduced flue gas volume, increased combustion temperature and the possibility of retrofit existing incineration plants. In the present paper, studies of oxy-fuel combustion of waste materials, in particular, municipal solid waste and sewage sludge are presented and summarized. The study shows the opportunities and challenges that have to be addressed to fully exploit the potential of the oxy-fired incineration plant.

© 2020 The Authors. Published by Elsevier Ltd. This is an open access article under the CC BY license (<http://creativecommons.org/licenses/by/4.0/>).

## 1. Introduction

Nowadays, climate change is a major challenge for scientists around the world that needs to be addressed immediately. Therefore, some actions have been taken in recent years. For instance, during the 21st Conference of the Parties of the United Nations Framework Convention on Climate Change (UNFCCC), representatives of member states established the common goal of decrease greenhouse gases (GHGs) emissions to maintain global average temperature well below 2°C above pre-industrial levels and to pursue efforts to limit the growth to 1.5°C [1]. To achieve the set goal, the EU commission prepared Energy Roadmap to 2050, which highlights that almost complete transition to renewable energy sources (97% of RES in electricity consumption) is crucial to decarbonize the energy sector. Besides, in most scenarios, the implementation of carbon capture and storage (CCS) is taken into account since it is currently considered the only technology that can significantly reduce carbon dioxide emissions from large-scale energy generation systems [2,3].

Carbon capture processes comprise pre-combustion, post-

combustion, and oxy-fuel combustion, which includes chemical looping combustion [4]. At present, post-combustion is considered the most mature technology for carbon capture with minimum impact on the existing systems and is therefore widely used. However, the main drawback is a large energy penalty since the separation of CO<sub>2</sub> from the exhaust gases after air combustion is a complicated process. As a result, the efficiency of the power plant drops by 8–12%, which is economically unfavourable [5]. A considerably better way in terms of efficiency is the pre-combustion system that is usually combined with IGCC plant, however, it is still unreliable, expensive and needs further development to become competitive [5,6]. Although oxy-fuel combustion (OFC) is not yet industrially applicable, it is the most promising among available technologies mostly due to easy CO<sub>2</sub> capture and the low efficiency penalty (around 4% mainly caused by CO<sub>2</sub> compression). Moreover, according to Pettinau et al. [5] if oxy-fuel combustion were commercial, it would be the best option for near-zero CO<sub>2</sub> emission power generation. In addition, application of oxy-fuel combustion reduces the volume of flue gas, increases the boiler efficiency, eliminates nitrogen oxides (NO<sub>x</sub>), stabilizes the temperature and allows modernization of existing systems [5,7,8].

Nevertheless, problems that scientists highlighted are the high capital cost investment, as well as energy consumption of the air

\* Corresponding author.

E-mail address: [paulina.wienchol@polsl.pl](mailto:paulina.wienchol@polsl.pl) (P. Wienchol).

separation unit (ASU), because currently the only available technology that can meet the requirements for a large amount of high purity oxygen is based on cryogenic distillation. Hence, investigation of new methods of air separation, such as oxygen transport membrane, ion-transport membranes or chemical looping, is essential to increase the efficiency of the oxy-fuel combustion process [8,9]. Taking into account that chemical looping technology can significantly improve the oxy-fuel combustion process, it has attracted the attention of scientists recently [10]. It is also considered as a next-generation CO<sub>2</sub> capture process [11]. Chemical looping air separation can be applied in both oxy-fired and IGCC plants instead of ASU resulting in the increase of net plant efficiency by around 3%, the reduction of capital investment by roughly 10–18% and the decrease in electricity cost by 7–12% [12].

### 1.1. Oxy-fuel combustion of solid fuels

Oxy-fuel combustion (Fig. 1) involves the replacement of air as an oxidant into high purity oxygen, usually above 95 vol%, and recirculated flue gas. Consequently, produced flue gas stream contains mainly carbon dioxide and water vapour that can be easily removed by condensation. Finally, carbon dioxide can be purified, compressed and stored in a geological formation [13], or used in geothermal technology [14,15], in agriculture [16], and for the production of biofuels, such as methanol (CH<sub>3</sub>OH) and dimethyl ether (CH<sub>3</sub>OCH<sub>3</sub>) [17] creating the carbon capture storage and utilization (CCUS) system.

The employment of a mixture of oxygen and carbon dioxide instead of air significantly affects the combustion process, therefore the technology of oxy-fuel combustion should be carefully integrated with the rest of the system. For example, the heat transfer profile differs due to the higher concentration of three-atomic gases (CO<sub>2</sub>, H<sub>2</sub>O) with different physical and chemical properties, such as emissivity and heat capacity. It was thoroughly examined both numerically and experimentally by several researchers [18–23]. It was found that both the convective and radiative heat transfers were higher under the oxy-fuel conditions. The ignition, flame propagation, and stability under oxy-fuel combustion were evaluated in Ref. [24–29]. It was reported that ignition delay increased and flame speed decreased during oxy-combustion due to higher heat capacity of CO<sub>2</sub> and lower O<sub>2</sub> diffusivity in CO<sub>2</sub>. Besides, many attempts have been made [30–35] aimed at estimating emission of pollutants during oxy-fuel combustion. Studies showed that under oxy-fuel combustion (a) emission of NO<sub>x</sub>, SO<sub>2</sub> and CO can be reduced, however, it highly depended on oxygen concentration in O<sub>2</sub>/CO<sub>2</sub> mixture (with higher amount of oxygen, pollution emission decreased), (b) a big impact on gas emission had a type of fuel and (c) emissions differed since volumetric flue gas flow rate was reduced and flue gas stream was recycled.

Over the past decade, the number of studies on oxy-fuel combustion has increased drastically, as shown in Fig. 2. Currently, there are many literature reviews concerning oxy-combustion of

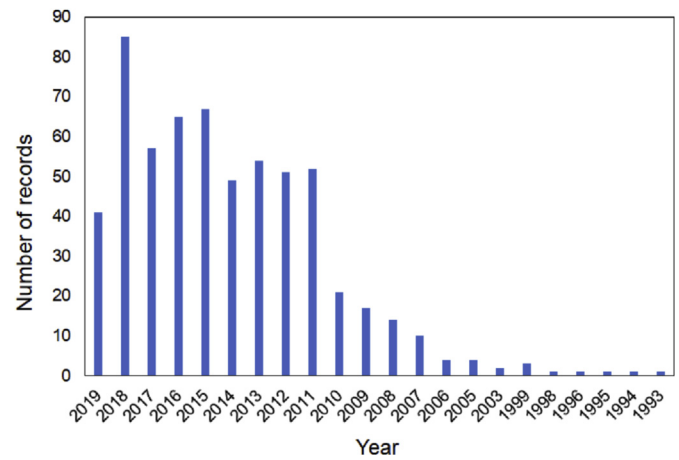


Fig. 2. The number of publications on oxy-fuel combustion, source: Web of Science (WoS).

coal since this is the most widespread fuel [36–41]. Authors focused on the trends and current issues, associated mainly with the retrofitting of existing power plants. Nevertheless, they pointed out that oxy-fuel combustion is a cost-effective and technically feasible method of CO<sub>2</sub> capture. Recently, biomass has started to play a key role in the energy sector due to the excessive depletion of non-renewable resources. It was found that biomass can support countries that do not have natural energy resources, thereby reducing their energy dependence and increasing energy security [42]. Thus, Liu et al. [43] published the first review on oxy-fuel co-combustion of coal and biomass in fluidized bed boiler, at which they underlined that such technology attracted attention in both the academic and industry sectors.

The presented works indicate that oxy-fuel combustion is a potentially efficient technology, which can be introduced to both new and existing power plants as well as for different types of fuels, such as biomass. A large number of studies have shown that oxy-coal combustion technology has evolved in recent decades, but there are still many research questions that have been noted by scientists. The concerns are related to the implementation of OFC technology in existing power plants and the use of low-quality fuels, such as biomass or municipal solid waste. One of the biggest challenges of oxy-fuel combustion is the high energy consumption of ASU, therefore to improve the performance of oxy-fired power plants a crucial aspect is research on effective methods of air separation.

### 1.2. Waste composition

By 2050, the amount of waste is expected to increase from 2.01 billion tonnes to 3.4 billion tonnes [44]. Until then, the waste

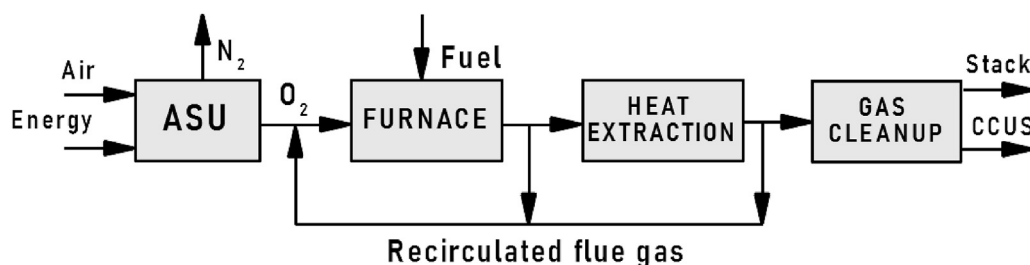


Fig. 1. Schematic draw of the oxy-fuel combustion process.

management sector should develop so that waste does not become a dangerous threat to the environment and human health. As stated in the European Directive [45], biomass is a biodegradable fraction of products, waste, and residues from a biological origin, including municipal solid waste. Thus, such MSW as, paper, cardboard, wood, cloth, green waste, and food can be classified as a renewable source of energy, what from a legal and economic point of view can be crucial in the development of systems based on recovering energy from waste because renewable energy is more often financially and politically supported.

According to the World Bank [44], the composition of waste varies around the world mainly due to the value of the gross domestic product (GDP) and consumption pattern. Middle- and low-income countries generate about 64% of materials with biological origin. While, in high-income countries, MSW contains mostly inorganic fractions with high calorific value, which can be recycled. However, barely 28% of MSW, which comes from developed countries is biogenic [46]. As can be observed in Fig. 3, globally, more than half of the waste has a biological origin.

Taking into account that waste is not only available worldwide but also the average heating value of the waste is approximately 10 MJ/kg [47], using waste as a source of valuable energy seems reasonable and could be a key factor for sustainable development and the circular economy, which aims to maintain the value of products, materials and resources as long as possible, to reduce waste and resources consumption.

### 1.3. Bio-energy with CCS

Since oxy-fuel combustion can be applied to any type of fuel used for thermal power production, the interest of research on the combustion in  $O_2/CO_2$  atmosphere of biomass has recently increased. Speaking of the use of biomass as the source of energy in a system integrated with carbon capture and storage technology, one should not forget about the bio-energy with carbon capture and storage (BECCS or BioCCS) process. It is a combination of two  $CO_2$  mitigation methods, which in consequence give a net-zero or negative carbon dioxide emission [48], and thus cools the Earth. According to Gładysz and Ziębik [49] the cumulative  $CO_2$  emission of net electricity production for oxy-fuel combustion of biomass is  $-0.2722 \text{ kgCO}_2/\text{M}_{el}$  and emissions from MSW incineration integrated with CCS system is around  $-0.7 \text{ kgCO}_2, eq/\text{kg}$  of wet MSW [50]. This shows that BioCCS technology can significantly contribute to the decarbonisation of Europe.

There are 20 BECCS projects worldwide, which relate to various bio-energy technologies, e.g. waste-to-energy plants (WtE) in Norway and the Netherlands, ethanol plants in France, Brazil and Sweden, biomass combustion and co-firing in Japan, two pulp and

paper plants in Sweden, biomass gasification in the United States and biogas plant in Sweden [50,51]. According to Bui et al. [52], Ricci and Selosse [53], the deployment of BECCS is technically possible, however, negative emissions are not covered by the Kyoto framework, thus the main drawbacks to commercially adopting this system is the lack of economic and political drivers supporting the technologies based on bioenergy with carbon capture. Therefore, it would be necessary to financially encourage electricity generation with negative  $CO_2$  emissions.

## 2. Aim and scope of the work

Understanding the importance of the role of bio-energy integrated with carbon capture technology in the sustainable development scenario leads to consideration of the oxy-fuel combustion of waste as a prospective solution for mitigating a climate change. Since currently, there is a lack of overview of the combustion of municipal solid waste and other problematic fuels, such as sewage sludge, in  $O_2/CO_2$  atmosphere the objective of the present work summarizes the current knowledge status of technology.

Section 3 contains an overview of available waste-to-energy technologies, in particular, thermal methods of energy recovery from waste since they are effective solutions for waste management that should be developed. Besides, the possibility of integration of WtE plants with carbon capture is presented and compared, as well as existing incineration plants with  $CO_2$  capture are discussed.

Section 4 is devoted to examining works on oxy-fuel combustion of waste since the oxy-incineration plant seems to be potentially a more effective way of waste disposal than those, which are available currently. The collected papers present the most important findings on the kinetic parameters obtained during thermal degradation of waste under different atmospheres, as well as the emission of pollutants and heavy metals during oxy-fuel combustion since these are key design parameters. Summarizing current knowledge is important in order to build reliable combustion modelling tools, necessary to optimize the combustion of specific types of waste and scale-up of furnaces. This article exposes opportunities that oxy-fuel combustion technology can bring and the challenges that need to be addressed before the implementation of oxy-fuel combustion of waste process.

## 3. Waste to energy technology

There are many options for waste management, i.e. composting, landfilling, recycling and utilizing waste for energy production. Although landfilling and dumping causes a negative impact on the environment due to uncontrolled methane release, this practice is a dominant method of waste management, especially in developing countries [54]. Unlike landfilling, energy recovery from waste is an efficient and ecological way of handling waste, however, the investment cost is relatively high. Therefore, most of the WtE plants are placed in high-income countries [55]. Waste-to-energy technologies include thermal conversion (pyrolysis, gasification, and incineration), biological conversion (anaerobic digestion), as well as a landfill with energy recovery [56]. WtE processes allow to reduce the volume of waste, recover energy and decrease fossil fuel consumption. Besides, waste is a cheap source of energy or can be even considered as an income since municipalities have to pay other parties to manage their waste. Thus, the WtE industry is developing dynamically and it is expected that the Waste-to-Energy industry will be worth approximately USD 37.6 billion in 2020 [57].

### 3.1. Pyrolysis

Pyrolysis is a decomposition of feedstock into gaseous, liquid

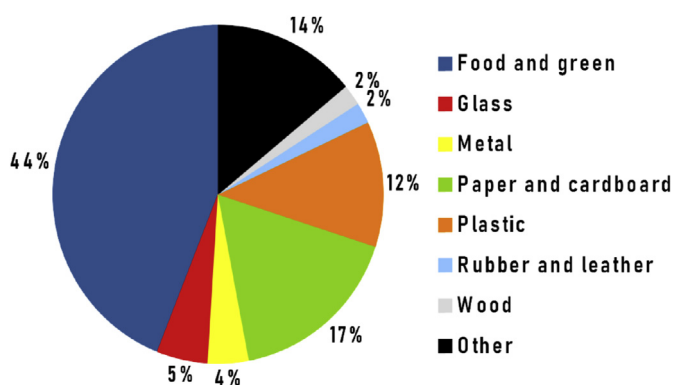


Fig. 3. Global waste composition, data source [44].

and solid materials at elevated temperatures between 300 °C and 650 °C in an inert atmosphere, for example, nitrogen or argon. Pyrolytic products vary depending on the feedstock composition and pyrolysis parameters, such as temperature, heating rate and residence time [55,58]. The main reason for employing the pyrolysis of MSW is bio-oil and synthesis gas production, which can be a substitute for transportation fuel or can be used in power generation and petrochemical industry [59]. Besides, produced char that is classified as a by-product can be used for water treatment applications or as an agricultural soil amendment. However, one of the problems the researchers have pointed out is that biofuels are heavily contaminated and require cleaning and the employment of sophisticated methods for improvement before use. Moreover, pyrolysis of waste is not economically viable and need further research [60].

### 3.2. Gasification (IGCC and IPGCC plants)

Gasification is partial oxidation with oxygen, produced by an Air Separation Unit (ASU) and steam at high temperatures during which carbonaceous materials are converted into syngas ( $\text{CO}_2$ ,  $\text{H}_2$ ,  $\text{CO}$ ,  $\text{CH}_4$ ) [55]. Depending on the process temperature, gasification (800–1200°C) and plasma gasification (from 5000°C up to 15 000 °C) are distinguished [61]. Typically, a technology that employs gasification is the Integrated Gasification Combined Cycle (IGCC), while the process that utilizes plasma gasification is the Integrated Plasma Gasification Combined Cycle (IPGCC). Both methods allow for the carbon capture resulting in zero- $\text{CO}_2$  emission power generation [62]. There are several studies concerning plants based on the MSW gasification and plasma gasification [63–66], as well as co-gasification of waste and other fuels [67,68] to produce not only electricity but also district heat and gaseous hydrogen. The overall conclusion is that gasification-based systems are very efficient and can handle problematic low-grade fuels. In addition, the gasification plant is highly flexible and depending on the desired product, the gasifying agent should be modified. If the main objective is the production of hydrogen, the steam should be injected into the reactor, while during electric power generation, using oxygen-enriched air is recommended. In general, gasification is a promising method of waste management, however, there is currently only one commercial plant that uses waste as an energy source in the gasification process for electricity and heat production. Furthermore, the cost required for gas cleaning is higher than in the case of waste incineration.

### 3.3. Chemical looping (CLC plant)

During chemical looping combustion, two reactors are employed. Fuel is introduced in the fuel reactor, in which it is oxidized by metal oxide. The reduced metal oxide is then transferred into the air reactor where it is oxidized. Similarly to oxy-fuel combustion, the exhaust gas from fuel reactor only contains  $\text{CO}_2$  and  $\text{H}_2\text{O}$  and consequently, carbon dioxide can be easily captured after condensation [69,70]. To date, only a few studies focused on chemical looping combustion/gasification of waste. Moreover, works regard mostly the fate of heavy metals, such as chlorine or cadmium since it is considered that the emission of heavy metals is one of the challenges in the CLC and CLG of waste [71].

Bi et al. [72] studied the impact of different oxygen carriers on dioxins formation during chemical looping combustion. They found that CLC based on  $\text{CaSO}_4$  effectively inhibits the formation of PCDD/Fs. While Zhao and Wang [11], Ma et al. [73] established that *in situ* gasification-chemical looping combustion using  $\text{CaO}$ -decorated  $\text{Fe}_2\text{O}_3/\text{Al}_2\text{O}_3$  as oxygen carrier is highly efficient and suppress the PCDD/Fs emission.

### 3.4. Incineration (MSWI plant)

Incineration is the full oxidative combustion of waste in a furnace at high temperatures between 850°C and 1200°C. Among the thermal treatment of waste methods, incineration is the most mature and widely used technique [74]. Furthermore, according to Dong et al. [75], from the life cycle assessment (LCA) point of view, the incineration process is currently better than pyrolysis and gasification-melting due to the highly efficient flue gas cleaning section, use of combined heat and power (CHP) cycle and the recycling of ash.

The first waste incineration plants were introduced in the 19th century during the Industrial Revolution and were intended exclusively to utilize waste. However, this changed in the mid-20th century, when oil prices soared, resulting in the idea of waste-to-energy technology [57]. Today, according to Kaza et al. [44], about 11% of municipal waste is treated through modern incineration plants that correspond to roughly 1200 incinerators around the world. It means that the application of carbon capture in incineration plants could cause a sudden decrease in  $\text{CO}_2$  emission in the near future. In Poland, the waste-to-energy sector is developing rapidly. There are currently seven municipal solid waste incineration plants (MSWI) with a total capacity equal to almost one million tonnes of waste per year, which corresponds to 9% of the MSW produced in the country [76]. Moreover, there is planned that the number of incineration plants will increase up to 30 [77]. In Norway, meanwhile, waste management is well-developed, i.e. 58% of waste is recycled or incinerated. The WtE plant's number is 17 (total capacity is around 1.70 Mt/year), including one incineration plant in Oslo with implemented carbon capture and storage (CCS) system [78].

#### 3.4.1. Modern waste incineration

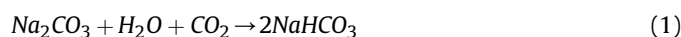
Modern waste incineration plants are not only obligated to comply with environmental protection regulations but also have to face a difficult challenge to arouse public confidence and acceptance. Therefore, more and more plants are designed in an integral way with the environment. For example, a combined heat and power (CHP) waste incineration plant in Copenhagen that in addition to excellent efficiency, also has a recreation area, which includes a ski slope, viewpoint and climbing wall [79].

Currently, there are three main groups of MSWI technologies: (a) moving grate, (b) rotary kiln and (c) fluidized bed incinerators [57], of which grate boilers are used in 80% of WtE plants worldwide [80]. During the combustion of MSW, many pollutants are produced, including fly ashes, heavy metals, carbon compounds, acid gases, and others, and they have to be removed according to limits included in European Union documents or in other national regulations. To fulfill the requirements waste incineration plants should be planned and designed in accordance with the guidelines of the "Best Available Techniques (BAT) for Waste Incineration" document [80]. Moreover, in order to ensure complete combustion of waste, the EU Parliament introduced the Directive, which requires all installations to keep the incineration or co-incineration gases for at least 2 seconds at a temperature of at least 850°C, whereas incineration process of hazardous waste with a content of more than 1% of halogenated organic substances expressed as chlorine must occur at 1100°C for at least 2 seconds. To guarantee proper conditions, the plant should be equipped with auxiliary burners.

#### 3.4.2. Incineration with $\text{CO}_2$ capture

Currently, to the best knowledge of authors, there are four incineration plants that are coupled with a carbon capture system. They are located in Norway (Klemetsrud CHP), Japan (Saga City)

and in the Netherlands (Twence and AVR plant). AVR plant, Twence and Saga City are examples of the CCU facilities. In Japan, an alkaline aqueous amine method of carbon capture is introduced designed by Toshiba. The obtained carbon dioxide is used for local crops cultivation and algae cultures formation [81]. In this way, the waste incineration plant captures 10 tonnes of carbon dioxide every day [82]. AVR is the first waste-to-energy company with a large-scale CO<sub>2</sub> capture system. In 2019, 60 000 tonnes of carbon dioxide was expected to be captured, liquefied and transported to end-users that was mainly greenhouse agriculture industry. In the future, AVR will seek to capture 800 000 tonnes of CO<sub>2</sub> per year and use it in building materials (concrete) or chemical industry for plastic and biofuels production, supporting the local circular economy [83]. While, at Twence waste incineration plant, 830 000 tonnes of waste is processed annually, producing 405 000 MWh of electricity and 1.5 million GJ of thermal energy for district heating [84]. The CO<sub>2</sub> capture process was implemented in 2011. Carbon dioxide is scrubbed from the flue gas stream, purified and used to produce a sodium bicarbonate slurry (SBC) according to equation (1).



Then, SBC is injected to remove the acid components from the flue gas, such as HF, HCl and SO<sub>2</sub>. Consequently, the incineration plant is more independent of the operating costs, because expenditures for the flue gas cleaning can be reduced, and global carbon footprint is lower [85]. Waste incineration plant in Oslo (Klemetsrud) processing around 400 000 tonnes of non-recyclable waste. As a result, 55 MW of heat and 10.5 MW of electricity is produced for city residents. The carbon capture method that will be implemented in the plant is based on amine absorption and it will reduce the carbon dioxide emission by 400 000 tonnes every year. The plant in Klemetsrud will be an example of a CCS facility, therefore it is foreseen that carbon dioxide will be permanently stored in the North Sea [86].

Presented examples have indicated that carbon capture can be successfully implemented in a waste incineration plant resulting in near-zero (or even negative) CO<sub>2</sub> emission power generation. As shown, carbon dioxide capture methods used in waste incineration plants so far are based on post-combustion since this method is relatively easy to implement and the most mature. However, sequestration of CO<sub>2</sub> after air-combustion is very complex and reduces efficiency by 14.7%. While according to Tang et al. [87] oxy-fuel combustion would reduce the efficiency of the incineration plant by 12.6%. Additionally, Ding et al. [88] shows that after the optimization of the oxy-fired incineration plant, the decrease in efficiency can achieve the level of 9.57%. Key parameters, which could improve the oxy-fuel combustion process are the recirculation of flue gas, which can be used to heat the molecular sieve regeneration gas of ASU and the primary condensate as well as the waste heat generated by ASU compressors, which also can be utilized to heat the primary condensate. The issue that can occur in the case of oxy-fuel combustion is that it requires more adaptations to the incineration plant compared to post-combustion, thus uncertainties in process performance are higher.

According to Sathre et al. [89], the energy penalty for the use of CCS technology in WtE plants would be reduced to 7% in the future (Fig. 4). It can be accomplished by the employment of highly efficient MSW gasification technology integrated with a gas turbine (IGCC), in which CO<sub>2</sub> is separated from hydrogen that is relatively easier than the separation of carbon dioxide from nitrogen. Thus, the energy penalty of pre-combustion is potentially lower than that of post-combustion. The next option for reduction of energy penalty of CCS can be presumably the development of air separation

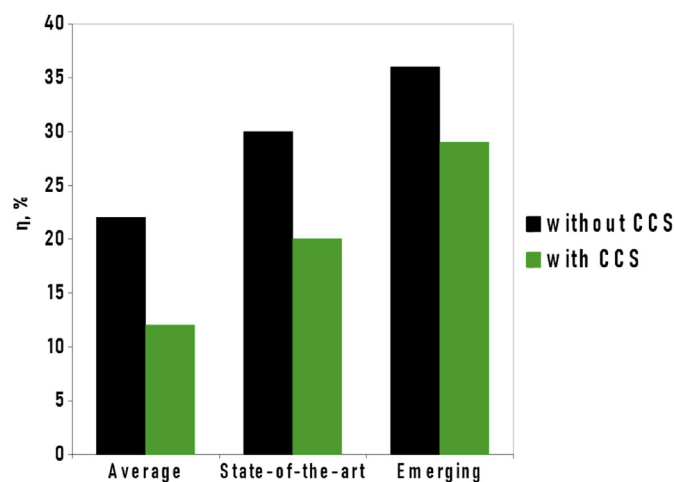


Fig. 4. Efficiency of WtE plants with and without CCS in dependence of development level, data source: Sathre et al. [89].

methods in oxy-fuel combustion and replacement of cryogenic distillation by more efficient technologies, such as chemical looping air separation.

Nevertheless, it is difficult to say whether a 7% decrease in efficiency will be sufficient to make carbon capture technology attractive to waste incineration plants. In our view, carbon capture technology should be improved to reduce the efficiency of incineration plants as little as possible. However, taking into account that waste is cheap, partly organic and widely available, a decrease in efficiency is not as relevant as in the case of coal-fired power plants.

#### 4. Oxy-fuel combustion of MSW

Application of oxy-fuel combustion in the incineration plant is noteworthy since, except carbon capture, it can bring several merits, such as an increase in process temperature due to higher oxygen concentration and the decrease of the auxiliary fuel consumption that is usually used to keep the required temperature. Besides, oxy-fuel combustion causes that the volume of flue gas decreases to roughly 1/5 since during air combustion, approximately 80% of the flue gas is nitrogen. As a result, the efficiency of the boiler is higher, which is confirmed by Tang et al. [87] and it also allows to reduce the size of the flue gas cleaning devices, thus the investment costs will be probably lower. Higher oxygen concentration results in greater oxidation of hydrocarbons. Besides, due to the absence of nitrogen in flue gas, the concentration of pollutants is higher, so the efficiency of desulphurisation or other impurities removal can increase. To the best of the authors' knowledge, with the exception of waste from sewage sludge, there is currently a lack of available research on oxy-fuel combustion of waste in pilot facilities. The papers that will be presented focus mainly on thermal degradation of waste samples under various conditions, with particular emphasis on combustion parameters such as ignition, combustion rate, and burnout, as well as gaseous and heavy metal emissions in order to draw conclusions and propose the possibilities of further technology development.

##### 4.1. Thermogravimetric analysis

To obtain useful data of thermal behaviour and calculate kinetic parameters that can be used to model the oxy-fired combustion chamber, the first logical step of the research is the analysis of

thermal decomposition of various waste feedstocks, separately and as fuel mixture, under different conditions, i.e. various heating rates, atmospheres or temperatures. To carry out the study, thermogravimetric analysis (TGA) is usually employed, which is often coupled with Fourier-transform infrared spectroscopy (FTIR), gas chromatography (GC) or mass spectrometry (MS) to identify gaseous products that are released during the process.

#### 4.1.1. Pyrolysis of MSW in CO<sub>2</sub> and N<sub>2</sub> atmosphere

Pyrolysis is an important initial stage of the combustion process since it determines such parameters as ignition, the stability of flame, product distribution and burnout. Therefore, in most cases, oxy-fuel combustion and pyrolysis are examined in parallel or pyrolysis is investigated before oxy-fuel combustion tests [90]. Lai et al. [91] investigated pyrolysis of waste in different atmospheres, including N<sub>2</sub>, CO<sub>2</sub> and N<sub>2</sub>/CO<sub>2</sub> mixtures. The results showed that under the carbon dioxide conditions the volatilization occurred between 200°C and 550°C, while above 650°C the thermal decomposition of mineral and the char gasification took place. Furthermore, authors noted that replacement of N<sub>2</sub> by CO<sub>2</sub> encouraged the char gasification and solid residue differed remarkably since in the nitrogen atmosphere residues were char and ash and in CO<sub>2</sub> residues were practically ash.

The next study, conducted by Tang et al. [90] concerned the pyrolysis of rubber, plastics, wood, paper, textile and kitchen waste in CO<sub>2</sub> atmosphere. They used thermogravimetric analyzer (TGA) coupled with Fourier transform infrared (FTIR). The results showed that CO<sub>2</sub> below 600°C behaved as the inert atmosphere. Whereas, above 600°C atmosphere changed the location of DTG peaks as well as formation mechanisms. Authors observed that CO<sub>2</sub> atmosphere inhibits polymerization reactions of tars and intensifies cracking of tars into gases. Moreover, it was found that pyrolysis in CO<sub>2</sub> at high temperatures enhances char cracking and its reactivity as well as decreases the amount of char. What is more, they suggested that these phenomena may affect the char combustion and fuel burnout during oxy-fuel combustion. Tang et al. [92] employed tubular electrical furnace to investigate char characteristics, including the analysis of char pore structure, during pyrolysis of waste in N<sub>2</sub> and CO<sub>2</sub> atmospheres. Results confirmed the previous findings that char reacted with CO<sub>2</sub> at high temperature. Since at the temperature of 800°C, the pore surface area of CO<sub>2</sub> char was smaller than of char obtained in N<sub>2</sub> atmosphere.

Petrochemical wastewater is also considered a problematic waste material, especially in countries where the petroleum and petrochemical industry has a vast scale, such as China, because improper management of wastewater sludge can cause serious environmental pollution. In Ref. [93] authors investigated pyrolysis of petrochemical wastewater sludge in N<sub>2</sub> and CO<sub>2</sub> atmospheres. Similarly to previous studies, they found that at lower temperatures CO<sub>2</sub> behaves as an inert atmosphere. Moreover, they distinguished three stages of material decomposition under CO<sub>2</sub> conditions: drying, devolatilization and char-CO<sub>2</sub> gasification at high

temperatures, while under N<sub>2</sub> conditions only two steps (drying and devolatilization). Additionally, they observed that curves of weight loss are moved in toward direction, which means that reactions are delayed. It can be explained by higher density and specific heat of CO<sub>2</sub> compared to N<sub>2</sub> as well as different radiative properties.

Summarizing findings on pyrolysis of different waste materials under N<sub>2</sub> and CO<sub>2</sub> atmosphere one should be said that at low temperatures there is no significant differences between atmospheres, while at high temperatures, CO<sub>2</sub> acts like a gasification agent that reacts with char. These conclusions are supported by Ref. [94–96], and they can be explained by the fact that char-CO<sub>2</sub> gasification is highly endothermic reaction, which means that it requires a lot of energy, and therefore occurs only at high temperatures.

#### 4.1.2. Combustion of MSW under CO<sub>2</sub>/O<sub>2</sub> conditions

Lai et al. [97] examined combustion process of MSW, they employed different atmospheres to compare the results, namely N<sub>2</sub>/O<sub>2</sub> and CO<sub>2</sub>/O<sub>2</sub> with various O<sub>2</sub> concentrations. Besides, kinetic parameters were calculated based on the nth order reaction fitting model. Table 1 presents the results of the kinetic analysis. Scientists found that the largest decrease in sample weight was between 200°C and 540°C, and the maximum mass loss rates increased when oxygen concentration was higher. Moreover, higher heating rates resulted in superior weight loss rate and some reactions can be overlapped. Besides, the authors claimed that the three-step reaction model can adjust the mass loss of samples accordingly.

In [98–100] authors presented a thermogravimetric analysis of waste materials combustion under CO<sub>2</sub>/O<sub>2</sub> conditions in order to obtain kinetic parameters (Table 1) and evaluate the thermal degradation of different feedstocks. The conclusion was that the direct replacement of nitrogen with carbon dioxide negatively affects combustion since ignition is delayed and the maximum weight loss rate is lower. However, as the oxygen concentration in the CO<sub>2</sub>/O<sub>2</sub> mixture increases, the combustion parameters approach those occurring during air combustion. The similar combustion performance as under 80%N<sub>2</sub>/20%O<sub>2</sub> conditions was obtained in 70%CO<sub>2</sub>/30%O<sub>2</sub> atmosphere. It should be stressed out that similar observations were noted during the oxy-combustion of coal and other fuels [36,38] and it was ascribed to the lower heat loss caused by a decreased amount of diluent gas (CO<sub>2</sub>) as well as enhanced heat transfer and oxygen propagation. Besides, they reported that reactions of char oxidation (Eq. (2)) and calcium carbonate decomposition (Eq. (3)) during the oxy-fuel combustion was inhibited to toward direction due to a very high carbon dioxide concentration. While at elevated temperatures (around 900°) Boudouard reaction (Eq. (4)) appeared.



**Table 1**  
Results of kinetic analyses of different waste materials in 80%CO<sub>2</sub>/20%O<sub>2</sub> atmosphere.

Material	logA <sub>1</sub> , 1/s	E <sub>1</sub> , kJ/mol	n1	logA <sub>2</sub> , 1/s	E <sub>2</sub> , kJ/mol	n2	logA <sub>3</sub> , 1/s	E <sub>3</sub> , kJ/mol	n3	Correlation coefficient	Source
MSW <sub>1</sub>	19.692	209.443	3.137	11.456	145.744	1.465	2.277	58.302	2.119	0.999647	[97]
MSW <sub>2</sub>	19.08	209.44	3.14	11.46	145.74	1.47	2.28	58.30	2.20	0.999647	[99]
PCV	12.87	165.72	1.53	10.37	185.89	2.69	-2.80	11.22	0.07	0.999882	[100]
Leather	11.93	150.36	2.09	6.55	128.3	2.99	13.09	349.58	0.46	0.998619	
Rubber	3.79	91.64	2.65	2.93	132.27	0.17	7.10	195.49	3.47	0.995446	
Paper	11.5	157.7	3.9	32.5	255.8	0.8	-5.6	90.5	0.4	0.998266	[98]
Fruit waste	6.4	97.4	4.6	32.0	250.0	0.3	-1.6	86.2	1.0	0.994585	
Plant residue	6.7	93.7	1.0	2.4	58.0	2.9	6.5	39.0	1.2	0.998081	



Oxy-fuel combustion of petrochemical wastewater sludge was presented in Ref. [93]. Authors examined combustion under different combustion parameters, including the atmosphere, heating rate and oxygen concentration, using a thermogravimetric analyser (TGA). They found that the combustion rate in the  $\text{CO}_2/\text{O}_2$  atmosphere was lower compared to  $\text{N}_2/\text{O}_2$ , because of different properties of gases. Moreover, higher heating rates can result in quicker ignition and better burnout. While an enriched oxygen atmosphere can intensify heat production. Besides, Niu et al. [101] investigated the oxy-fuel combustion of sewage sludge. The results indicated that (a) the decomposition of sewage sludge consisted of two peaks that were located at devolatilization and oxidation periods, (b) the thermal lag decreased with increasing heating rate, (c) during combustion in  $\text{O}_2/\text{CO}_2$  atmosphere at an analogous concentration of oxygen as in air combustion, combustion performance was worse and (d) ignition index and comprehensive performance indices of the sample in 30% $\text{O}_2$ /70% $\text{CO}_2$  were similar to that obtained during air combustion.

In conclusion, presented studies indicated that direct replacement of nitrogen by carbon dioxide causes that the ignition is delayed and the combustion rate is lower. Nevertheless, some authors reported that with the higher content of oxygen in  $\text{CO}_2/\text{O}_2$  mixture the combustion performance can be improved, and the most similar combustion characteristics to air burning were obtained in 30% $\text{O}_2$ /70% $\text{CO}_2$  atmosphere. Besides, the model-fitting was the most frequently chosen approach for calculating kinetic parameters of MSW degradation. This is the most practical approach to estimate kinetic parameters, while there are other theoretical approaches that are also in use, for example, density functional theory (DFT) [10].

#### 4.2. Heavy metals

During combustion of municipal solid waste (MSW), knowledge about heavy metal behaviour is crucial for the control of emission of pollutants since, in comparison with other solid fuels, such as coal or biomass, the waste contains a relatively high amount of heavy metals that are highly harmful to both natural environment and human health. Furthermore, the amount of ash can be a serious issue in the combustion process since there is a high risk of slagging, bed agglomeration, fouling and corrosion of the devices, as well as ash, could inhibit a heat transfer and consequently, decrease combustion efficiency [102]. Sørnum et al. [103,104] studied the impact of varying operational parameters and the composition of waste on the devolatilization, chemical composition of heavy metals and condensing behaviour under air combustion conditions in a grate furnace, using equilibrium calculations. Whereas, Wang et al. [105] used X-ray spectroscopy (SEM-EDX) and X-ray fluorescence (XRF) to characterise ash deposits from municipal solid waste-to-energy (WtE) plants.

The first study of the behaviour of heavy metals during oxy-fuel combustion of municipal solid waste was presented by Tang et al. [106]. Authors used a lab-scale electrically heated tube furnace to assess the impact of MSW combustion in various atmospheres on hazardous heavy metals (Pb, Cd, Zn, Cr, Ni and Cu) in the bottom ashes. The overall conclusion was that the  $\text{CO}_2/\text{O}_2$  atmosphere increased enrichment of heavy metals in bottom ashes, which meant that a lower amount of heavy metals was in the fly ash and thus, the emission to the atmosphere was lower. The effect of temperature on evaporation of heavy metals was the most

pronounced for the medium volatile metal Pb, and the smallest for the low volatiles Cr and Ni. Moreover, change in temperature had a bigger impact on (PVC) than for wood sawdust and paper mixture. Nevertheless, the content of heavy metals in ashes during oxy-fuel combustion was higher than China's requirements of soil environmental quality standards.

The volatilization of cadmium, chromium and zinc during the oxy-fuel combustion of food waste and plastic (PVC) in a lab-scale tubular furnace was studied by Ke et al. [107]. In general, the results indicated that the amount of ash was greater for food waste. Besides, during oxy-fuel combustion, ash rate of food waste was bigger than during air combustion. However, at higher temperatures, the amount of ash rate decreased because of decomposition of  $\text{CaCO}_3$ . While, the ash rate of PVC did not change notably after the replacement of nitrogen by carbon dioxide and it was explained by the fact that PVC did not contain calcium carbonate, which reacted with  $\text{CO}_2$ . Moreover, the volatilization of Cd and Cr was lower in oxy-combustion conditions, however, the volatilization of Zn increased in  $\text{CO}_2/\text{O}_2$  atmosphere. Furthermore, researchers claimed that incineration operating conditions just slightly reduce the volatilization of heavy metals and using sorbents is required to meet the requirements.

Magdziarz et al. [102], Jang et al. [108] studied the sewage sludge ashes from combustion in  $\text{N}_2/\text{O}_2$  and  $\text{CO}_2/\text{O}_2$  atmospheres in a 12-kW bench-scale circulating fluidized-bed combustor. The temperature of the process was held at 850°C and different  $\text{CO}_2/\text{O}_2$  ratios were tested. Moreover, such analytical techniques as X-ray diffraction (XRD), SEM-EDX and TG-DSC were applied to perform analyses of ashes. Generally, results showed that the main compounds of the ashes of sewage sludge are  $\text{SiO}_2$ ,  $\text{Fe}_2\text{O}_3$ ,  $\text{P}_2\text{O}_5$ ,  $\text{CaO}$ ,  $\text{Al}_2\text{O}_3$ ,  $\text{MgO}$ ,  $\text{TiO}_2$ ,  $\text{K}_2\text{O}$ ,  $\text{Na}_2\text{O}$  and  $\text{SO}_3$ . Moreover, the combustion atmosphere did not influence significantly the chemical composition of ash and corrosion should not be a problem during oxy-fuel combustion of sewage sludge due to low levels of potassium, sodium and chlorine. Thus, sewage sludge can be successfully combusted in oxy-fuel technology.

##### 4.2.1. Sorbents effect

The next works focused on finding effective sorbents to control the emission of heavy metals. Tang et al. [109] investigated the behaviour of copper (Cu), nickel (Ni) and zinc (Zn) during oxy-fuel combustion of tire rubber and high-density polyethylene (HDPE) under  $\text{N}_2/\text{O}_2$  and  $\text{CO}_2/\text{O}_2$  atmosphere with the addition of limestone and calcium oxide (CaO). Results demonstrated that the replacement of  $\text{N}_2$  by  $\text{CO}_2$  as well as the addition of limestone decreased the evaporation of heavy metals. Moreover, the capture efficiency of limestone for Zn, Cu and Ni was affected by the waste composition. In the case of tire rubber, combustion in  $\text{CO}_2/\text{O}_2$  atmosphere favoured the capture of Zn, Cu and Ni, but not in the case of HDPE. Although the performance of limestone was worse than CaO for capturing Cu and Ni, the cost of limestone was lower than CaO. Therefore, limestone offered the potential for a low-cost effective medium to control heavy metals during MSW combustion.

Furthermore, Ke et al. [110] studied the effect of the temperature of the furnace, sorbents types and ratio between carbon dioxide and oxygen on adsorption of heavy metals (Al, Cr and Zn). They found that at higher temperatures more aluminium was in the bottom ash, however, the volatilization of zinc increased. Besides,  $\text{CaCO}_3$  did not absorb Al, while calcium oxide (nature or modified) had an excellent performance for Al capture. None of the sorbents could capture the chromium.  $\text{CO}_2/\text{O}_2$  ratio had a large impact on the capture of Cr and Zn but did not affect Al, and the decrease of  $\text{CO}_2/\text{O}_2$  ratio helped capture Cr and Zn.

Summarizing, the heavy metal problem is a very complex issue and there is still not enough research on heavy metals behaviour



during oxy-fuel combustion. Studies presented in this paper show that a major impact on heavy metals had the composition of waste and process temperature. The oxy-fuel combustion of waste requires the use of sorbents to reduce volatilization of heavy metals, and the addition of the limestone can be an effective method to control the heavy metals.

#### 4.2.2. Emissions

A major concern associated with waste combustion is pollution emission, therefore they are subject to the research of many scientists. Emissions are highly related to fuel composition as well as combustion conditions. Tang et al. [111] investigated the oxy-fuel combustion of MSW and the effect of heating rate, temperature, and oxygen concentration on NO<sub>x</sub> and SO<sub>2</sub> emissions. The results showed that both temperature and atmosphere have an impact on emission levels. In the case of NO<sub>x</sub>, with increasing oxygen concentration in the CO<sub>2</sub>/O<sub>2</sub> atmosphere, emission was higher. Besides, replacement of N<sub>2</sub> by CO<sub>2</sub> decreased NO<sub>x</sub> emission only at a temperature above 800°C, and reduced SO<sub>2</sub> emission when the temperature was below 1000°C. At 1000°C, in order to simultaneously remove SO<sub>2</sub> and NO<sub>x</sub> in 80%CO<sub>2</sub>/20%O<sub>2</sub> atmosphere sorbents were required. While Sung et al. [112] presented an investigation on oxy-fuel co-combustion of sewage sludge and wood pellets. Experiments were performed in a 30 kWth CFB system. They continuously registered the temperature and the concentration of O<sub>2</sub>, CO<sub>2</sub>, CO and NO in flue gases and evaluated the impact of fuel composition, oxygen injection rates, and flue gas recirculation. They observed that the most uniform temperature gradient appeared at 60% of the flue gas recirculation rate and the CO and NO concentration decreased to 0.91% and 14 ppm, respectively. Moreover, Dai et al. [113] performed co-combustion of PVC and food waste in CO<sub>2</sub>/O<sub>2</sub> atmospheres to gain the knowledge of the HCl emission due to high content of chlorine in the waste. They found that temperature as well as CO<sub>2</sub>/O<sub>2</sub> ratio have an impact on Cl–HCl conversion.

## 5. Conclusion

The work provides the overview of currently available CO<sub>2</sub> capture methods, with particular attention to oxy-fuel combustion since it is considered as a most promising method of carbon capture methods. Besides, a review of waste-to-energy facilities is presented and the possibilities of their integration with CO<sub>2</sub> capture technology. Among available methods of thermal conversion of waste to energy, gasification is considered as the most efficient, however, it is currently only one commercial IGCC plant, in which waste is a source of energy. In addition, cleaning of the syngas is expensive causing that from the LCA perspective, incineration is still a better option for waste management. A promising method of waste utilization, which potentially increase of overall plant's performance is chemical looping combustion/gasification. Besides, it was found that using CaSO<sub>4</sub> as an oxygen carrier demonstrates a significant reduction of dioxins, however, this method is far from commercial use. While incineration is the most mature and common technique of WtE systems (the number of operating incinerators is more than 1200) and the application of carbon capture in existing plants will contribute to a large reduction of CO<sub>2</sub> concentration in the atmosphere and mitigate climate change.

Nowadays, there are four incineration plants, in which post-combustion carbon capture technology is successfully integrated. However, it was found that CO<sub>2</sub> capture based on the MEA technique results in a large energy penalty. Hence, to decrease the plant's efficiency drop causing by carbon capture process, further research should be focused on the implementation of more efficient methods of carbon sequestration, such as oxy-fuel

combustion that according to Ref. [88] can reduce the drop in efficiency to 9.57%. However, this result was obtained under the assumption of the steady-state process. To obtain more reliable results and predict the behaviour of the system in changing conditions, dynamic simulations of the oxy-incineration plant should be studied, especially that municipal solid waste are non-homogeneous materials [70,114].

It is expected that application of oxy-fuel combustion in incineration plant (a) decreases the energy penalty of the use of CCS, (b) reduces exhaust gas stream by 80% compared to air combustion and thus, increases boiler efficiency, (c) increases of process temperature due to higher oxygen concentration and results in smaller auxiliary fuel consumption and (d) decreases emission of NO<sub>x</sub> and other pollutants. However, it should be remembered that O<sub>2</sub>/CO<sub>2</sub> atmosphere affects the combustion process significantly and MSW is very demanding fuel. Some crucial aspects of the quality of bottom and fly ash and air leakage in the feeding system still remain unsolved. Thus, oxy-fuel combustion should be integrated very carefully to the incineration plant. Besides, to improve the efficiency of oxy-fuel combustion the new air separation method with lower energy demand should be developed.

From the literature review of the current state of knowledge of oxy-fuel combustion of waste the following conclusions can be made:

- During the pyrolysis of waste materials, the replacement of N<sub>2</sub> to CO<sub>2</sub> has a significant impact only at high temperatures (usually above 600°C) since the reaction between carbon dioxide and char is highly endothermic.
- Combustion performance highly depends on oxygen concentration, flue gas recirculation, and type of fuel. Researchers reported that during oxy-fuel combustion in 30%O<sub>2</sub>/70%CO<sub>2</sub> atmosphere, the combustion characteristic is similar to those obtained during air combustion.
- The most often employed method to calculate the kinetic parameters is model-fitting method and during degradation of MSW three steps are considered.
- The fate of heavy metals is ambiguous because it largely depends on the composition of the waste, but it can be stated that during oxy-fuel combustion more heavy metals are found in bottom ashes, and therefore less heavy metals are emitted to the atmosphere. Nevertheless, sorbents should be used to reduce heavy metal emissions to acceptable standards.

### 5.1. Future work

As shown, oxy-fuel combustion of waste is a very promising technology that can be implemented in hundreds of waste incineration plants in Europe and worldwide, but it still requires a lot of research. In our opinion, the investigation of oxy-fuel combustion should be mainly focused on (a) searching of optimal O<sub>2</sub>/CO<sub>2</sub> ratio to minimize the emission level and maximize the combustion performance, (b) research on new air separation methods, for example, chemical looping, and (c) looking for the most favourable adaptation of oxy-fuel combustion to incineration plant, for example by using of waste heat to power the auxiliary devices, such as ASU and compressors. Besides, further research should consist of combining the kinetic data of individual fuels with the waste incinerator chamber model, which will enable the design of furnaces optimized for the disposal of a particular type of waste, as well as analyses of dynamic simulations of the oxy-incineration plants.

## Declaration of competing interest

The authors declare that they have no known competing financial interests or personal relationships that could have appeared to influence the work reported in this paper.

## CRedit authorship contribution statement

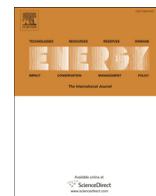
**Paulina Wienchol:** Methodology, Investigation, Writing - original draft, Writing - review & editing, Visualization. **Andrzej Szląk:** Conceptualization, Methodology, Writing - review & editing, Supervision. **Mario Ditaranto:** Conceptualization, Writing - review & editing, Supervision.

## References

- [1] United Nations Climate Change. The paris agreement. <https://unfccc.int/process-and-meetings/the-paris-agreement/the-paris-agreement>. [Accessed 22 February 2019].
- [2] European Commission. Roadmap 2050 - imact assessment and scenario analysis (2012) 1–100. <http://www.roadmap2050.eu/reports>.
- [3] Bennaceur K, Gielen D, Kerr T, Tam C. CO<sub>2</sub> capture and storage: a key carbon abatement option. OECD; 2008.
- [4] Raza A, Gholami R, Rezaee R, Rasouli V, Rabiei M. Significant aspects of carbon capture and storage—a review. *Petroleum*; 2018.
- [5] Pettinau A, Ferrara F, Tola V, Cau G. Techno-economic comparison between different technologies for co<sub>2</sub>-free power generation from coal. *Appl Energy* 2017;193:426–39.
- [6] Sahraei MH, McCalden D, Hughes R, Ricardez-Sandoval L. A survey on current advanced igcc power plant technologies, sensors and control systems. *Fuel* 2014;137:245–59.
- [7] Gerbelová H, Van Der Spek M, Schakel W. Feasibility assessment of co<sub>2</sub> capture retrofitted to an existing cement plant: post-combustion vs. oxy-fuel combustion technology. *Energy Procedia* 2017;114:6141–9.
- [8] Wu F, Argyle MD, Dellenback PA, Fan M. Progress in o<sub>2</sub> separation for oxy-fuel combustion—a promising way for cost-effective co<sub>2</sub> capture: a review. *Prog Energy Combust Sci* 2018;67:188–205.
- [9] Portillo E, Alonso-Fari-nas B, Vega F, Cano M, Navarrete B. Alternatives for oxygen-selective membrane systems and their integration into the oxy-fuel combustion process: a review. *Separ Purif Technol* 2019:115708.
- [10] Yuan Y, You H, Ricardez-Sandoval L. Recent advances on first-principles modeling for the design of materials in co<sub>2</sub> capture technologies. *Chin J Chem Eng* 2019;27:1554–65.
- [11] Zhao H, Wang J. Chemical-looping combustion of plastic wastes for in situ inhibition of dioxins. *Combust Flame* 2018;191:9–18.
- [12] Cormos C-C. Energy and cost efficient manganese chemical looping air separation cycle for decarbonized power generation based on oxyfuel combustion and gasification. *Energy* 2020;191:116579.
- [13] Zheng L. Oxy-fuel combustion for power generation and carbon dioxide (CO<sub>2</sub>) capture. Elsevier; 2011.
- [14] Miranda-Barbosa E, Sigfússon B, Carlsson J, Tzimas E. Advantages from combining ccs with geothermal energy. *Energy Procedia* 2017;114:6666–76.
- [15] Tarkowski R, Uliasz-Misiak B. Prospects for the use of carbon dioxide in enhanced geothermal systems in Poland. *J Clean Prod* 2019;229:1189–97.
- [16] Li Y, Ding Y, Li D, Miao Z. Automatic carbon dioxide enrichment strategies in the greenhouse: a review. *Biosyst Eng* 2018;171:101–19.
- [17] Rahman FA, Aziz MMA, Saidur R, Bakar WAWA, Hainin M, Putrajaya R, Hassan NA. Pollution to solution: capture and sequestration of carbon dioxide (co<sub>2</sub>) and its utilization as a renewable energy source for a sustainable future. *Renew Sustain Energy Rev* 2017;71:112–26.
- [18] Li D, Liu X, Wang C, Xu K, Zha Q, Lv Q, Feng Y, Zhong J, Che D. Numerical study on combustion and heat transfer properties under oxy-fuel condition in a 600mw utility boiler. *Energy Procedia* 2017;105:4009–14.
- [19] Kez V, Liu F, Consalvi J, Strohle J, Epple B. A comprehensive evaluation of different radiation models in a gas turbine combustor under conditions of oxy-fuel combustion with dry recycle. *J Quant Spectrosc Radiat Transf* 2016;172:121–33.
- [20] Guo J, Hu F, Jiang X, Huang X, Li P, Liu Z, Zheng C. Experimental and numerical investigations on heat transfer characteristics of a 35mw oxy-fuel combustion boiler. *Energy Procedia* 2017;114:481–9.
- [21] Bhuiyan AA, Naser J. Numerical modelling of oxy fuel combustion, the effect of radiative and convective heat transfer and burnout. *Fuel* 2015;139:268–84.
- [22] Smart JP, Patel R, Riley GS. Oxy-fuel combustion of coal and biomass, the effect on radiative and convective heat transfer and burnout. *Combustion and ame* 2010;157:2230–40.
- [23] Yang X, Clements A, Szuhánszki J, Huang X, Moguel OF, Li J, Gibbins J, Liu Z, Zheng C, Ingham D, et al. Prediction of the radiative heat transfer in small and large scale oxy-coal furnaces. *Appl Energy* 2018;211:523–37.
- [24] Shan F, Lin Q, Zhou K, Wu Y, Fu W, Zhang P, Song L, Shao C, Yi B. An experimental study of ignition and combustion of single biomass pellets in air and oxy-fuel. *Fuel* 2017;188:277–84.
- [25] Wang Z, Xiong Y, Cheng X, Liu M. Experimental study on the ame propagation characteristics of heavy oil oxy-fuel combustion. *J Energy Inst* December 2019;92(6):1630–40.
- [26] Tanui JK, Kioni PN, Mirre T, Nowitzki M. The effect of carbon dioxide on ame propagation speed of wood combustion in a fixed bed under oxy-fuel conditions. *Fuel Process Technol* 2018;179:285–95.
- [27] Taniguchi M, Shibata T, Kobayashi H. Prediction of lean ammability limit and ame propagation velocity for oxy-fuel fired pulverized coal combustion. *Proc Combust Inst* 2011;33:3391–8.
- [28] Jovanović R, Swiatkowski B, Kakietek S, Škobalj P, Lazović I, Cvetinović D. Mathematical modelling of swirl oxy-fuel burner ame characteristics. *Energy Convers Manag* 2019;191:193–207.
- [29] Liu J, Liu Z, Chen S, Santos SO, Zheng C. A numerical investigation on ame stability of oxy-coal combustion: effects of blockage ratio, swirl number, recycle ratio and partial pressure ratio of oxygen. *International Journal of Greenhouse Gas Control* 2017;57:63–72.
- [30] Duan Y, Duan L, Wang J, Anthony EJ. Observation of simultaneously low co, nox and so<sub>2</sub> emission during oxy-coal combustion in a pressurized uidized bed. *Fuel* 2019;242:374–81.
- [31] Ostrycharczyk M, Krochmalny K, Czerep M, Pawlak-Kruczek H, Zgóra J, Baranowski M. Examinations of the sulfur emission from pulverized lignite fuel, under pyrolysis and oxy-fuel combustion condition. *Fuel* 2019;241:579–84.
- [32] Sher F, Pans MA, Sun C, Snape C, Liu H. Oxy-fuel combustion study of biomass fuel in a 20 kwth uidized bed combustor. *Fuel* 2018;215:778–86.
- [33] Izquierdo M, de las Obras-Loscertales M, de Diego L, García-Labiano F, Mendiara T, Abad A, Gayán P, Adánez J. Mercury emissions from coal combustion in uidized beds under oxy-fuel and air conditions: inuence of coal characteristics and o<sub>2</sub> concentration. *Fuel Process Technol* 2017;167:695–701.
- [34] Shimokuri D, Fukuba S, Ishizuka S. Fundamental investigation on the fuel-nox emission of the oxy-fuel combustion with a tubular ame burner. *Proc Combust Inst* 2015;35:3573–80.
- [35] Shah IA, Gou X, Zhang Q, Wu J, Wang E, Liu Y. Experimental study on nox emission characteristics of oxy-biomass combustion. *J Clean Prod* 2018;199:400–10.
- [36] Buhre BJ, Elliott LK, Sheng C, Gupta RP, Wall TF. Oxyfuel combustion technology for coal-fired power generation. *Prog Energy Combust Sci* 2005;31:283–307.
- [37] Wall TF. Combustion processes for carbon capture. *Proc Combust Inst* 2007;31:31–47.
- [38] Toftegaard MB, Brix J, Jensen PA, Glarborg P, Jensen AD. Oxy-fuel combustion of solid fuels. *Prog Energy Combust Sci* 2010;36:581–625.
- [39] Scheffknecht G, Al-Makhadmeh L, Schnell U, Maier J. Oxy-fuel coal combustion: a review of the current state-of-the-art. *International Journal of Greenhouse Gas Control* 2011;5:S16–35.
- [40] Chen L, Yong SZ, Ghoniem AF. Oxy-fuel combustion of pulverized coal: characterization, fundamentals, stabilization and cfd modeling. *Prog Energy Combust Sci* 2012;38:156–214.
- [41] Singh RI, Kumar R. Current status and experimental investigation of oxy-fired uidized bed. *Renew Sustain Energy Rev* 2016;61:398–420.
- [42] Bilgili F, Kocak E, Bulut U, Kuşkaya S. Can biomass energy be an efficient policy tool for sustainable development? *Renew Sustain Energy Rev* 2017;71:830–45.
- [43] Liu Q, Shi Y, Zhong W, Yu A. Co-firing of coal and biomass in oxy-fuel fluidized bed for co<sub>2</sub> capture: a review of recent advances. *Chin J Chem Eng* October 2019;27(10):2261–72.
- [44] Kaza S, Yao L, Bhada-Tata P, Van Woerden F. What a waste 2.0: a global snapshot of solid waste management to 2050. World Bank Publications; 2018.
- [45] Union E. Directive 2009/28/ec of the european parliament and of the council of 23 april 2009 on the promotion of the use of energy from renewable sources and amending and subsequently repealing directives 2001/77/ec and 2003/30/ec. *Official Journal of the European Union* 2009;5:2009.
- [46] Mukherjee C, Denney J, Mbonimpa E, Slagley J, Bhowmik R. A review on municipal solid waste-to-energy trends in the USA. *Renew Sustain Energy Rev* 2020;119:109512.
- [47] Porteous A. Why energy from waste incineration is an essential component of environmentally responsible waste management. *Waste Manag* 2005;25:451–9.
- [48] Pires JCM, da Cunha Goncalves AL. Bioenergy with carbon capture and storage: using natural resources for sustainable development. Academic Press; 2019.
- [49] Iadysz PG, Ziebiak A. Environmental analysis of bio-ccs in an integrated oxy-fuel combustion power plant with co<sub>2</sub> transport and storage. *Biomass Bioenergy* 2016;85:109–18.
- [50] Pour N, Webley PA, Cook PJ. Potential for using municipal solid waste as a resource for bioenergy with carbon capture and storage (beccs). *International Journal of Greenhouse Gas Control* 2018;68:1–15.
- [51] Pour N, Webley PA, Cook PJ. A sustainability framework for bioenergy with carbon capture and storage (beccs) technologies. *Energy Procedia* 2017;114:6044–56.
- [52] Bui M, Fajardy M, Mac Dowell N. Bio-energy with carbon capture and storage

- (beccs): opportunities for performance improvement. *Fuel* 2018;213:164–75.
- [53] Ricci O, Selloso S. Global and regional potential for bioelectricity with carbon capture and storage. *Energy Pol* 2013;52:689–98.
- [54] Jouhara H, Czajczyńska D, Ghazal H, Krzyżyńska R, Anguilano L, Reynolds A, Spencer N. Municipal waste management systems for domestic use. *Energy* 2017;139:485–506.
- [55] Kumar A, Samadder SR. A review on technological options of waste to energy for effective management of municipal solid waste. *Waste Manag* 2017;69:407–22.
- [56] Moya D, Aldás C, López G, Kaparaju P. Municipal solid waste as a valuable renewable energy resource: a worldwide opportunity of energy recovery by using waste-to-energy technologies. *Energy Procedia* 2017;134:286–95.
- [57] Makarichi L, Jutidamrongphan W, Techato K-a. The evolution of waste-to-energy incineration: a review. *Renew Sustain Energy Rev* 2018;91:812–21.
- [58] Basu P. Biomass gasification, pyrolysis and torrefaction: practical design and theory. Academic press; 2018.
- [59] Sipra AT, Gao N, Sarwar H. Municipal solid waste (msw) pyrolysis for bio-fuel production: a review of effects of msw components and catalysts. *Fuel Process Technol* 15 June 2018;175:131–47.
- [60] Gandidi IM, Susila MD, Pambudi NA. Production of valuable pyrolytic oils from mixed municipal solid waste (msw) in Indonesia using non-isothermal and isothermal experimental. *Case studies in thermal engineering* 2017;10:357–61.
- [61] Chhabra V, Shastri Y, Bhattacharya S. Kinetics of pyrolysis of mixed municipal solid waste—a review. *Procedia environmental sciences* 2016;35:513–27.
- [62] Matsakas L, Gao Q, Jansson S, Rova U, Christakopoulos P. Green conversion of municipal solid wastes into fuels and chemicals. *Electron J Biotechnol* 2017;26:69–83.
- [63] Hognert J, Nilsson L. The small-scale production of hydrogen, with the co-production of electricity and district heat, by means of the gasification of municipal solid waste. *Appl Therm Eng* 2016;106:174–9.
- [64] Mazzoni L, Janajreh I. Plasma gasification of municipal solid waste with variable content of plastic solid waste for enhanced energy recovery. *Int J Hydrogen Energy* 2017;42:19446–57.
- [65] Begum S, Rasul M, Cork D, Akbar D. An experimental investigation of solid waste gasification using a large pilot scale waste to energy plant. *Procedia Engineering* 2014;90:718–24.
- [66] Rudra S, Tesfagaber YK. Future district heating plant integrated with municipal solid waste (msw) gasification for hydrogen production. *Energy* 2019;180:881–92.
- [67] Cormos C-C. Hydrogen and power co-generation based on coal and biomass/solid wastes co-gasification with carbon capture and storage. *Int J Hydrogen Energy* 2012;37:5637–48.
- [68] Mazzoni L, Janajreh I, Elagrouty S, Ghenai C. Modeling of plasma and entrained ow co-gasification of msw and petroleum sludge. *Energy* 2020:117001.
- [69] Lyngfelt A. Chemical-looping combustion of solid fuels—status of development. *Appl Energy* 2014;113:1869–73.
- [70] Lucio M, Ricardez-Sandoval LA. Dynamic modelling and optimal control strategies for chemical-looping combustion in an industrial-scale packed bed reactor. *Fuel* 2020;262:116544.
- [71] Chen P, Sun X, Gao M, Ma J, Guo Q. Transformation and migration of cadmium during chemical-looping combustion/gasification of municipal solid waste. *Chem Eng J* 2019;365:389–99.
- [72] Bi W-z, Zhao R-d, Chen T-j, Wu J-l, Wu J-h. Study on the formation of pccdd/fs in pvc chemical looping combustion. *J Fuel Chem Technol* 2015;43:884–9.
- [73] Ma J, Wang J, Tian X, Zhao H. In-situ gasification chemical looping combustion of plastic waste in a semi-continuously operated uidized bed reactor. *Proc Combust Inst* 2019;37:4389–97.
- [74] Dastjerdi B, Strezov V, Kumar R, Behnia M. An evaluation of the potential of waste to energy technologies for residual solid waste in new south wales, Australia. *Renew Sustain Energy Rev* 2019;115:109398.
- [75] Dong J, Tang Y, Nzihou A, Chi Y, Weiss-Hortala E, Ni M. Life cycle assessment of pyrolysis, gasification and incineration waste-to-energy technologies: theoretical analysis and case study of commercial plants. *Sci Total Environ* 2018;626:744–53.
- [76] Malinauskaitė J, Jouhara H, Czajczyńska D, Stanchev P, Katsou E, Rostkowski P, Thorne RJ, Colon J, Ponsá S, Al-Mansour F, et al. Municipal solid waste management and waste-to-energy in the context of a circular economy and energy recycling in europe. *Energy* 2017;141:2013–44.
- [77] Cyranka M, Jurczyk M, Pająk T. Municipal waste-to-energy plants in Poland—current projects. In: *E3S Web of conferences*, vol. 10. EDP Sciences; 2016. 00070.
- [78] Lausset C, Cherubini F, Oreggioni GD, del Alamo Serrano G, Becidan M, Hu X, Rørstad PK, Strømman AH. Norwegian wasteto- energy: climate change, circular economy and carbon capture and storage. *Resour Conserv Recycl* 2017;126:50–61.
- [79] Hulgaard T, MSc IS. Integrating waste-to-energy in copenhagen, Denmark. In: *Proceedings of the institution of civil engineers-civil engineering*, vol. 171. Thomas Telford Ltd; 2018. p. 3–10.
- [80] Jurczyk M, Mikus M, Dziedzic K. Flue gas cleaning in municipal waste-to-energy plants—part 1. *Infrastruktura i Ekologia Terenów Wiejskich*; 2016.
- [81] Saga City: the world's best kept secret (for now) - global CCS Institute. <https://www.globalccsinstitute.com/news-media/insights/saga-city-the-worlds-best-kept-secret-for-now/>; 2018.
- [82] Toshiba : News Release (10 Aug. Toshiba complete installation of world's first commercial-use CCU system in incineration plant, 2016. <https://www.toshiba.co.jp/about/press/2016%7b%5f%7d08/pr1001.htm>; 2016.
- [83] PRESS RELEASE Waste-to-energy company tackles CO2 emissions with large-scale CO2 capture installation. Technical Report; 2018.
- [84] Kearns DT. Waste-to-energy with ccs: a pathway to carbon-negative power generation. 2019.
- [85] Huttenhuis P, Roeloffzen A, Versteeg G. CO2 capture and re-use at a waste incinerator. *Energy Procedia* 2016;86:47–55.
- [86] Svaalestuen J, Bekken SG, Eide LI. CO2 capture technologies for energy intensive industries. *Energy Procedia* 2017;114:6316–30.
- [87] Tang Y, Ma X, Lai Z, Chen Y. Energy analysis and environmental impacts of a msw oxy-fuel incineration power plant in China. *Energy Pol* 2013;60:132–41.
- [88] Ding G, He B, Cao Y, Wang C, Su L, Duan Z, Song J, Tong W, Li X. Process simulation and optimization of municipal solid waste fired power plant with oxygen/carbon dioxide combustion for near zero carbon dioxide emission. *Energy Convers Manag* 2018;157:157–68.
- [89] Sathre R, Gustavsson L, Le Truong N. Climate effects of electricity production fuelled by coal, forest slash and municipal solid waste with and without carbon capture. *Energy* 2017;122:711–23.
- [90] Tang Y, Ma X, Wang Z, Wu Z, Yu Q. A study of the thermal degradation of six typical municipal waste components in co2 and n2 atmospheres using tga-ftir. *Thermochim Acta* 2017;657:12–9.
- [91] Lai Z, Ma X, Tang Y, Lin H. Thermogravimetric analysis of the thermal decomposition of msw in n2, co2 and co2/n2 atmospheres. *Fuel Process Technol* 2012;102:18–23.
- [92] Tang Y, Ma X, Lai Z, Lin H, Wu J. Char characteristics of municipal solid waste prepared under n2 and co2 atmospheres. *J Anal Appl Pyrol* 2013;101:193–8.
- [93] Chen J, Mu L, Cai J, Yao P, Song X, Yin H, Li A. Pyrolysis and oxy-fuel combustion characteristics and kinetics of petrochemical wastewater sludge using thermogravimetric analysis. *Bioresour Technol* 2015;198:115–23.
- [94] Kwon EE, Kim S, Lee J. Pyrolysis of waste feedstocks in co2 for effective energy recovery and waste treatment. *Journal of CO2 Utilization* 2019;31:173–80.
- [95] Policella M, Wang Z, Burra KG, Gupta AK. Characteristics of syngas from pyrolysis and co2-assisted gasification of waste tires. *Appl Energy* 2019;254:113678.
- [96] Chen S, Meng A, Long Y, Zhou H, Li Q, Zhang Y. Tga pyrolysis and gasification of combustible municipal solid waste. *J Energy Inst* 2015;88:332–43.
- [97] Lai Z, Ma X, Tang Y, Lin H. A study on municipal solid waste (msw) combustion in n2/o2 and co2/o2 atmosphere from the perspective of tga. *Energy* 2011;36:819–24.
- [98] Lai Z, Ma X, Tang Y, Lin H, Chen Y. Thermogravimetric analyses of combustion of lignocellulosic materials in n2/o2 and co2/o2 atmospheres. *Bioresour Technol* 2012;107:444–50.
- [99] Tang Y, Ma X, Lai Z. Thermogravimetric analysis of the combustion of microalgae and microalgae blended with waste in n2/o2 and co2/o2 atmospheres. *Bioresour Technol* 2011;102:1879–85.
- [100] Tang Y, Ma X, Lai Z, Fan Y. Thermogravimetric analyses of co-combustion of plastic, rubber, leather in n2/o2 and co2/o2 atmospheres. *Energy* 2015;90:1066–74.
- [101] Niu S, Chen M, Li Y, Xue F. Evaluation on the oxy-fuel combustion behavior of dried sewage sludge. *Fuel* 2016;178:129–38.
- [102] Magdziarz A, Kosowska-Golachowska M, Kijo-Kleczkowska A, Środa K, Wolski K, Richter D, Musia I T. Analysis of sewage sludge ashes from air and oxy-fuel combustion in a circulating uidized-bed. In: *E3S Web of conferences*, vol. 10. EDP Sciences; 2016. 00054.
- [103] Sorum L, Frandsen FJ, Hustad JE. On the fate of heavy metals in municipal solid waste combustion part i: devolatilisation of heavy metals on the grate. *Fuel* 2003;82:2273–83.
- [104] Sorum L, Frandsen FJ, Hustad JE. On the fate of heavy metals in municipal solid waste combustion. part ii. from furnace to filter. *Fuel* 2004;83:1703–10.
- [105] Wang L, Øye B, Skreiberg Ø, Becidan M, Vatland PS, Fossum M, Stuen J. Characterization of ash deposits from municipal solid waste (msw) incineration plants. *Energy Procedia* 2017;142:630–5.
- [106] Tang Y, Ma X, Yu Q, Zhang C, Lai Z, Zhang X. Heavy metal enrichment characteristics in ash of municipal solid waste combustion in co2/o2 atmosphere. *Waste Manag* 2015;43:247–54.
- [107] Ke C, Ma X, Tang Y, Zheng W, Wu Z. The volatilization of heavy metals during co-combustion of food waste and polyvinyl chloride in air and carbon dioxide/oxygen atmosphere. *Bioresour Technol* 2017;244:1024–30.
- [108] Jang H-N, Kim J-H, Back S-K, Sung J-H, Yoo H-M, Choi HS, Seo Y-C. Combustion characteristics of waste sludge at air and oxyfuel combustion conditions in a circulating uidized bed reactor. *Fuel* 2016;170:92–9.
- [109] Tang Y, Ma X, Zhang C, Yu Q, Fan Y. Effects of sorbents on the heavy metals control during tire rubber and polyethylene combustion in co2/o2 and n2/o2 atmospheres. *Fuel* 2016;165:272–8.
- [110] Ke C, Ma X, Tang Y, Tang F, Zheng W. Effects of natural and modified calcium-based sorbents on heavy metals of food waste under oxy-fuel combustion. *Bioresour Technol* 2019;271:251–7.
- [111] Tang Y, Ma X, Lai Z, Zhou D, Lin H, Chen Y. Nox and so2 emissions from municipal solid waste (msw) combustion in co2/o2 atmosphere. *Energy*

- 2012;40:300–6.
- [112] Sung J-H, Back S-K, Jeong B-M, Kim J-H, Choi HS, Jang H-N, Seo Y-C. Oxy-fuel co-combustion of sewage sludge and wood pellets with ue gas recirculation in a circulating uidized bed. *Fuel Process Technol* 2018;172:79–85.
- [113] Dai M, Yu Z, Tang Y, Ma X. Hcl emission and capture characteristics during pvc and food waste combustion in CO<sub>2</sub>/O<sub>2</sub> atmosphere. *J Energy Inst* 10 October 2019. Available online, In press.
- [114] Sachajdak A, Lappalainen J, Mikkonen H. Dynamic simulation in development of contemporary energy systems—oxy combustion case study. *Energy* 2019;181:964–73.



# Thermogravimetric and kinetic study of thermal degradation of various types of municipal solid waste (MSW) under N<sub>2</sub>, CO<sub>2</sub> and oxy-fuel conditions



Paulina Wienchol<sup>a,\*</sup>, Agnieszka Korus<sup>a</sup>, Andrzej Szlęk<sup>a</sup>, Mario Ditaranto<sup>b</sup>

<sup>a</sup> Department of Thermal Technology, Silesian University of Technology, ul. Konarskiego 22, 44-100, Gliwice, Poland

<sup>b</sup> SINTEF Energy Research, Sem Sælands vei 11, 7034, Trondheim, Norway

## ARTICLE INFO

### Article history:

Received 20 October 2021

Received in revised form

14 February 2022

Accepted 21 February 2022

Available online 24 February 2022

### Keywords:

Oxy-fuel combustion

MSW

Thermogravimetric analysis

Kinetic analysis

Isoconversional methods

## ABSTRACT

Oxy-fuel combustion is one carbon capture and sequestration (CCS) technique that uses both O<sub>2</sub> and recirculated flue gas as an oxidiser. As a result, the produced gas is composed mainly of CO<sub>2</sub> and H<sub>2</sub>O, which makes its sequestration more cost-effective. Changing the atmosphere from N<sub>2</sub> to CO<sub>2</sub> affects combustion behaviour. To study the impact of the atmosphere on the combustion process, the thermal degradation of representative types of municipal solid waste (MSW) under N<sub>2</sub>, CO<sub>2</sub>, and O<sub>2</sub>/CO<sub>2</sub> atmospheres was analysed using a thermogravimetric (TG) instrument. Nonisothermal degradation experiments were conducted, and three heating rates were examined. Isoconversional methods were employed to determine kinetic data. Comparing N<sub>2</sub> and CO<sub>2</sub> atmospheres, it was found that below 600 °C, the shape of TG curves was not affected significantly. However, above 600 °C under CO<sub>2</sub> atmosphere, a second peak appeared, which indicated gasification reactions of the char with carbon dioxide. In the presence of oxygen, the second peak was shifted to lower temperatures, indicating that thermal decomposition with O<sub>2</sub> was more rapid. The reported kinetic parameters provide fundamental information on the conversion of solid waste. Thus, they are essential for designing chambers dedicated to the oxy-combustion of waste.

© 2022 Elsevier Ltd. All rights reserved.

## 1. Introduction

The European Union has seen an increasing trend in generated municipal solid waste (MSW). The amount of waste produced per capita in the EU increased by 7.5% in 2019 compared to 1995 [1]. This trend is caused by progressive urbanisation, population and economic growth, as well as the consumptive lifestyle of European Union citizens. The increase in the amount of generated waste raises the issue of how to treat it. Fig. 1 presents the European waste management pattern (data from 2018). As can be observed, recycling plays a leading role in the waste disposal process, especially in highly-developed countries. Recycling allows for recovering materials and thus, according to the Circular Economy Package [2], recycling together with prevention and re-use is the most preferable method of waste management. However, the issue of waste that cannot be recycled remains, and significant amounts of such

waste are currently landfilled in Europe (average 40%). Landfills release methane with a global warming potential (GWP) 28 times higher than CO<sub>2</sub>. In addition, they can leach hazardous pollutants into groundwater as well as emit toxic fumes and dust [3]. Although the thermal treatment technique is much more expensive than landfilling due to strict emission standards, it is an environmentally more favourable waste management method as it recovers energy from non-recyclable waste and prevents its harmful disposal [4]. The waste-to-energy industry can also help local and regional authorities meet their environmental and economic goals [5]. According to [6], in 2018, there were 492 WtE plants in 22 European countries, in which 96 million tonnes of waste were thermally treated.

Compared to other thermal treatment techniques, like gasification and pyrolysis, incineration is the most mature, developed, and cost-effective technology [7]. Although modern incineration plants are equipped with advanced and effective air pollution controls (APCs), they are still a source of CO<sub>2</sub> emissions [8]. However, according to the black Deal document [9], the European Union aims to achieve net-zero blackhouse gas emissions by 2050. This

\* Corresponding author.

E-mail address: [paulina.wienchol@polsl.pl](mailto:paulina.wienchol@polsl.pl) (P. Wienchol).

Nomenclature		Greek letters	
<i>Abbreviations</i>		$\alpha$	Conversion rate,
CCUS	Carbon Capture, Utilisation and Storage	$\beta$	Heating rate, K/min
DT	Ash Deformation Temperature	$\epsilon$	Relative error
FC	Fixed Carbon	<i>Subscripts</i>	
FT	Ash Flow Temperature	0	initial
HT	Ash Hemisphere Temperature	char	char burnout process
MC	Moisture Content	f	final
MEA	Monoethanolamine	pyro	pyrolysis process
MSW	Municipal Solid Wastes	t	at any time
OFC	Oxy-fuel combustion	<i>Symbols</i>	
PVC	Polyvinyl chloride	A	Pre-exponential factor, 1/s
SCG	Spent Coffee Grounds	E	Energy activation, kJ/mol
SST	Ash Shrinkage Starting Temperature	k	rate constant, 1/s
Tex	Textiles	m	Mass, kg
VM	Volatiles Matter	R	Universal gas constant, J/molK
WtE	Waste to Energy	R <sup>2</sup>	Correlation coefficient,
		T	Temperature, K

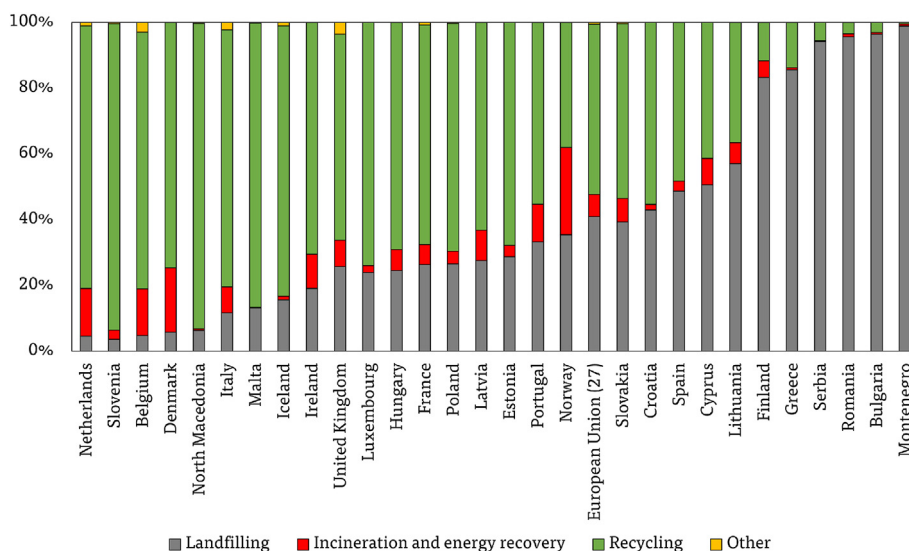


Fig. 1. Waste management in Europe in 2018 (based on data available Eurostat [1]).

strategy aims to “transform EU into a fair and prosperous society, with a modern, resource-efficient and competitive economy where there are no net emissions of greenhouse gases in 2050, and where economic growth is decoupled from resource use”. To meet this challenge, all sectors of the economy will be obligated to reduce or eliminate CO<sub>2</sub> emissions. For the waste-to-energy sector, the only possible method to avoid carbon dioxide emissions is to implement carbon capture and utilisation or storage (CCUS) technology [8]. Moreover, due to the fact that about 65% of carbon contained in waste is biogenic, the emission of CO<sub>2</sub> over the full cycle is negative [10]. According to the studies conducted by Pour et al. [11] and Bisinella et al. [12], MSW incineration with CO<sub>2</sub> capture can eliminate about 0.7 net kg CO<sub>2,eq</sub> from the atmosphere per kg of wet MSW burned, and thereby lower climate change impacts despite the energy used by the capture unit. Besides, authors in [13] suggest that carbon can be used for various purposes, for example the hydrogenated production of chemicals including synthesis of

methane, methanol, dimethyl ether (DME), and formic acid. Furthermore, as noted in our previous paper [8], the most energy-intensive unit in oxy-MSW incineration system is the air separation unit (ASU). Therefore, to improve oxy-fuel combustion technology, CO<sub>2</sub> hydrogenation can be coupled with water electrolysis process in order to obtain pure oxygen for use as an oxidiser. As Pratschner et al. [14] state, combining oxy-fuel combustion with CCU technologies is a promising system configuration for future power-to-liquid plants which use large-scale electrolyzers.

Currently, worldwide there are four incineration plants where CO<sub>2</sub> capture is planned. These plants include one in Oslo (Klemetsrud WtE plant) which is aiming for permanent CO<sub>2</sub> storage in the North Sea, two plants in the Netherlands (Twence and AVR plants) which exemplify carbon capture and utilisation technology (CCU), and a plant in Japan (Saga City) that utilises CO<sub>2</sub> to cultivate crops and create algae cultures. However, the CO<sub>2</sub> capture method employed in the aforementioned plants is based on the post-

combustion technique [8]. Tang et al. [15] used life cycle assessment (LCA) analysis and found that incineration plants integrated with carbon capture technology based on the oxy-fuel combustion technique are superior in terms of energy efficiency and environmental impacts compared to the MEA post-combustion method.

### 1.1. Literature overview of oxy-MSW incineration

This study focuses on oxy-waste combustion (OWC) technology, which relies on the use of oxygen as an oxidiser instead of air. As a consequence, the produced gas contains mainly carbon dioxide and water vapour, and thus the CO<sub>2</sub> is easier to separate than for the post-combustion method, since it relies on straightforward water condensation [16]. So far oxy-fuel combustion technology was deeply investigated for fossil fuels such as coal or natural gas. Comprehensive reviews of these studies are readily available [17,18]. However, OFC for incineration is novel, and so there is a dearth of research which would provide fundamental knowledge on this process [15]. Due to the absence of nitrogen in the oxidiser, the exhaust gas volume is about 5 times lower, and thereby the concentration of pollutants is higher [19]. Therefore the cleaning of flue gas is easier and more cost-efficient, because smaller equipment can be used [20]. Application of OFC technology in incineration plants results in elevated process temperature due to the high oxygen content in the boiler. This temperature rise increases combustion efficiency and consequently exergy efficiency since the combustion process is a major contributor to exergy destruction (about 60%) [16,21].

Oxy-fuel technology is expected to enable other process improvements, such as a) reduction or even complete elimination of the auxiliary fossil fuel consumption typically used to keep the required process temperature (thus decreasing CO<sub>2</sub> emission), and b) decrease of heavy hydrocarbons (dioxins and furans) emissions by enhanced oxidation of these compounds. Tests of these potential benefits should be addressed in future research. One foreseeable concern with the proposed technology, due to the increased temperature of the process, is possibility of ash melting issue since municipal solid waste contains a high content of organic compounds with a low ash melting point. Therefore recirculation of dry flue gas, which consists mainly of carbon dioxide, is planned to control the temperature [22].

Until now, most studies on oxy-MSW combustion compared the thermal degradation of individual MSW materials [23,24] and their blends [25–27] using thermogravimetric analysis under N<sub>2</sub> and CO<sub>2</sub> atmospheres. As emphasised by those studies, pyrolysis and gasification are important steps of MSW combustion that require further investigation to acquire fundamental data and gain comprehensively understanding of their mechanisms. The results indicated that direct replacement of N<sub>2</sub> by CO<sub>2</sub> affects weight loss rates and the reactions occurring above 600 °C, while at lower temperature CO<sub>2</sub> acts as inert atmosphere. In addition, it was shown that atmosphere affects the composition and amount of the obtained gaseous products. The authors also noticed that blends of materials can hinder the burnout and char-CO<sub>2</sub> reaction.

Combustion behaviour using a TGA instrument under N<sub>2</sub>/O<sub>2</sub> and CO<sub>2</sub>/O<sub>2</sub> conditions [28–31] was investigated for mixed wastes only. The authors claimed that the 30% oxygen content in the CO<sub>2</sub>/O<sub>2</sub> atmosphere achieved a similar combustion performance as air, and thus oxy-fuel combustion technique needs knowledge from oxygen-enriched combustion technology. Apart from that, some researchers investigated emissions of pollutants [32,33] and heavy metals migration under N<sub>2</sub>/O<sub>2</sub> and CO<sub>2</sub>/O<sub>2</sub> [34,35].

The first tests on a lab-scale reactor dedicated to oxy-MSW combustion were described in [36]. This study showed that the model MSW can be successfully incinerated under various oxy-fuel

conditions, provided that the oxygen concentration in the oxidiser is carefully adjusted. The results also indicated that there are no insurmountable barriers to the further development of oxy-MSW combustion. However, kinetic parameters are needed to understand what happens during the experiments and to be able to accurately model these effects. As can be seen, the research to date has mainly focused on understanding the thermal behaviour of MSW, while the kinetic analysis has not been carried out exhaustively. Therefore, a reliable set of kinetic parameters of decomposition for typical MSW components under CO<sub>2</sub> and O<sub>2</sub>/CO<sub>2</sub> is lacking. These parameters would express the quantitative differences between atmospheric composition and could be used for oxy-MSW combustion process modelling [8].

### 1.2. Research objectives

The general aim of this work was to gain fundamental knowledge on the impact of the process atmosphere on the stages of feedstock degradation, such as devolatilisation and char burnout. To accomplish this goal, thermogravimetric analysis (TGA) of thermal decomposition of representative types of municipal solid waste (MSW), such as textiles (Tex), spent coffee grounds (SCG), and PVC was performed under N<sub>2</sub>, CO<sub>2</sub> and O<sub>2</sub>/CO<sub>2</sub> atmospheres. The specific goal of this research was to determine the global kinetic parameters, such as energy activation (E<sub>a</sub>) and pre-exponential factor (A), of these processes in various atmospheres as well as to compare different approaches of obtaining kinetic data. To complete this task, four model-free methods were used: Friedman, Ozawa-Flynn-Wall, Kissinger-Akahira-Sunose and Vyazovkin. Such an extensive kinetic analysis of waste material decomposition under various conditions has not been found in the literature so far, and thus it is a scientific novelty of this work. Results of this research will also contribute to the development of oxy-MSW incineration technology by providing data for use in the modelling of such systems.

Section 2 presents analyses of the selected waste materials and experimental methodology. Section 3 explains the theoretical fundamentals of isoconversional methods that were used to calculate kinetic parameters. Results of thermogravimetric study as well as kinetic analysis are illustrated and discussed in Section 4. Finally, conclusions and recommendations for future works are summarised in Section 5.

## 2. Materials and methods

### 2.1. Feedstock characterisation and analysis

Textiles (Tex), spent coffee grounds (SCG), and polyvinyl chloride (PVC) were used as waste materials in this study. Textiles were chosen for the research since over 69% of textile waste is currently landfilled, which risks soil and groundwater contamination by heavy metals used in the production process [37]. Therefore, more sustainable techniques for its management should be sought. Cotton, which is comprised almost exclusively of cellulose [38] (i.e. a glucose polymer) was used in this study. Coffee is a globally popular beverage prepared from roasted coffee beans, with about 500 billion cups consumed every year [39]. Currently, spent coffee grounds have no significant market and hence are problematic for disposal, but their relatively high chemical energy content makes them a potentially valuable feedstock [40]. SCG are also used here as an example of an organic material. PVC was selected to represent plastic materials due to its common occurrence in MSW. Moreover, since 38–66% of the chlorine content of MSW originates from PVC, this material is responsible for the formation of many chloro-compounds released during MSW incineration [30,38].

Proximate and ultimate analyses of the chosen materials were carried out according to appropriate standards for alternative fuels: PN-EN ISO 15414-3:2011, PN-EN ISO 15402:2011 and PN-EN ISO 15403:2011 for moisture, volatile matter, and ash determination, respectively; PN-EN 15407:2011 and PN-EN 15408:2011 for C, H, N, S, Cl analyses. Results of the analyses are presented in Table 1. The analyses were outsourced to accredited laboratory, where all parameters were determined using accredited methods. The results of proximate analysis for PVC and textiles were similar, owing to the fact that both materials are polymers, even though the textile is a natural polymer and PVC is synthetic [38,41]. The SCG, being an organic material, is rich in hemicellulose, cellulose, lignin, fat, and protein [42]. The presence of lignin affects the higher quantity of fixed carbon. As shown, SCG has the highest calorific value and fixed carbon content, but also produced the largest quantity of ash.

Ash composition and its characteristic melting points are shown in Tables 2 and 3. Ash shrinkage starting temperature (SST) is defined as the temperature at which the area of the sample falls below 95% of the original sample area at 550 °C. Since shrinkage can be caused by sintering, in this study SST is treated as a limiting temperature of the process on the grate. As can be observed, the SST of the sample is relatively low due to a high content of alkaline compounds (CaO, MgO, Na<sub>2</sub>O, K<sub>2</sub>O) and CO<sub>2</sub> in ash. Table 3 presents also ash deformation temperature (DT), ash hemisphere temperature (HT), and ash flow temperature (FT).

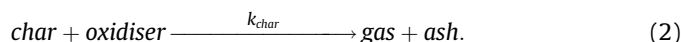
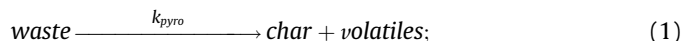
### 2.2. Thermogravimetric instrument and procedure

An experimental campaign was carried out at standard atmospheric pressure using a TGA/DSC analyser (Netzsch STA 409 PC Luxx) with a sensitivity of 0.001 mg and accuracy of 1% of the measurement range. The textile samples were cut and ground to size 0.05 mm. Coffee grounds and PVC powder were used as received, with sizes 0.5 mm and 0.2 mm, respectively. Before each experiment, samples were dried for 2–3 h at 105 °C to remove moisture. The initial weight of the samples was 5 ± 0.1 mg. Sample mass loss profiles were determined based on dynamic heating runs, with the linear temperature increase from 100 to 1000 °C at heating rates (β) of 5, 10 and 15 K/min. Each experiment was replicated to evaluate the reproducibility of the results. Three different atmospheres were examined: (a) inert 100 vol% N<sub>2</sub>, (b) gasifying 70/30 vol% CO<sub>2</sub>/N<sub>2</sub> and (c) oxidising with 63/7/30 vol% CO<sub>2</sub>/O<sub>2</sub>/N<sub>2</sub>. In the oxidising atmosphere, the flows were selected to achieve conditions similar to those of an actual combustion chamber, while accommodating the associated limitation of the bed temperature. This means that the temperature of the fuel bed should not exceed the temperature of ash melting, which for organic waste ash is relatively low (630 °C). For this purpose, calculations of the adiabatic temperature of the process depending on the oxidant composition were performed. These calculations showed that to prevent ash melting, the maximum molar fraction of oxygen in the oxidant should not exceed 10%.

### 3. Kinetic theory and calculations

The main goal of any kinetic analysis is to parameterise the

chemical process rate and gain knowledge on the process mechanism [43]. Kinetic parameters are useful in modelling energy systems based on fuel combustion, such as fixed-bed and fluidised-bed boilers, since they allow for predicting the thermal behaviour of the feedstock [44] as well as can provide guidance for design and optimization of reactors [45]. In this study, it is assumed that thermochemical processes are simply described as one-step global reactions:



The chemical reaction rate is expressed as follows:

$$\frac{d\alpha}{dt} = k(T)f(\alpha) \tag{3}$$

where t is time (s); T is temperature (K); α is the conversion rate; f(α) is the differential reaction model; and k(T) is a temperature-dependent rate constant described by the Arrhenius equation:

$$k(T) = A \exp \frac{-E}{RT} \tag{4}$$

here A is the pre-exponential factor (s<sup>-1</sup>); E is the apparent activation energy (J/mol); and R is the universal gas constant (8314 J/molK). The conversion rate is defined as:

$$\alpha(t) = \frac{m_0 - m(t)}{m_0 - m_f} \tag{5}$$

where m<sub>0</sub> is initial mass (mg); m(t) is mass as a function of time (mg); and m<sub>f</sub> is the final mass (mg).

By integrating Eq. (3), the integral form g(α) of the reaction model can be obtained:

$$\int_0^\alpha \frac{d\alpha}{f(\alpha)} = g(\alpha) = \frac{A}{\beta} \int_{T_0}^T \exp \left( -\frac{E}{RT} \right) dT \tag{6}$$

Because the foregoing integral does not have an analytical solution, a number of approximate solutions have been proposed in the past, albeit with poor precision. Current methods use numerical integration to compute integrals with very high accuracy [43].

If the activation energy does not vary significantly with the conversion rate, the process can be described by single effective activation energy. Otherwise the process is likely to involve two or more steps having differing activation energy [46].

#### 3.1. Model-free methods

The isoconversional approach to solid-state kinetics allows retrieving kinetic data, i.e. activation energies E(α) and pre-exponential factors A(α), without the knowledge of the reaction model. Thus it is also known as a model-free method.

**Table 1**  
Proximate and ultimate analysis of samples.

Symbol	MC	VM	FC	Ash	C	H	O	N	S	Cl	LHV
Unit	% (ar)					% (db)					kJ/kg (db)
T	3.3	91.6	7.98	0.42	45.11	6.55	48.08	0.20	0.02	0.037	16 380
SCG	1.9	80.5	17.33	2.17	52.28	6.92	38.19	2.41	0.13	0.073	20 470
PVC	0.1	93.6	6.3	<0.1	38.31	5.18	13.77	<0.01	0.13	42.6	20 010



**Table 2**  
Composition of ash.

Symbol	SiO <sub>2</sub>	Fe <sub>2</sub> O <sub>3</sub>	Al <sub>2</sub> O <sub>3</sub>	Mn <sub>3</sub> O <sub>4</sub>	TiO <sub>2</sub>	CaO	MgO	SO <sub>3</sub>	P <sub>2</sub> O <sub>5</sub>	Na <sub>2</sub> O	K <sub>2</sub> O	BaO	SrO	Cl	CO <sub>2</sub>
Unit									%						
T	31.8	2.18	3.67	0.09	1.74	22.2	4.89	11.6	2.01	7.91	3.04	0.40	0.20	1.05	6.24
SCG	1.79	0.62	0.78	0.15	0.06	12.0	9.54	6.13	12.4	0.64	40.0	0.02	0.07	0.92	13.9

**Table 3**  
Characteristic ash melting points in an oxidising atmosphere.

Symbol	SST	DT	HT	FT
Unit	°C			
T	770	1190	1240	1240
SCG	630	1230	>1500	>1500

Isoconversional methods are divided into categories: a) differential, such as Friedman; b) integral, for example the Ozawa-Flynn-Wall (OFW), Kissinger-Akahira-Sunose (KAS), and Vyazovkin methods. Compared to differential methods, integral methods are versatile due to their higher tolerance to experimental noise. Differentiation propagates the effect of noise, reducing the accuracy of the results. On the other hand, integral methods use approximations that can entail inaccuracies. All model-free methods are broadly discussed in a series of articles published by The International Confederation for Thermal Analysis and Calorimetry (ICTAC) Kinetics Committee [43,47]. In this study, both an experimental campaign and kinetic analysis were carried out based on these recommendations.

According to the isoconversional principle, the process rate at a constant extent of conversion  $\alpha$  is a function of temperature exclusively [46]. For constant  $\alpha$ , the following equations can be derived from Eq. (3) by taking the first logarithmic derivative:

$$\left[ \frac{\partial \ln(d\alpha/dt)}{\partial T^{-1}} \right]_{\alpha} = \left[ \frac{\partial \ln k(T)}{\partial T^{-1}} \right]_{\alpha} + \left[ \frac{\partial \ln f(\alpha)}{\partial T^{-1}} \right]_{\alpha} \quad (7)$$

Because  $\alpha$  is constant,  $f(\alpha)$  is also constant, and the second term in the right-hand side of Eq. (4) is zero; thus:

$$\left[ \frac{\partial \ln(d\alpha/dt)}{\partial T^{-1}} \right]_{\alpha} = \frac{-E_{\alpha}}{R} \quad (8)$$

### 3.1.1. Friedman method

The most common differential isoconversional approach, the Friedman method can be applied to calculate the activation energy according via [48]:

$$\ln \left( \frac{d\alpha}{dt} \right) = \ln A + \ln f(\alpha) - \frac{E}{RT} \quad (9)$$

Activation energy ( $E_a$ ) can be easily determined from the slope of a plot of  $\ln(d\alpha/dt)$  against  $1/T$ .

### 3.1.2. Ozawa-Flynn-Wall method

The OFW method uses the Doyle approximation to compute  $g(\alpha)$  [49]:

$$\ln(\beta_i) = \ln \left[ \frac{AE}{Rg(\alpha)} \right] - 5.331 - 1.052 \frac{E}{RT} \quad (10)$$

Apparent activation energy ( $E_a$ ) can be obtained from a plot of the natural logarithm of heating rates  $\ln(\beta_i)$  versus  $1/T$ , which represents the linear relation with a given value of the conversion at

different heating rates.

### 3.1.3. Kissinger-Akahira-Sunose method

A more accurate approximation introduced by Murray and White leads to a frequently used technique called the Kissinger-Akahira-Sunose (KAS) method [50]:

$$\ln \left( \frac{\beta_i}{T^2 \alpha_i} \right) = \ln \left( \frac{A_{\alpha} R}{E_{\alpha}} \right) - \ln g(\alpha) - E_{\alpha} RT_{\alpha,i} \quad (11)$$

The plot of  $\ln \beta/T^2$  versus  $1/T$  for constant value of  $x$  will be a straight line. The  $E$  can be determined by the gradient of the curve, which is simply  $-E/R$ .

### 3.1.4. Vyazovkin method

The most modern method, called Vyazovkin, employs a series of experiments performed at different heating rates to calculate  $E_{\alpha}$  by minimising the following function [46]:

$$\varphi(E_{\alpha}) = \sum_{i=1}^n \sum_{j \neq i}^n \frac{I(E_{\alpha}, T_{\alpha,i}) \beta_j}{I(E_{\alpha}, T_{\alpha,j}) \beta_i} \quad (12)$$

where the temperature integral

$$I(E_{\alpha}, T_{\alpha}) = \int_0^{T_{\alpha}} \exp \left( \frac{-E_{\alpha}}{RT} \right) dT = \frac{E_{\alpha}}{R} \cdot p(x) \quad (13)$$

is solved numerically. Minimisation is repeated for each value of  $\alpha$  to obtain the dependence of  $E_{\alpha}$  on  $\alpha$ . The function  $p(x)$  can be expressed by the fourth Senum and Yang approximation:

$$p(x) = \frac{e^{-x}}{x} \approx \frac{x^3 + 18x^2 + 88x + 96}{x_4 + 20x^3 + 120x_2 + 240x + 120} \quad (14)$$

## 3.2. Calculations

All the calculations for this study were performed with Netzsch Kinetics Neo (NKN) software (v.2.5.0.1), supported with MS Excel and MATLAB. Friedman, OFW, and Vyazovkin analyses were conducted using the NKN package at a resolution of 0.01 for  $\alpha$ . To assess the degree of matching between fitting results and experimental data, the mean value of relative error was calculated defined as:

$$\bar{\varepsilon} = \frac{1}{n} \sum_{i=1}^n \frac{y_{measured_i} - y_{calculated_i}}{y_{measured_i}} \quad (15)$$

here  $y_{measured_i}$  is the actual value of the weight loss for the given temperature (%);  $y_{calculated_i}$  is the calculated value of the weight loss for the given temperature based on obtained kinetics (%);  $n$  is the number of measurements.

## 4. Results and discussion

### 4.1. TGA and DTG results

The mass loss (TGA) and the mass loss rate (DTG) profiles of each studied waste materials under inert, gasifying, and oxidising atmospheres at heating rates of 5, 10, and 15 K/min are illustrated in Figs. 2–4 for textile, spent coffee grounds and PVC samples, respectively. The presented graphs each represent one measurement. To check the repeatability of the measurements, the mean difference was calculated between the values of the weight loss ( $\Delta_{TGA}$ ) and the weight loss rate ( $\Delta_{DTG}$ ) of samples for duplicates. The results are presented in Table 4. As can be observed, the best accordance between mass loss profiles for all feedstocks appeared under inert conditions. The mean difference between weight loss curves increased in gasifying and oxidising atmospheres and was relatively high, except for the spent coffee grounds sample. However, the mean difference between DTG curves was at acceptable levels for all performed experiments. It should be underlined that the biggest difference between TGA profiles occurred at high temperatures, where the mass of the sample was small, which can be explained by the high sensitivity of the balance used. Therefore, we concluded that the results could be used for kinetic calculations, while reported residual masses should be treated with caution due to device uncertainty. This finding is supported by the results of Tables 5–7, where the main characteristics of TGA and DTG curves are summarised. These tables list the temperature range in which the decomposition took place, the temperature at which the maximal mass loss rate (DTG) occurred, and the final percentage of solid residue, along with their standard deviations ( $\sigma$ ). As can be seen, the standard deviations calculated for solid residues are relatively high in almost all cases, sometimes exceeding the value

itself. However, for DTG peak temperature ( $^{\circ}\text{C}$ ) and DTG max ( $\%/min$ ), the standard deviations are negligible. This allows for the conclusion that the nature of the thermogravimetric analysis does not allow for precise determination of the final mass of the sample, but it records the dynamic mass change well.

#### 4.1.1. Effects of the atmosphere on thermal decomposition of MSW

As shown in Fig. 2, the degradation of a textile sample under inert conditions occurred in one step between 230 and 400  $^{\circ}\text{C}$  (for  $\beta = 10$  K/min), confirming the sample was of predominantly (almost pure cellulose). When the temperature was higher than 400  $^{\circ}\text{C}$ , almost all material was decomposed with a very low solid residue, similar to results obtained by Yang et al. [51]. Under gasifying conditions below 600  $^{\circ}\text{C}$ , there were no significant differences between atmospheres, and DTG curves practically coincided, as reported in the literature [23,26]. However, different specific heat capacities and diffusion rates of  $\text{N}_2$  and  $\text{CO}_2$  result in a decrease of the weight loss rate of the peaks corresponding to volatile release [23]. At temperatures above 600  $^{\circ}\text{C}$  carbon dioxide starts to react with the remaining char, which is depicted by the second peak on the graph. However, due to the small amount of fixed carbon and ash in the sample, the peak is very weak ( $-0.6\%/min$  for  $\beta = 10$  K/min). In the oxidising atmosphere, the presence of oxygen accelerates degradation (occurring at lower temperatures) and a final combustion process can be observed. The final mass under  $\text{CO}_2$  and  $\text{O}_2/\text{CO}_2$  atmospheres is practically the same. These findings are confirmed by study reported in [52].

The thermal degradation of spent coffee grounds, which are presented in Fig. 3, started at a lower temperature than for textiles. This observation indicated the presence of hemicellulose in the feedstock and finishes at higher temperature (until 560  $^{\circ}\text{C}$ ), which can be caused by the presence of lignin in SCG sample. Also, three

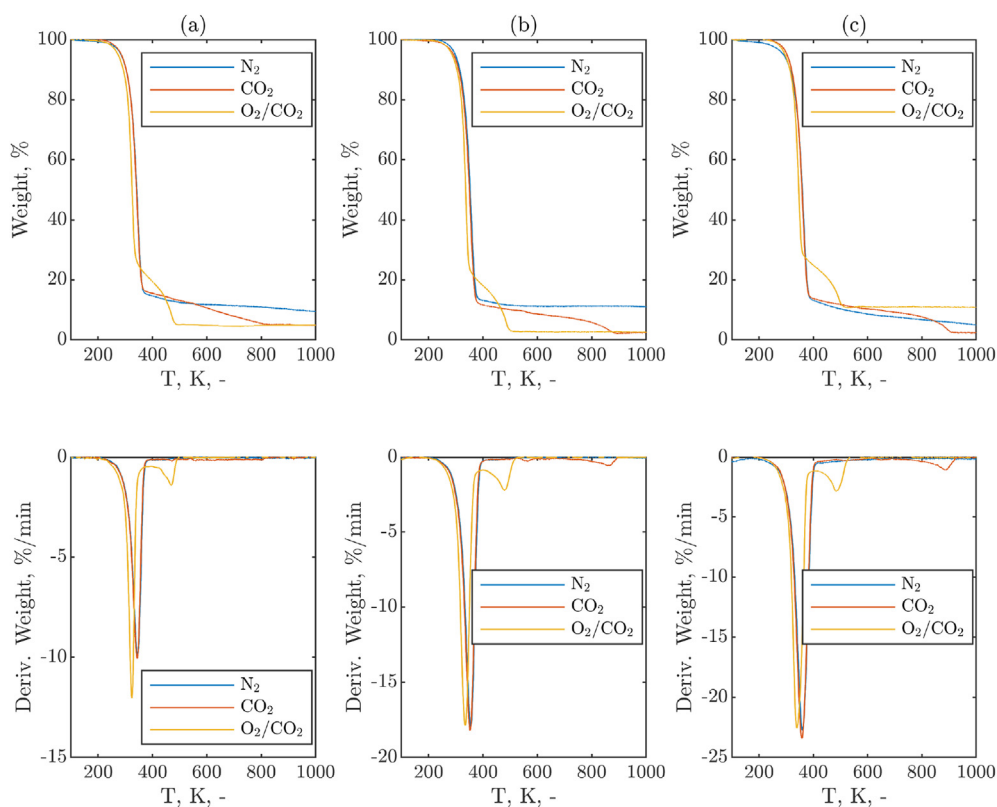


Fig. 2. TGA and DTG curves of textiles under  $\text{N}_2$ ,  $\text{CO}_2$  and  $\text{O}_2/\text{CO}_2$  atmospheres at a) 5, b) 10 and c) 15  $\text{Kmin}^{-1}$

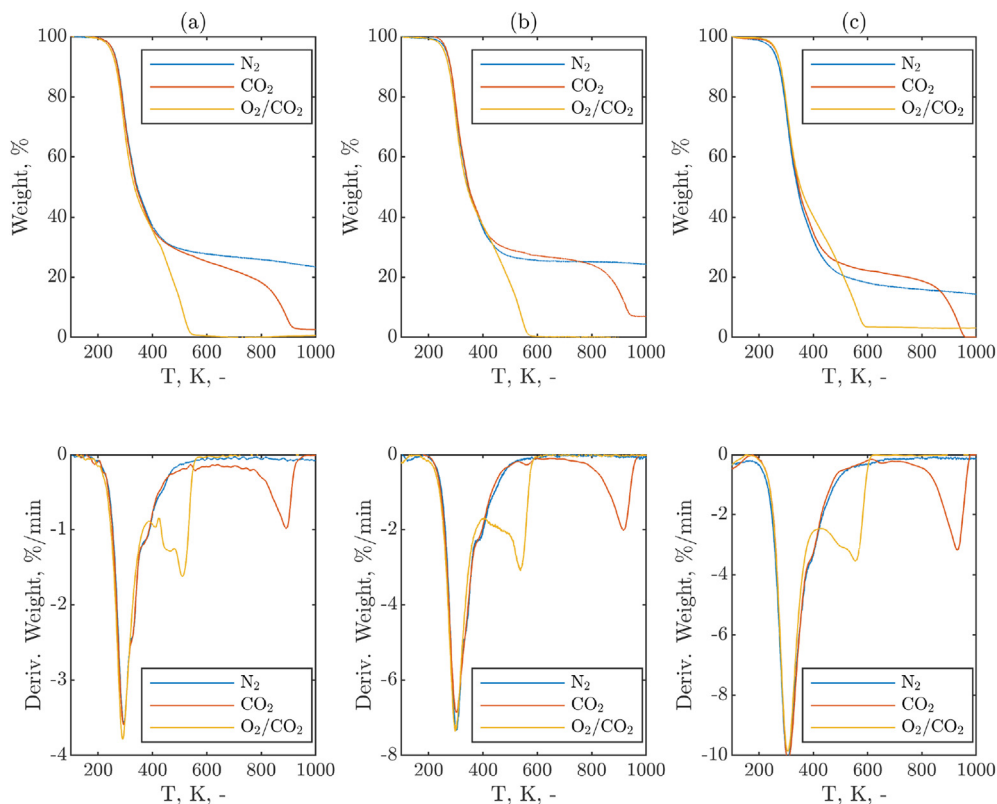


Fig. 3. TGA and DTG curves of spent coffee grounds under N<sub>2</sub>, CO<sub>2</sub> and O<sub>2</sub>/CO<sub>2</sub> atmospheres at a) 5, b) 10 and c) 15 Kmin<sup>-1</sup>

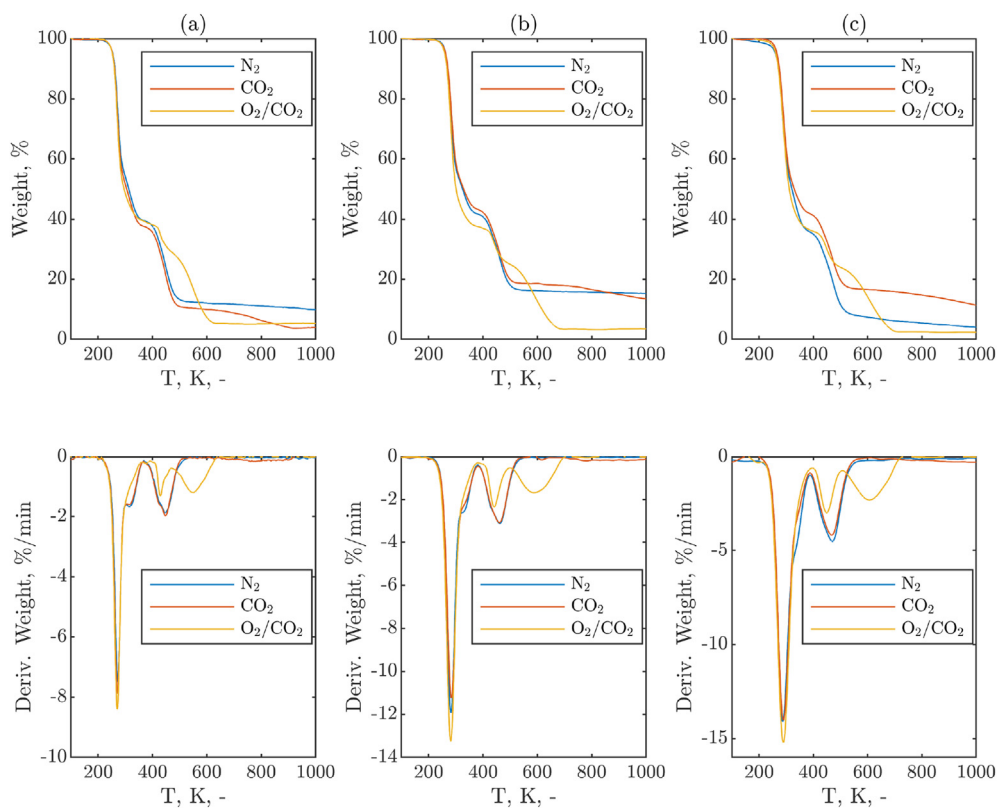


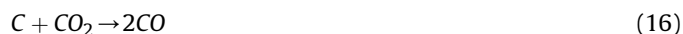
Fig. 4. TGA and DTG curves of PVC under N<sub>2</sub>, CO<sub>2</sub> and O<sub>2</sub>/CO<sub>2</sub> atmospheres at a) 5, b) 10 and c) 15 Kmin<sup>-1</sup>

**Table 4**  
The mean difference ( $\overline{\Delta\%}$ ) between the sample weight losses for the two measurements for 10 K/min.

Sample	Atmosphere	$\overline{\Delta_{TGA}}, \%$	$\overline{\Delta_{DTG}}, \% \text{ min}$
Tex	inert	1.05	0.017
	gasifying	9.75	0.136
	oxidising	14.30	0.178
SCG	inert	3.20	0.041
	gasifying	6.21	0.090
	oxidising	1.14	0.010
PVC	inert	2.01	0.032
	gasifying	1.10	0.019
	oxidising	5.19	0.072

shoulders can be perceived on the DTG curve. The first one is almost imperceptible and occurs at approximately 335 °C, a second shoulder was very pronounced and appears at 390 °C and the third shoulder can be noticed at 420 °C. Brachi et al. [40] implied these shoulders indicate that degradation does not occur in a single-step and can be attributed to the degradation of other organic compounds, such as proteins, carbohydrates, fats, fatty acids, amino acids, polysaccharides, etc., as well as the chemical recombination of pyrolytic derivatives produced by the primary pyrolysis. As Kim et al. [53] suggested, due to the fact that the reaction rate for dehydrogenation is proportional to the temperature, volatilisation in SCGs is initiated first and then dehydrogenation via thermal cracking is started, which is depicted by the second vertex. In N<sub>2</sub>

atmosphere, the solid residue was relatively high due to the high content of char in the sample. As in the case of textiles, below 600 °C, the DTG curves practically overlapped, however, it can be noticed that the shoulder at 420 °C does not exist. At higher temperature, similarly to the textile sample, a second peak was observed and the final mass was lower than under inert atmosphere. However, due to the higher content of char in the sample, the second peak was stronger (−2.0%/min). These results have also been found in other studies, for example in [23]. As literature reports, they can be explained by the following mechanisms. First, carbon dioxide can hinder secondary char formation by breaking and reacting with tars. Second, CO<sub>2</sub> can react directly with the char according to the Boudouard reaction (Eq. (16)) [26,54]:



Under O<sub>2</sub>/CO<sub>2</sub> conditions, the degradation of the spent coffee sample was shifted to lower temperatures (similar to the textile sample) and at temperature above 600 °C only ash remained.

As can be observed in Fig. 4, the PVC sample decomposed in two steps when carrier gas was N<sub>2</sub> and CO<sub>2</sub>, while three-step decomposition occurred in the case of oxidising atmosphere. The first step is ascribed to dehydrochlorination and polyene chain formation (between 220 and 380 °C). The second step is linked to the degradation of polyene chains between 380 and 530 °C [55], formation of alkyl aromatics with remaining char, including condensation and dehydrogenation reactions with deep dealkylation,

**Table 5**  
Characteristics of TGA and DTG curves of samples under inert atmosphere.

Sample	Heating rate, K/min	Solid Residue at 1000 °C, %	$\sigma$	DTG peak temperature, °C	$\sigma$	DTG max, %/min	$\sigma$	Temperature range, °C
Tex	5	9.3	1.22	344.8	0.11	−9.9	0.25	237.9–380.5
	10	11.2	1.27	354.5	0.26	−17.9	0.11	229.7–400.3
	15	4.3	6.82	360.2	0.50	−22.7	1.76	207.8–409.5
SCG	5	18.0	2.62	294.1	0.19	−3.7	0.08	184.6–527.8
	10	23.8	2.40	302.3	0.61	−7.0	0.16	190.3–560.2
	15	13.7	1.24	305.0	0.78	−10.2	0.27	194.0–651.8
PVC	5	9.7	3.62	271.8, 447.8	0.06, 0.79	−7.5, −1.9	0.01, 0.06	196.6–370.2, 370.2–512.9
	10	15.0	1.95	281.9, 457.9	0.03, 0.81	−11.9, −3.1	0.02, 0.05	215.9–382.4, 382.4–533.0
	15	3.6	8.11	287.1, 468.7	0.53, 0.97	−14.06, −4.5	0.38, 0.03	204.7–386.6, 386.6–559.7

**Table 6**  
Characteristics of TGA and DTG curves of samples under gasifying atmosphere.

Sample	Heating rate, K/min	Solid Residue at 1000 °C, %	$\sigma$	DTG peak temperature, °C	$\sigma$	DTG max, %/min	$\sigma$	Temperature range, °C
Tex	5	4.9	2.32	343.8	0.08	−10.1	0.15	227.4–379.1
	10	2.4	8.60	352.7, 864.6	0.38, 0.02	−18.2, −0.6	0.16, 0.03	238.6–394.8, 836.2–896.4
	15	2.3	0.58	358.0, 889.3	0.29, 2.34	−23.4, −1.1	1.22, 0.70	245.1–409.2, 850.9–922.5
SCG	5	2.6	12.30	293.8, 892.5	0.10, 1.06	−3.6, −1.0	0.42, 0.13	207.9–513.0, 777.8–932.1
	10	6.9	5.59	302.1, 917.9	0.03, 1.05	−6.9, −2.0	0.26, 0.03	204.0–523.5, 779.7–971.0
	15	0	2.99	306.6, 930.6	0.06, 3.90	−10.2, −3.2	0.16, 0.24	202.1–610.4, 780.8–982.8
PVC	5	3.9	1.39	270.8, 447.3	0.34, 0.30	−7.9, −2.0	0.06, 0.08	214.0–365.2, 365.2–509.0
	10	13.4	0.64	284.0, 461.5	0.32, 0.61	−11.2, −3.1	0.54, 0.08	211.3–381.5, 381.5–531.2
	15	11.3	2.49	289.8, 468.1	0.22, 1.67	−14.0, −4.2	0.50, 0.08	199.8–387.8, 397.8–563.0

**Table 7**  
 Characteristics of TGA and DTG curves of samples under oxidising atmosphere (10 vol% of oxygen in the oxidiser).

Sample	Heating rate, K/min	Solid Residue at 1000 °C,%	$\sigma$	DTG peak temperature, °C	$\sigma$	DTG max, %/min	$\sigma$	Temperature range, °C
Tex	5	4.9	2.02	324.1, 469.3	0.42, 0.98	-12.0, -1.4	0.82, 0.02	233.7–500.2
	10	2.5	13.4	333.9, 479.6	1.06, 1.56	-17.8, -2.4	2.84, 0.23	237.1–517.6
	15	10.9	8.67	339.2, 483.1	1.23, 2.09	-22.6, -2.8	1.15, 0.22	208.9–537.8
SCG	5	0.6	10.39	290.4, 509.7	0.25, 3.45	-3.8, -1.6	0.35, 0.15	185.5–566.0
	10	1.5	1.20	299.8, 537.3	1.21, 1.98	-6.8, -2.8	0.18, 0.04	184.0–598.9
	15	3.1	5.73	306.0, 555.3	1.74, 2.59	-9.9, -3.5	0.51, 0.74	183.6–618.4
PVC	5	5.2	2.30	270.2,	1.20,	-8.4,	0.09,	213.6–355.5,
				428.5,	1.46,	-1.3,	0.04,	392.0–470.3,
				549.3	2.09	-1.2	0.03	470.3–635.6
	10	3.5	5.41	281.5,	1.12,	-13.5,	0.90	211.3–376.5,
				440.7,	2.08,	-2.3,	0.19,	398.9–498.5,
				589.5	2.58	-1.7	0.38	498.5–703.9
	15	2.3	5.35	289.4,	0.06,	-15.2,	0.62,	212.1–393.5,
				448.3,	0.55,	-3.0,	0.15,	393.5–506.6,
				606.5	1.18	-2.3	0.03	506.6–723.9

isomerization, chain scission, crosslinking, and aromatization [56]. The CO<sub>2</sub> atmosphere did not affect degradation significantly, while in an oxidising atmosphere, the shape of peaks was modified, indicating that reaction mechanisms were different when oxygen was present. A third peak appeared at temperature 590 °C and the final mass was the lowest, indicating the formation of char and its combustion in the last stage of degradation.

4.1.2. Effects of the heating rate on thermal decomposition of MSW

In general, with increasing heating rate, the DTG peaks shifted toward a higher temperature range without a significant change in their shape (Tables 5–7). The maximum values of DTG peaks were generally greater for higher heating rates, which was also noticed by other researchers [40,57,58]. It demonstrated that the process is

delayed with the raised heating rate. As authors in [58] implied, it can be caused by the fact that the heat transfer of the sample particles is decreased at the high heating rate, which is not favourable to the degradation of the feedstock. When analysing the results of the final sample masses, no clear trends emerged. In most cases, the percentage of solid residue at  $\beta = 10$  K/min was the highest. However, due to the lack of reproducibility in the results for the final masses, this result should be investigated further.

4.2. Kinetic analysis

In this section, results of the kinetic study based on isoconversional approach are presented for the examined samples under various conditions. The plots of energy activation ( $E_a$ ) computed

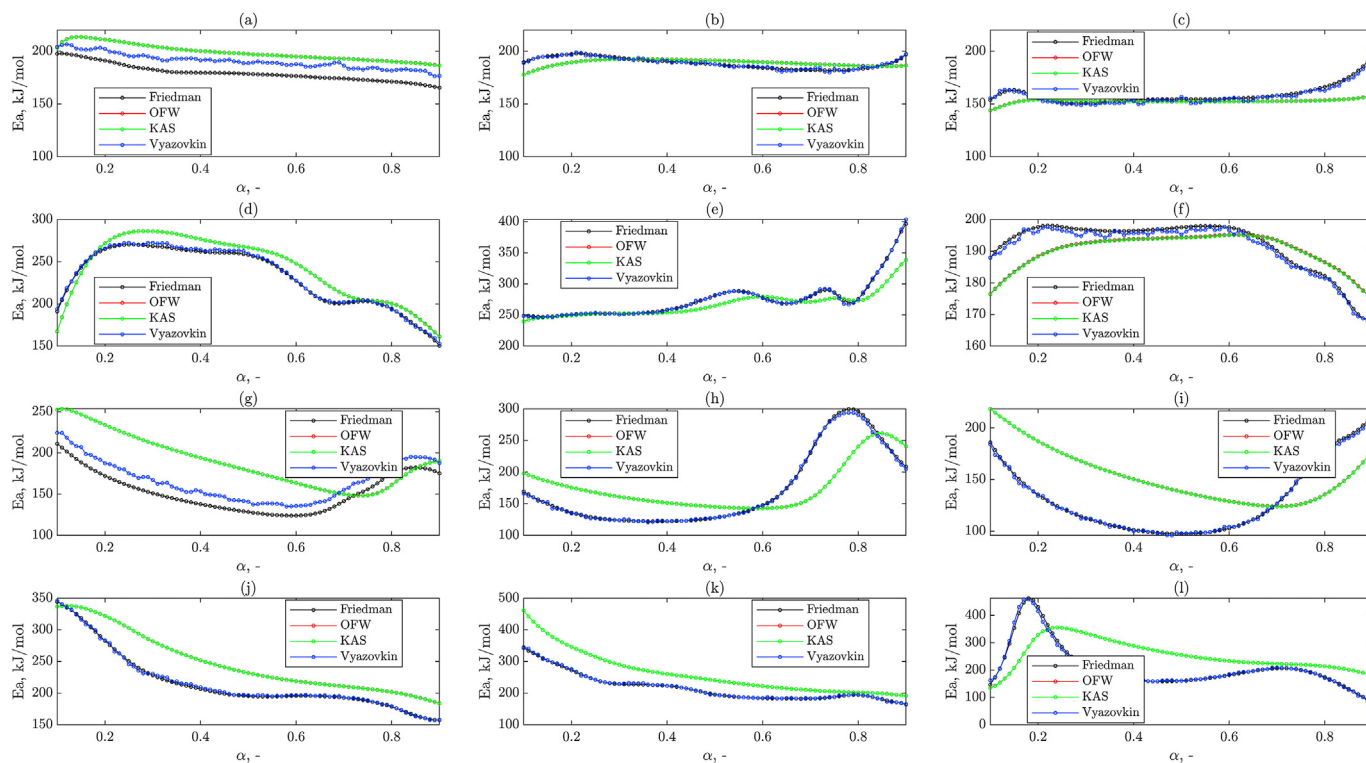


**Fig. 5.** Activation energy as a function of conversion rate for pyrolysis of the following: textiles in a) inert, b) gasifying, and c) oxidising atmosphere; spent coffee grounds in d) inert, e) gasifying, and f) oxidising atmosphere; PVC (first peak) in g) inert, h) gasifying, and i) oxidising atmosphere; PVC (second peak) in j) inert, k) gasifying, and l) oxidising atmosphere.

**Table 8**  
Kinetic parameters of samples pyrolysis in N<sub>2</sub>, CO<sub>2</sub> and O<sub>2</sub>/CO<sub>2</sub> calculated using all methods.

Atmosphere	Sample	Parameter	Friedman	OFW	KAS	Vyazovkin
Inert	SCG	Ea, kJ/mol	232.1	242.1	241.9	233.4
		A, log(1/s)	17.7	19.1	19.1	17.8
		R <sup>2</sup>	0.99959	0.98783	0.98759	0.99956
	T	Ea, kJ/mol	179.4	198.8	198.7	190.5
		A, log(1/s)	12.9	14.6	14.6	13.8
		R <sup>2</sup>	0.99991	1.00000	1.00000	0.99986
	PVC <sub>1peak</sub>	Ea, kJ/mol	153.0	189.8	189.7	166.7
		A, log(1/s)	11.9	15.5	15.6	13.2
		R <sup>2</sup>	0.99974	0.99009	0.98340	0.99932
	PVC <sub>2peak</sub>	Ea, kJ/mol	216.4	248.0	247.9	216.9
		A, log(1/s)	13.2	15.6	15.7	13.3
		R <sup>2</sup>	0.99732	0.99073	0.98827	0.99997
Gasifying	SCG	Ea, kJ/mol	274.7	266.7	266.6	274.6
		A, log(1/s)	21.3	21.2	21.2	21.3
		R <sup>2</sup>	0.99991	0.99085	0.98897	0.99984
	T	Ea, kJ/mol	188.9	189.0	188.9	188.8
		A, log(1/s)	13.7	13.7	13.8	13.7
		R <sup>2</sup>	0.99976	0.99917	0.99817	0.99978
	PVC <sub>1peak</sub>	Ea, kJ/mol	171.9	175.3	175.2	171.0
		A, log(1/s)	13.6	14.0	14.1	13.5
		R <sup>2</sup>	0.97352	0.97106	0.99340	0.99951
	PVC <sub>2peak</sub>	Ea, kJ/mol	216.5	261.1	261.0	217.2
		A, log(1/s)	13.3	16.7	16.7	13.3
		R <sup>2</sup>	0.99732	1.00000	1.00000	0.55475
Oxidising	SCG	Ea, kJ/mol	192.0	190.1	190.0	191.0
		A, log(1/s)	14.8	14.9	15.0	14.7
		R <sup>2</sup>	0.99998	0.98712	0.98708	0.99996
	T	Ea, kJ/mol	158.8	152.8	152.6	157.5
		A, log(1/s)	11.6	10.9	10.9	11.5
		R <sup>2</sup>	0.99989	0.98847	0.99064	0.99985
	PVC <sub>1peak</sub>	Ea, kJ/mol	131.2	153.1	153.0	130.9
		A, log(1/s)	10.0	12.1	12.1	9.9
		R <sup>2</sup>	0.99982	0.99631	0.99753	0.99976
	PVC <sub>2peak</sub>	Ea, kJ/mol	207.1	253.3	253.1	206.7
		A, log(1/s)	12.9	16.3	16.3	12.9
		R <sup>2</sup>	0.99823	0.99014	0.99023	0.99809

with the KAS, FWO, Friedman, and Vyazovkin for conversion degree range of 0.1–0.9 are presented. Average values of energy activation and pre-exponential factor are tabulated together with correlation coefficient (R<sup>2</sup>). Under gasifying and oxidising conditions, two thermal degradation sub-processes were evident, namely the release of volatiles and char burnout. Therefore, the obtained kinetic data can be directly used in the oxy-MSW combustion models, in which individual stages of waste combustion are considered. For each process, apparent activation energy, which is the energy barrier for a chemical reaction to appear as well as a pre-exponential factor, i.e. the frequency of vibrations of the activated complex [43], were calculated.

#### 4.2.1. Pyrolysis sub-process

Fig. 5a–c present apparent activation energy in the conversion degree function α for devolatilisation of the textile sample in N<sub>2</sub>, CO<sub>2</sub>, and O<sub>2</sub>/CO<sub>2</sub>, respectively. The energy activation value for the textile samples did not vary significantly within the conversion range, indicating that pyrolysis of textiles can be described by a single effective activation energy. This result could mean that the process has a single-step [46]. The value of Ea under N<sub>2</sub> atmosphere was between 176 and 206 kJ/mol, in CO<sub>2</sub> between 180 and 199 kJ/mol, while in O<sub>2</sub>/CO<sub>2</sub> between 149 and 197 kJ/mol.

Activation energy for pyrolysis of the spent coffee grounds sample in inert, gasifying and oxidising atmospheres is shown in Fig. 5d–f. The values of energy activation of the spent coffee grounds pyrolysis fluctuate more, which can be attributed to the heterogeneous composition of the sample (cellulose, hemicellulose, lignin and extracts). These fluctuations indicate the presence

of an intricate reaction system, including parallel, competitive, and complex reactions, which would best be described by multi-step kinetics. The activation energy was in the range 152–272 kJ/mol under inert and gasifying conditions, and was 168–197 kJ/mol when oxygen was present.

Unlike textiles and coffee grounds, PVC devolatilisation consists of two peaks, the activation energy of each peak in conversion rate function was calculated and presented in Fig. 5g–i and Fig. 5j–l. For both peaks, the activation energy varied throughout the conversion range, which confirmed that PVC undergoes a very intricate pyrolytic decomposition related to several different reaction types. The value of Ea for the first peak is in the range of 135–224 kJ/mol, 120–293 kJ/mol, and 95–205 kJ/mol in N<sub>2</sub>, CO<sub>2</sub> and O<sub>2</sub>/CO<sub>2</sub>, respectively. For the second stage of PVC pyrolysis, the value of Ea fluctuated in the range of 158 and 346 kJ/mol, 191 and 461 kJ/mol, as well as 82 and 459 kJ/mol in N<sub>2</sub>, CO<sub>2</sub> and O<sub>2</sub>/CO<sub>2</sub> atmosphere, respectively.

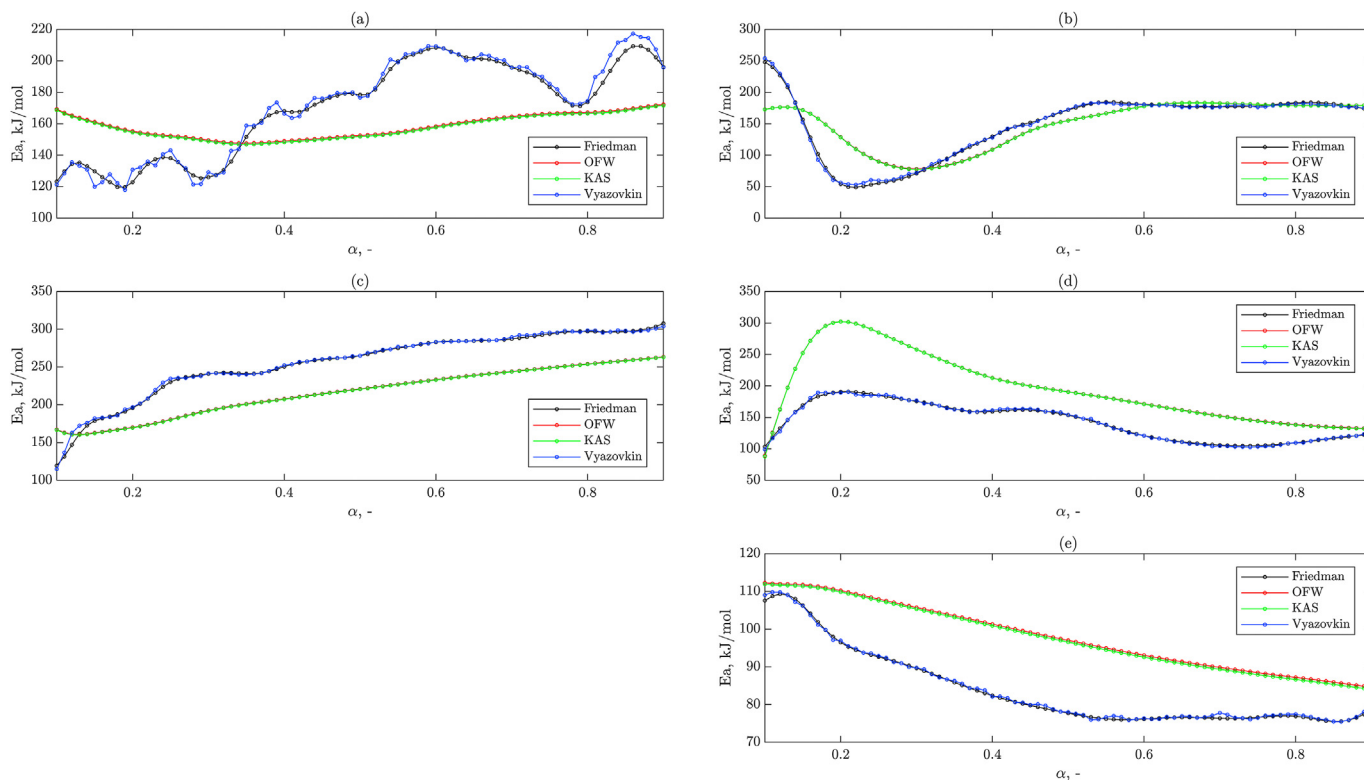
Interestingly, it was observed that activation energy as a function of conversion rate showed similar trends for all atmospheres across all calculation methods. The results obtained by OFW and KAS methods were more stable, which confirmed that Friedman differential method is more susceptible to noise in experimental data. However, it has to be noted that integral methods involve an intrinsic error in the calculation of activation energy due to the integration of temperature. Thus, the results obtained with Friedman method are relatively more reliable than those obtained with OFW and KAS methods theoretically [59].

Table 8 summarises the results of the kinetic analysis for sample devolatilisation. As can be observed, the Friedman differential method and Vyazovkin method yielded almost identical average values of Ea, which were slightly lower than those from the other integral methods. On the other hand, the average Ea values calculated by the KAS method were almost the same as those calculated by the OFW method. This was the case even though the KAS method is based on a more accurate approximation developed by Murray and White.

In the case of the spent coffee sample, the average value of Ea was generally greater than for textiles, meaning that SCG decomposition was more energy-intensive, most likely due to its more complex composition. The first peak of PVC pyrolysis (originating from dehydrochlorination) was characterised by a lower value of the activation energy compared to the second peak, indicating that the second stage of PVC degradation, i.e. polymeric chain decomposition, required more energy. The similar results were obtained by Xu et al. [60]. However, they found that PVC pyrolysis activation energy was 48.11–49.79 kJ/mol and 109.78–113.59 kJ/mol for the first and second stage, respectively. The discrepancy in the results can be caused by the different conditions of the process (higher heating rate, carrier gas flow, etc.). Tang et al. [31] retrieved kinetic parameters under oxy-fuel conditions at O<sub>2</sub> concentration of 20% in the oxidiser. Similar to this study, it was found that the value of activation energy of the second degradation stage is the highest, while the Ea of the char burnout is the lowest.

Moreover, it can be seen that under inert and gasification conditions the mean values of energy activation and the pre-exponential factor differed by about 20 kJ/mol, similar difference in Ea values was observed in the studies performed in Refs. [61,62]. Such a slight difference in Ea values indicates that at lower temperatures, carbon dioxide behaves as an inert atmosphere and does not affect the degradation significantly, which was also observed in- [23]. Under oxidising conditions, the average values of Ea is the smallest, which can be ascribed to the presence of highly reactive oxygen which facilitated decomposition.

Even considering the uncertainties of the kinetic parameter results, most of the parameter sets were determined with high



**Fig. 6.** Activation energy as a function of conversion rate for char burnout: textiles in a) gasifying and b) oxidising atmosphere; spent coffee grounds in c) gasifying and d) oxidising atmosphere; PVC in e) oxidising atmosphere.

**Table 9**

Kinetic parameters of char burnout in CO<sub>2</sub> and O<sub>2</sub>/CO<sub>2</sub> atmosphere calculated using all methods.

Atmosphere	Sample	Parameter	Friedman	OFW	KAS	Vyazovkin	
Gasifying	SCG	Ea, kJ/mol	255.4	216.6	216.2	256.2	
		A, log(1/s)	8.9	7.1	7.0	8.9	
		R <sup>2</sup>	0.99988	0.99513	0.99761	0.99986	
		T	Ea, kJ/mol	170.0	158.3	157.6	171.6
			A, log(1/s)	5.5	4.9	4.7	5.6
Oxidising	SCG	R <sup>2</sup>	0.99800	0.81140	0.97364	0.99710	
		Ea, kJ/mol	142.3	195.4	195.1	142.2	
		A, log(1/s)	7.1	11.0	11.0	7.1	
		R <sup>2</sup>	1.00000	1.00000	1.00000	1.00000	
		T	Ea, kJ/mol	148.5	149.4	149.1	148.7
A, log(1/s)	8.4		8.7	8.6	11.2		
PVC	PVC	R <sup>2</sup>	0.99989	0.99392	0.99407	0.99988	
		Ea, kJ/mol	83.8	97.9	97.4	84.0	
		A, log(1/s)	2.5	3.5	3.2	2.6	
		R <sup>2</sup>	0.99960	0.97573	0.99336	0.99942	

precision, as evidenced by R<sup>2</sup> values close to unity (R<sup>2</sup> > 0.98). This means that these results have the relatively reliable accuracy. Moreover, it can be concluded that isoconversional methods are able to calculate the kinetic parameters of the pyrolysis process in different atmospheres for both lignocellulosic and plastic materials. However, in some cases, the correlation coefficient was unsatisfactory. For example, R<sup>2</sup> for the second peak of PVC pyrolysis in CO<sub>2</sub> obtained based on the Vyazovkin method was only 0.555. These methods can be inappropriate for materials whose decomposition consists of parallel and independent reactions.

#### 4.2.2. Char burnout process

The global kinetics of gasification and/or oxidation of char, as

indicated by an additional peak at elevated temperature (Figs. 2–4), were calculated analogously to the pyrolysis process. The activation energies of char burnout for textiles, spent coffee grounds, and PVC samples in CO<sub>2</sub> and O<sub>2</sub>/CO<sub>2</sub> atmospheres are presented in Fig. 6a–e. The average values of E<sub>a</sub> are presented in Table 9.

For the char burnout process in gasifying conditions, the opposite phenomenon is observed, namely E<sub>a</sub> calculated based on the Friedman and Vyazovkin methods was larger than when calculated using integral methods. However, similarly to previous results, E<sub>a</sub> trends calculated using integral methods were smoother. For textile samples, the value of E<sub>a</sub> under CO<sub>2</sub> atmosphere was between 120 and 217 kJ/mol, while in O<sub>2</sub>/CO<sub>2</sub> is in the range of 52 and 254 kJ/mol. For SCG, E<sub>a</sub> was between 114 and 303 kJ/mol as well as 99 and 190 kJ/mol, for CO<sub>2</sub> and O<sub>2</sub>/CO<sub>2</sub> atmosphere, respectively. While for the PVC sample, E<sub>a</sub> is in the range of 75 and 109 kJ/mol. In all cases, the value of R<sup>2</sup> was above 0.97, except for one case, namely E<sub>a</sub> of char gasification of textile retrieved using OFW method (R<sup>2</sup> = 0.811). However, this is still an acceptable result and it can be stated that calculated values are reliable. Moreover, it should be remembered that these results are valid for an oxygen concentration 10%. Using these results for other oxygen concentrations in the oxidiser could introduce unacceptable error.

#### 4.3. Models verification

To verify the accuracy of each method, the TGA curves were reproduced as shown in Fig. 7 and Fig. 8, as well as the mean relative error ( $\bar{\epsilon}$ ) between the experimental data and the calculated weight loss curves was determined and reported in Table 10. As can be observed, for all methods the relative error is very small, which confirms that model-free methods are suitable for determination of

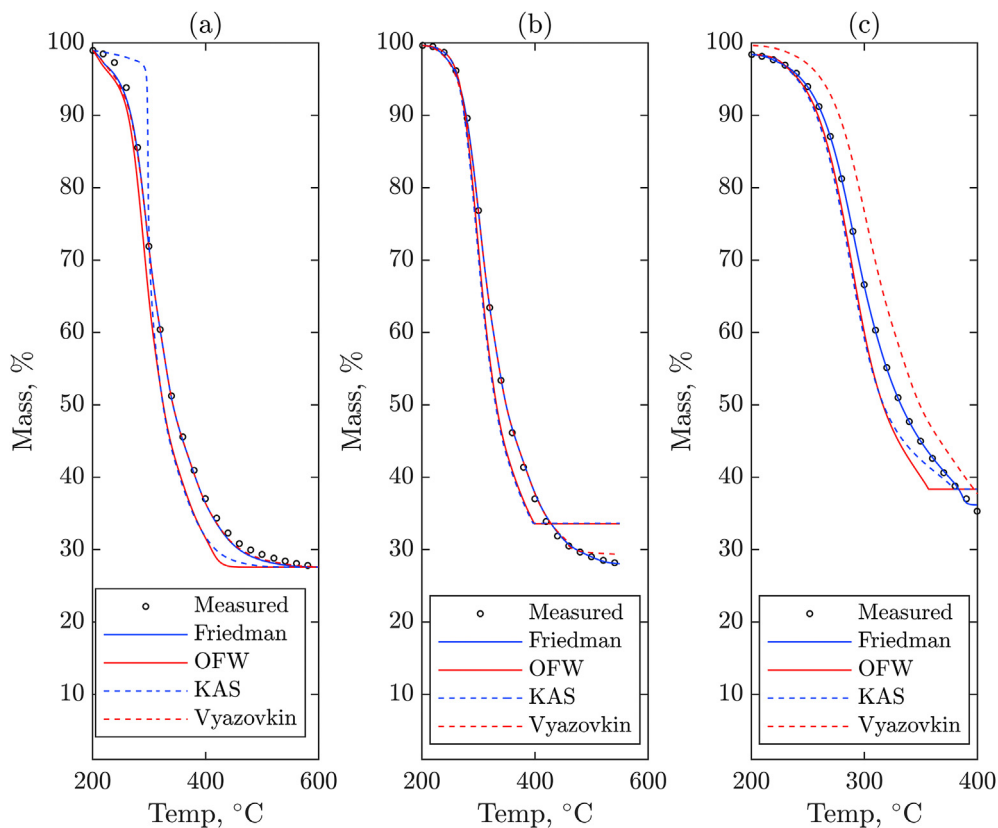


Fig. 7. Reproduced TGA curves of SCG pyrolysis under a) inert, b) gasifying and c) oxidising atmospheres with measured values.

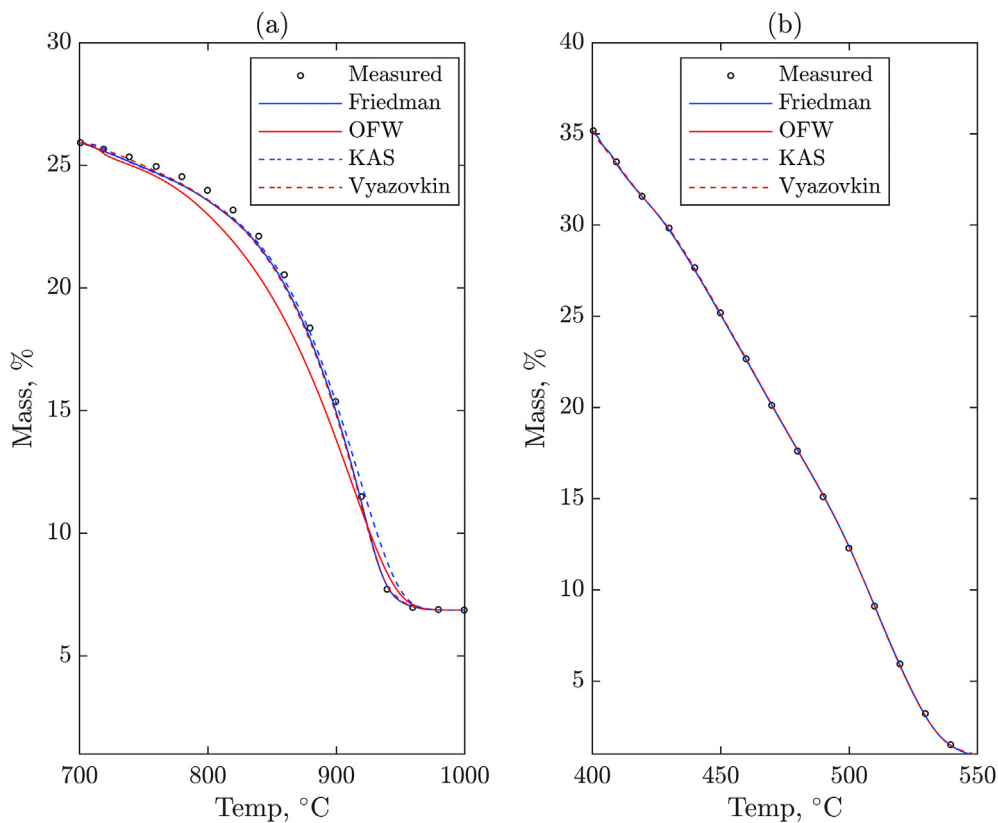


Fig. 8. Reproduced TGA curves of SCG char burnout under different atmospheres with measured values.



**Table 10**

The mean relative error ( $\bar{\varepsilon}$ ) between the actual and calculated values of sample weight loss for all methods for 10 K/min.

Sample	Atmosphere	Process	$\bar{\varepsilon}_{\text{Friedman}}$	$\bar{\varepsilon}_{\text{OFW}}$	$\bar{\varepsilon}_{\text{KAS}}$	$\bar{\varepsilon}_{\text{Vyazovkin}}$
Tex	Inert	Pyrolysis	0.020	3.173	3.174	0.024
		Pyrolysis	0.039	2.901	2.880	0.040
		Char burnout	0.010	1.412	1.201	0.020
	Oxidising	Pyrolysis	0.011	0.287	0.273	0.021
		Char burnout	0.001	0.116	0.116	0.000
SCG	Inert	Pyrolysis	0.090	0.203	0.076	0.102
		Pyrolysis	0.043	0.040	0.054	0.056
		Char burnout	0.003	0.009	0.006	0.003
	Oxidising	Pyrolysis	0.002	0.090	0.103	0.003
		Char burnout	0.000	0.232	0.232	0.000
PVC	Inert	Pyrolysis (I stage)	0.170	0.570	0.590	0.180
		Pyrolysis (II stage)	0.020	0.790	0.650	0.010
	Gasifying	Pyrolysis (I stage)	0.014	0.055	0.036	0.051
		Pyrolysis (II stage)	0.000	0.002	0.001	0.000
	Oxidising	Pyrolysis (I stage)	0.008	0.081	0.029	0.029
		Pyrolysis (II stage)	0.002	0.043	0.002	0.002
		Char burnout	0.000	0.011	0.044	0.000

kinetic data of waste degradation. It should be noticed, that in all calculation cases, Friedman and Vazovkin methods yields the smallest value of  $\bar{\varepsilon}$  (below 0.180), they are considered as the most accurate and they are recommended for further studies.

## 5. Conclusion

In this work, thermal degradation of various types of waste materials (coffee grounds, textiles, and PVC) in different atmospheres, i.e. an inert, gasifying and oxidising, was studied to obtain kinetic parameters of pyrolysis and char burnout processes. Kinetic parameters were calculated using Netzsch Kinetics Neo software (v.2.5.0.1). The most important findings are as follows:

- Results showed that shifting atmosphere from inert to gasifying does not influence the thermal decomposition of samples below 600 °C, and the kinetic parameters for pyrolysis are similar in N<sub>2</sub> and CO<sub>2</sub> atmosphere. However, in the gasifying atmosphere, the second peak appears above 600 °C during the decomposition of lignocellulosic materials that is ascribed to CO<sub>2</sub>-char reactions. In the case of lignocellulosic materials, the O<sub>2</sub>/CO<sub>2</sub> atmosphere causes that reactions with char and carrier gas is more rapid and occurs at a lower temperature, thus it partially overlaps the pyrolysis process, which is demonstrated by DTG curves as well as larger fluctuations in the activation energy above a certain value of  $\alpha$ .
- Results of PVC degradation in various atmospheres indicate that this plastic follows different reaction mechanisms compared to lignocellulosic materials and change of atmosphere affects its thermal decomposition differently. These results point out that each group of waste should be investigated separately in order to create successful models of oxy-MSW combustion and further develop this technology.
- The energy activation of textile pyrolysis was 190.5 kJ/mol, 188.8 kJ/mol, and 157.5 kJ/mol, for SCG sample, 233.4 kJ/mol, 274.6 kJ/mol, and 191.0 kJ/mol and for PVC Ea was 166.7 kJ/mol, 171.0 kJ/mol, and 130.9 kJ/mol (I stage) as well as 216.9 kJ/mol, 217.2 kJ/mol and, 206.7 kJ/mol (II stage) for inert, gasifying and oxidising atmospheres, respectively. For SCG char burnout, Ea was 256.2 kJ/mol and 142.2 kJ/mol for gasifying and oxidising atmospheres, respectively. For char burnout process of textile sample, Ea was 171.6 kJ/mol and 148.7 kJ/mol for gasifying and oxidising atmospheres, respectively. Finally, energy activation of char burnout of PVC sample under oxidising atmosphere was

84.0 kJ/mol. These sets of kinetic data obtained using different isoconversional methods can be directly used in the modelling of oxy-MSW incineration systems.

- It was found that the kinetic parameters calculated by the methods of Friedman and Vyazovkin are more efficient than OFW and KAS for studied materials, because the theoretical curves reproduced based on kinetic data obtained using these methods best reflected the measurement results.
- It should be remembered that waste incineration is feasible and implemented on a large scale. However, the investigated oxy-waste incineration technology can improve the process and thereby increase the variety of the waste that could be incinerated.

### 5.1. Future work

In the future, a mathematical model of oxy-waste combustion in a moving grate furnace will be developed to investigate heat transfer between solid and gas phases, along with combustion characteristics. The model will include such processes as pyrolysis and char burnout based on chemical kinetics obtained in this article. Subsequently, optimization of the O<sub>2</sub>/CO<sub>2</sub> ratio and its feeding will be performed to avoid the ash melting problem.

### Credit author statement

Conceptualization: Andrzej Szlęk, Mario Ditaranto, Paulina Wienchol. Methodology: Paulina Wienchol, Agnieszka Korus. Investigation: Paulina Wienchol, Agnieszka Korus. Writing - Original Draft: Paulina Wienchol, Agnieszka Korus. Writing - Review & Editing: Andrzej Szlęk, Mario Ditaranto. Visualization: Paulina Wienchol. Supervision: Andrzej Szlęk, Mario Ditaranto. Project administration: Paulina Wienchol. Funding acquisition: Paulina Wienchol.

### Declaration of competing interest

The authors declare that they have no known competing financial interests or personal relationships that could have appeared to influence the work reported in this paper.

### Acknowledgement

The work of PW is supported by the Statutory Fund of the Faculty of Energy and Environmental Engineering of the Silesian University of Technology (grant no. BKM-579/RIE6/2020). MD was supported by the Research Council of Norway through the CAPE-WASTE project (grant no. 281869) and the ERANET Cofund ACT NEWEST-CCUS project (grant no. 305062).

### References

- [1] Eurostat SE. Municipal waste statistics. 2017. 2019-02-18, [https://ec.europa.eu/eurostat/statistics-explained/index.php/Municipal\\_waste\\_statistics](https://ec.europa.eu/eurostat/statistics-explained/index.php/Municipal_waste_statistics).
- [2] Liobikienė G, Butkus M. The European Union possibilities to achieve targets of europe 2020 and paris agreement climate policy. *Renew Energy* 2017;106: 298–309.
- [3] Scheutz C, Kjeld A, Fredenslund AM. Methane emissions from Icelandic landfills—a comparison between measured and modelled emissions. *Waste Manag* 2022;139:136–45.
- [4] Lu J-W, Zhang S, Hai J, Lei M. Status and perspectives of municipal solid waste incineration in China: a comparison with developed regions. *Waste Manag* 2017;69:170–86.
- [5] Makarichi L, Juditadrongphan W, Techato K-a. The evolution of waste-to-energy incineration: a review. *Renew Sustain Energy Rev* 2018;91:812–21.
- [6] Confederation of European waste-to-energy plants. Waste-to-energy plants in europe in 2018; 2021. Accessed: 2021-04-02, <https://www.cewep.eu/waste-to-energy-plants-in-europe>

- to-energy-plants-in-europe-in-2018/.
- [7] Dastjerdi B, Strezov V, Kumar R, Behnia M. An evaluation of the potential of waste to energy technologies for residual solid waste in new south wales, Australia. *Renew Sustain Energy Rev* 2019;115:109398.
  - [8] Wienchol P, Szlęk A, Ditaranto M. Waste-to-energy technology integrated with carbon capture—challenges and opportunities. *Energy* 2020;198:117352.
  - [9] Communication from the commission to the european parliament, the council, the european economic and social committee and the committee of the regions. the european green deal. Accessed: 2021-06-18, [https://ec.europa.eu/info/sites/info/files/european-green-deal-communication\\_en.pdf](https://ec.europa.eu/info/sites/info/files/european-green-deal-communication_en.pdf); 2019.
  - [10] Lucquiaud M, Herraiz L, Su D, Thomson C, Chalmers H, Becidan M, Ditaranto M, Roussanaly S, Anantharaman R, Moreno Mendaza J, et al. Negative emissions in the waste-to-energy sector: an overview of the newest-ccus programme. 2021.
  - [11] Pour N, Webley PA, Cook PJ. A sustainability framework for bioenergy with carbon capture and storage (beccs) technologies. *Energy Proc* 2017;114:6044–56.
  - [12] Bisinella V, Hulgaard T, Riber C, Damgaard A, Christensen TH. Environmental assessment of carbon capture and storage (ccs) as a post-treatment technology in waste incineration. *Waste Manag* 2021;128:99–113.
  - [13] Christensen TH, Bisinella V. Climate change impacts of introducing carbon capture and utilisation (ccu) in waste incineration. *Waste Manag* 2021;126:754–70.
  - [14] Pratschner S, Skopec P, Hrdlicka J, Winter F. Power-to-green methanol via co<sub>2</sub> hydrogenation—a concept study including oxyfuel fluidized bed combustion of biomass. *Energies* 2021;14:4638.
  - [15] Tang Y, Ma X, Lai Z, Chen Y. Energy analysis and environmental impacts of a msw oxy-fuel incineration power plant in China. *Energy Pol* 2013;60:132–41.
  - [16] Yadav S, Mondal S. A review on the progress and prospects of oxy-fuel carbon capture and sequestration (ccs) technology. *Fuel* 2022;308:122057.
  - [17] Buhre BJ, Elliott LK, Sheng C, Gupta RP, Wall TF. Oxy-fuel combustion technology for coal-fired power generation. *Prog Energy Combust Sci* 2005;31:283–307.
  - [18] Toftgaard MB, Brix J, Jensen PA, Glarborg P, Jensen AD. Oxy-fuel combustion of solid fuels. *Prog Energy Combust Sci* 2010;36:581–625.
  - [19] Sher F, Pans MA, Sun C, Snape C, Liu H. Oxy-fuel combustion study of biomass fuels in a 20 kwth fluidized bed combustor. *Fuel* 2018;215:778–86.
  - [20] Markewitz P, Kuckshinrichs W, Leitner W, Linszen J, Zapp P, Bongartz R, Schreiber A, Müller TE. Worldwide innovations in the development of carbon capture technologies and the utilization of co<sub>2</sub>. *Energy Environ Sci* 2012;5:7281–305.
  - [21] Vilardi G, Verdone N. Exergy analysis of municipal solid waste incineration processes: the use of o<sub>2</sub>-enriched air and the oxy-combustion process. *Energy* 2022;239:122147.
  - [22] Magnanelli E, Mosby J, Becidan M. Scenarios for carbon capture integration in a waste-to-energy plant. *Energy* 2021;227:120407.
  - [23] Tang Y, Ma X, Wang Z, Wu Z, Yu Q, A. Study of the thermal degradation of six typical municipal waste components in co<sub>2</sub> and n<sub>2</sub> atmospheres using tg-ftir. *Thermochim Acta* 2017;657:12–9.
  - [24] Policella M, Wang Z, Burra KG, Gupta AK. Characteristics of syngas from pyrolysis and co<sub>2</sub>-assisted gasification of waste tires. *Appl Energy* 2019;254:113678.
  - [25] Lai Z, Ma X, Tang Y, Lin H. Thermogravimetric analysis of the thermal decomposition of msw in n<sub>2</sub>, co<sub>2</sub> and co<sub>2</sub>/n<sub>2</sub> atmospheres. *Fuel Process Technol* 2012;102:18–23.
  - [26] Chen S, Meng A, Long Y, Zhou H, Li Q, Zhang Y. Tga pyrolysis and gasification of combustible municipal solid waste. *J Energy Inst* 2015;88:332–43.
  - [27] Déparrois N, Singh P, Burra K, Gupta A. Syngas production from co-pyrolysis and co-gasification of polystyrene and paper with co<sub>2</sub>. *Appl Energy* 2019;246:1–10.
  - [28] Lai Z, Ma X, Tang Y, Lin H. A study on municipal solid waste (msw) combustion in n<sub>2</sub>/o<sub>2</sub> and co<sub>2</sub>/o<sub>2</sub> atmosphere from the perspective of tga. *Energy* 2011;36:819–24.
  - [29] Lai Z, Ma X, Tang Y, Lin H, Chen Y. Thermogravimetric analyses of combustion of lignocellulosic materials in n<sub>2</sub>/o<sub>2</sub> and co<sub>2</sub>/o<sub>2</sub> atmospheres. *Bioresour Technol* 2012;107:444–50.
  - [30] Tang Y, Ma X, Lai Z, Fan Y. Thermogravimetric analyses of co-combustion of plastic, rubber, leather in n<sub>2</sub>/o<sub>2</sub> and co<sub>2</sub>/o<sub>2</sub> atmospheres. *Energy* 2015;90:1066–74.
  - [31] Tang Y, Ma X, Lai Z, Zhou D, Chen Y. Thermogravimetric characteristics and combustion emissions of rubbers and polyvinyl chloride in n<sub>2</sub>/o<sub>2</sub> and co<sub>2</sub>/o<sub>2</sub> atmospheres. *Fuel* 2013;104:508–14.
  - [32] Tang Y, Ma X, Lai Z, Zhou D, Lin H, Chen Y. Nox and so<sub>2</sub> emissions from municipal solid waste (msw) combustion in co<sub>2</sub>/o<sub>2</sub> atmosphere. *Energy* 2012;40:300–6.
  - [33] Tang Y, Ma X, Lai Z. Thermogravimetric analysis of the combustion of microalgae and microalgae blended with waste in n<sub>2</sub>/o<sub>2</sub> and co<sub>2</sub>/o<sub>2</sub> atmospheres. *Bioresour Technol* 2011;102:1879–85.
  - [34] Ke C, Ma X, Tang Y, Zheng W, Wu Z. The volatilization of heavy metals during co-combustion of food waste and polyvinyl chloride in air and carbon dioxide/oxygen atmosphere. *Bioresour Technol* 2017;244:1024–30.
  - [35] Tang Y, Ma X, Zhang C, Yu Q, Fan Y. Effects of sorbents on the heavy metals control during tire rubber and polyethylene combustion in co<sub>2</sub>/o<sub>2</sub> and n<sub>2</sub>/o<sub>2</sub> atmospheres. *Fuel* 2016;165:272–8.
  - [36] Becidan M, Ditaranto M, Carlsson P, Bakken J, Olsen MN, Stuen J. Oxyfuel combustion of a model msw—an experimental study. *Energies* 2021;14:5297.
  - [37] Yousef S, Eimontas J, Striugas N, Tatarians M, Abdelnaby MA, Tuckute S, Kliucininkas L. A sustainable bioenergy conversion strategy for textile waste with self-catalysts using mini-pyrolysis plant. *Energy Convers Manag* 2019;196:688–704.
  - [38] Becidan M. Experimental studies on municipal solid waste and biomass pyrolysis. 2007.
  - [39] Li X, Strezov V, Kan T. Energy recovery potential analysis of spent coffee grounds pyrolysis products. *J Anal Appl Pyrol* 2014;110:79–87.
  - [40] Brachi P, Santes V, Torres-Garcia E. Pyrolytic degradation of spent coffee ground: a thermokinetic analysis through the dependence of activation energy on conversion and temperature. *Fuel* 2021;120995.
  - [41] Zhou H, Meng A, Long Y, Li Q, Zhang Y. An overview of characteristics of municipal solid waste fuel in China: physical, chemical composition and heating value. *Renew Sustain Energy Rev* 2014;36:107–22.
  - [42] Banu JR, Kavitha S, Kannah RY, Kumar MD, Atabani A, Kumar G, et al. Bio-refinery of spent coffee grounds waste: viable pathway towards circular bioeconomy. *Bioresour Technol* 2020;302:122821.
  - [43] Vyazovkin S, Burnham AK, Criado JM, Pérez-Maqueda LA, Popescu C, Sbirrazzuoli N. Ictac kinetics committee recommendations for performing kinetic computations on thermal analysis data. *Thermochim Acta* 2011;520:1–19.
  - [44] Weber R. Extracting mathematically exact kinetic parameters from experimental data on combustion and pyrolysis of solid fuels. *J Energy Inst* 2008;81:226–33.
  - [45] Qiao Y, Xu F, Xu S, Yang D, Wang B, Ming X, Hao J, Tian Y. Pyrolysis characteristics and kinetics of typical municipal solid waste components and their mixture: analytical tg-ftir study. *Energy Fuels* 2018;32:10801–12.
  - [46] Vyazovkin S. Isoconversional kinetics of thermally stimulated processes. Springer; 2015.
  - [47] Vyazovkin S, Chrissafis K, Di Lorenzo ML, Koga N, Pijolat M, Roduit B, Sbirrazzuoli N, Suñol JJ. Ictac kinetics committee recommendations for collecting experimental thermal analysis data for kinetic computations. *Thermochim Acta* 2014;590:1–23.
  - [48] Friedman HL. Kinetics of thermal degradation of char-forming plastics from thermogravimetry. application to a phenolic plastic. In: *Journal of polymer science part C: polymer symposia*, vol. 6. Wiley Online Library; 1964. p. 183–95.
  - [49] Flynn JH, Wall LA. General treatment of the thermogravimetry of polymers 1966;70:487.
  - [50] Akahira T, Sunose T. Method of determining activation deterioration constant of electrical insulating materials. *Res Rep Chiba Inst Technol (Sci Technol)* 1971;16:22–31.
  - [51] Yang H, Yan R, Chen H, Lee DH, Zheng C. Characteristics of hemicellulose, cellulose and lignin pyrolysis. *Fuel* 2007;86:1781–8.
  - [52] Moltó J, Font R, Conesa JA, Martín-Gullón I. Thermogravimetric analysis during the decomposition of cotton fabrics in an inert and air environment. *J Anal Appl Pyrol* 2006;76:124–31.
  - [53] Kim Y, Lee J, Yi H, Tsang YF, Kwon EE. Investigation into role of co<sub>2</sub> in two-stage pyrolysis of spent coffee grounds. *Bioresour Technol* 2019;272:48–53.
  - [54] Kwon EE, Kim S, Lee J. Pyrolysis of waste feedstocks in co<sub>2</sub> for effective energy recovery and waste treatment. *J CO<sub>2</sub> Util* 2019;31:173–80.
  - [55] Ma W, Rajput G, Pan M, Lin F, Zhong L, Chen G. Pyrolysis of typical msw components by py-gc/ms and tg-ftir. *Fuel* 2019;251:693–708.
  - [56] Özsin G, Pütün AE. Tga/ms/ft-ir study for kinetic evaluation and evolved gas analysis of a biomass/pvc co-pyrolysis process. *Energy Convers Manag* 2019;182:143–53.
  - [57] Merdun H, Laougé ZB. Kinetic and thermodynamic analyses during co-pyrolysis of greenhouse wastes and coal by tga. *Renew Energy* 2021;163:453–64.
  - [58] Ding G, He B, Yao H, Cao Y, Su L, Duan Z. Co-combustion behaviors of municipal solid waste and low-rank coal semi-coke in air or oxygen/carbon dioxide atmospheres. *J Therm Anal Calorim* 2021;143:619–35.
  - [59] Yan J, Jiao H, Li Z, Lei Z, Wang Z, Ren S, Shui H, Kang S, Yan H, Pan C. Kinetic analysis and modeling of coal pyrolysis with model-free methods. *Fuel* 2019;241:382–91.
  - [60] Xu F, Wang B, Yang D, Hao J, Qiao Y, Tian Y. Thermal degradation of typical plastics under high heating rate conditions by tg-ftir: pyrolysis behaviors and kinetic analysis. *Energy Convers Manag* 2018;171:1106–15.
  - [61] Yousef S, Eimontas J, Striugas N, Abdelnaby MA. Pyrolysis and gasification kinetic behavior of mango seed shells using tg-ftir-gc-ms system under n<sub>2</sub> and co<sub>2</sub> atmospheres. *Renew Energy* 2021;173:733–49.
  - [62] Huang J, Zhang J, Liu J, Xie W, Kuo J, Chang K, Buyukada M, Evrendilek F, Sun S. Thermal conversion behaviors and products of spent mushroom substrate in co<sub>2</sub> and n<sub>2</sub> atmospheres: kinetic, thermodynamic, tg and py-gc/ms analyses. *J Anal Appl Pyrol* 2019;139:177–86.



# A comparative study on thermochemical decomposition of lignocellulosic materials for energy recovery from waste: Monitoring of evolved gases, thermogravimetric, kinetic and surface analyses of produced chars

Paulina Copik<sup>a,\*</sup>, Agnieszka Korus<sup>a</sup>, Andrzej Szlęk<sup>a</sup>, Mario Ditaranto<sup>b</sup>

<sup>a</sup> Department of Thermal Technology, Silesian University of Technology, Gliwice, Poland

<sup>b</sup> SINTEF Energy Research, Trondheim, Norway

## ARTICLE INFO

Handling editor: Krzysztof (K.J.) Ptasiński

### Keywords:

Municipal solid waste  
Char  
Oxy-fuel combustion  
Gasification  
Pyrolysis  
Waste-to-energy

## ABSTRACT

Increased waste generation caused by the growth of urbanisation rate forces scientists and policymakers to rapidly develop and implement optimal waste management strategies. Since there are many ways to waste treatment and each waste material has different physicochemical properties, they should be investigated separately. This paper presents the results of an experimental investigation on the thermal decomposition of the spent coffee grounds (SCG) and textiles under various atmospheres using a vertical tube furnace. In the study, different analytical techniques are used, such as gas chromatography (GC), gas adsorption for surface area and porosity determination, Fourier-transform infrared spectroscopy (FTIR), and thermogravimetric analysis (TGA). Results indicated that SCG sample yielded more calorific pyrolytic gas (209.8 kJ/mol) than TEX (198.7 kJ/mol). O<sub>2</sub>/CO<sub>2</sub> atmosphere fasten the fuel decomposition. Concerning biochar, it can be concluded that fast pyrolysis influenced their combustion performance, for example, its ignition temperature, TEX<sub>slow</sub> (475.4 °C) > SGS<sub>slow</sub> (470.5 °C) and TEX<sub>fast</sub> (469.6 °C) > SGS<sub>fast</sub> (415.0 °C), maximum weight loss rates and reactivity. This study will provide a better understanding of thermochemical degradation of waste and allows for developing optimal routes of waste utilisation.

## 1. Introduction

Due to increasing urbanisation, in the future, most people will inhabit big cities. Metropolises have numerous challenges, including traffic, excessive waste generation, and air and water pollution. Thus, appropriate municipal solid waste (MSW) management is one of the key elements for the sustainable development of urban areas. After recycling, energy recovery from waste is the most favourable method of waste management, in line with the concept of a circular economy. As a result, local governments can reduce greenhouse gas footprints, dispose of waste effectively and create new workplaces [1–3]. Besides, the use of waste as a source of energy can decrease fossil fuel depletion and mitigate climate change.

There are plenty of possibilities for extracting energy from waste: for example, via gasification in the presence of sub-stoichiometric air to produce syngas; through pyrolysis, which operates in the absence of oxygen to give various valuable pyrolytic products, such as pyrolytic gas, bio-oil and biochar; and full oxidation (combustion), which allows

for heat and electricity production with a reduction in waste volume of up to 90% [4]. All these methods are generally known as waste-to-energy (WtE) technologies, with incineration currently being the most mature and superior in large-scale applications [5]. Although pyrolysis and gasification are growing in popularity [6], the variability of feedstock is the main obstacle to fully developing these technologies, since a high degree of pre-treatment is required.

Nevertheless, biochar, which is derived from organic waste pyrolysis, has great potential in environmental and industrial applications owing to its unique physicochemical features [7]. The properties of biochar directly depend on the feedstocks and process conditions employed, which were widely reviewed by Weber and Quicker [8]. Since biochar has desirable fuel properties, such as higher energy density and good grindability, it could potentially be a useful solution where a waste incineration plant could not be deployed close to a city, addressing key issues, including expensive transportation and poor grindability, associated with the direct use of waste as a fuel [9,10].

Although the incineration sector has evolved over the past decades

\* Corresponding author.

E-mail address: [paulina.wienchol@polsl.pl](mailto:paulina.wienchol@polsl.pl) (P. Copik).

and the problem of harmful furans and dioxins has been eliminated, there is still an issue regarding carbon dioxide emissions from the part of the carbon contained in the waste that is not of biological origin [2]. Therefore, a step forward in incineration technology development is the implementation of Carbon Capture and Utilisation or Storage (CCUS) techniques in WtE plants, which will lead to negative CO<sub>2</sub> emissions from biogenic carbon in waste, thus decreasing atmospheric CO<sub>2</sub> [11].

Among CCUS technologies, oxy-fuel is considered the most promising method, mostly due to the high partial pressure of carbon dioxide in the flue gas, which results in less energetic carbon capture compared to the post-combustion method [12]. Furthermore, using oxygen instead of air causes the exhaust gas volume to be about five times lower, and thereby gas cleaning is cheaper because fewer materials need to be used to construct an air pollution control system [13]. Since combustion in an oxygen atmosphere also results in a higher process temperature, the implementation of the oxy-fuel combustion technique in an incineration plant can eliminate the consumption of auxiliary fossil fuel, which is usually used to keep the required temperature [14].

An in-depth understanding of the thermal degradation properties of individual waste materials under various conditions is crucial to provide an optimised utilisation method for municipal solid waste. In the literature, we can find studies of these properties, which are usually product characteristics. Li et al. [15] investigated the bioenergy generation potential of spent coffee grounds (SCG) during pyrolysis at two heating rates of 10 and 60 °C/min using the thermogravimetric technique. The pyrolysis efficiency was estimated at 77–85 %, depending on the moisture content of the feedstock. Kelkar et al. [16] used a screw-conveyor pyrolysis reactor to assess the effects of reactor temperature and residence time during the fast pyrolysis on the overall and organic yield of liquid product. Bio-oil production and the effect on its quality of process temperatures ranging from 673 K to 873 K were also investigated by Bok et al. [17]. They found that CO<sub>2</sub> and CO, as well as CH<sub>4</sub> are the three main volatile products during SCG pyrolysis, while in the bio-oils, palmitic and linoleic acids were the dominant compounds, indicating its great potential for further biodiesel production.

Biochar derived from SCG pyrolysis was evaluated by Christou et al. [18] as a soil conditioner for boosting plant growth, while Cho et al. [19] used nano Fe(III) oxide (FO) as an additive material in spent coffee ground (SCG) pyrolysis under a CO<sub>2</sub> atmosphere and investigated its impacts on syngas generation and biochar adsorptive properties. Various researchers have analysed [20–22] pyrolysis using CO<sub>2</sub> as a reaction medium in lab-scale reactors. They observed that by using carbon dioxide, the generation of syngas is enhanced, while condensable hydrocarbons (e.g., tar) are reduced. In the most recent study, Primaz et al. [23] used a thermogravimetric method to study SCG pyrolysis and combustion processes and determine kinetic parameters. Studies on the co-pyrolysis of SCG and other fuels, such as plastics, have also been reported, for example, in Ref. [24]. Results indicated that co-pyrolysis improve the performance of the process.

Studies on the pyrolysis and gasification of waste textiles (TEX), such as polyester fiber, cotton, and wool, using thermogravimetric analysis, X-ray diffraction (XRD), and scanning electron microscopy (SEM) were presented in Refs. [25,26]. Tang et al. [27] employed TGA-FTIR analysis to investigate pyrolysis in N<sub>2</sub> and CO<sub>2</sub> atmosphere of six different waste materials, including TEX. The outcomes showed that the growth rate of CO absorbance in CO<sub>2</sub> is significantly faster than in N<sub>2</sub>, indicating waste pyrolysis in carbon dioxide can increased the syngas production at higher temperatures.

As the literature reports [28], there are limited studies comparing fast and slow biomass and waste pyrolysis. Up to now, fast and slow pyrolysis of sugarcane bagasse [29], cherry seed [30] and macadamia nutshell [31] have been performed. However, the effect of the heating rate on the physicochemical properties of biochar derived from banana waste and forest residue was reported in two articles [9,28]. Moreover, no study was found on the combustion characteristics of biochar obtained from fast and slow pyrolysis.

This study is the continuation of our previous research on the thermogravimetric and kinetic analysis of thermal degradation of three different waste materials under various atmospheres, where we retrieved chemical kinetic parameters, such as energy activation (E<sub>a</sub>) and pre-exponential factor (A), of pyrolysis and char burnout processes using model-free methods [32]. In this work, we employed the same reaction gases as previously, namely inert (N<sub>2</sub>), gasifying (CO<sub>2</sub>) and oxy-combustion (O<sub>2</sub>/CO<sub>2</sub>); however, we used a laboratory-scale reactor to compare the thermal behaviour of TEX and SCG.

TEX sample was chosen since approximately 113 million metric tons of textile fibers were produced worldwide in 2021. Natural fibers such as cotton or wool had a production volume of 25.4 million metric tons, whereas chemical fibers accounted for the remaining 88.2 million [33]. Over 69 % of TEX waste is currently landfilled, which risks soil and groundwater contamination by heavy metals used in the production process [34]. A popular beverage made from roasted coffee beans, coffee is consumed all around the world. The estimated amount of coffee consumed worldwide in 2020 was 167.26 million bags, up 1.9 % from the 164.13 million bags recorded in 2019 [35]. Currently, spent coffee grounds have no significant market and hence are problematic for disposal, but their relatively high chemical energy content makes them a potentially valuable feedstock [20]. In the paper, we also prepared waste-derived chars under different pyrolytic conditions and subjected them to further kinetic analysis to evaluate the influence of the size of the sample on the chemical kinetics through a comparison of the kinetic parameters of the char burnout process calculated in a previous paper [32] and within this work. To the best of our knowledge, the combustion properties, as well as kinetic and surface analyses of carbonized SCG and TEX obtained at varied heating rates, have not been widely studied. So, we have focused on a) gas evolution during the thermal degradation of waste materials under different atmospheres to evaluate these materials as energy carriers, and b) biochar properties obtained during fast and slow pyrolysis of used waste samples, which will provide information on the ability of this material for adsorption processes, its reactivity and combustibility, depending on process conditions. This work will contribute the development of studies on waste thermal conversion processes since it provides new knowledge on waste thermal behaviour as well as essential experimental data, which can be used as an input or for the validation of various mathematical models.

## 2. Methodology

### 2.1. Materials

For this study, representative examples of MSW were used, such as TEX and SCG, since they are available worldwide, and their management is considered a common global issue [34]. The detailed characterisation of the materials employed, including proximate and ultimate analyses as well as ash composition analysis, was described in our previous paper [32].

For this study, the chemical composition of the raw material was tested according to the PN-92/P-50092 Standard for plant biomass. The cellulose content was determined by the Seifert method using a mixture of acetylacetone and dioxane, the lignin content using the Tappi method using concentrated sulfuric acid, the holocellulose content using sodium chlorite, and the amount of material soluble in organic solvents by the Soxhlet method. The hemicellulose content was calculated as the difference between that of holocellulose and cellulose. The average results with standard deviations are presented in Table 1.

For experimental purposes, samples were cut and ground before the tests down to a size of 0.1 mm. The initial weight of the samples was 2 ± 0.5 g, while the height of the bed was 2 cm.

**Table 1**  
Chemical composition of tested samples.

Symbol	Extractive substances		Cellulose		Lignin		Hemicellulose		Holocellulose	
	$\bar{x}$	$\sigma$	$\bar{x}$	$\sigma$	$\bar{x}$	$\sigma$	$\bar{x}$	$\sigma$	$\bar{x}$	$\sigma$
Unit	%									
SCG	15.5	0.6	18.1	0.4	23.8	0.4	33.4	0.6	51.5	0.5
Tex	3.1	0.2	89.6	0.3	1.6	0.2	9.9	0.6	99.5	0.3

## 2.2. Experimental apparatus

### 2.2.1. Thermochemical degradation process

To investigate the thermal degradation of various waste materials depending on the atmosphere employed, as well as producing chars for further analysis, tests were carried out in a custom-built laboratory-scale experimental rig. The main part of the test rig was a tubular reactor located inside an electrical furnace. Selected gases were introduced into the upper part of the quartz tube reactor. The employed test stand can be used for either a gravimetric or an evolved gas method. The description of the stand and its operation in both modes has been discussed in detail in the article by Korus et al. [36].

In the evolved gas mode, three different atmospheres were used: (a) inert, 100 vol% N<sub>2</sub>, (b) gasifying, 100 vol% CO<sub>2</sub>, and (c) oxidising, 90/10 vol% CO<sub>2</sub>/O<sub>2</sub>, with a total flow of 400 ml/min to assess the gas evolution profiles during different processes, such as pyrolysis, gasification and oxy-combustion. The temperature of the process varied from ambient temperature to 800 °C for an inert atmosphere, and to 1100 °C for the other atmospheres, with a constant heating rate of 15 K/min. Afterward, samples were kept in the reactor for a 30 min isotherm at the final temperature for the given atmosphere. Gas samples were taken at 90 s intervals and analysed post-run with GC-TCD. Each experiment was replicated to evaluate the reproducibility of the results. The temperature of the sample was registered with a thermocouple inserted into the reactor, and the mean value was reported for each sampling interval.

In the fast pyrolysis experiment, only inert conditions were employed. The sample was placed into a crucible attached to the rod, while the furnace panel was in the upper position so that the reactor was above the sample holder. A high heating rate of ca. 1700 °C/min was achieved by lowering the furnace, which was pre-heated up to 800 °C and constantly purged with N<sub>2</sub>, so that it rapidly enclosed the sample that was waiting in the ambient atmosphere.

Apart from the lab-scale test stand, the SCG char was also produced in a muffle furnace by inserting a crucible with a lid (dedicated to volatile matter analysis) containing a 2 g sample into a furnace heated to 800 °C for 7 min.

Due to the small amount of the sample, the collection and analysis of the liquid products were not feasible. Thus, we calculated the percentage of liquids by the difference in weights and assumed that they contained volatile organic compounds and water vapour.

### 2.2.2. Gas sampling and analysis

To evaluate the effect of the atmosphere on the gaseous products during thermal decomposition, gases were captured into gas bags behind the reactor at 90 s intervals, during degradation processes. To analyse the gathered gas, a gas chromatograph (Agilent 6890 N) was used, which detected six different gases (CO<sub>2</sub>, CO, CH<sub>4</sub>, H<sub>2</sub>, N<sub>2</sub> and O<sub>2</sub>). The conditions for the analysis of the gaseous products have been presented in detail in the study of Korus et al. [37].

## 2.3. Characterisation of solid products

### 2.3.1. Thermogravimetric analysis

Thermal degradation under oxy-fired conditions of the obtained chars was carried out at standard atmospheric pressure using a TGA/DSC analyser (Netzsch STA 409 PC Luxx) with a sensitivity of 0.001 mg and an accuracy of 1% of the measurement range.

Before each experiment, samples were dried for 2–3 h at 105 °C to remove moisture. To avoid heat and mass transfer limitations, the initial weight of the samples was 5 mg. Sample mass loss profiles were determined based on dynamic heating runs, with a linear temperature increase from 100 to 1000 °C at heating rates ( $\beta$ ) of 5, 10 and 15 K/min. All the experiments were performed under an oxy-combustion atmosphere with a total flow rate of 100 ml/min, with 10% oxygen and 90% carbon dioxide, using 30 ml/min nitrogen as a purge gas. Blank experiments were carried out to obtain the baselines, used to subtract the buoyancy effect, calibrating the experiments with samples.

The obtained TG and DTG curves were used to evaluate the parameters of char oxy-combustion, such as the temperature at which the fuel sample starts to burn, which is known as the ignition temperature ( $T_i$ ), the temperature at which sample combustion is completed, which is the burnout temperature ( $T_f$ ) and the maximum peak temperature ( $T_p$ ).  $T_i$  was determined by the tangent method described in Ref. [38],  $T_f$  was defined as the temperature at which the combustion rate decreases to 1 wt%/min at the end of the combustion process [39], and  $T_p$  represented the temperature corresponding to the peak of the DTG profile.

The characteristic temperatures were correlated with various combustibility indexes such as the ignition index ( $D_i$ ), which refers how quickly or slowly the fuel was ignited, the burnout index ( $D_f$ ), and the combustion indexes, such as  $S$ ,  $H_f$  and  $C$  given by Mureddu et al. [40] (Eqs. (1)–(5)).

$$D_i = \frac{DTG_{max}}{t_p t_i} \quad (1)$$

where  $DTG_{max}$  is the maximum combustion rate,  $t_p$  is the corresponding time of the maximum peak, and  $t_i$  is the ignition time.

$$D_f = \frac{DTG_{max}}{\Delta t_{1/2} t_f} \quad (2)$$

where  $\Delta t_{1/2}$  is the time range for  $\frac{DTG}{DTG_{max}} = 0.5$  and  $t_f$  is the burnout time.

The  $S$  index reflects the ignition, combustion, and burnout properties of a fuel. The larger the value of the  $S$  index, the higher the combustion activity is.

$$S = \frac{DTG_{max} DTG_{mean}}{T_f T_i^2} \quad (3)$$

where  $DTG_{mean}$  represents the mean combustion rate.

$H_f$  describes the rate and intensity of the combustion process. The smaller the value of the  $H_f$  index, the better the combustion properties are [41].

$$H_f = T_p \ln \left( \frac{\Delta T_{1/2}}{DTG_{max}} \right) \quad (4)$$

$C$  is the flammability index, which is described as:

$$C = \frac{DTG_{max}}{T_i^2} \quad (5)$$

These indicators are widely used for the evaluation of the combustion performance of different fuels, for example, coal [42,43], biomass [40,44], and hydrochars [45].

### 2.3.2. Kinetic analysis

The results of thermogravimetric analysis at various heating rates were also used to calculate the kinetic parameters. In this study, an isoconversional approach to solid-state kinetics was employed, which allowed kinetic data to be retrieved, i.e., activation energies,  $E(\alpha)$ , and then, pre-exponential factors,  $A(\alpha)$ , without any knowledge of the reaction model. A detailed description of model-free methods can be found in Refs. [32,46–48]. In this study, differential Friedman, as well as integral Vyazovkin techniques, were used. All the calculations within the presented study were performed with Netzsch Kinetics Neo software (v.2.5.0.1) supported with MS Excel software. Friedman and Vyazovkin analyses were conducted as implemented in the Netzsch software, with a results resolution of 0.01 for  $\alpha$ .

### 2.3.3. Porosity and surface analysis

The surface area and pore size distribution (PSD) of the residual chars created during feedstock conversion under the inert atmosphere were calculated using dual two-dimensional non-local density functional theory (2D-NLDFT) models developed by Jagiello and Olivier [49], for  $N_2$  adsorption at 77 K and  $CO_2$  adsorption at 273 K. Isotherms were collected with a Micromeritics TriStar II 3020 analyser. The  $N_2$  isotherm provided insight into the mesopores, while the  $CO_2$  adsorption accounted for the micropores  $<10 \text{ \AA}$ . The PSD calculations were performed using the SAIEUS software that allows the simultaneous fitting of two measured isotherms with the respective theoretical kernels [50]. Additionally, specific surface area calculated with classical Brunauer–Emmett–Teller (BET) method using  $N_2$  isotherm was provided as the reference.

Attenuated total reflectance Fourier transform infrared spectroscopy (ATR-FTIR) was used to examine the surface of the residues from the TEX and SCG decomposition. Spectra constructed from 32 scans, with a resolution of  $4 \text{ cm}^{-1}$  within the range of  $4000\text{--}700 \text{ cm}^{-1}$  wavenumbers were taken with a PerkinElmer Spectrum 100 spectrometer. Two repetitions were made for each sample and the averaged spectra are reported herein.

## 3. Results and discussion

### 3.1. Thermal degradation process

#### 3.1.1. Effect of the atmosphere on product distribution

Firstly, the product distribution after the pyrolysis, gasification and oxidation experiments described in section 2.2.1 was calculated for both samples, as shown in Fig. 1. After the slow pyrolysis process, the solid phase accounted for 21 % and 10 % of the SCG and the TEX samples, which were in agreement with a proximate analysis of the used samples presented in Ref. [32], which means that all volatile matter have been

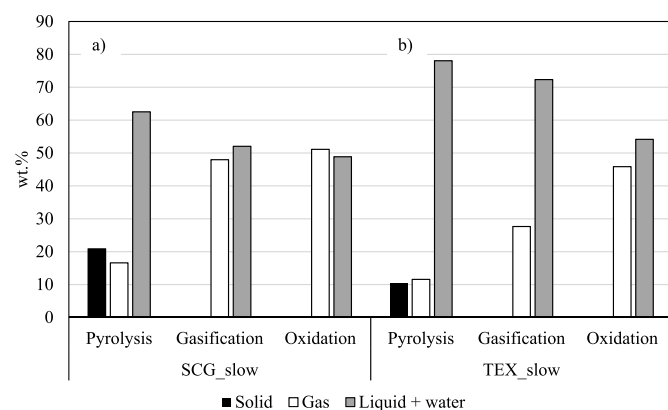


Fig. 1. Product distribution after tests under different atmospheres using a) SCG and b) TEX samples.

released from the samples and only char remains. The gaseous phase was around 17 % and 12 % for SCG slow and TEX\_slow after the pyrolysis process. The remaining mass was assumed to be converted into the liquid products and for both samples, it was the largest part. Similar findings for pyrolysis of lignocellulosic materials can be found in several articles, for example, [51,52].

In gasifying and oxidising atmospheres, a larger share of gaseous products, a smaller part of liquid yield, and a lack of solid phase can be observed than in the inert atmosphere, suggesting complete conversion of char as well as secondary reactions of tar. According to Yue et al. [53], it was caused by the fact that more cracking reactions occurred and more oxygen-containing functional groups (i.e. carbonyl group) were produced when  $CO_2$  was present. Oxygen-containing functional groups were easier to combine with the hydrogen radical producing water, which involved in gasification with char, resulting in the decreasing of liquid phase yield.

#### 3.1.2. Effect of the atmosphere on gaseous products

Gas evolution profiles during the thermal degradation of TEX and SCG under different conditions are presented in Figs. 2–4. For TEX pyrolysis, the evolution of three gases, namely  $CO_2$ ,  $CO$  and  $CH_4$ , was registered. Since during the gasification and oxidation tests,  $CO_2$  was consumed rather than produced, it was not reported in this article. Although a small amount of  $H_2$  could also be observed in the chromatograms from TEX decomposition, the concentrations were below the limit of quantification (3000 ppm), and thus they were not presented in this study. It is plausible that some heavier hydrocarbons, such as acetylene and ethylene, were formed as well, yet the instrumental methods applied for the analysis did not allow their detection. The yields of  $H_2$  from the thermal degradation of SCG were high enough to be quantified and reported.

To assess the reproducibility of the results from both experiments, the standard deviation was calculated and presented in graphs. As can be seen, the values of  $CO$ ,  $CH_4$  as well as  $CO_2$  (in the case of the inert atmosphere) are consistent, meaning that the tests were carried out correctly and that the selected methodology was appropriate. There was a slight discrepancy in the case of hydrogen production, which may be the result of its low level in the sample. However, after integrating the area under the curve, the values of the hydrogen formed during both experiments are similar, namely 1.9 mmol and 2.2 mmol.

Comparing the inert and gasifying atmospheres, it was observed that below  $600 \text{ }^\circ\text{C}$ , there were no significant differences in the gaseous products. In both atmospheres, the maximum peak of  $CO$  was around  $0.15 \text{ mmol/min}$  and appeared at  $380 \text{ }^\circ\text{C}$  (TEX) and  $0.20 \text{ mmol/min}$  at  $350 \text{ }^\circ\text{C}$  for SCG, while the  $CH_4$  peak height is of  $0.03 \text{ mmol/min}$  and occurred at  $550 \text{ }^\circ\text{C}$  for TEX, and  $0.07 \text{ mmol/min}$  at  $560 \text{ }^\circ\text{C}$  for SCG. However, in the gasifying atmosphere, a second peak of  $CO$  could be distinguished above  $700 \text{ }^\circ\text{C}$  with a height of  $2.5 \text{ mmol/min}$  (TEX) and  $5.8 \text{ mmol/min}$  (SCG), which resulted from the Boudouard reaction of char with  $CO_2$  (Eq. (6)). Similar findings were reported in Refs. [54,55].



For both the examined materials, the mechanism of devolatilization was not changed by the switch of the atmosphere from inert to gasifying, as revealed by the similarities in the intensity and temperature range of the  $CH_4$  and the first  $CO$  peaks. For TEX, the ratio of carbon evolved as  $CH_4$  and  $CO$  generated during devolatilization in  $N_2$  and  $CO_2$  was equal to 0.89 and 0.83. While for SCG, it was 0.73 and 0.75, for  $CH_4$  and  $CO$ , respectively. These results could indicate that the amount of  $CO_2$  produced during the volatiles release process in the gasifying atmosphere was also comparable to that obtained during pyrolysis in an inert atmosphere. The amounts of carbon released in the later stage of gasification, where the gasification of the solid residue occurred, corresponded to the amount of char recovered from the reactor after the pyrolysis, i.e., 10% for TEX and 20% for SCG. This observation

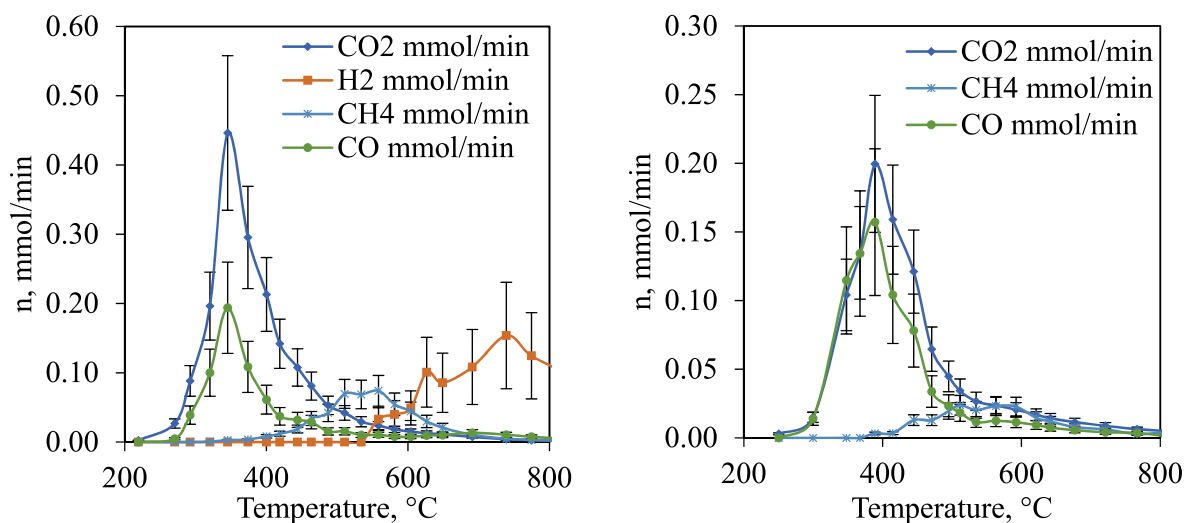


Fig. 2. Gas evolution during the thermal degradation of a) SCG and b) TEX under  $N_2$  atmosphere.

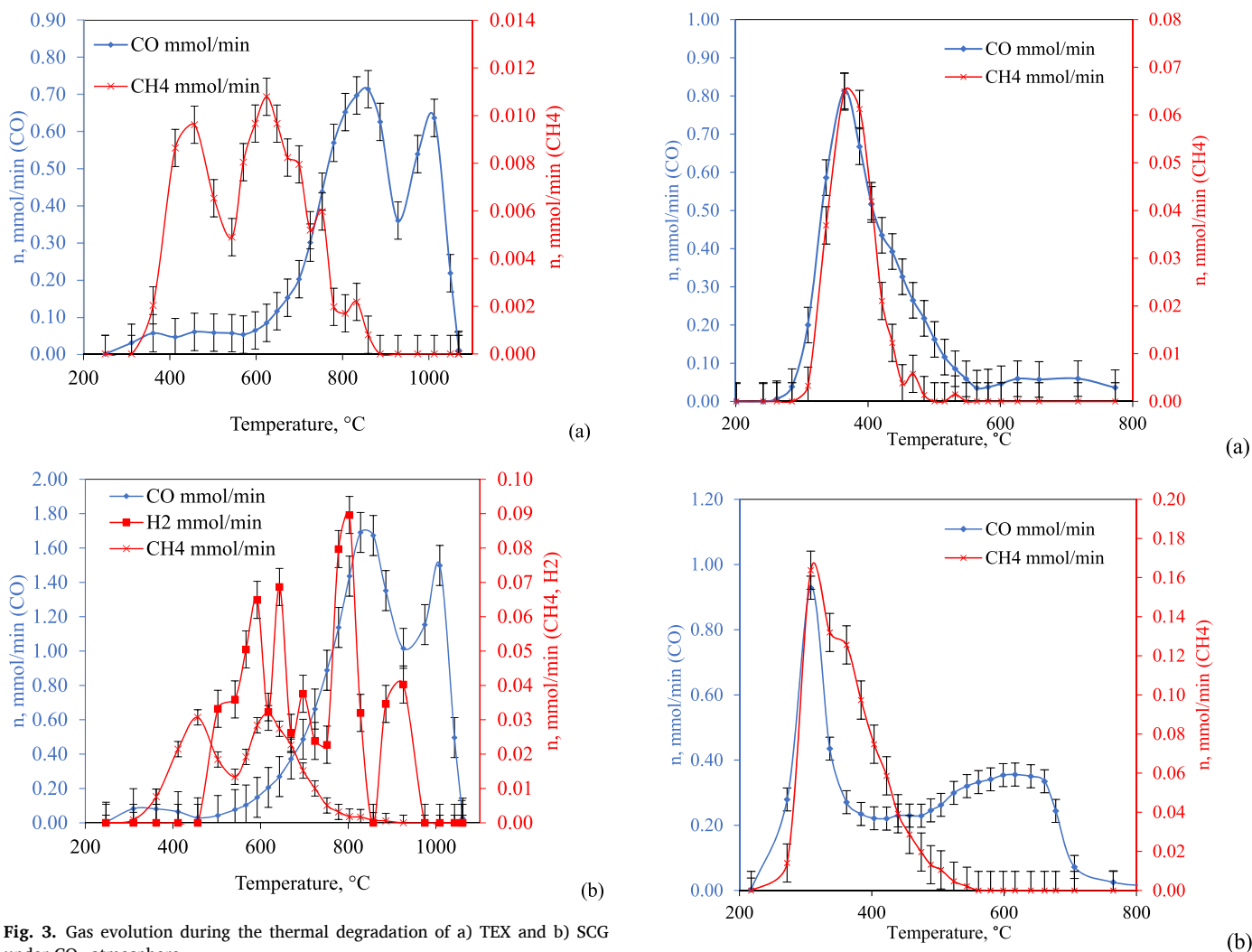


Fig. 3. Gas evolution during the thermal degradation of a) TEX and b) SCG under  $CO_2$  atmosphere.

Fig. 4. Gas evolution during the thermal degradation of a) TEX and b) SCG under  $O_2/CO_2$  atmosphere.

corroborated the finding that similar yields of volatiles were released from the samples during their devolatilization in  $N_2$  and  $CO_2$ .

The observed differences in the  $CH_4$  and  $H_2$  yields from the two materials could have been caused by their structural differences

(Table 1). These gases were formed in the later stage of the devolatilization process and were most likely the result of the secondary reactions between the primary char and the primary volatiles adsorbed on its surface. At sufficiently high temperatures, the volatiles underwent polymerisation, forming  $H_2$  during the dehydrogenation of the aromatic rings. Meanwhile, functional groups were released from the substituted compounds in the form of methane and some light hydrocarbons. Substantial quantitative and qualitative differences in the volatiles released from the TEX and SCG could be expected. The TEX sample is composed mainly of cellulose, and its decomposition during the primary pyrolysis consisted of two possible pathways: a) depolymerization to anhydro-oligosaccharides, monomeric anhydrosugars and their derivatives, which formed the majority of the char, and b) pyranose ring scission to light species, including  $H_2O$ ,  $CH_4$ ,  $CO$  and  $CO_2$  [56–58]. On the other hand, SCG comprises hemicellulose and lignin along with the cellulose constituent. Hemicellulose, the most labile compound, is a matrix of polysaccharides, while lignin, the most thermally stable, comprises highly interconnected and cross-linked p-hydroxyphenyl, syringyl and guaiacyl units [59]. The more complex structure of SCG likely resulted in a higher yield of the heavy and highly substituted compounds, resulting in the more intense release of  $H_2$  and  $CH_4$  from the secondary reactions of the volatiles.

In the oxidising atmosphere, most gases were released over a temperature range of 300–550 °C due to the presence of highly reactive oxygen, which can be observed in Fig. 4. The peaks of  $CH_4$  and  $CO$  corresponded to the highest oxygen uptake, i.e. 85 % for TEX and 95% for SCG. In this atmosphere, the formation of  $CH_4$  occurred at the same temperature as the initial  $CO$  and  $CO_2$  release. These results suggested that differences occurred in the devolatilization of the samples in the presence of oxygen. In the inert conditions, methane and hydrogen were produced at higher temperature (above 500 °C) due to the secondary reactions of tars adsorbed on the char (demethylation and dehydrogenation), whereas, when oxygen was supplied, the tars underwent homogenous reactions with  $O_2$  immediately after their release from the sample, i.e., at temperatures of around 300 °C. Tar decomposition in the gas phase resulted in the loss of functional groups, releasing  $CH_4$ , and ring opening reactions, which yielded  $CO$  and  $CO_2$ , significantly increasing the molar flows of these compounds. No  $H_2$  was detected in the oxidation tests of both samples as it was instantaneously combusted to  $H_2O$ .

The pyrolytic gas composition from SCG and TEX pyrolysis is presented in Fig. 5. The results indicated that gas produced during the SCG pyrolysis contained more hydrogen and methane, and thus it had a slightly higher value of LHV, namely, 209.8 kJ/mol. For TEX pyrolysis, the LHV of the pyrolytic gas was 198.7 kJ/mol.

### 3.1.3. Effect of the reaction atmosphere on the solid residue

Figs. 6 and 7 show the solid residue after the experiments. In the  $N_2$  atmosphere, char was formed with a mass of 10 % and 20 % of the initial weight of the TEX and SCG, respectively. The higher weight of solid residue generated during spent coffee grounds pyrolysis can be ascribed to the occurrence of lignin in the sample, which contributes to char formation [27,55,60]. Under gasifying and oxidising conditions, the solid residue comprised only a small amount of ash and thus it was not quantified. Visual examination of the residues formed under the  $CO_2$  atmosphere suggested complete char gasification, which correlates with the similar amounts of carbon released during gasification and combustion tests (Fig. 1). Thus, it is presumed that the solid residue is almost ash. Similar findings were observed in Refs. [27,60]. Over 4 times higher ash content in SCG, compared with textiles as reported in Ref. [32], resulted in a more abundant residue from the gasification and combustion of this sample. The different colours of the gasification and combustion residues might result from the different form of inorganic compounds, as  $CO_2$  is a weaker oxidising agent than  $O_2$ . Under the oxidising atmosphere, the resulting ash took a greenish colour, which could be explained by the existence of silicates, such as magnesium iron silicate with the chemical formula  $(Mg, Fe)_2SiO_4$  or by the occurrence of iron (Fe) and sulphur (S) in the ash, which under the influence of high temperature formed iron sulphide [61]. Nevertheless, research on produced ash under oxy-MSW combustion should be further investigated.

The ATR-FTIR spectra of each residue are presented in Fig. 8. The pyrolytic chars had a very poorly developed spectra, suggesting a high level of the graphitisation, with barely visible increase in absorption around 1600 and 1000  $cm^{-1}$ , plausibly from some residual  $C=O$  and  $C-O$  structures, respectively. The spectra of the gasification residues were relatively flat, the increased band at 1000  $cm^{-1}$  in the solids obtained from SCG gasification most likely arose from the presence of quartz wool residue that contaminated the sample, as its powdered form did not allow for clean removal from the wool plug.

The most interesting spectra were observed for the ash from

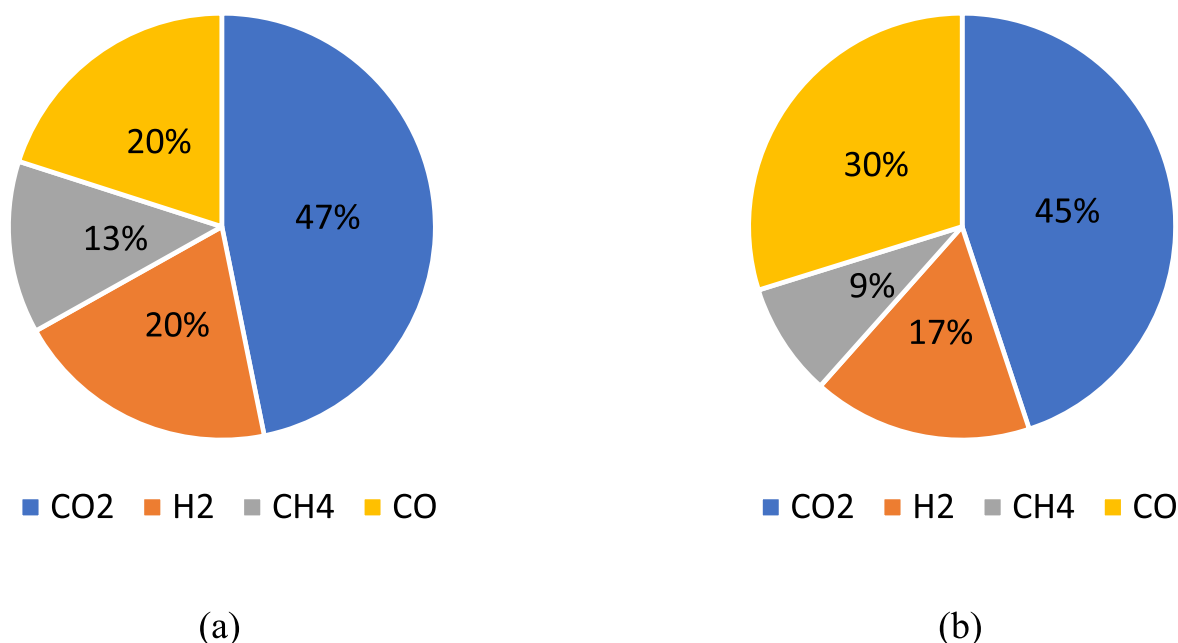


Fig. 5. Composition of the pyrolytic gas for a) SCG and b) TEX sample.



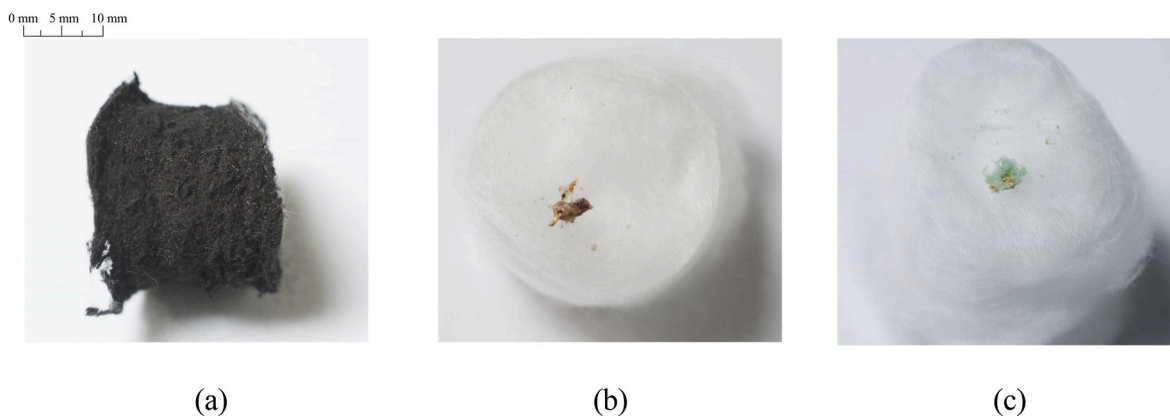


Fig. 6. Solid residue after thermal degradation of textiles under a) inert, b) gasifying and c) oxidising conditions.

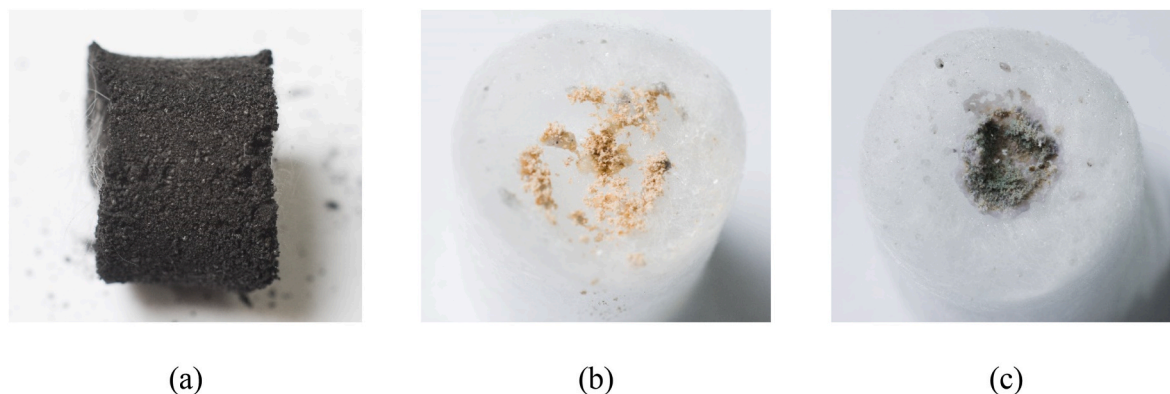


Fig. 7. Solid residue after thermal degradation of coffee grounds under a) inert, b) gasifying and c) oxidising conditions.

oxidation tests; the residue from the textiles had an especially pronounced absorption around the  $1000\text{ cm}^{-1}$  suggest high content of  $\text{SiO}_2$  [62], corroborating the TEX ash composition analysis [32]. The bands at  $1600$  and  $1390\text{ cm}^{-1}$  in the SCG residue likely result from the  $\text{K}_2\text{O}$  [63], the main compound of the SCG ash.

### 3.2. Characterisation of the pyrolytic char formed under different conditions

Thermal degradation under the inert atmosphere performed using lab-scale reactor in the slow and fast pyrolysis mode as well as muffle furnace (described in Section 2.2.1) resulted in the formation of residual pyrolytic chars abundant enough to be analysed with the gas adsorption method for surface area and pore size distribution calculations as well as with the thermogravimetric method for calculating the burning features and kinetic data.

#### 3.2.1. Surface area and pore size distribution

The total surface area ( $S_{\text{total}}$ ) and total pore volume ( $V_{\text{total}}$ ) of the TEX and SCG chars were obtained using the dual two dimensional version of the non-local density functional theory (2D-NLDFT) model fitted simultaneously to the  $\text{CO}_2$  and  $\text{N}_2$  isotherms (Table 2). Incorporating  $\text{CO}_2$  isotherm into the calculations allowed accounting for the micropores inaccessible to the nitrogen molecules, giving more accurate results. The specific surface area according to the Brunauer–Emmett–Teller (BET) method based on the  $\text{N}_2$  isotherm was provided for an easier comparison with literature reports. Besides the cumulative values, the dual model was primarily used to approximate the pore size distribution (PSD) in chars (Fig. 9).

The porosity of the TEX and SCG chars developed to a different

extent, regardless of the pyrolysis conditions. Although microporous, the TEX chars from slow and fast pyrolysis possessed some larger pores that were able to facilitate  $\text{N}_2$  molecules. On the other hand, the SCG char had extremely ultramicroporous structure –  $\text{N}_2$  failed to enter the pores and even  $\text{CO}_2$  adsorption was almost negligible (Fig. 10). Most pores in the PSDs of microporous samples calculated with the dual model originate from the  $\text{CO}_2$  measurement. Inclusion of the  $\text{CO}_2$  isotherm is responsible for the dramatic difference between the total ( $S_{\text{total}}$ ) and BET surface area of all examined chars, highlighting the importance of using appropriate probe molecules while examining microporous carbons [64].

The differences in the porosity of the TEX and SGS chars can be attributed to the properties of feedstock, as the same preparation conditions were applied during their preparation. The textiles are comprised of pure cellulose fibres, while spent coffee grounds have a substantial amount of lignin, which is strongly cross-linked and more resistant to thermal degradation. Thus, in the case of SCG conversion, the development of the porosity of the cellulose residue was most likely hindered, as the escape of its volatiles was suppressed by the liquid derivatives of lignin decomposition, as observed by Chua et al. [65].

Highly microporous structure of the cellulose char has been previously reported, e.g. by Brunner et al. [66] where the surface areas in the range of  $300\text{--}600\text{ cm}^2/\text{g}$  were calculated from the  $\text{CO}_2$  adsorption while the calculation based on the  $\text{N}_2$  isotherms estimated the specific surface of  $1\text{--}5\text{ m}^2/\text{g}$ . Surface area of SCG chars as low as  $1\text{--}1.5\text{ m}^2/\text{g}$  was evaluated with  $\text{N}_2$  adsorption by Vardon et al. [67] and Stylianou et al. [68].

TEX char from fast pyrolysis developed significantly lower porosity compared to the slow process, as the high heating rate could hinder the release of volatiles [69]. In case of SCG, the increased porosity of the fast

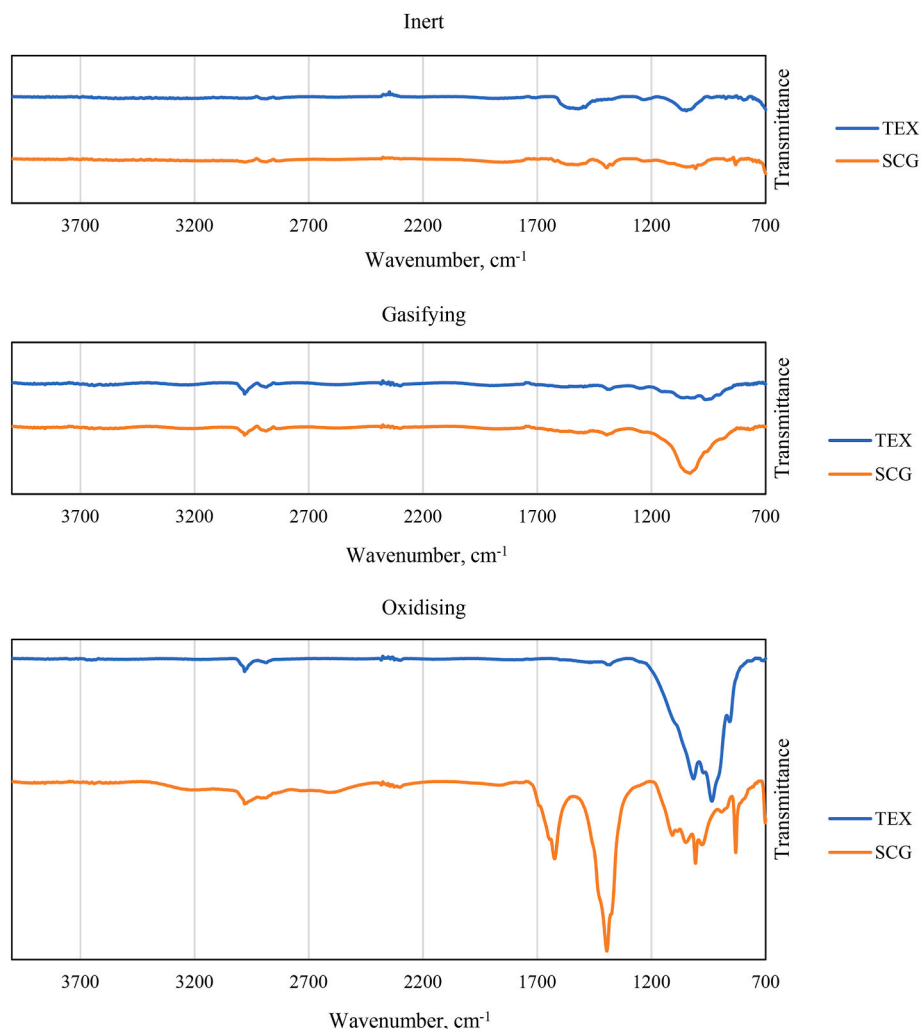


Fig. 8. ATR-FTIR spectra of the solid residues from the textiles (TEX) and spent coffee grounds (SCG) conversion under inert, gasifying, and oxidising atmospheres.

Table 2

Total surface area ( $S_{total}$ ) and pore volume ( $V_{total}$ ) calculated from the dual 2D-NLDFT model and the BET surface area of the TEX and SCG chars from the slow, fast, and muffle furnace pyrolysis.

	$S_{total}$ , m <sup>2</sup> /g	$V_{total}$ , cm <sup>3</sup> /g	BET, m <sup>2</sup> /g
TEX_slow	710	0.243	81.1
TEX_fast	479	0.165	14.1
SGS_slow	65	0.025	0.9
SGS_fast	120	0.076	0.8
SGS_muffle	585	0.176	1.3

pyrolysis chars should be considered with caution; this sample had extremely low porosity and thus even CO<sub>2</sub> adsorption was extremely small, resulting in a poor fitting, which might have biased the PSD, as suggested by the unaccounted-for shift of the ultramicropore peak. Since the purely inert atmosphere yielded char that was de facto non-porous, the additional SCG pyrolysis test was performed in the muffle furnace using the closed-lid crucible, i.e., under highly depleted oxidiser concentration. This setup, although less controlled, might better reflect the conditions in the real combustion chamber. Indeed, the SCG char from the muffle furnace experiment developed more pores, suggesting that, despite the rapid volatiles release, some oxidising gases managed to access the surface of the sample.

### 3.2.2. Thermal analyses

The thermogravimetric experimental results for the obtained chars are presented and compared by using thermogravimetric (TG) profiles and differential thermogravimetric (DTG) curves (Figs. 10–12). The features of the combustion acquired from the thermal analysis technique, summarised in Table 3, were used to effectively compare the reactivity and combustibility of chars resulting from the fast and slow pyrolysis of the selected waste (referred to as Fast TEX, Fast SCG, Slow TEX, and Slow SCG as appropriate).

Generally, it can be observed that the curve consists of one main mass loss, it can be ascribed to the combustion of char. During the oxidation char step, all the curves show a main peak that indicates the temperature corresponding to the maximum reaction rate. The maximum rate of weight loss in %/min during the main degradation process was Fast TEX (11.92) > Slow TEX (11.21) > Muffle furnace SCG (8.14) > Fast SCG (6.25) > Slow SCG (6.14). The lower maximum value of DTG and average weight loss rate for chars derived from SCG could be considered evidence of the low reactivity of lignin [70].

As presented, with an increased heating rate ( $\beta$ ), DTG profiles shift to higher temperatures, and the rate of mass loss rises since the heat transfer is not as effective as it was for lower heating rates. It suggests that the degradation process is slower with the increasing of  $\beta$  that a higher heating rate causes the maximum combustion rate to be increased. The reason is the enhancement of mass transfer results from heat transfer intensification. This can be attributed to the fact that the heating of solid particles occurs more gradually at lower heating rates,

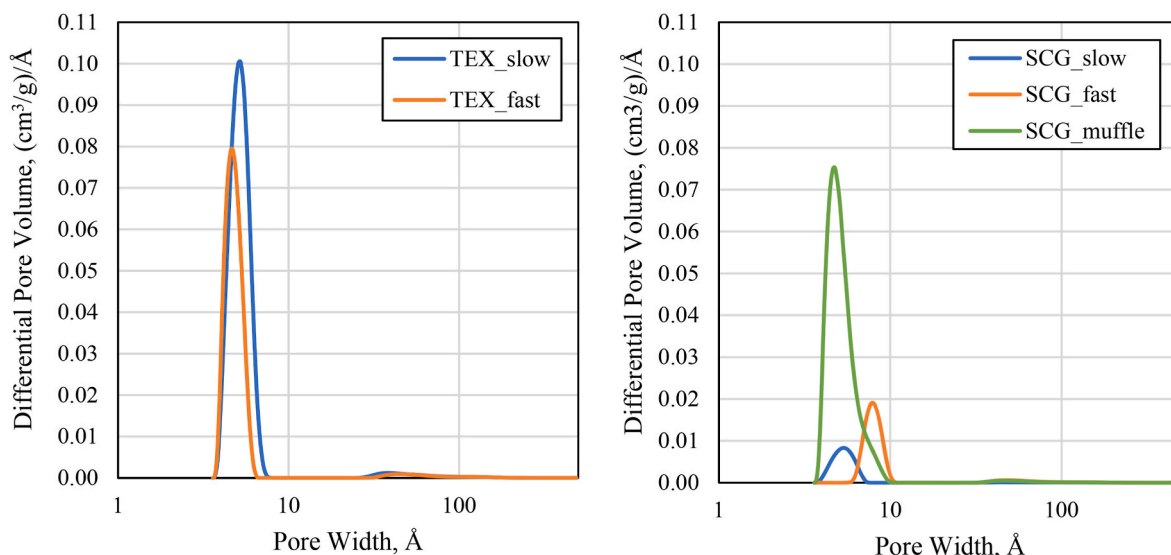


Fig. 9. Pore size distribution (PSD) in (a) textile (TEX) and (b) spent coffee grounds (SCG) from slow and fast pyrolysis, and muffle furnace pyrolysis (CO<sub>2</sub> adsorption at 273 K showed in the small graph).

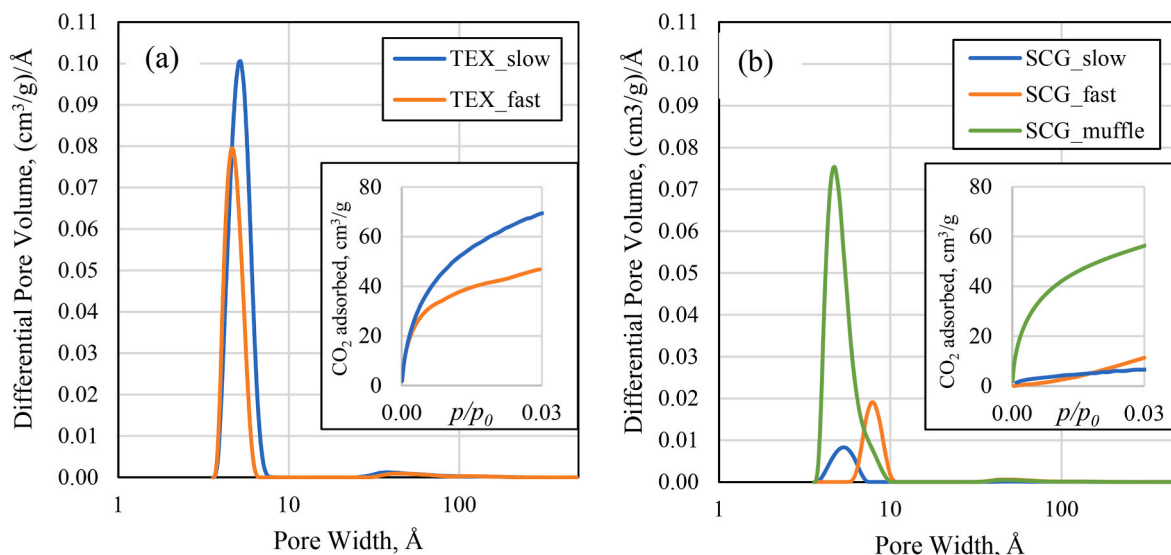


Fig. 10. TG and DTG curves of char derived from spent coffee grounds a) slow, b) fast pyrolysis and c) fast pyrolysis in muffle furnace.

thus leading to an improved and more effective heat transfer to the inner part and among the particles. Similar findings were also observed in Refs. [25,32,40,58].

Besides, as it can be seen, in all studied cases fast pyrolysis shifted the maximum peaks into lower temperatures and increased their values, for example, the maximum peak of TEX-char is 11.92 and 11.21%/min at occurs at 537.5 and 541.9 °C for fast and slow pyrolysis, respectively. SCG-char sample maximum peak is 6.25 and 6.14%/min and appears at the temperature of 513.4 °C and 574.9 °C for fast and slow pyrolysis, respectively. Interestingly, not only the reaction rate, but also the type of reactor is significant for the properties of biochar since the maximum peak of SCG-char derived from muffle furnace increased up to 8.14%/min and took place at 470.4 °C.

For both, fast and slow pyrolysis, the ignition temperature ( $T_i$ ) of char derived from SCG was lower than of that from textiles, namely, TEX\_slow (475.4 °C) > SGS\_slow (470.5 °C) and TEX\_fast (469.6 °C) > SGS\_fast (415.0 °C). The fastest ignition occurred for SGC\_muffle (400.1 °C). This indicates that both the SCG sample itself and the method of obtaining it, i.e. by fast pyrolysis, favour higher biochar

reactivity.

Regarding combustion performance, firstly, we assessed the ignition index ( $D_i$ ). As reported in Table 3, the heating rate of the pyrolysis process influenced the ignition index and the expected trend can be seen, namely the higher ignition index corresponds to the lower ignition temperatures within one material, for example,  $D_i$  of TEX\_slow is lower than that of TEX\_fast. Comparing two feedstocks, TEX and SCG, a different tendency has been observed, implying that the ignition index may not be the only factor to be concerned, related to the ignition temperature. As Mureddu et al. [40] reported, it could be due to the higher content of ash in the sample, which can affect oxygen diffusion and heat transfer. This results in lower temperatures of ignition of SCG than that of the TEX-derived chars even if the ignition index of the TEX samples is higher than that of the SCG. The ignition index of the SCG-char produced in the muffle furnace was similar to TEX chars.

The values of S index for TEX-char samples are generally greater than SCG-char, meaning a better combustion performance of these samples. Comparing slow and fast pyrolysis, it can be noticed that higher heating rates result in char with superior combustion characteristics. Finally, the

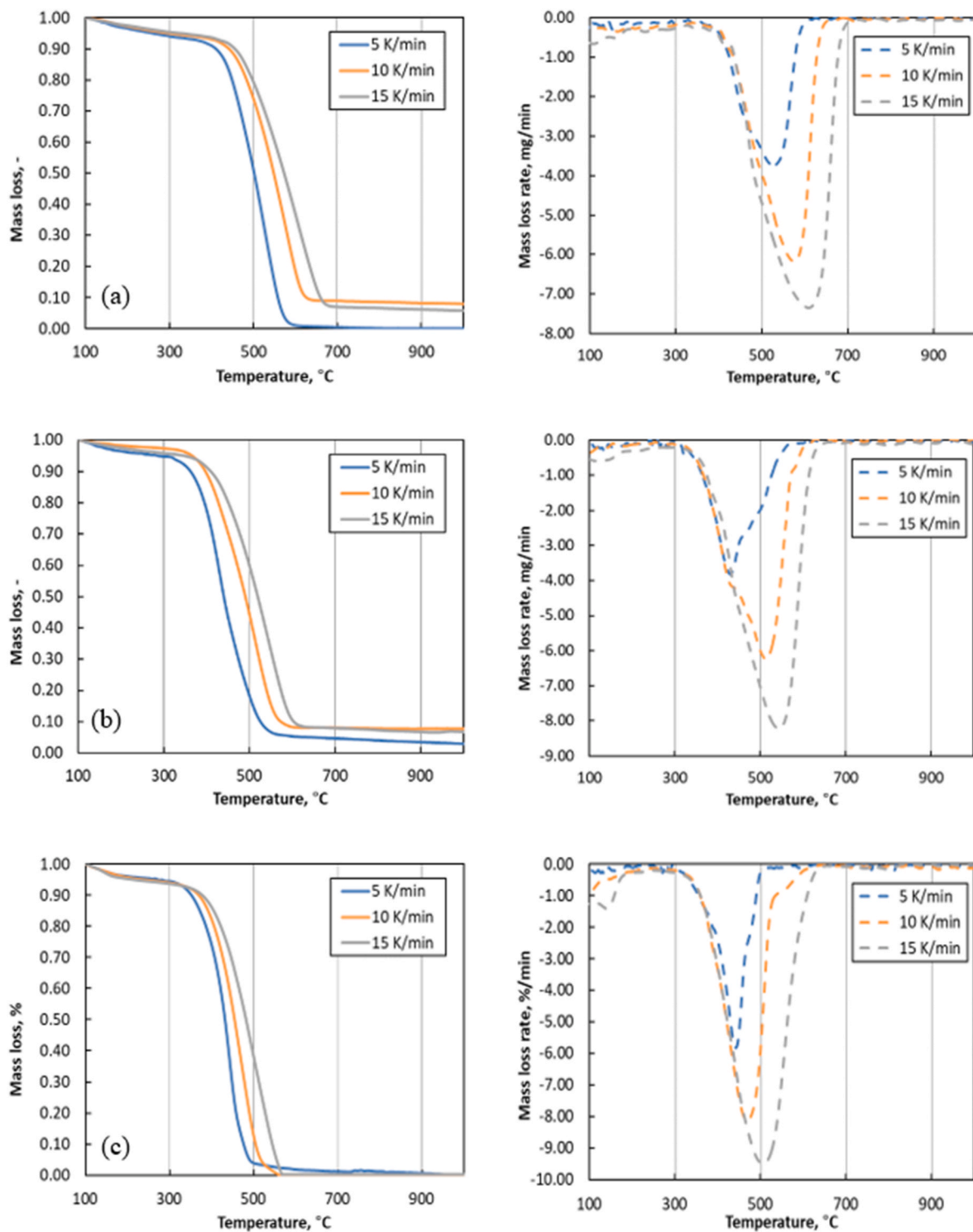


Fig. 11. TG and DTG curves of char derived from spent coffee grounds a) slow, b) fast pyrolysis and c) fast pyrolysis in muffle furnace.

trend of  $H_f$  index follows the ignition and burnout indexes, showing smaller values for TEX-derived char samples, thus confirming their better combustion properties. Surprisingly, char derived from SCG pyrolysis in muffle furnace had the smallest value of  $H_f$ , which implies its high reactivity and intense combustion. C is adopted to evaluate the combustion stability of chars. The C indexes of the five kinds of chars are between  $27.7 \times 10^{-6}$  and  $54.0 \times 10^{-6}$ , among which the C index of TEX\_fast is the highest, indicating that the combustion stability of this sample is the best.

Comparing the values of characteristic combustion parameters, such as Ti, S, C, and  $H_f$ , calculated in this work with values from the literature, it can be concluded that char derived from SGS\_muffle has the properties most similar to coal [40,71].

### 3.2.3. Kinetic analysis

The isoconversional method can obtain more accurate apparent activation energy ( $E_a$ ) without assuming the structure function  $f(x)$ . In Tables 4–5, the average values of  $E_a$  and  $\log(A)$  for SCG and TEX chars,

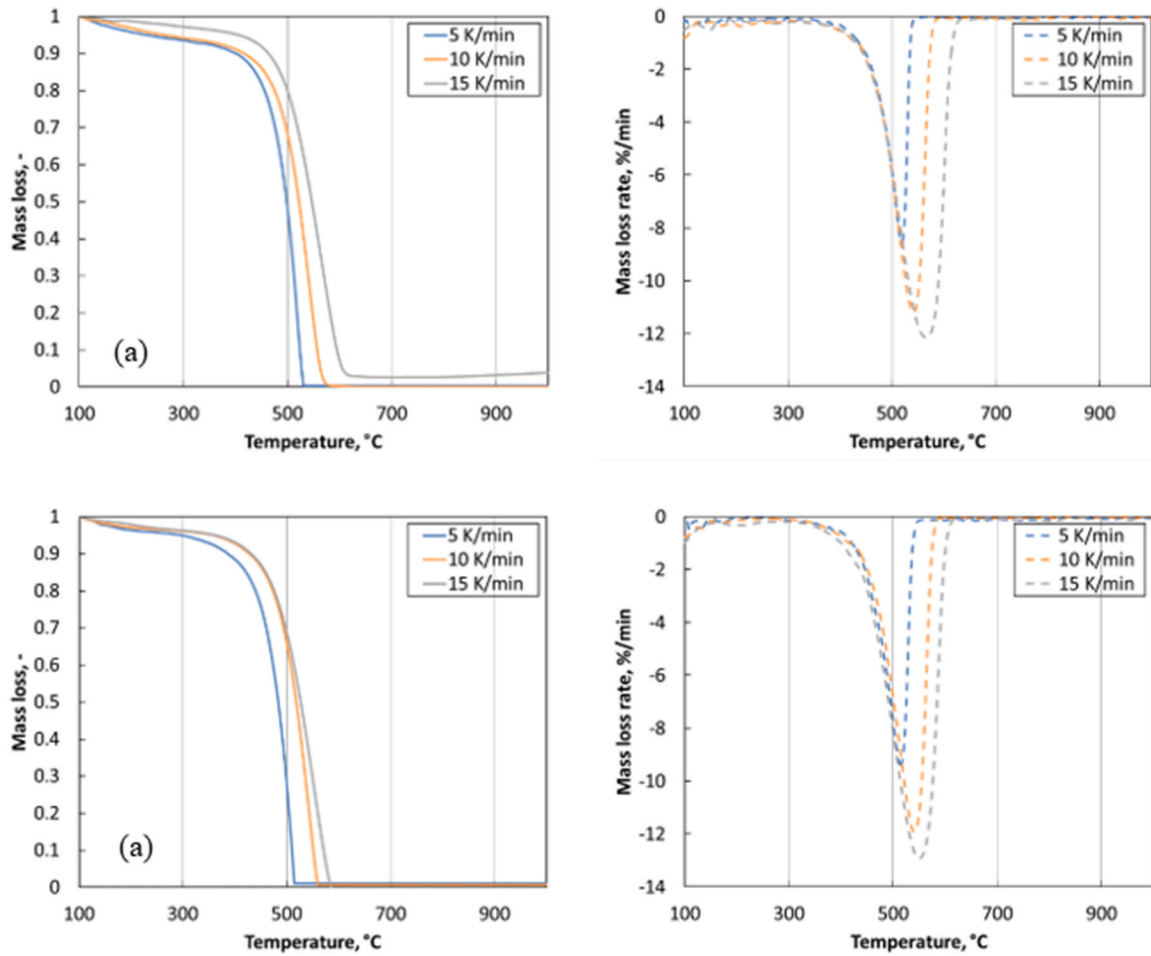


Fig. 12. TG and DTG curves of char derived from textiles a) slow and b) fast pyrolysis.

Table 3

Main oxy-combustion parameters of tested chars.

Sample	SGS_slow	SGS_fast	SGS_muffle	TEX_slow	TEX_fast
Ignition Temperature, °C	470.5	415.0	400.1	475.4	469.6
Peak temperature, °C	574.9	513.4	470.4	541.9	537.5
Burnout temperature, °C	663.3	623.4	619.2	606.3	598.4
Ignition time, min	52.9	47.3	45.8	53.4	52.7
Peak time, min	63.5	57.3	52.9	60.1	59.7
Burnout time, min	72.5	68.3	67.4	66.8	65.8
DTG <sub>max</sub> , %/min	6.14	6.25	8.14	11.21	11.92
DTG <sub>mean</sub> , %/min	0.85	0.84	0.97	0.93	0.99
$\Delta t_{1/2}$ , min	53.6	46.8	46.8	55.7	55.3
$D_i$ , wt.%/min <sup>3</sup> · 10 <sup>-3</sup>	1.813	2.305	3.360	3.493	3.789
$D_b$ , wt.%/min <sup>4</sup> · 10 <sup>-5</sup>	2.504	3.406	4.878	5.013	5.487
$S$ , wt.%/(min <sup>4</sup> · °C <sup>2</sup> ) · 10 <sup>-8</sup>	3.564	4.909	7.966	7.621	9.026
$H_b$ , °C · 10 <sup>3</sup>	3.750	2.148	1.844	2.055	2.002
$C$ , °C · 10 <sup>-6</sup>	27.736	36.290	50.850	49.601	54.053

Table 4

Kinetic parameters of oxy-combustion of SCG derived chars.

Sample	SCG_slow		SCG_fast		SCG_muffle	
	Friedman	Vyazovkin	Friedman	Vyazovkin	Friedman	Vyazovkin
Average value of energy activation, kJ/mol	73.5	72.8	69.5	70.6	51.9	52.0
Average value of pre-exponential factor, Log(1/s)	2.162	2.104	2.057	2.144	1.130	1.173

**Table 5**  
Kinetic parameters of oxy-combustion of TEX derived chars.

Sample Method	TEX_slow		TEX_fast	
	Friedman	Vyazovkin	Friedman	Vyazovkin
Average value of energy activation, kJ/mol	80.2	80.1	116.1	116.4
Average value of pre-exponential factor, Log(1/s)	2.905	2.908	5.308	5.333

respectively, are summarised. In this study, both Friedman's and Vyazovkin's methods yield similar results, which is consistent with our previous research [32].

Based on kinetic analysis, it was observed that in the case of SCG sample, higher heating itself did not have a strong influence on the activation energy of the char; it was slightly decreased by around 3 kJ/mol. However, char produced by using muffle furnace resulted in more reactive sample, and the value of  $E_a$  for SCG\_muffle is 52 kJ/mol. As we stated before, it can be caused by the entry of oxygen into the furnace during the pyrolysis process, and thus more developed porosity and reactivity.

The larger differences can be observed in the case of TEX-derived chars. Increasing the heating rate resulted in higher  $E_a$  (kJ/mol), namely,  $TEX_{fast}$  (116.1) >  $TEX_{slow}$  (80.2). It can be also explained by the fact that slow pyrolysis developed significantly greater porosity compared to the fast devolatilization process.

#### 4. Conclusions

In this study, the thermal degradation of TEX and SCG in different atmospheres, i.e. inert, gasifying, and oxidising (with  $O_2/CO_2$ ), was studied to evaluate the gas evolution profiles and analyse the solid residues. Additionally, chars derived from slow and fast pyrolysis were subjected to analysis. The results showed that shifting the atmosphere from inert to gasifying does not affect the thermal decomposition of samples below 600 °C. However, in the gasifying atmosphere, the second peak of CO appears above 600 °C during the solid residue decomposition due to  $CO_2$ -char reactions. In the  $O_2/CO_2$  atmosphere, the degradation of the solid residue occurs at lower temperatures and the immediate decomposition of volatiles can be observed due to the presence of the reactive oxygen. A similar share of carbon in the gaseous products was observed for gasification and oxidation test, suggesting nearly complete waste conversion.

Comparing the pyrolytic gas from the two materials, it can be concluded that the SCG sample yielded more calorific gas, which was richer in hydrogen and methane due to its more complex structure (larger amounts of hemicellulose and lignin).

The study shows the importance of the atmosphere during waste devolatilization and solid residue formation. The observed differences should be accounted for while modelling the WtE plants (including pyrolysis, gasification, and oxy- or air-incineration). Moreover, the residue formation under different atmospheres is an important aspect,

#### Nomenclature

##### Abbreviations

$C$	flammability index
$D_i$	ignition index
$D_f$	burnout index
FTIR	Fourier-transform infrared spectroscopy
GC	Gas Chromatograph
$H_f$	stability index
MSW	Municipal Solid Waste

since certain compounds in the ash can lead to corrosion and have a low temperature of melting point, for example,  $SiO_2$  and  $K_2O$ , which leads to a requirement for costly cleaning and maintenance, and thus reduces the economic viability of the plant. These results also indicate that each group of waste should be investigated separately in order to create successful models of MSW utilisation technologies.

Regarding the properties of chars produced during the slow and fast pyrolysis of the investigated waste, it can be concluded that a higher heating rate resulted in chars with a lower porosity and, thus, lower reactivity: the study showed a direct correlation. The reason for this relationship can be that at a high heating rate, the release of volatiles could be hindered. Besides, SCG-chars were characterised by poorer developed pore structures than TEX-chars. However, as the study proved, next to the heating rate, the method of sample preparation was important as well since SCG-chars prepared in a muffle furnace developed their specific surface better due to the possible access of oxygen in the process. Chars obtained from fast pyrolysis are characterised by superior combustion performance, lower temperature of ignition, higher maximum weight loss rates, and better stability.

This deep insight into the thermochemical conversion of waste, including the monitoring of gas evolution and product analysis, as well as the study of the combustion properties of the received chars under different conditions will provide a better understanding of these processes and aid the development of optimum routes for waste treatment.

#### Credit author statement

Paulina Copik: Conceptualization; Methodology; Investigation; Resources; Data Curation; Writing - Original Draft; Writing - Review & Editing; Visualization; Project administration; Funding acquisition. Agnieszka Korus: Methodology; Investigation; Writing - Original Draft; Writing - Review & Editing. Andrzej Szłek: Conceptualization; Supervision. Mario Ditaranto: Conceptualization; Supervision.

#### Declaration of competing interest

The authors declare that they have no known competing financial interests or personal relationships that could have appeared to influence the work reported in this paper.

#### Data availability

Data will be made available on request.

#### Acknowledgements

This research is supported by the National Science Centre (Project no. UMO-2021/41/N/ST8/02548) and Ministry of Education and Science (Poland) under statutory research funds of the Faculty of Energy and Environmental Engineering of SUT (08/060/RGZ200275-24). MD participation was funded by the Research Council of Norway through the ERANET Cofund ACT NEWEST-CCUS project (grant # 305062).

SCG	Spent Coffee Grounds
S	combustion activity index
TEX	Textiles
TGA	thermogravimetric analysis
WtE	Waste to Energy
$\beta$	Heating rate

## References

- [1] Kaya K, Ak E, Yaslan Y, Oktug SF. Sustainable computing : informatics and systems waste-to-energy framework : an intelligent energy recycling management. *Sustain Comput Informatics Syst* 2021;30:100548. <https://doi.org/10.1016/j.suscom.2021.100548>. March.
- [2] Makarichi L, Jutidamrongphan W, Techato K. The evolution of waste-to-energy incineration: a review. *Renew Sustain Energy Rev* Aug. 2018;91:812–21. <https://doi.org/10.1016/j.rser.2018.04.088>.
- [3] Babu R, Veramendi PMP, Rene ER. Case Studies in Chemical and Environmental Engineering Strategies for resource recovery from the organic fraction of municipal solid waste. *Case Stud Chem Environ Eng* 2021;3:100098. <https://doi.org/10.1016/j.csee.2021.100098>. March.
- [4] Kumar A, Samadder SR. A review on technological options of waste to energy for effective management of municipal solid waste. *Waste Manag* 2017;69:407–22. <https://doi.org/10.1016/j.wasman.2017.08.046>.
- [5] Yi S, Jang Y, An AK. Potential for energy recovery and greenhouse gas reduction through waste-to-energy technologies. *J Clean Prod* 2018. <https://doi.org/10.1016/j.jclepro.2017.12.103>.
- [6] Dong J, Tang Y, Nzihou A, Chi Y. Key factors influencing the environmental performance of pyrolysis, gasification and incineration Waste-to-Energy technologies. *Energy Convers Manag* 2019;196:497–512. <https://doi.org/10.1016/j.enconman.2019.06.016>. May.
- [7] Yargicoglu EN, Yamini B, Reddy KR, Spokas K. Physical and chemical characterization of waste wood derived biochars. *WASTE Manag*; 2014. <https://doi.org/10.1016/j.wasman.2014.10.029>.
- [8] Weber K, Quicker P. Properties of biochar. *Fuel* 2018;217:240–61. <https://doi.org/10.1016/j.fuel.2017.12.054>. January.
- [9] Wang L, Li T, Várhegyi G, Skreirev Ø, Løvås T. CO<sub>2</sub> gasification of chars prepared by fast and slow pyrolysis from wood and forest residue: a kinetic study. *Energy Fuel* 2018;32(1):588–97. <https://doi.org/10.1021/acs.energyfuels.7b03333>.
- [10] Abdullah H, Wu H. Biochar as a fuel: 1. Properties and grindability of biochars produced from the pyrolysis of mallee wood under slow-heating conditions. *Energy Fuel* 2009;23(8):4174–81. <https://doi.org/10.1021/ef900494t>.
- [11] Pour N, Webley PA, Cook PJ. Potential for using municipal solid waste as a resource for bioenergy with carbon capture and storage (BECCS). *Int J Greenh Gas Control* 2018;68:1–15.
- [12] Tang YT, Ma XQ, Lai ZY, Chen Y. Energy analysis and environmental impacts of a MSW oxy-fuel incineration power plant in China. *Energy Pol* 2013;60:132–41. <https://doi.org/10.1016/j.enpol.2013.04.073>.
- [13] Buhre BJP, Elliott LK, Sheng CD, Gupta RP, Wall TF. Oxy-fuel combustion technology for coal-fired power generation. *Prog Energy Combust Sci* 2005;31(4):283–307.
- [14] Wienchol P, Szłęk A, Ditaranto M. Waste-to-energy technology integrated with carbon capture – challenges and opportunities. *Energy* May 2020;198:117352. <https://doi.org/10.1016/j.energy.2020.117352>.
- [15] Li X, Strezov V, Kan T. Energy recovery potential analysis of spent coffee grounds pyrolysis products. *J Anal Appl Pyrolysis* 2014. <https://doi.org/10.1016/j.jaap.2014.08.012>.
- [16] Kelkar S, et al. Pyrolysis of spent coffee grounds using a screw-conveyor reactor. *Fuel Process Technol* 2015;137:170–8. <https://doi.org/10.1016/j.fuproc.2015.04.006>.
- [17] Pil J, Seok H, Seok Y, Chae H, Joon S. Fast pyrolysis of coffee grounds : characteristics of product yields and biocrude oil quality. *Energy* 2012;47(1):17–24. <https://doi.org/10.1016/j.energy.2012.06.003>.
- [18] Christou A, et al. Effects of biochar derived from the pyrolysis of either biosolids, manure or spent coffee grounds on the growth, physiology and quality attributes of field-grown lettuce plants. *Environ Technol Innov* 2022;26:102263. <https://doi.org/10.1016/j.eti.2021.102263>.
- [19] Cho D-W, et al. Adsorption of potentially harmful elements by metal-biochar prepared via Co-pyrolysis of coffee grounds and Nano Fe(III) oxides. *Chemosphere* 2023;319:136536. <https://doi.org/10.1016/j.chemosphere.2022.136536>.
- [20] Kim Y, Lee J, Yi H, Fai Tsang Y, Kwon EE. Investigation into role of CO<sub>2</sub> in two-stage pyrolysis of spent coffee grounds. *Bioresour Technol* 2019;272:48–53. <https://doi.org/10.1016/j.biortech.2018.10.009>.
- [21] Cho DW, Lee J, Yoon K, Ok YS, Kwon EE, Song H. Pyrolysis of FeCl<sub>3</sub>-pretreated spent coffee grounds using CO<sub>2</sub> as a reaction medium. *Energy Convers Manag* 2016;127:437–42. <https://doi.org/10.1016/j.enconman.2016.09.036>.
- [22] Kibret HA, Kuo Y-L, Ke T-Y, Tseng Y-H. Gasification of spent coffee grounds in a semi-fluidized bed reactor using steam and CO<sub>2</sub> gasification medium. *J Taiwan Inst Chem Eng* 2021;119:115–27. <https://doi.org/10.1016/j.jtice.2021.01.029>.
- [23] Primaz C, Gil-Castell O, Ribes-Greus A. Strategies towards thermochemical valorisation of spent coffee grounds (SCG): kinetic analysis of the thermal and thermo-oxidative decomposition. *Biomass Bioenergy* 2023;174:106840. <https://doi.org/10.1016/j.biombioe.2023.106840>.
- [24] Fu J, et al. Co-circularity of spent coffee grounds and polyethylene via co-pyrolysis: characteristics, kinetics, and products. *Fuel* 2023;337:127061. <https://doi.org/10.1016/j.fuel.2022.127061>.
- [25] Wen C, Wu Y, Chen X, Jiang G, Liu D. The pyrolysis and gasification performances of waste textile under carbon dioxide atmosphere. *J Therm Anal Calorim* 2017;128(1):581–91. <https://doi.org/10.1007/s10973-016-5887-7>.
- [26] Wu Y, Wen C, Chen X, Jiang G, Liu G, Liu D. Catalytic pyrolysis and gasification of waste textile under carbon dioxide atmosphere with composite Zn-Fe catalyst 2017;166:115–23. <https://doi.org/10.1016/j.fuproc.2017.05.025>.
- [27] Tang YT, Ma XQ, Wang ZH, Wu Z, Yu QH. A study of the thermal degradation of six typical municipal waste components in CO<sub>2</sub> and N<sub>2</sub> atmospheres using TGA-FTIR. *Thermochim Acta* 2017. <https://doi.org/10.1016/j.tca.2017.09.009>.
- [28] Abdullah N, Mohd R, Syairah N, Aziz M, Rabie M, Disa N. Banana pseudo-stem biochar derived from slow and fast pyrolysis process. *Heliyon* 2023;9(1):e12940. <https://doi.org/10.1016/j.heliyon.2023.e12940>.
- [29] Al Arni S. Comparison of slow and fast pyrolysis for converting biomass into fuel. *Renew Energy* 2017;124:197–201. <https://doi.org/10.1016/j.renene.2017.04.060>.
- [30] Duman G, Okutucu C, Ucar S, Stahl R, Yanik J. The slow and fast pyrolysis of cherry seed. *Bioresour Technol* 2011;102(2):1869–78. <https://doi.org/10.1016/j.biortech.2010.07.051>.
- [31] Hasan MM, Rasul MG, Khan MMK. The effects of slow and fast pyrolysis on the yields and properties of produced bio-oils from macadamia nutshell. *AIP Conf Proc* 2022;2681(1). <https://doi.org/10.1063/5.0114965>.
- [32] Wienchol P, Korus A, Szłęk A, Ditaranto M. Thermogravimetric and kinetic study of thermal degradation of various types of municipal solid waste (MSW) under N<sub>2</sub>, CO<sub>2</sub> and oxy-fuel conditions. *Energy Jun. 2022*;248:123573. <https://doi.org/10.1016/j.energy.2022.123573>.
- [33] Industrievereinigung Chemiefaser, "Production volume of chemical and textile fibers worldwide from 1975 to 2021," <https://www.ivc-ev.de/sites/default/files/informationsmaterial-dateien/IVCJahresbrochure2022.pdf> (accessed August. 8, 2023).
- [34] Yousef S, et al. A sustainable bioenergy conversion strategy for textile waste with self-catalysts using mini-pyrolysis plant, vol. 196. June; 2019. p. 688–704. <https://doi.org/10.1016/j.enconman.2019.06.050>.
- [35] International Coffee Organization. World coffee consumption. 2021. World coffee consumption, <http://www.ico.org/prices/new-consumption-table.pdf>. [Accessed 2 August 2023].
- [36] Korus A, et al. Kinetic parameters of petroleum coke gasification for modelling chemical-looping combustion systems. *Energy* 2021;232. <https://doi.org/10.1016/j.energy.2021.120935>.
- [37] Korus A, Samson A, Szłęk A. Catalytic conversion of toluene over a biochar bed under an inert atmosphere – the comparison of chars from different types of wood and the role of selected metals. *Fuel* 2020;279:118468. <https://doi.org/10.1016/j.fuel.2020.118468>. March.
- [38] Ma BG, Li XG, Xu L, Wang K, Wang XG. Investigation on catalyzed combustion of high ash coal by thermogravimetric analysis. *Thermochim Acta* 2006;445(1):19–22. <https://doi.org/10.1016/j.tca.2006.03.021>.
- [39] Lu JJ, Chen WH. Investigation on the ignition and burnout temperatures of bamboo and sugarcane bagasse by thermogravimetric analysis. *Appl Energy* 2015;160:49–57. <https://doi.org/10.1016/j.apenergy.2015.09.026>. 2015.
- [40] Mureddu M, Dessì F, Orsini A, Ferrara F, Pettinau A. Air- and oxygen-blown characterization of coal and biomass by thermogravimetric analysis. *Fuel* 2018;212:626–37. <https://doi.org/10.1016/j.fuel.2017.10.005>. April.
- [41] Niu SL, Lu CM, Han KH, Zhao JL. Thermogravimetric analysis of combustion characteristics and kinetic parameters of pulverized coals in oxy-fuel atmosphere. *J Therm Anal Calorim* 2009;98(1):267–74. <https://doi.org/10.1007/s10973-009-0133-1>.
- [42] Tang L, et al. Thermogravimetric analysis of the combustion characteristics and combustion kinetics of coals subjected to different chemical demineralization processes. *ACS Omega* 2022;7(16):13998–4008. <https://doi.org/10.1021/acsomega.2c00522>.
- [43] Ma B-G, Li X-G, Xu L, Wang K, Wang X-G. Investigation on catalyzed combustion of high ash coal by thermogravimetric analysis. *Thermochim Acta* 2006;445(1):19–22. <https://doi.org/10.1016/j.tca.2006.03.021>.
- [44] Chen J, et al. Co-combustion of sewage sludge and coffee grounds under increased O<sub>2</sub>/CO<sub>2</sub> atmospheres: thermodynamic characteristics, kinetics and artificial neural network modeling. *Bioresour Technol* 2018;250:230–8. <https://doi.org/10.1016/j.biortech.2017.11.031>. September 2017.
- [45] Wilk M, Ślíz M, Lubieniecki B. Hydrothermal co-carbonization of sewage sludge and fuel additives: combustion performance of hydrochar. *Renew Energy* 2021;178:1046–56. <https://doi.org/10.1016/j.renene.2021.06.101>.
- [46] Vyazovkin S, et al. Thermochimica Acta ICTAC Kinetics Committee recommendations for collecting experimental thermal analysis data for kinetic computations 2014;590:1–23. <https://doi.org/10.1016/j.tca.2014.05.036>.

- [47] Vyazovkin S. *Isoconversional kinetics of thermally stimulated processes*. Springer; 2015.
- [48] Vyazovkin S, Burnham AK, Criado JM, Pérez-maqueda LA, Popescu C, Sbirrazzuoli N. Thermochimica Acta ICTAC Kinetics Committee recommendations for performing kinetic computations on thermal analysis data. *Thermochim Acta* 2011;520(1–2):1–19. <https://doi.org/10.1016/j.tca.2011.03.034>.
- [49] Jagiello J, Olivier JP. 2D-NLDFT adsorption models for carbon slit-shaped pores with surface energetical heterogeneity and geometrical corrugation. *Carbon N. Y.* 2012;55(2):70–80. <https://doi.org/10.1016/j.carbon.2012.12.011>.
- [50] Jagiello J. Stable numerical solution of the adsorption integral equation using splines. *Langmuir Aug.* 1994;10(8):2778–85. <https://doi.org/10.1021/la00020a045>.
- [51] Hosoya T, Kawamoto H, Saka S. Pyrolysis gasification reactivities of primary tar and char fractions from cellulose and lignin as studied with a closed ampoule reactor. *J Anal Appl Pyrolysis* 2008;83(1):71–7. <https://doi.org/10.1016/j.jaap.2008.06.002>.
- [52] Sobek S, Werle S. Solar pyrolysis of waste biomass: a comparative study of products distribution, in situ heating behavior, and application of model-free kinetic predictions. *Fuel* 2021;292:120365. <https://doi.org/10.1016/j.fuel.2021.120365>. February.
- [53] Yue C, Gao P, Tang L, Chen X. Effects of N<sub>2</sub>/CO<sub>2</sub> atmosphere on the pyrolysis characteristics for municipal solid waste pellets. *Fuel* 2022;315:123233. <https://doi.org/10.1016/j.fuel.2022.123233>. November 2021.
- [54] Kwon EE, Kim S, Lee J. Pyrolysis of waste feedstocks in CO<sub>2</sub> for effective energy recovery and waste treatment. *J CO<sub>2</sub> Util* 2019;31:173–80. <https://doi.org/10.1016/j.jcou.2019.03.015>. February.
- [55] Ali M, Yousef S, Eimontas J, Stri N. Pyrolysis and gasification kinetic behavior of mango seed shells using TG-FTIR-GC-MS system under N<sub>2</sub> and CO<sub>2</sub> atmospheres 2021;173. <https://doi.org/10.1016/j.renene.2021.04.034>.
- [56] Ma W, Rajput G, Pan M, Lin F, Zhong L, Chen G. Pyrolysis of typical MSW components by Py-GC/MS and TG-FTIR. *Fuel* 2019;251:693–708. <https://doi.org/10.1016/j.fuel.2019.04.069>. January.
- [57] Lu Q, Yang X, Dong C, Zhang Z, Zhang X, Zhu X. Influence of pyrolysis temperature and time on the cellulose fast pyrolysis products : analytical Py-GC/MS study. *J Anal Appl Pyrolysis* 2011;92(2):430–8. <https://doi.org/10.1016/j.jaap.2011.08.006>.
- [58] Chen S, Meng A, Long Y, Zhou H, Li Q, Zhang Y. TGA pyrolysis and gasification of combustible municipal solid waste. *J Energy Inst* 2015;88(3):332–43. <https://doi.org/10.1016/j.joei.2014.07.007>.
- [59] Senneca O, Cerciello F, Russo C, Wütscher A, Muhler M, Apicella B. Thermal treatment of lignin , cellulose and hemicellulose in nitrogen and carbon dioxide. *Fuel* 2020;271:117656. <https://doi.org/10.1016/j.fuel.2020.117656>. March.
- [60] Tang Y, Ma X, Lai Z, Lin H, Wu J. Char characteristics of municipal solid waste prepared under N<sub>2</sub> and CO<sub>2</sub> atmospheres. *J Anal Appl Pyrolysis* 2013;101:193–8. <https://doi.org/10.1016/j.jaap.2013.01.010>.
- [61] Wang L, Hustad JE, Skreiberg Ø, Skjevraak G, Grønli M. A critical review on additives to reduce ash related operation problems in biomass combustion applications. *Energy Proc* 2012;20(1876):20–9. <https://doi.org/10.1016/j.egypro.2012.03.004>.
- [62] Criado M, Fernández-Jiménez A, Palomo A. Alkali activation of fly ash: effect of the SiO<sub>2</sub>/Na<sub>2</sub>O ratio: Part I: FTIR study. *Microporous Mesoporous Mater* Nov. 2007; 106(1–3):180–91. <https://doi.org/10.1016/J.MICROMESO.2007.02.055>.
- [63] Kim DH, Mudiyansele K, Szanyi J, Kwak JH, Zhu H, Peden CHF. Effect of K loadings on nitrate formation/decomposition and on NO<sub>x</sub> storage performance of K-based NO<sub>x</sub> storage-reduction catalysts. *Appl Catal B Environ* Oct. 2013;142 (143):472–8. <https://doi.org/10.1016/J.APCATB.2013.05.063>.
- [64] Jagiello J, Ania C, Parra JB, Cook C. Dual gas analysis of microporous carbons using 2D-NLDFT heterogeneous surface model and combined adsorption data of N<sub>2</sub> and CO<sub>2</sub>. *Carbon N. Y.* 2015;91:330–7. <https://doi.org/10.1016/j.carbon.2015.05.004>.
- [65] Chua YW, Wu H, Yu Y. Effect of cellulose–lignin interactions on char structural changes during fast pyrolysis at 100–350 °C. *Proc Combust Inst Jan.* 2021;38(3): 3977–86. <https://doi.org/10.1016/J.PROCI.2020.08.014>.
- [66] Brunner PH, Roberts PV. The significance of heating rate on char yield and char properties in the pyrolysis of cellulose. *Carbon N. Y. Jan.* 1980;18(3):217–24. [https://doi.org/10.1016/0008-6223\(80\)90064-0](https://doi.org/10.1016/0008-6223(80)90064-0).
- [67] Vardon DR, et al. Complete utilization of spent coffee grounds to produce biodiesel, bio-oil, and biochar. *ACS Sustainable Chem Eng* Oct. 2013;1(10):1286–94. [https://doi.org/10.1021/SC400145W/SUPPL\\_FILE/SC400145W\\_SI\\_001.PDF](https://doi.org/10.1021/SC400145W/SUPPL_FILE/SC400145W_SI_001.PDF).
- [68] Stylianou M, et al. Physicochemical and structural characterization of biochar derived from the pyrolysis of biosolids, cattle manure and spent coffee grounds. *J Energy Inst* Oct. 2020;93(5):2063–73. <https://doi.org/10.1016/J.JOEI.2020.05.002>.
- [69] Angin D. Effect of pyrolysis temperature and heating rate on biochar obtained from pyrolysis of safflower seed press cake. *Bioresour Technol* 2013;128:593–7. <https://doi.org/10.1016/j.biortech.2012.10.150>.
- [70] Garcia E, Ejim IF, Liu H. Thermogravimetric analysis of co-combustion of a bituminous coal and coffee industry by-products. *Thermochim Acta* 2022;715: 179296. <https://doi.org/10.1016/j.tca.2022.179296>.
- [71] Yuan Y, He Y, Tan J, Wang Y, Kumar S, Wang Z. Co-Combustion Characteristics of Typical Biomass and Coal Blends by Thermogravimetric Analysis 2021;9:1–11. <https://doi.org/10.3389/fenrg.2021.753622>. October.





Co-published by  
**Institute of Fluid-Flow Machinery**  
Polish Academy of Sciences  
**Committee on Thermodynamics and Combustion**  
Polish Academy of Sciences

Copyright©2024 by the Authors under licence CC BY 4.0

<http://www.imp.gda.pl/archives-of-thermodynamics/>



# Simplified mathematical model of oxy-fuel combustion of municipal solid waste on the grate furnace: effect of different flue gas recirculation rates and comparison with conventional mode

Paulina Copik<sup>\*a</sup>, Andrzej Szłęk<sup>a</sup>, Mario Ditaranto<sup>b</sup>

<sup>a</sup>Department of Thermal Engineering, Silesian University of Technology, Gliwice, Poland

<sup>b</sup>SINTEF Energy Research, Trondheim, Norway

Received: 2024-01-27; revised: 2024-07-03; accepted: 2024-07-16

## Abstract

Bioenergy carbon capture technology (BioCCS or BECCS) plays a key role in the European Green Deal, which aims to decarbonize industry and energy sectors, resulting in the production of energy with negative CO<sub>2</sub> emissions. Due to the biogenic origin of carbon contained in municipal solid waste (MSW), the application of carbon capture in waste incineration plants can be classified as BioCCS. Thus, this technology has attracted scientists' attention recently since it reduces excessive waste and emissions of carbon dioxide. Currently, there are four incineration plants in the Netherlands, Norway and Japan, in which CO<sub>2</sub> capture is implemented; however, they are based on the post-combustion technique since it is the most mature method and not requires many changes in the system. Nevertheless, the separation of CO<sub>2</sub> from the flue gas flow, which contains mostly nitrogen, is complex and causes a large drop in the total performance of the system. Oxy-fuel combustion technology involves the replacement of air as an oxidizer into high purity oxygen and recirculated exhaust gas. As a result, CO<sub>2</sub>-rich gas is produced that is practically ready for capture. The main goal of the study is to develop a mathematical model of oxy-waste combustion to answer the research questions, such as how the composition of oxidant that is supplied to the process affects the combustion performance. The model includes all important processes taking place within the chamber, such as pyrolysis, char burnout and gas combustion over the grate. The results of the work will contribute to the development of oxy-waste incineration plants and will be useful for design purposes.

**Keywords:** oxy-fuel combustion; mathematical modelling; municipal solid waste; carbon capture

Vol. 4(2024) doi: 10.24425/ather.2024.151233

## 1. Introduction

Municipal solid waste (MSW) is recognized as an inevitable result of human activity, rapid urbanization, and economic growth. By 2050, global waste production is expected to increase from 2.01 billion tonnes in 2016 to 3.40 billion tonnes [1]. The waste-to-energy (WtE) industry is of unquestionable significance for non-recyclable waste disposal and plays a key role in the waste management hierarchy established in the Euro-

pean Union (EU) Waste Framework Directive [2]. A grate furnace is a mature and reliable technique for waste incineration that is also able to destroy and remove toxic organic substances [3]. As stated in [4], in the EU, the proportion of MSW incineration plants making use of moving grate technology is 88%.

## Nomenclature

$\bar{a}$	Planck-mean absorption coefficient
$H_i$	Physical enthalpy, kJ/kg
$k_i$	kinetic rate constant, 1/s
$k_{diff}$	coefficient of mass transfer
$\dot{m}_i$	mass flow, kg/s
$A_i$	pre-exponential factor or frequently factor, 1/s
$E_i$	the energy activation, kJ/mol
$R$	the universal gas constant, J/(kmolK)
$r_c$	the ratio of CO/CO <sub>2</sub> formation rate
$c_p$	the specific heat capacity, J/(kgK)
$C_i$	the overall mass diffusion-limited constant, s/K <sup>0.75</sup>
$Q_{rad}$	heat of radiation, kW
$Q_{reac}$	heat of reaction, kW
$Q_{comb}$	heat of combustion, kW
$T_{bed}$	temperature of fuel bed, K
$T_{gas}$	temperature of surrounding gases, K

## Abbreviations and Acronyms

ASU	Air Separation Unit
BECCS	Bioenergy Carbon Capture and Storage
CCS	Carbon Capture and Storage
GDP	Gross Domestic Product
LCA	Life Cycle Assessment
LHV	Lower Heating Value
MEA	Monoethanolamine
MSW	Municipal Solid Waste
OFC	Oxy-fuel combustion
TGA	Thermogravimetric analysis
WtE	Waste-to-energy

A step forward in the development of WtE plants is the integration of incinerators with carbon capture and storage (CCS) technology to become carbon dioxide negative [5]. The described system is called bio-energy carbon capture technology (BioCCS or BECCS) and consists of CO<sub>2</sub> removal from the atmosphere through feedstock with biological origin, which is then thermally converted to obtain energy. The resulting biogenic carbon dioxide is captured and permanently stored, for instance, in a geologic formation, and the biomass is regrown [6].

The opportunities and challenges that need to be addressed to fully exploit the great potential of BECCS technologies based on MSW are summarised in our previous work [7], in which we concluded that among all CCS techniques, oxy-fuel combustion (OFC) is a promising technology in terms of energy efficiency and environmental impact.

OFC involves increasing the partial pressure of carbon dioxide in the exhaust gases in order to facilitate and reduce the costs of its sequestration [8]. The schematic diagram of the oxy-MSW incineration plant is presented in Figure 1. The process consists of the employment of O<sub>2</sub> instead of air as an oxidizer, resulting in a temperature increase. In the case of waste usually having a moderated or low calorific value, oxy-incineration is favourable

since it reduces the consumption of auxiliary fossil fuels (it is often used to keep the required temperature in the MSW combustor, causing inevitable CO<sub>2</sub> emissions). Moreover, due to the absence of nitrogen, the volume of the flue gas stream is about 5 times lower, which facilitates the cleaning of flue gas and allows for reducing the size of equipment [9]. It can also be foreseen that an increase in the partial pressure of oxygen will intensify the oxidation of complex hydrocarbons. However, the issue with ash melting may occur due to the elevated temperature of the process. To control the temperature in the furnace, oxygen can be diluted with flue gas, which mainly consists of carbon dioxide and water vapour.

Till now, studies on oxy-waste combustion were focused on the assessment of the operation of the entire system, e.g. authors in [10–12] simulated the MSW incineration plant working under oxy-fuel combustion conditions and using exergy and life cycle assessment (LCA) analyses evaluated its exergy and energy efficiency as well as its effect on the environment. Results indicated that the total weighted resource consumption and total weighted environment potential of MSW oxy-fuel incineration were lower than MSW incineration with CO<sub>2</sub> capture via monoethanolamine (MEA) absorption. The authors also emphasised that the electric power consumption of air separation unit

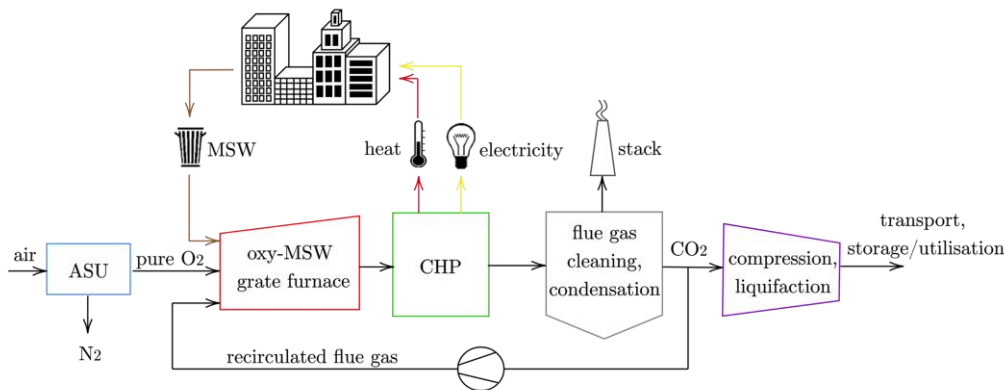


Fig. 1. Schematic diagram of the oxy-fuel incineration plant.

(ASU) was the major influencing parameter, followed by the electric power consumption of CO<sub>2</sub> compressor, while transport distance had small influence on the results.

Experience from previous research on the oxy-combustion of fossil fuels, like coal, has shown that combustion chemistry and radiative heat transfer are altered due to the significantly higher partial pressures of carbon dioxide and water vapor in the flue gas [9,13–15]. Therefore, in the studies on oxy-waste combustion, the thermogravimetric technique was widely employed by many researchers to assess the thermal behaviour of waste, determine chemical kinetics and study gaseous emission in O<sub>2</sub>/N<sub>2</sub> and O<sub>2</sub>/CO<sub>2</sub> atmospheres [16–20]. Authors indicated that at the same oxygen concentration, the DTG peak values in the oxy-fuel atmosphere were lower than those in the air atmosphere indicating that CO<sub>2</sub> has a higher inhibitory effect as well as NO<sub>x</sub> and SO<sub>2</sub> emissions were reduced at some temperatures under O<sub>2</sub>/CO<sub>2</sub> atmosphere. Thermogravimetric analysis plays a vital role in research on the oxy-waste combustion process since it allows for relatively cost-effective and straightforward experimental data collection compared to tests using full-scale furnaces. As stated in [7], obtained kinetic data from TGA analysis can be further used in mathematical and numerical modelling of the oxy-MSW combustion process.

In the literature, few works on the experimental investigation of oxy-waste combustion using lab-scale reactors can be also found, for example in [21,22]. Based on the results, authors concluded that such challenges as combustion chamber design, local O<sub>2</sub> concentrations, flue gas recirculation strategy as well as primary and secondary measures for NO<sub>x</sub> should be further investigated. By now, only one study concerns an experimental campaign on OFC of wood chips using a pilot-scale facility [23]. The results of the tests indicated that the OFC of the biomass fuel is feasible but differs significantly from that of air combustion. The CO<sub>2</sub> concentration in the dry flue gas could be increased to around 73% with 5.7% excess O<sub>2</sub>. Compared to air combustion, the emission of CO was higher during oxy-fired conditions, and the maximum temperature along the combustion chamber was lower.

Mathematical modeling is a powerful tool for furnace design and performance optimisation for various combustion systems without having to resort to scaling up results from lab-scale experiments, which is generally complicated by the strong interaction between turbulence, reaction kinetics, heat release and radiation. Research focused on mathematical modelling of waste and biomass combustion on the grate furnace (Fig. 2) can be found in several articles, for example in [24–29]. Authors developed models of non-fossil solid fuels combustion with the various levels of complexity that can be used for different purposes. All established models include such processes as drying, devolatilization, gas and char oxidation based on chemical kinetic to study different combustion indicators, e.g. temperature profiles, ignition and emission of pollutants. Since biomass and municipal solid waste contain high proportions of volatile matter, Yang et al. [30] built a 1-d model of solid fuel bed combustion to examine the effect of devolatilisation rate of the waste

fuels on the process. In [31], authors developed two-dimensional unsteady state model to investigate the effects of moisture content on combustion characteristics. Studies showed that due to the high moisture content of the feedstock, the evaporation process consumes a large amount of heat and can take about 2/3 of the whole combustion process. Research presented in [32] compared 2-d and 3-d models of waste combustion and investigated the effects of particle size, waste throughput, and residence time on the bed incineration performance. Yu et al. [33] developed a three-dimensional mathematical model as a tool for furnace structure design and operation conditions optimization when the straw combustion is in oxygen-enriched or air atmospheres. Such parameters as temperature, CO and NO were calculated. The results of simulations showed that combustion in an oxygen-enriched atmosphere is superior to combustion in conventional air. A comprehensive review of modelling approaches of biomass and waste combustion is presented in [34] and [35], respectively.

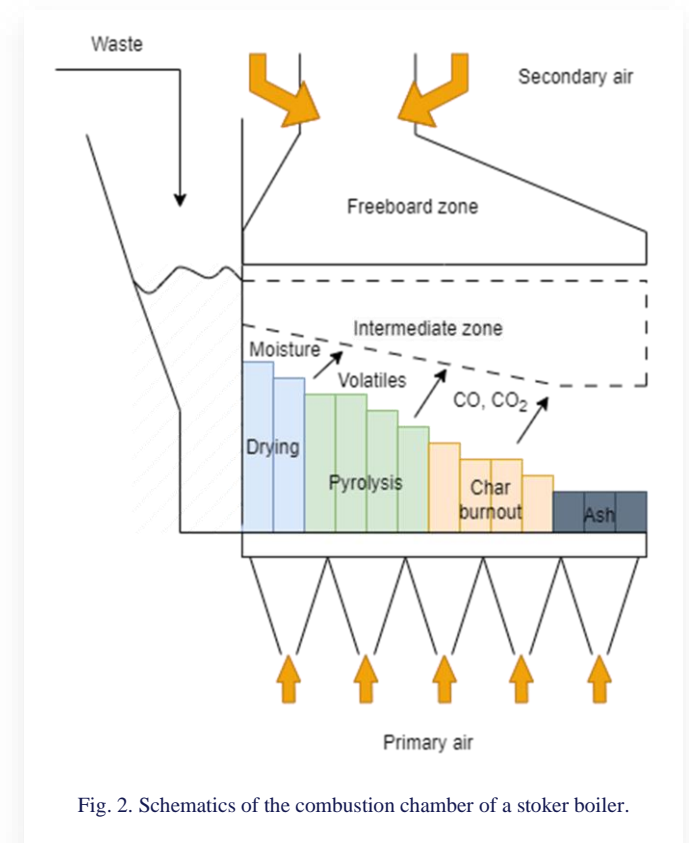


Fig. 2. Schematics of the combustion chamber of a stoker boiler.

Up to now, one paper on CFD simulation of biomass thermal conversion under air/oxy-fuel conditions in a reciprocating grate boiler was found in the literature [36]. The effect of O<sub>2</sub>/recycled flue gas (CO<sub>2</sub>) ratios on flame temperature distribution, species concentration, char burnout, and fuel consumption have been studied and substantial differences were noticed compared with combustion in air atmosphere. The numerical prediction showed that the gas temperature profile in oxy-fuel conditions with 25% oxygen concentration by volume in the oxidizer is closer to the referenced air-fired combustion.

To the best of the authors' knowledge, mathematical models of oxy-waste combustion in a moving grate furnace have not yet been described in the literature. Therefore, in this paper, a mathematical model of waste combustion for a full-scale moving grate MSWI plant under air- and oxy-fired conditions is demonstrated and compared. The model is developed using MATLAB Software. First, the air combustion model is validated by comparison with full-scale plant data. The validated model is then modified for an oxygen-fired system and used to study the effects of the atmosphere and oxidant distribution on important process outcomes.

Section 2 presents the studied system as well as model assumptions and equations. In Section 3, the process and calculation data used for this work are presented. The results are illustrated and discussed in Section 4. Finally, conclusions and recommendations for future works are summarised in Section 5.

## 2. Mathematical model development

### 2.1. Overview and assumptions

The scheme of considered MSW grate furnace is shown in Figure 3. The combustion chamber is divided into three calculation sections: (a) grate, (b) intermediate zone, and (c) freeboard. In the model, the

air in the grate zone is heated and partially consumed in the waste oxidation processes. The rest of the heated air and gases such as volatiles, water vapour, carbon dioxide and carbon monoxide escape from the grate zone. In the case of air combustion, the primary and secondary air is considered to be humid air. Temperature and relative humidity determine the absolute water content of air. For oxy-combustion, the oxidant is oxygen from the ASU and recycled exhaust gases. The composition of the oxidant that was adopted during the simulations is given in Table 2 (Section 3).

As Hoang et al. [35] stated, the coupling between the waste bed and the freeboard is a concern during mathematical modelling. Therefore, in this study, the intermediate zone is proposed, in which the released combustible gases like carbon monoxide and volatile matter are partially combusted with the surplus oxidizer from the grate zone; thus, heat is released above the grate. The reactions follow a chemical equilibrium. Such a solution has not yet been found in the literature.

In the freeboard, oxidiser is supplied again to ensure the complete combustion of remaining combustible gases. The produced flue gas contains mainly CO<sub>2</sub>, H<sub>2</sub>O, and excess O<sub>2</sub>. Thus, after water condensation, CO<sub>2</sub> can be easily compressed and transported.

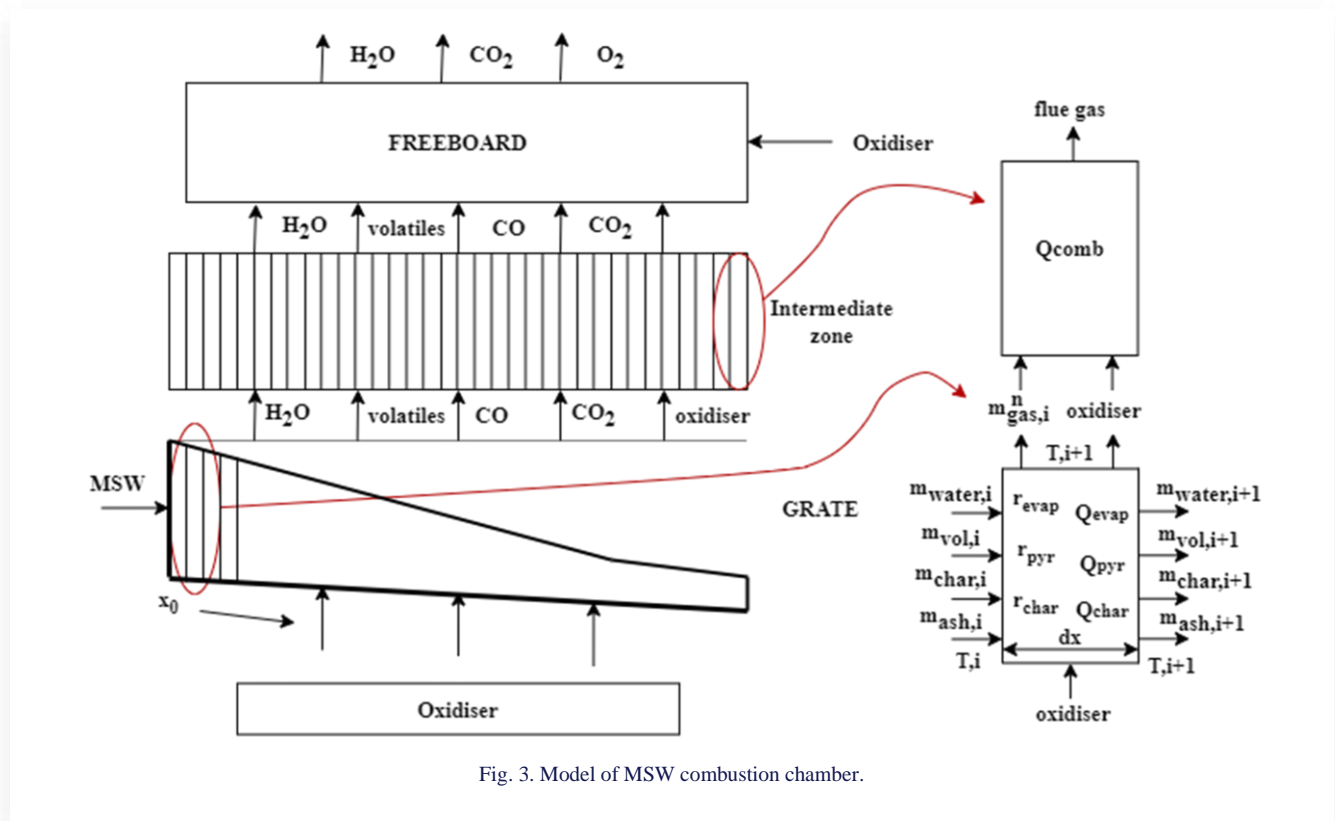


Fig. 3. Model of MSW combustion chamber.

grate zone contains solid fuel particles. The oxidizer at the initial temperature and fresh fuel flow into the grate zone, where in the first stage is heated by surrounding gases by radiation, which provides energy for the evaporation and devolatilization. Then, the remained char reacts with oxidiser, which is supplied to the furnace, generating CO and CO<sub>2</sub>. Therefore, fuel conversion processes take place in the grate zone, releasing or absorbing heat. This approach is consistent with most models of the solid fuels combustion on the grate found in the literature [34,37]. The

The main assumptions:

- Waste is described by proximate and ultimate analysis
- Model is steady state
- Modelled grate and intermediate zones are one dimensional; freeboard is modelled as 0-d;

- Grate and intermediate zones are discretized in the direction of the moving grate as a series of control volumes. State variables within each control volume are homogeneous;
- Pyrolysis and char burnout zones that take place on the grate are taken into account based on one-step chemical kinetics;
- Combustion of volatiles and gases produced during char burnout zone that takes place over the grate is complete.

## 2.2. Materials

Municipal solid waste is a mixture of paper, plastic, food, textiles, tires/rubber, glass and others. Determining the physico-chemical properties of municipal solid waste is often problematic due to the high variability and heterogeneity of the feedstock [38]. The composition of waste varies depending on the level of GDP, lifestyle of society, but may also vary depending on the season [7]. However, it can be assumed that general properties of Europe's MSW are as follows: a) relatively high moisture content of 10-20%, b) high VM content at about 60-80% (dry basis), c) the ash fraction exceeds 10%, and d) level of FC is about 10-20%. The average ultimate MSW composition also can be proposed (daf basis): 40-50% C; 25-35% O; 5-7% H; 0.5-2% N; 0.1- 0.2% S; 0.1-0.2% Cl with a moisture content of 20-40% and an ash content of 15-30% [39].

In this study, we took the properties of waste, such as spent coffee grounds, described in detail in our previous study on kinetic analysis [20], but because the tested materials were dry, the amount of moisture was adjusted to match waste that is typically combusted in waste incineration plants. The proximate and ultimate analyses are presented in Table 1.

$$\frac{\dot{m}_{tot,i} C_{tot,i} dT_i}{dx} = H_{bed,i} - H_{bed,i+1} + Q_{rad,i} + H_{ox,i}^{in,grate} - H_{ox,i+1}^{out,grate} + Q_{reac,i} - H_{gas,i+1}^{out,grate} \quad (3)$$

where  $Q_{rad,i}$  is heat of radiation, kW/m;  $H_{ox,i}^{in,grate}$  and  $H_{ox,i+1}^{out,grate}$  are the enthalpy of the oxidant at the inlet and outlet of the i-th control volume, kW/m;  $Q_{reac,i}$  is the heat of the reactions (evaporation, pyrolysis, char oxidation) of the i-th control volume, kW/m;  $H_{bed,i-1}$  and  $H_{bed,i+1}$  are the physical enthalpy of the solid bed in the adjacent i-th control volume, kW/m;  $H_{gas,i+1}^{out,grate}$  is the physical enthalpy of the gaseous phase escaping i-th control volume, kW/m,  $\dot{m}_{tot,i}$  is defined as:

$$\dot{m}_{tot,i} = \dot{m}_{water,i} + \dot{m}_{waste,i} + \dot{m}_{char,i} + \dot{m}_{ash,i} \quad (4)$$

Where  $\dot{m}_{water,i}$ ,  $\dot{m}_{waste,i}$ ,  $\dot{m}_{char,i}$  and  $\dot{m}_{ash,i}$  are the mass flow of the water, dry waste, char and ash in the solid bed, kg/(s·m).

### 2.3.1 Moisture evaporation zone

Table 1. Fuel analyses.

Proximate analysis (dry basis, wt%)					
Moisture (ar, wt%)	Volatile matter (db, wt%)		Fixed carbon (db, wt%)	Ash content (db, wt%)	
20	57.77		7.62	34.61	
Ultimate analysis (dry basis, wt%)					
LHV, kJ/kg	C	H	O	N	S
14 784	43.50	5.50	15.28	0.13	0.01

## 2.3. Mass and energy balances

The mass flow loss in each control volume is calculated as follows:

$$\frac{d\dot{m}_{tot,i}}{dx} = -k_j \cdot dt \cdot \dot{m}_i \quad (1)$$

where  $d\dot{m}_{tot,i}$  is the mass flow loss of the the fuel, kg/s; dx is the length of the control volume, m;  $k_j$  is the rate of the j-th process (drying, pyrolysis, char burn-out), 1/s; dt is fuel residence time, s; described as:

$$dt = \frac{dx}{v} \quad (2)$$

where v is grate velocity, m/s

The energy balance for the municipal solid waste bed is modeled as:

The rate of moisture release from solids can be expressed as [27,28,40]:

$$r_{evp} = A_s h_s (C_{w,s} - C_{w,g}) \text{ when } T_s < 100 \text{ } ^\circ\text{C} \quad (5)$$

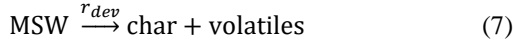
or

$$r_{evp} = \frac{Q_{rad}}{H_{evp}} \text{ when } T_s \geq 100 \text{ } ^\circ\text{C} \quad (6)$$

where  $k_{evp}$  is the reaction rate of evaporation, kg/s;  $H_{evp}$  is the evaporation heat of the moisture in the solid, kJ/kg;  $h_s$  is the convective mass transfer coefficient, m/s (calculated according to Ref. [34]);  $C_{w,s}$ ,  $C_{w,g}$  is the moisture concentration in the solid phase and gas phase, respectively, kg/m<sup>3</sup>;  $A_s$  is particle surface area, m<sup>2</sup>; and  $Q_{rad}$  is radiation heat transfer, kW.

### 2.3.2 Devolatilisation zone

Pyrolysis is a crucial stage of combustion, where volatile compounds are released and the char is formed. Due to the complexity of pyrolysis process, in this study, devolatilization of waste is described by a one-step global reaction (Equation (7)).



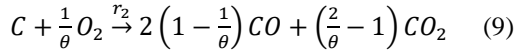
The rate of volatiles formation is taken from an Arrhenius type of expression (Eq. 8)). The data used during calculation are presented in Table 3.

$$k_{dev} = A_1 \exp \left[ \frac{-E_1}{RT_{grate}} \right] \quad (8)$$

where  $A_1$  is pre-exponential factor or frequently factor, 1/s;  $E_1$  is the energy activation, kJ/mol;  $R$  - the universal gas constant, J/(kmolK).

### 2.3.3 Char burnout zone

Due to reactivity of  $\text{CO}_2$  diluent, char combustion is influenced by various mechanisms, such as reduced oxygen mass transfer in  $\text{CO}_2$ , the lower temperature due to the higher heat capacity of  $\text{CO}_2$  and the char- $\text{CO}_2$  gasification reactions [41]. In this study, the oxidizing (exothermic) reaction of char with oxygen is considered (Eq. (9)), in which  $\text{CO}_2$  and  $\text{CO}$  are produced.



where  $\theta$  is the stoichiometric ratio for char oxidation defined as follow:

$$\frac{\dot{m}_{gas,i} c_{gas,i} dT_i}{dx} = H_{ox,i}^{out,grate} + H_{gas,i}^{out,grate} + Q_{comb,i} - H_{gas,i}^{out,intermediate\ zone} \quad (14)$$

where  $Q_{comb,i}$  is heat of partial combustion of volatiles and combustible gases, kW/m;  $H_{gas,i}^{out,intermediate\ zone}$  is the enthalpy of the produced gas at the outlet of the  $i$ -th control volume, kW/m.

### 2.4. Heat transfer between solid and gaseous phases

Since high temperature occurs in the combustion chamber, this model assumes that radiation is the dominant heat transfer mechanism (Eq. 15).

$$Q_{rad,i} = \frac{\varepsilon_{bed} + 1}{2} A \sigma (\varepsilon_{gas} T_{gas}^4 - \sigma_{gas} T_{bed}^4) \quad (15)$$

The emissivity  $\varepsilon_{bed}$  depends on the material, temperature and surface condition. In our simulations we used a constant emissivity of  $\varepsilon_{bed} = 0.8$  for waste bed, but different emissivities can be used for different fractions if data are available.  $T_{gas}$  is a temperature of the freeboard, K;  $T_{bed}$  is a temperature of the grate, K;  $\sigma$  is the Stefan-Boltzmann constant,  $\sigma = 5.67 \times 10^{-8} \text{ W} \cdot \text{m}^{-2} \cdot \text{K}^{-4}$ .

To calculate the radiative properties of the gases in the furnace ( $\varepsilon_{gas}$  and  $\alpha_{gas}$ ), the weighted sum of the gray gases model (WSGGM) is used, which was introduced by Hottel and Sarofim [43] and due to its simplicity and relatively high accuracy, it was further developed and used by many researchers [38,44].

$$\theta = \frac{1 + \frac{1}{r_c}}{\frac{1}{2} + \frac{1}{r_c}} \quad (10)$$

where  $r_c$  is the ratio of  $\text{CO}/\text{CO}_2$  formation rate, which can be estimated by Eq. (11) [26]:

$$r_c = \frac{\text{CO}}{\text{CO}_2} = 12 \exp \left( -\frac{3300}{T_{char}} \right) \quad (11)$$

Char reaction rate that can be generally expressed as [42]:

$$k_i = \frac{k_{kin,i} k_{diff,i}}{k_{kin,i} + k_{diff,i}} \quad (12)$$

where  $k_{kin,i}$  is kinetic rate constant for oxidizing and reductive reaction,  $\text{kg}/(\text{m}^2 \cdot \text{sPa})$ ;  $k_{diff,i}$  is coefficient of mass transfer for oxidizing and reductive reaction,  $\text{kg}/(\text{m}^2 \cdot \text{sPa})$ .

$$k_{kin,i} = A_i \exp \left[ \frac{-E_i}{RT_{char}} \right] \quad (13)$$

where  $C_i$  is the overall mass diffusion-limited constant,  $\text{s}/\text{K}^{0.75}$ ;  $d_p$  is diameter of char particle, m;  $T_\infty$  temperature of surrounding gas, K.

### 2.3.4 Intermediate zone – gaseous phase partial combustion

The energy balance of intermediate zone is calculated as follow:

In the WSGG model, the Planck-mean absorption coefficient of the gas mixture over a path length is determined by [41,45]:

$$\bar{\alpha} = -\ln(1 - \varepsilon/s) \quad (16)$$

where  $s$  is the radiation beam length, and  $\varepsilon$ , the gas emissivity. The latter is calculated from:

$$\varepsilon = \sum_i a_{\varepsilon,i}(T) (1 - \exp(-\kappa_i p_i s)) \quad (17)$$

where  $a_{\varepsilon,i}$  is the emissivity weighting factor for gray gas  $i$ ,  $\kappa_i$  and  $p_i$  are the pressure absorption coefficient ( $1/\text{m} \cdot \text{atm}$ ) and partial pressure (atm) of the absorbing gas  $i$ , respectively.

The emissivity weighting factors are polynomial correlations that can be given as a function of the gas temperature:

$$a_{\varepsilon,i} = \sum_j b_{\varepsilon,i,j} T^{j-1} \quad (18)$$

It should be noted that most of the already established coefficients of WSGGM are suitable only for the air-fired combustion conditions, where the molar fractions ratio of carbon dioxide and water vapour differs from oxy-fuel combustion, and using them in the oxy-fired conditions may lead to uncertain levels of inaccuracy. Therefore, with the growing popularity of oxygen-fired systems, some scientists have expanded the set of coefficients with those dedicated to oxy-fuel combustion, for example, in [45,46].

### 3. Calculation data

Physical data and process data (Tab. 2) of the full-scale incineration plant were provided by the Returkraft WtE plant in Kristiansand (Norway). A description of the waste incineration process at the studied plant is available in the article [38].

Table 2. Physical data and process data.

Parameter	Unit	Value
Grate length	m	10.2
Grate width	m	6.3
Height to the top of 1st pass	m	19.15
Waste throughput capacity	t/h	18
Primary air distribution (5 zones) (air-fired mode)	%	8 – 29 – 37 – 23 – 3
Primary air temperature	°C	110
Primary air flow rate	m <sup>3</sup> /h	53669
Secondary air temperature	°C	110
Secondary air flow rate	m <sup>3</sup> /h	39945
Grate speed	m/s	0.002
Oxidiser composition (air-fired mode)	vol. %	21% O <sub>2</sub> – 79% N <sub>2</sub>
Relative humidity	%	95
Oxidiser composition (oxy-fired mode)	vol. %	95% O <sub>2</sub> – 5% N <sub>2</sub>
Wet recirculated flue gas composition (oxy-fired mode)	mol %	55.5% CO <sub>2</sub> – 27.7% H <sub>2</sub> O – 12.2% O <sub>2</sub> – 4.4% N <sub>2</sub>
Flue gas molar flow	kmol/s	0.9429

As we mentioned earlier, in this study individual steps of the fuel thermal decomposition were taken into account based on chemical kinetics. To determine the kinetic parameters of waste materials, an experimental campaign on the thermogravimetric instrument and lab-scale reactor was performed. Firstly, we performed the TGA analysis of sample pyrolysis in N<sub>2</sub> and CO<sub>2</sub> atmospheres and retrieved the kinetic data, employing isoconversional methods, also known as model-free (Friedman and Vyazovkin). According to the isoconversional principle, the process rate at a constant extent of conversion  $\alpha$  is a function of temperature [47]. Then, we used a lab-scale reactor to produce waste chars and we subjected them to thermogravimetric analysis in air and oxy-fired conditions. These studies were in detail described in our previous works [20,21]. Table 3 shows the kinetic data used in the mathematical model in the air- and oxy-fired mode.

Other calculation data, such as, the physical properties of used waste used in the model are summarized in Table 4.

For the simulation of waste combustion system, the MATLAB

Table 3. Kinetic data used in the mathematical model in the air- and oxy-fired mode.

Parameter	Unit	Value
A <sub>dev,air</sub>	1/s	10 <sup>17.7</sup>
E <sub>dev,air</sub>	kJ/mol	232100
A <sub>dev,oxy</sub>	1/s	10 <sup>21.3</sup>
E <sub>dev,oxy</sub>	kJ/mol	274700
A <sub>char,air</sub>	1/s	10 <sup>4.79</sup>
E <sub>char,air</sub>	kJ/mol	104372
A <sub>char,oxy</sub>	1/s	136.56
E <sub>char,oxy</sub>	kJ/mol	72137

Table 4. Physical properties of waste used in the model [24,27,29]

Parameter	Unit	Value
Heat capacity of water, $c_{water}$	kJ/kgK	4.187
Heat capacity of dry waste, $c_{waste}$		1.5+0.001·T
Heat capacity of char, $c_{char}$		0.44+0.001·T·7·10 <sup>-8</sup> T <sup>2</sup>
Heat capacity of ash, $c_{ash}$		0.8
Bed emissivity, $\epsilon_{bed}$	-	0.8
Gas emissivity (air-fired system), $\epsilon_{gas,air}$	-	0.4143
Gas emissivity (oxy-fired system), $\epsilon_{gas,oxy}$	-	0.4816

software was used. The equations were solved using Newton-Raphson method and a mesh array of 10 200 was employed.

### 4. Results and discussion

In the study, firstly simulations of the incineration chamber in the air-fired mode were performed, using assumptions and equations presented in Section 2 and input data presented in Section 3. The results of these calculations, such as temperature of the

grate and intermediate zone as well as mass flow of the waste in the function of the grate length, together with the model verification are provided as a "reference" and presented in Section 4.1. Validated model was then modified to the oxy-fired mode using the input data from Section 3. The results of the analysis of oxy-fired system are presented in Section 4.2.

#### 4.1. Reference simulation and comparison with process data

Figure 4a presents temperature of the grate and intermediate zone as well as fuel mass flow in the function of the grate length. As can be observed, fuel combustion on the grate occurs gradually. Firstly, the fuel heats up and dries (Zone I), then when the grate reaches a temperature of around 450 °C, volatile matters are released. The drying and pyrolysis processes end at a distance of 2 m of the grate. Directly above the grate, in the inter-

Nevertheless, it is worth mentioning that in the char burnout zone, the temperature should not exceed 800°C due to the presence of organics in the waste, such as plant residues and food leftovers with a very low ash melting point temperature of around 825°C [48].

Figure 5 presents a comparison of the temperature of the free-board between the air-fired model and the real measurements (with the calculated average value) in the incineration plant. Figure 6 shows measurements and the calculated value of the oxygen content in the flue gas at the outlet. The relative difference between the calculated and measured temperature and oxygen content is 4.8% and 10.2%, respectively. Thus, it was found that the air-fired model was sufficiently accurate and work on the model in the oxy-combustion mode began.

#### 4.2. Oxy combustion model

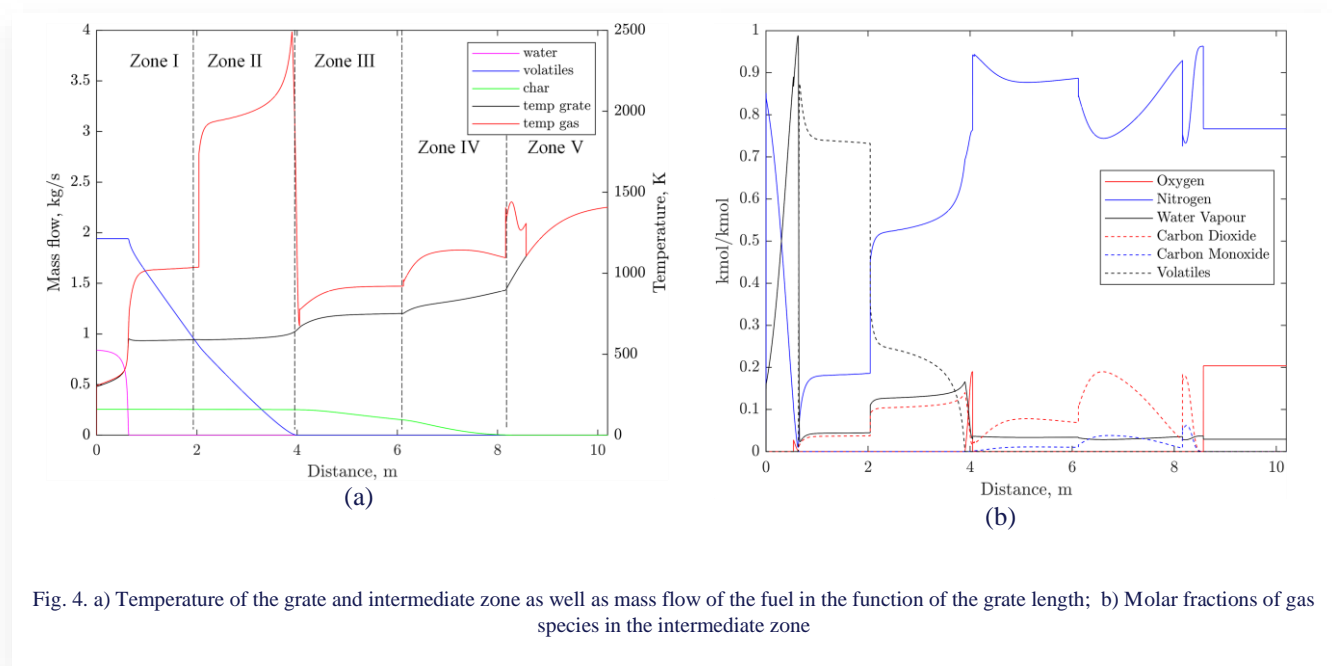


Fig. 4. a) Temperature of the grate and intermediate zone as well as mass flow of the fuel in the function of the grate length; b) Molar fractions of gas species in the intermediate zone

mediate zone, the volatiles partially burn, releasing heat and causing temperature growth up to 2000 K (Zone II). After the pyrolysis process, the waste char begins to slowly oxidize, and over a grate length of 8 m the fuel is burned out (Zones III and IV). In the fifth zone, the air mass flow is reduced and only ash remains. Similar findings regarding weight loss on the grate, burnout and grate temperatures have been found in the literature [27,28,30,38]. The different zones shown in Figure 4a correspond to the air distribution according to data obtained from an incinerator in Norway (Table 2).

Figure 4b presents the molar fractions of gas species in the intermediate zone. As can be seen, oxygen quickly drops from 21% to below 1%, meaning that is consumed during most of the process on the grate, which indicates that locally air-lean (or fuel-rich) conditions dominate the bed combustion processes [33]. After the complete combustion of the fuel, the intermediate zone is filled only with air. Results indicate that during the char oxidation CO<sub>2</sub> generation is more intensive. The produced carbon monoxide will be further combusted in the intermediate zone above the grate generating heat.

This section presents the results of the simulations of the oxy-waste combustion chamber. To assess the influence of different factors, such as flue gas recirculation ratio, oxygen distribution, and oxidizer temperature, we studied three different cases:

- 1) The first analysed case involved introducing oxygen into the combustion chamber, with lambda ( $\lambda$ ) equal to 0.52, along with recirculated exhaust gas in the ratio of 15, 20, and 25%.
- 2) The second analysed case comprised checking the influence of oxidant distribution. This was achieved by first supplying recirculated flue gas to the combustion



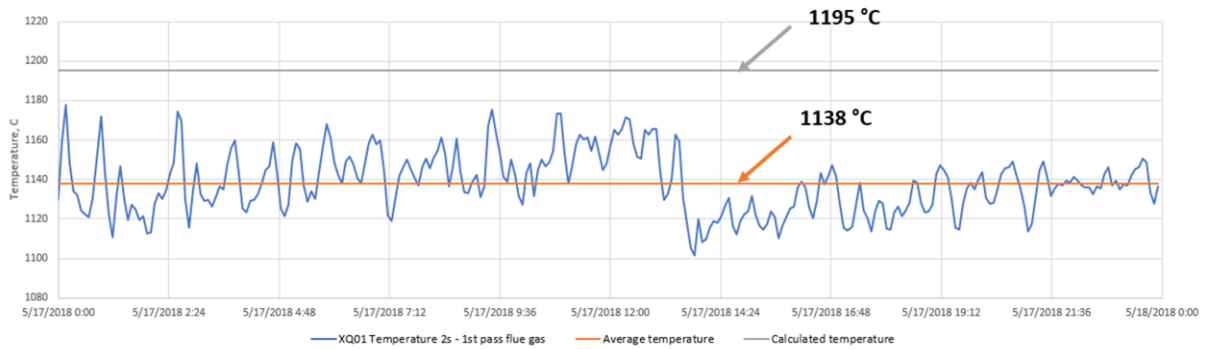


Fig. 5. Comparison between real temperature in the furnace (freeboard zone) and simulation (WtE Returkraft plant data)

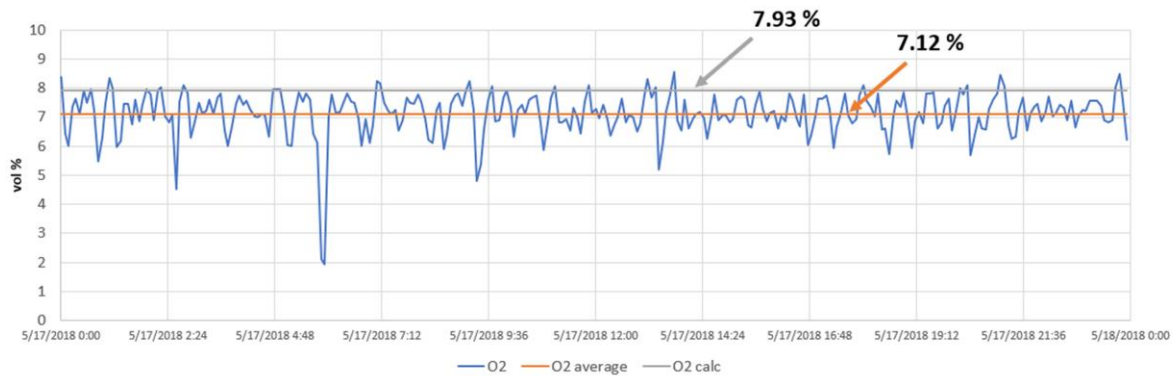


Fig. 6. Comparison between oxygen content in the flue gas at the outlet and simulation (WtE Returkraft plant data)

chamber, and only after the volatile matters had volatilized, introducing oxygen (in the amount as in the first case).

- 3) In the third case, the most favorable oxygen distribution was taken (determined from the previous cases) and the influence of 3 different oxidant temperatures on the process was checked.

#### 4.2.1 Effect of the flue gas recirculation

Oxy-fuel combustion changes many parameters inside the furnace due to change in overall thermal environment in the furnace. A major effect is visible on temperature distribution which happens due to CO<sub>2</sub> rich combustion environment. Figure 7 presents the radiative heat transfer between gas and solid phase for air- and oxy-fired conditions. As can be observed, oxy-fired system is characterized by higher radiative heat flux than combustion in air atmosphere, which can be also observed in other comparative studies on air- and oxy-fired systems [41,49].

Figure 8 shows the temperatures of the grate and intermediate zone as well as the mass flow of the waste in the function of the grate length. As can be observed, the higher the degree of flue gas recirculation, the lower the temperature of the grate and the intermediate zone, which confirms that recirculation can effectively control the temperature in the combustion chamber. The reason for that is the change in the environment of the furnace, as CO<sub>2</sub> and H<sub>2</sub>O contained in flue gas have a different specific

heat capacity than N<sub>2</sub>. The increased amount of recycled flue gas, and thus the higher amount of heat released by combustion, is absorbed, which decreases the temperature of the process [36,50].

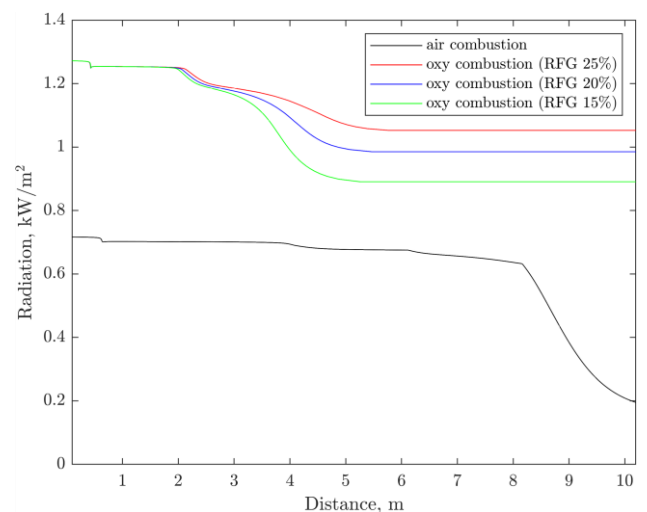


Fig. 7. Radiative heat transfer for air- and oxy-fired system

The next finding obtained in this research is that using oxygen during waste combustion raises the temperature and speeds up the process. For instance, combustion ends at 4 m for a recirculation rate of a 15%, 4.5 m for a 20% rate, and at 5.5 m for 25%. This means that, in addition to the lower exhaust gas volume and thus, smaller equipment used for flue gas cleaning (as discussed in Section 1), the size of the combustion chambers operating under oxy-fuel conditions may be lowered by 30–50% when compared to the conventional mode of combustion.

The oxygen needed to complete the oxy-waste combustion pro-

Table 5. Oxygen demand for different oxy-fired conditions

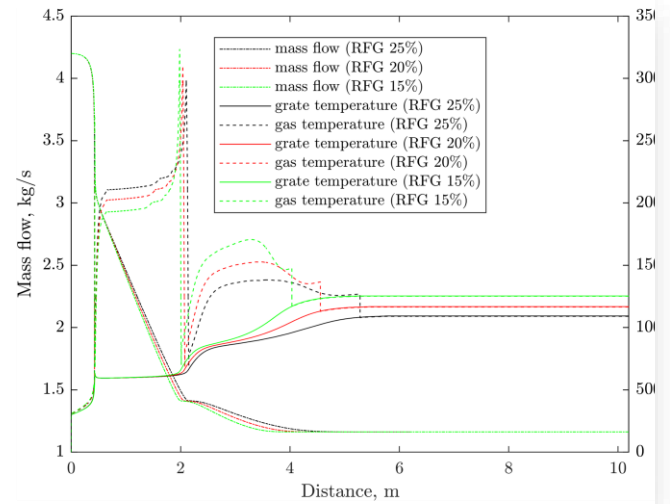
Parameter	Unit	Value		
FGR ratio	%	15	20	25
Total oxygen demand	kmol/s	0.0969	0.1027	0.1085
Oxygen from ASU	kmol/s	0.0795		
The share of oxygen in the oxidant	%	33	37	43

cess (total and oxygen produced in ASU) is compiled in Table 5. A larger flue gas recirculation ratio corresponds with a higher oxygen content in the oxidiser. This is because components that oxidize, like oxygen, carbon dioxide, and water vapour, are present in the recirculated gases. Additionally, the percentage of oxygen in the oxidant was determined for each case and ranged from 33% to 34%.

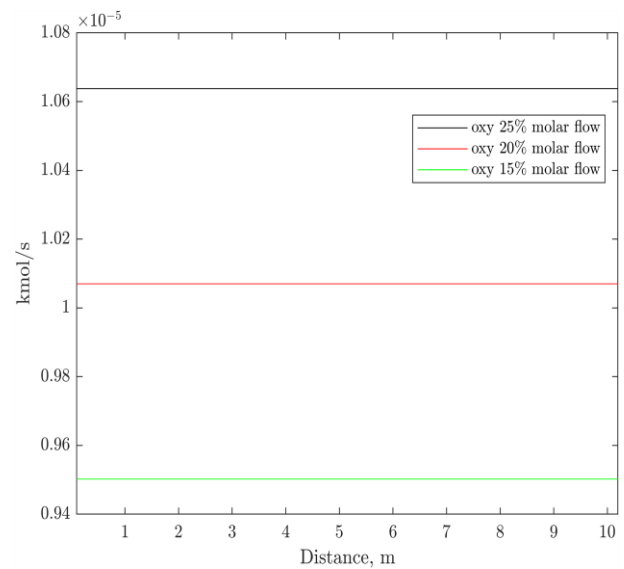
Nevertheless, we found that temperature in the intermediate zone can exceed up to 3000 K, when the volatiles are partially combusted, and the temperature at the grate can exceed the temperature of the waste ash melting point. Thus we analysed the second case, in which we limited the oxygen supply only to char oxidation zone. The drying and devolatilization processes were carried out in the atmosphere of recycled flue gases (with the ratios of 15, 20 and 25%).

#### 4.2.2 Effect of oxygen distribution

Analogously to the previous results, Figures 9 and 10 show the temperature of the grate and intermediate zone as well as the weight flow of the waste in the function of the grate length for the three different ratios of flue gas recirculation. The results imply that the use of recirculated flue gas for evaporation and pyrolysis processes is feasible. Limiting oxygen slightly extends the process and significantly decreases the temperature in the combustion chamber (Fig. 9). Moreover, the radiative heat transfer profile in this case is more similar to air combustion



(a)



(b)

Fig. 8. a) Temperature of the grate and intermediate zone as well as mass flow of the fuel in the function of the grate length b) oxidant distribution along the grate

Table 6. Oxygen demand for different oxy-fired conditions

Parameter	Unit	Value		
FGR ratio	%	15%	20%	25%
Total oxygen demand	kmol/s	0.0290	0.0232	0.0174
The share of oxygen in the oxidant	%	25		

(Fig. 10). The oxygen share in the oxidant for the each case was equal to 25%.

Regarding the oxygen demand, in the second case studied, the required amount of oxygen in the process decreased significantly as shown in Table 6. This results in lower consumption

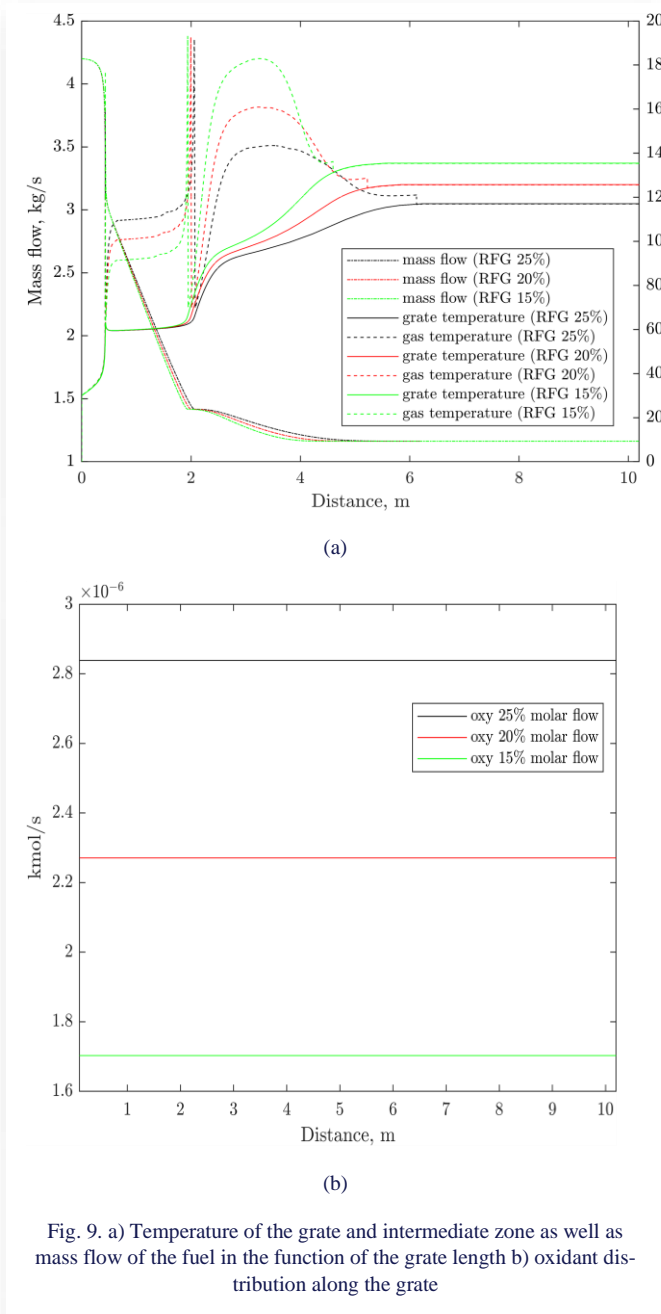


Fig. 9. a) Temperature of the grate and intermediate zone as well as mass flow of the fuel in the function of the grate length b) oxidant distribution along the grate

of electricity to power the air separation unit, which is employed to produce pure oxygen. As various studies have shown [7,51], the ASU is the most energy-intensive device in the oxy-fuel combustion systems; Therefore, in studies on oxy-waste incineration, the key parameter that will allow the selection of the optimal oxidant distribution strategy should be the demand for oxygen.

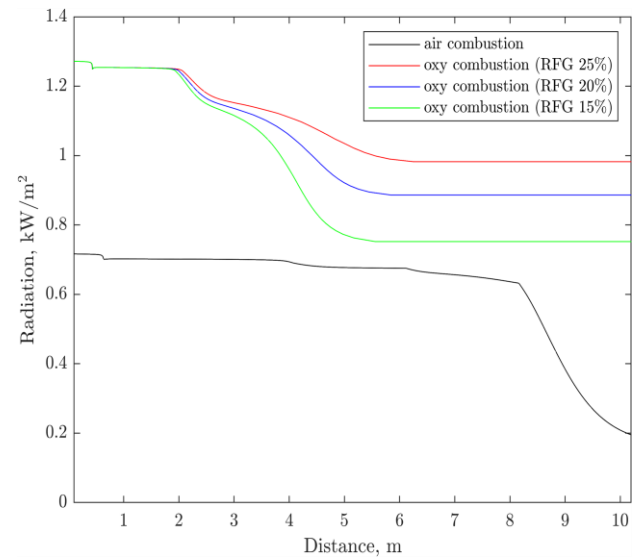


Fig. 10. Radiative heat transfer for air- and oxy-fired system

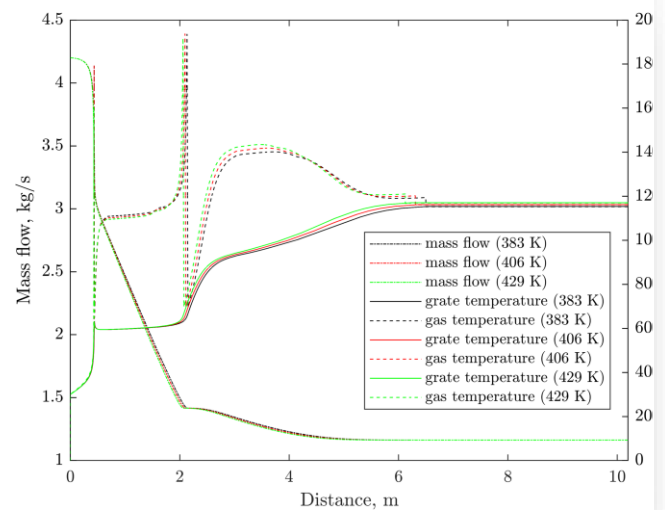


Fig. 11. Temperature of the grate and intermediate zone as well as mass flow of the fuel in the function of the grate length

#### 4.2.3 Effect of oxidizer temperature

In the last case, we analysed the influence of the temperature of the oxidizer on the process. We selected the conditions used in the second case (with the 25% of recirculated flue gas) and investigated three different temperatures of 383, 406 and 429 K. The results presented in the Figure 11 indicate that the temperature of the oxidiser does not affect the process significantly.

### 5. Conclusions

This study shows the first attempt at mathematical modeling of real scale oxy-waste incineration, which is a scientific novelty

of this work. As a result, the 1-d model of oxy-MSW combustion in a grate furnace is developed and analysed. The processes that were considered on the grate comprised waste drying, pyrolysis, the heterogeneous reactions of char and O<sub>2</sub>/CO<sub>2</sub> based on the chemical kinetics as well as homogeneous reactions with gases in the intermediate zone (above the grate). Besides, heat and mass transfer between the gas and solid phases are comprised.

The presented results showed that such combustion parameters as temperature and the length of the process highly depend on oxidant composition:

- Increased content of oxygen in the supplied gas shortens the combustion process by around 30-50%
- Increased content of oxygen elevates the temperature in the gaseous reactions area
- Increased content of oxygen elevates the temperature in the grate
- Study also confirmed that flue gas recirculation effectively control the temperature of the process.
- Moreover, the results indicate that the use of recirculated exhaust gases as an oxidant is sufficient for the drying and pyrolysis process.

Thus, oxy-fuel combustion of waste in a grate furnace can provide improved burnout and higher temperature with a sustainable “CO<sub>2</sub>-less” thermal conversion of fuel.

Results will be useful especially for the design purposes of the oxy-MSW combustion process since they show the duration of the various stages of waste incineration, the amount and composition of the obtained products, as well as the approximate temperature of the gaseous and solid phases depending on the used oxidant.

## Acknowledgements

This research is supported by the National Science Centre (Project no. UMO-2021/41/N/ST8/02548) and Ministry of Education and Science (Poland) under statutory research funds of the Faculty of Energy and Environmental Engineering of SUT (08/060/RGZ200275-24). The work of MD is supported by the CLIMIT program of the Research Council of Norway (Grants number 281869 and 305062).

I would like to acknowledge WtE Returkraft plant for providing the operational data.

## References

- [1] Kaza, S., Yao, L., Bhada-Tata, P. & Van Woerden, F. (2018). What a Waste 2.0: A Global Snapshot of Solid Waste Management to 2050. *What a Waste 2.0 A Glob. Snapshot Solid Waste Manag. to 2050*. <https://doi.org/10.1596/978-1-4648-1329-0>
- [2] Cucchiella, F., D'Adamo, I. & Gastaldi, M. (2017). Sustainable waste management: Waste to energy plant as an alternative to landfill. *Energy Conversion and Management, Elsevier Ltd.* 131, 18–31. <https://doi.org/10.1016/j.enconman.2016.11.012>
- [3] Kumar, A. & Samadder, S.R. (2017). A review on technological options of waste to energy for effective management of municipal solid waste. *Waste Management, Elsevier Ltd.* 69, 407–22. <https://doi.org/10.1016/j.wasman.2017.08.046>
- [4] Makarichi, L., Jutidamrongphan, W. & Techato, K. (2018). The evolution of waste-to-energy incineration: A review. *Renewable and Sustainable Energy Reviews, Pergamon.* 91, 812–21. <https://doi.org/10.1016/J.RSER.2018.04.088>
- [5] Pour, N., Webley, P.A. & Cook, P.J. (2018). Potential for using municipal solid waste as a resource for bioenergy with carbon capture and storage (BECCS). *International Journal of Greenhouse Gas Control, Elsevier.* 68, 1–15.
- [6] Ramírez, S.E.T.K.B.A. (2021). Decarbonising Industry via BECCS: Promising Sectors, Challenges, and Techno-economic Limits of Negative Emissions. *Current Sustainable/Renewable Energy Reports, Springer International Publishing.* 253–62. <https://doi.org/10.1007/s40518-021-00195-3>
- [7] Wienchol, P., Szłęk, A. & Ditaranto, M. (2020). Waste-to-energy technology integrated with carbon capture – Challenges and opportunities. *Energy, 198,* 117352. <https://doi.org/10.1016/j.energy.2020.117352>
- [8] Buhre, B.J.P., Elliott, L.K., Sheng, C.D., Gupta, R.P. & Wall, T.F. (2005). Oxy-fuel combustion technology for coal-fired power generation. *Progress in Energy and Combustion Science, Elsevier.* 31, 283–307.
- [9] Toftegaard, M.B., Brix, J., Jensen, P.A., Glarborg, P. & Jensen, A.D. (2010). Oxy-fuel combustion of solid fuels. *Progress in Energy and Combustion Science, Elsevier Ltd.* 36, 581–625. <https://doi.org/10.1016/j.peccs.2010.02.001>
- [10] Ding, G., He, B., Cao, Y., Wang, C., Su, L., Duan, Z. et al. (2018). Process simulation and optimization of municipal solid waste fired power plant with oxygen/carbon dioxide combustion for near zero carbon dioxide emission. *Energy Conversion and Management, Elsevier Ltd.* 157, 157–68. <https://doi.org/10.1016/j.enconman.2017.11.087>
- [11] Tang, Y.T., Ma, X.Q., Lai, Z.Y. & Chen, Y. (2013). Energy analysis and environmental impacts of a MSW oxy-fuel incineration power plant in China. *Energy Policy, Elsevier.* 60, 132–41. <https://doi.org/10.1016/j.enpol.2013.04.073>
- [12] Vilardi, G. & Verdone, N. (2022). Exergy analysis of municipal solid waste incineration processes: The use of O<sub>2</sub>-enriched air and the oxy-combustion process. *Energy,* 239, 122147. <https://doi.org/https://doi.org/10.1016/j.energy.2021.122147>
- [13] Scheffknecht, G., Al-makhadmeh, L., Schnell, U. & Maier, J. (2011). Oxy-fuel coal combustion — A review of the current state-of-the-art. *International Journal of Greenhouse Gas Control,* 16–35. <https://doi.org/10.1016/j.ijggc.2011.05.020>

- [14] MONIKA KOSOWSKA-GOLACHOWSKA, AGNIESZKA KIJO-KLECZKOWSKA, ADAM LUCKOS, KRZYSZTOF WOLSKI, T.M. (2016). Oxy-combustion of biomass in a circulating fluidized bed Experimental Circulating fluidized bed combustor. *Archives of Thermodynamics*, 37, 17–30. <https://doi.org/10.1515/aoter-2016-0002>
- [15] Kindra, V.O. & Milukov, I.A. (2021). Thermodynamic analysis of cycle arrangements of the coal-fired thermal power plants with carbon capture Introduction. *Archives of Thermodynamics*, 42, 103–21. <https://doi.org/10.24425/ather.2021.139653>
- [16] Lai, Z.Y., Ma, X.Q., Tang, Y.T. & Lin, H. (2011). A study on municipal solid waste (MSW) combustion in N<sub>2</sub>/O<sub>2</sub> and CO<sub>2</sub>/O<sub>2</sub> atmosphere from the perspective of TGA. *Energy*, Elsevier Ltd. 36, 819–24. <https://doi.org/10.1016/j.energy.2010.12.033>
- [17] Tang, Y., Ma, X., Lai, Z. & Fan, Y. (2015). Thermogravimetric analyses of co-combustion of plastic, rubber, leather in N<sub>2</sub>/O<sub>2</sub> and CO<sub>2</sub>/O<sub>2</sub> atmospheres. *Energy*, Elsevier. 90, 1066–74.
- [18] Lai, Z.Y., Ma, X.Q., Tang, Y.T., Lin, H. & Chen, Y. (2012). Thermogravimetric analyses of combustion of lignocellulosic materials in N<sub>2</sub>/O<sub>2</sub> and CO<sub>2</sub>/O<sub>2</sub> atmospheres. *Bioresource Technology*, Elsevier Ltd. 107, 444–50. <https://doi.org/10.1016/j.biortech.2011.12.039>
- [19] Tang, Y., Ma, X., Lai, Z., Zhou, D. & Chen, Y. (2013). Thermogravimetric characteristics and combustion emissions of rubbers and polyvinyl chloride in N<sub>2</sub>/O<sub>2</sub> and CO<sub>2</sub>/O<sub>2</sub> atmospheres. *Fuel*, Elsevier Ltd. 104, 508–14. <https://doi.org/10.1016/j.fuel.2012.06.047>
- [20] Wienchol, P., Korus, A., Szlęk, A. & Ditaranto, M. (2022). Thermogravimetric and kinetic study of thermal degradation of various types of municipal solid waste (MSW) under N<sub>2</sub>, CO<sub>2</sub> and oxy-fuel conditions. *Energy*, Pergamon. 248, 123573. <https://doi.org/10.1016/J.ENERGY.2022.123573>
- [21] Copik, P., Korus, A., Szi, A. & Ditaranto, M. (2023). A comparative study on thermochemical decomposition of lignocellulosic materials for energy recovery from waste: Monitoring of evolved gases, thermogravimetric, kinetic and surface analyses of produced chars. 285. <https://doi.org/10.1016/j.energy.2023.129328>
- [22] Becidan, M., Ditaranto, M., Carlsson, P., Bakken, J., Olsen, M.N.P. & Stuen, J. (2021). Oxyfuel Combustion of a Model MSW—An Experimental Study. *Energies* 2021, Vol 14, Page 5297, Multidisciplinary Digital Publishing Institute. 14, 5297. <https://doi.org/10.3390/EN14175297>
- [23] Mack, A., Maier, J. & Scheffknecht, G. (2022). Modification of a 240 kWth grate incineration system for oxyfuel combustion of wood chips. *Journal of the Energy Institute*, 104, 80–8.
- [24] Shin, D. & Choi, S. (2000). The Combustion of Simulated Waste Particles in a Fixed Bed. *Combust. Flame*.
- [25] Yang, W., Ryu, C. & Choi, S. (2004). Unsteady one-dimensional model for a bed combustion of solid fuels. *Proc. Instn Mech. Engrs*.
- [26] Zhou, H., Jensen, A.D., Glarborg, P., Jensen, P.A. & Kavaliauskas, A. (2005). Numerical modeling of straw combustion in a fixed bed. *Fuel*, 84, 389–403. <https://doi.org/10.1016/j.fuel.2004.09.020>
- [27] Gu, T., Yin, C., Ma, W. & Chen, G. (2019). Municipal solid waste incineration in a packed bed: A comprehensive modeling study with experimental validation. *Applied Energy*, Elsevier Ltd. 247, 127–39. <https://doi.org/10.1016/j.apenergy.2019.04.014>
- [28] Hoang, Q.N., Van Caneghem, J., Croymans, T., Pittoors, R. & Vanierschot, M. (2022). A novel comprehensive CFD-based model for municipal solid waste incinerators based on the porous medium approach. *Fuel*, 326, 124963. <https://doi.org/https://doi.org/10.1016/j.fuel.2022.124963>
- [29] Wissing, F., Wirtz, S. & Scherer, V. (2017). Simulating municipal solid waste incineration with a DEM / CFD method – Influences of waste properties, grate and furnace design. *Fuel*, Elsevier Ltd. 206, 638–56. <https://doi.org/10.1016/j.fuel.2017.06.037>
- [30] Yang, Y.B., Yamauchi, H., Nasserzadeh, V. & Swithenbank, J. (2003). Effects of fuel devolatilisation on the combustion of wood chips and incineration of simulated municipal solid wastes in a packed bed. *Fuel*, 82, 2205–21. [https://doi.org/10.1016/S0016-2361\(03\)00145-5](https://doi.org/10.1016/S0016-2361(03)00145-5)
- [31] Sun, R., Ismail, T.M., Ren, X. & Abd El-Salam, M. (2015). Numerical and experimental studies on effects of moisture content on combustion characteristics of simulated municipal solid wastes in a fixed bed. *Waste Management*, Elsevier Ltd. 39, 166–78. <https://doi.org/10.1016/j.wasman.2015.02.018>
- [32] Xia, Z., Long, J., Yan, S., Bai, L., Du, H. & Chen, C. (2020). Two-Fluid Simulation of Moving Grate Waste Incinerator: Comparison of 2D and 3D Bed Models. *Energy*, Elsevier Ltd. 119257. <https://doi.org/10.1016/j.energy.2020.119257>
- [33] Yu, Z., Ma, X. & Liao, Y. (2010). Mathematical modeling of combustion in a grate-fired boiler burning straw and effect of operating conditions under air- and oxygen-enriched atmospheres. *Renewable Energy*, Elsevier Ltd. 35, 895–903. <https://doi.org/10.1016/j.renene.2009.10.006>
- [34] Khodaei, H., Al-Abdeli, Y.M., Guzzomi, F. & Yeoh, G.H. (2015). An overview of processes and

- considerations in the modelling of fixed-bed biomass combustion. *Energy*, Elsevier Ltd. p. 946–72. <https://doi.org/10.1016/j.energy.2015.05.099>
- [35] Hoang, Q.N., Vanierschot, M., Blondeau, J., Croymans, T., Pittoors, R. & Van Caneghem, J. (2021). Review of numerical studies on thermal treatment of municipal solid waste in packed bed combustion. *Fuel Communications*, Elsevier Ltd. 7, 100013. <https://doi.org/10.1016/j.fueco.2021.100013>
- [36] Karim, R., Ahmed, A., Alhamid, A., Sarhan, R. & Naser, J. (2020). CFD simulation of biomass thermal conversion under air / oxy-fuel conditions in a reciprocating grate boiler. *Renewable Energy*, Elsevier Ltd. 146, 1416–28. <https://doi.org/10.1016/j.renene.2019.07.068>
- [37] Yang, Y.B., Goh, Y.R., Zakaria, R., Nasserzadeh, V. & Swithenbank, J. (2002). Mathematical modelling of MSW incineration on a travelling bed. *Waste Management*, 22, 369–80. [https://doi.org/10.1016/S0956-053X\(02\)00019-3](https://doi.org/10.1016/S0956-053X(02)00019-3)
- [38] Magnanelli, E., Tranås, O.L., Carlsson, P., Mosby, J. & Becidan, M. (2020). Dynamic modeling of municipal solid waste incineration. *Energy*, Pergamon. 209, 118426. <https://doi.org/10.1016/J.ENERGY.2020.118426>
- [39] Becidan, M. (2007). *Experimental Studies on Municipal Solid Waste and Biomass Pyrolysis*. Norwegian University of Science and Technology.
- [40] Ismail, T.M., Abd El-Salam, M., El-Kady, M.A. & El-Haggag, S.M. (2014). Three dimensional model of transport and chemical late phenomena on a MSW incinerator. *International Journal of Thermal Sciences*, Elsevier Masson SAS. 77, 139–57. <https://doi.org/10.1016/j.ijthermalsci.2013.10.019>
- [41] Chen, L., Yong, S.Z. & Ghoniem, A.F. (2012). Oxy-fuel combustion of pulverized coal: Characterization, fundamentals, stabilization and CFD modeling. *Progress in Energy and Combustion Science*, Elsevier. 38, 156–214. <https://doi.org/10.1016/j.pecs.2011.09.003>
- [42] Toporov, D.D. (2014). Combustion of Pulverised Coal in a Mixture of Oxygen and Recycled Flue Gas. *Combust. Pulverised Coal a Mix. Oxyg. Recycl. Flue Gas*. p. 1–175. <https://doi.org/10.1016/C2013-0-19301-4>
- [43] C. Hottel, A.F.S. (1967). *Radiative Heat Transfer*. McGraw-Hill, New York.
- [44] Sadeghi, H., Hostikka, S., Crivelli, G. & Bordbar, H. (2021). Weighted-sum-of-gray-gases models for non-gray thermal radiation of hydrocarbon fuel vapors, CH<sub>4</sub>, CO and soot. *Fire Safety Journal*, Elsevier Ltd. 125, 103420. <https://doi.org/10.1016/j.firesaf.2021.103420>
- [45] Bordbar, M.H., Wezel, G. & Hyppänen, T. (2014). A line by line based weighted sum of gray gases model for inhomogeneous CO<sub>2</sub>-H<sub>2</sub>O mixture in oxy-fired combustion. *Combustion and Flame*, Elsevier Inc. 161, 2435–45. <https://doi.org/10.1016/J.COMBUSTFLAME.2014.03.013>
- [46] Alberti, M., Weber, R. & Mancini, M. (2020). New formulae for gray gas absorptivities of H<sub>2</sub>O, CO<sub>2</sub>, and CO. *Journal of Quantitative Spectroscopy and Radiative Transfer*, Elsevier Ltd. 255. <https://doi.org/10.1016/j.jqsrt.2020.107227>
- [47] Vyazovkin, S. (2015). *Isoconversional kinetics of thermally stimulated processes*. Springer,.
- [48] Butmankiewicz, T., Dziugan, P., Kantorek, M., Karcz, H. & Wierzbicki, K. (2012). Thermal disposal of municipal waste on a grid - is it a proper technology? *Archives of Waste Management and Environmental Protection*, 14, 13–28.
- [49] Smart, J.P., Patel, R. & Riley, G.S. (2010). Oxy-fuel combustion of coal and biomass, the effect on radiative and convective heat transfer and burnout. *Combustion and Flame*, The Combustion Institute. 157, 2230–40. <https://doi.org/10.1016/j.combustflame.2010.07.013>
- [50] Mureddu, M., Dessì, F., Orsini, A., Ferrara, F. & Pettinau, A. (2018). Air- and oxygen-blown characterization of coal and biomass by thermogravimetric analysis. *Fuel*, Elsevier. 212, 626–37. <https://doi.org/10.1016/j.fuel.2017.10.005>
- [51] Skorek-Osikowska, A., Bartela, Ł. & Kotowicz, J. (2015). A comparative thermodynamic, economic and risk analysis concerning implementation of oxy-combustion power plants integrated with cryogenic and hybrid air separation units. *Energy Conversion and Management*, Pergamon. 92, 421–30. <https://doi.org/10.1016/J.ENCONMAN.2014.12.079>